

CR160177

(NASA-CR-160166) DEVELOPMENT OF A PROTOTYPE
FLEXIBLE RADIATOR SYSTEM Final Report
(Vought Corp., Dallas, Tex.) 286 p
HC A13/MF A01

N79-24299

CSCI 20D

Unclas
22209

G3/34

DEVELOPMENT OF A PROTOTYPE FLEXIBLE RADIATOR SYSTEM

- FINAL REPORT -

2-30320/3R-52078

CONTRACT NO. NAS9-14776
DRL: T-1213, LINE ITEM 3
DRD: MA-1837TA

Submitted to:

THE NATIONAL AERONAUTICS AND SPACE ADMINISTRATION
JOHNSON SPACE CENTER
HOUSTON, TEXAS

by

VOUGHT CORPORATION
DALLAS, TEXAS 75265



DEVELOPMENT OF A PROTOTYPE FLEXIBLE RADIATOR SYSTEM

- FINAL REPORT -

2-30320/9R-52078

CONTRACT NO. NAS9-14776
DRL: T-1213, LINE ITEM 3
DRD: MA-1837TA

Submitted to:

THE NATIONAL AERONAUTICS AND SPACE ADMINISTRATION
JOHNSON SPACE CENTER
HOUSTON, TEXAS

by

VOUGHT CORPORATION
DALLAS, TEXAS 75265

PREPARED BY:

C. W. Hixon
C. W. Hixon

REVIEWED BY:

J. A. Oren
J. A. Oren

APPROVED BY:

R. L. Cox
R. L. Cox

J. C. Utterback
J. C. Utterback
Manager, Propulsion

TABLE OF CONTENTS

		<u>PAGE</u>
1.0	SUMMARY	1
2.0	INTRODUCTION	2
3.0	RADIATOR PANEL DESCRIPTION	6
4.0	RADIATOR PANEL FABRICATION	12
5.0	RADIATOR PANEL TESTING	15

APPENDICES

A	Program Progress Reports Nos. 1 - 25 (7 June 1978 - 31 December 1978)	A-1
B	Hypervelocity Impact Experiment Test Report	B-1
C	Heat Bonding Process Evaluation - Prototype Flexible Radiator	C-1
D	Instrumentation Error Analysis - Flexible Radiator Solar Degradation Test	D-1
E	Solar Degradation Test Quick Look Report	E-1

LIST OF FIGURES

		<u>PAGE</u>
1	Inflatable Radiator System	3
2	Prototype Flexible Radiator Panel and Assembly Table . . .	4
3	Prototype Flexible Radiator Panel	5
4	Flexible Radiator Fin Material	7
5	Inlet and Outlet Fluid Manifolds	9
6	Fluid Manifold Tube Connections	10
7	Flexible Radiator Stowed Configuration	11
8	Mold for Laminating Flexible Radiator Panel	13
9	Assembly of Fusion Bonding Radiator	14
10	Vought Drawing T213-SK08	16

1.0 SUMMARY

The Vought Corporation designed, fabricated and tested a prototype flexible space radiator under NASA/JSC contract number NAS9-14776 between June 1976 and December 1978. This report documents the design and fabrication technique of the resultant flexible space radiator. The radiator is a roll-up flexible panel with the transport fluid manifolds located at the ends of the 27 foot length. Fifty PFA Teflon flow tubes are sandwiched between the layers of silver wire mesh and sealed in the FEP Teflon film. The transport fluid flows from an inlet manifold through 25 panel flow tubes to the end of the radiator panel into a manifold which directs the fluid into the other 25 flow tubes on its return to the base of the radiator. Deployment/retraction of the flexible radiator panel is by low pressure inflation tubes (one along each side of the panel) which incorporate a flat spring. The spring supplies the retraction force to wind the radiator panel on a drum when the pressure in the inflation tubes is relieved.

Room ambient deployment tests of the radiator panel were conducted at Vought to verify the inflation tube/spring deployment/retraction capability. These tests were documented on 16 mm film. The panel was deployed in Chamber B at NASA-JSC for a thermal vacuum, solar spectrum exposure test. After approximately 100 hours of solar exposure, post-test inspection revealed no structural or optical properties degraded.

2.0

INTRODUCTION

The Vought Corporation began full scale development of the flexible space radiator concept in June 1976 under Contract to NASA-JSC. The flexible radiator has potential application as a supplementary heat rejection device on the Shuttle Orbiter. Figure 1 depicts a 4 KW heat rejection module and an early flexible fin concept. Design and fabrication effort on the soft-tube, flexible radiator culminated in a prototype radiator panel shown in Figures 2 and 3. This report presents the design details and fabrication techniques used to produce the contract deliverable end item.

Appendix A contains all the progress reports between June 1976 and December 1978, and may be consulted for the direction of the program on a monthly basis. Appendix B contains the results of a hypervelocity impact experiment test performed at the Texas A&M University facility. An investigation of bonding adhesives was made before the program was redirected to a fusion bonding process and the results of this investigation appear in Appendix C. Appendix D is an instrumentation error analysis of the solar degradation test documented in Appendix E.

INFLATABLE RADIATOR SYSTEM

SOFT TUBE DESIGN

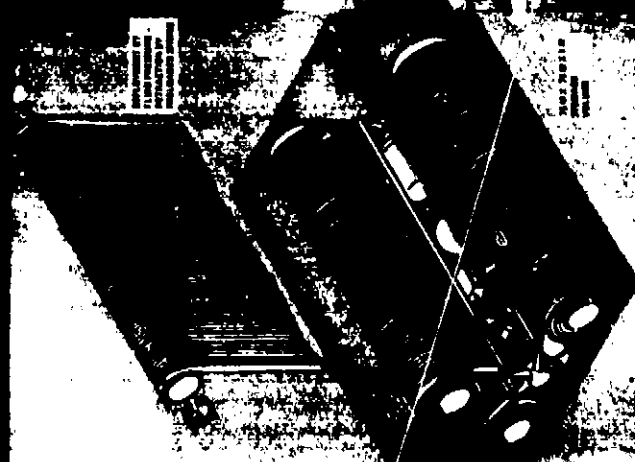


FIGURE 1



FIGURE 2
PROTOTYPE FLEXIBLE RADIATOR PANEL AND ASSEMBLY TABLE

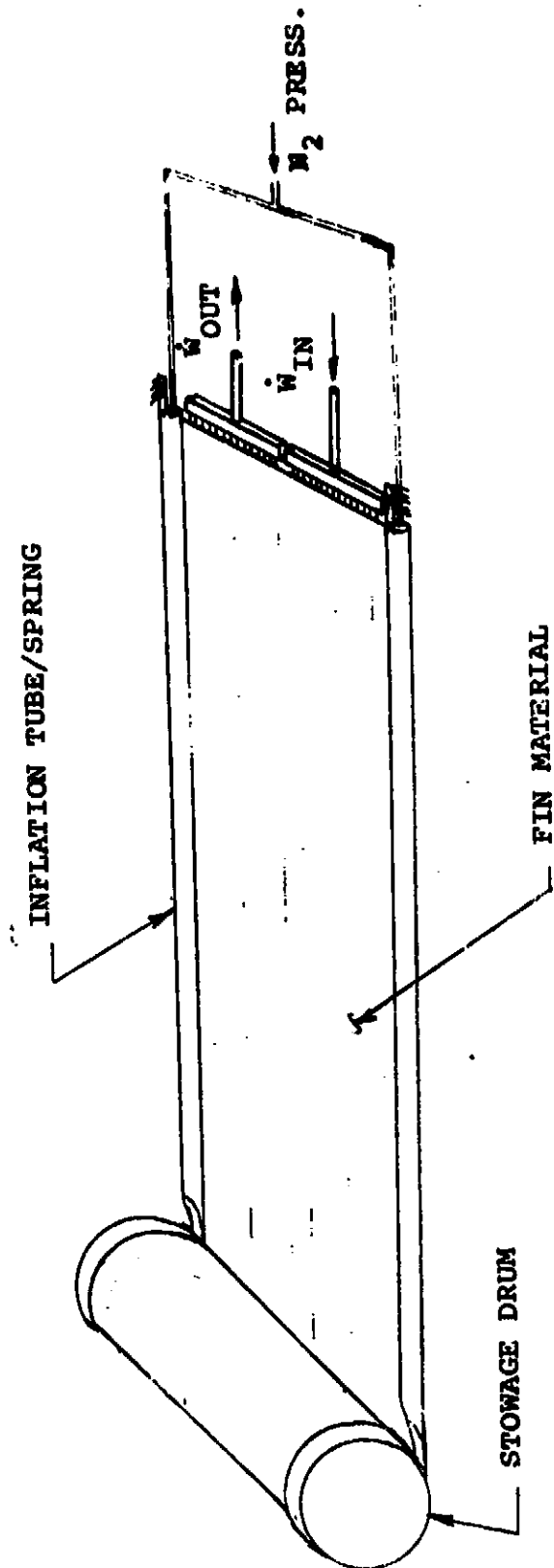


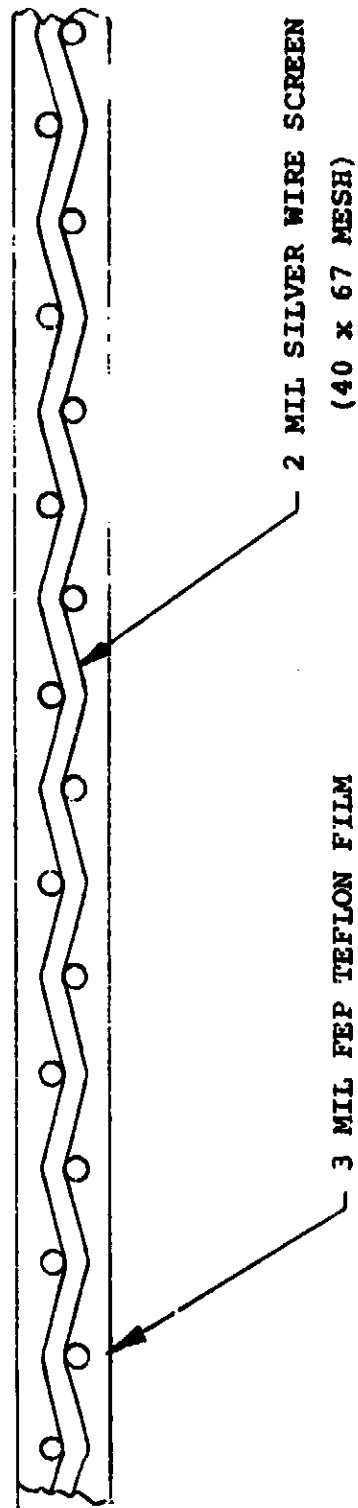
FIGURE 3
PROTOTYPE FLEXIBLE RADIATOR PANEL
(PARTIAL DEPLOYMENT)

3.0 RADIATOR PANEL DESCRIPTION

The prototype flexible radiator is designed to reject 1.33 KW to a 0°F sink using Coolanol 15 as the transport fluid with a 100°F radiator inlet temperature. The overall radiator dimensions in the deployed configuration are 3.3 feet wide by 27 feet long to give a total radiating area (from both sides) of 178 square feet. In the stowed configuration, the radiator rolls up on a drum 10 inches in diameter by 4 feet long to a final diameter of approximately 17 inches.

The prototype panel was constructed from six basic components: (1) the flexible fin, (2) panel flow tubes, (3) fluid manifolds, (4) deployment inflation tubes, (5) retraction springs, and (6) the stowage drum. Principal to the capability of the panel to reject heat is the fin material. The fin material fabrication was subcontracted to Schjeldahl, Inc. who used a newly developed continuous mill operation which hot-rolled a 40 x 67 silver wire mesh into 3 mil FEP Teflon film and vacuum deposited 1000 Å of silver covered by 150 Å of Inconel on one side of the Teflon film. Optical properties of the hot-rolled laminate steadily deteriorated after receipt of the material and the ensuing investigation revealed shortcomings in the manufacturing process which allowed the silver to tarnish in contact with the air. Deemed unuseable due to the large measured solar absorptance values, the deposited silver and Inconel were removed from the Teflon film and fin material became just the wire mesh imbedded in the film (Figure 4). Solar absorptance values of the mesh/film only were 0.16, which is approximately 13% lower than the lowest measured value of the original silvered material. The emissivity of the fusion bonded laminate was 0.70.

To distribute the heat from the transport fluid over the panel area, 50 flow tubes of PFA Teflon (1/8" O.D. x 1/16" I.D.) spaced .75" apart are used. These flow tubes run parallel to the long dimension of the radiator panel and connect to aluminum manifolds. The tube-to-manifold connections are made with standard Swagelok fittings, an adhesive, and tube inserts which allowed the fittings to capture the soft tubing without collapsing the tube wall. Dr. Fred Dawn of NASA-JSC recommended several adhesives for the connections and one (EC2216) manufactured by 3M proved very successful. Samples of these connections were tested for extended periods in a 200°F water bath at 100 psi without leakage.



NOTE: ONE LAYER OF TWO-
LAYER LAMINATE SH

FIGURE 4 FLEXIBLE RADIATOR FIN MATERIAL

The fluid manifolds distribute the flow to the panel such that 25 flow tubes receive inlet flow. At the drum end of the radiator, a second manifold collects the flow and directs it into the other 25 flow tubes on the return leg back along the panel into the outlet manifold (see Figures 5 and 6). The outlet manifold collects the transport fluid from the radiator and directs it back into the environmental control system.

The flexible radiator panel is stowed in approximately eight wraps on a 10 inch drum (see Figure 7). Four inch diameter inflation tubes made by Schjeldahl of Kevlar/mylar are attached along each side of the radiator panel. Specially prepared flat springs are incorporated in each inflation tube in a pocket along the drum side of the inflation tube. The retraction springs must be closely matched as to the magnitude of force each exerts. A mismatch in retraction spring force will not allow the radiator panel to wind-up in the original stowage volume. A spring adjustment capability was designed into the spring hold down to fine tune the panel deployment/retraction path. Panel deployment is achieved by pressurizing (≈ 1 psig) the inflation tubes which work against the retraction spring force to roll the stowage drum outward exposing increasing amounts of panel area.

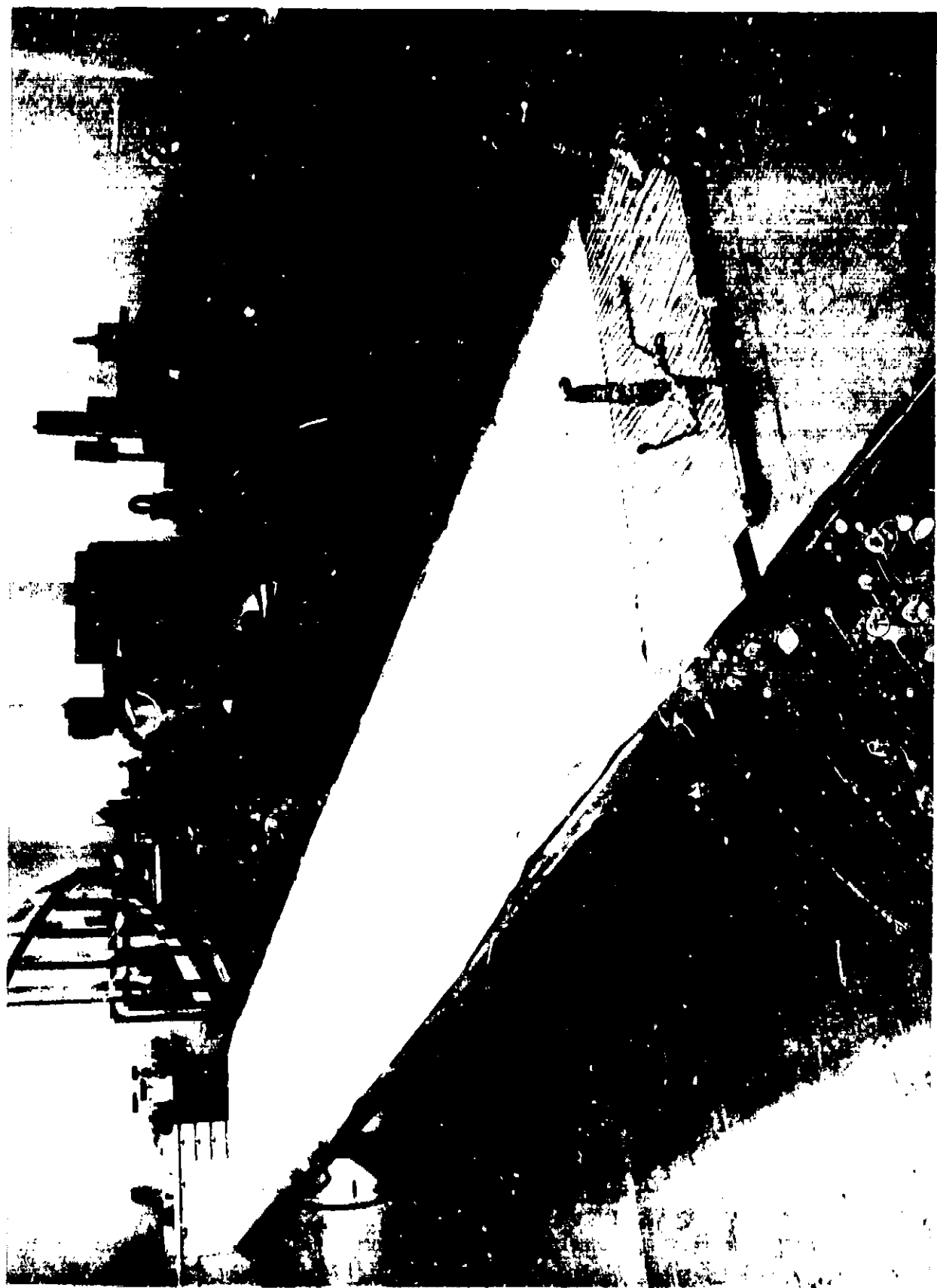


FIGURE 5 INLET AND OUTLET FLUID MANIFOLDS



FIGURE 6 FLUID MANIFOLD TUBE CONNECTIONS

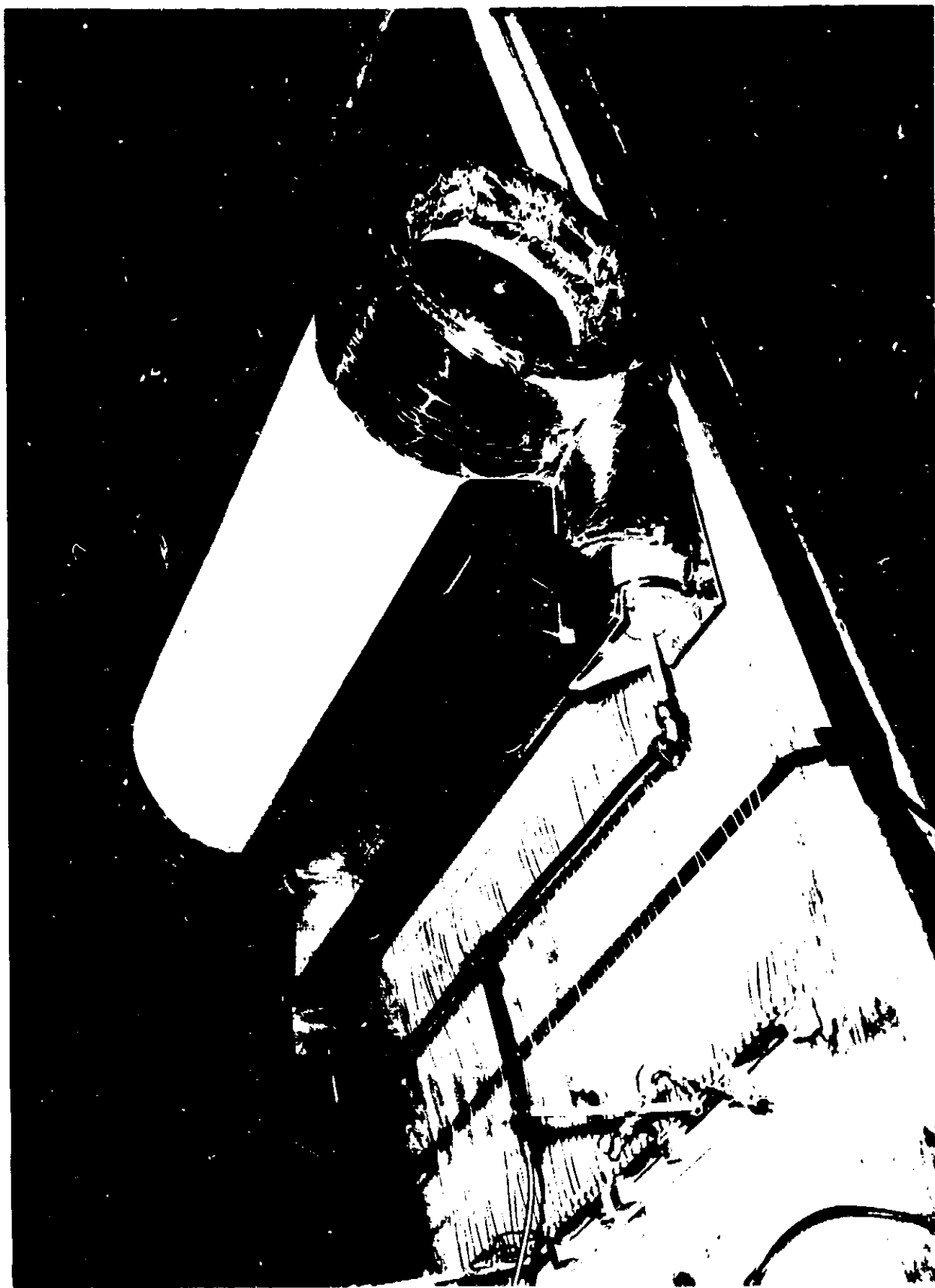


FIGURE 7 FLEXIBLE RADIATOR STOWED CONFIGURATION

4.0 RADIATOR PANEL FABRICATION

Fusion bonding was chosen as the method of forming the laminate of the two fin layers sandwiching the flow tubes. PFA Teflon tube material was used to guard against the tubes collapsing during the bonding process. An assembly table (see Figure 2) was constructed on which the complete radiator panel can be laid out. The table surface has 50 grooves spaced three-quarters of an inch apart (Figure 8). To aid in assembly, holes drilled in the grooves were connected to a vacuum source which pulled one layer of fin material into the grooves. Following operations sandwiched the flow tubes between the fin material in the grooves and a second layer of fin material with Kapton vacuum bagging material holding the flexible fin assembly together. The flexible fin assembly (Figure 9) on the assembly table was rolled into a 5.5' x 5.5' x 30' autoclave for the fusion bonding process. The autoclave was programmed to reach 570°F within $\pm 3^\circ\text{F}$ over a three hour heat-up period. The fusion bond attained between the layers of fin material and between the flow tubes and the fin material was very strong mechanically.

The retraction springs were purchased from Spring Engineers (Dallas) and sent to Schjeldahl, the inflation tube subcontractor. Schjeldahl bonded pockets along the inflation tubes to accommodate the retraction springs and delivered these to Vought as assemblies. The inflation tube assemblies were then attached to the edge of the radiator panel fin material in a fold of aluminized mylar material; the free edges of which were sown to the fin material.

Stowage drum fabrication and assembly is shown in Vought drawing T213-SK08 which is presented in Figure 10.

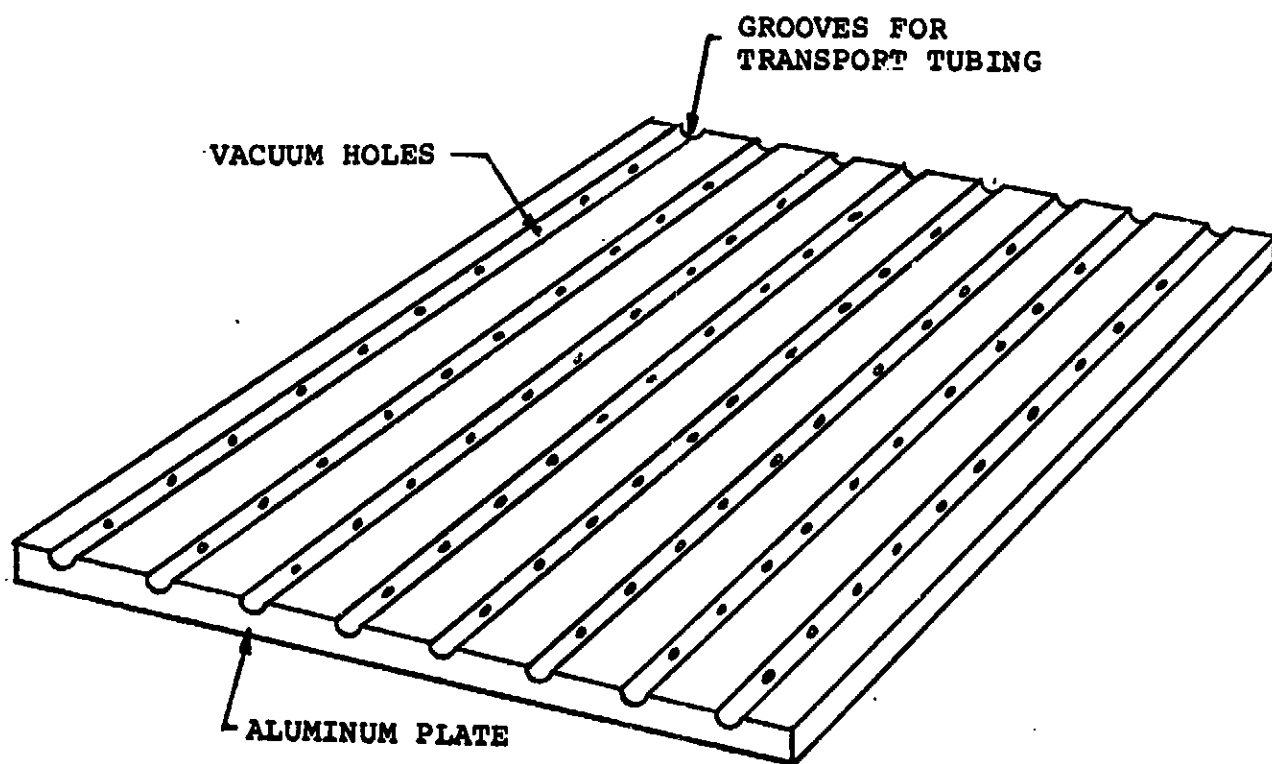


FIGURE 8
MOLD FOR LAMINATING FLEXIBLE RADIATOR PANEL

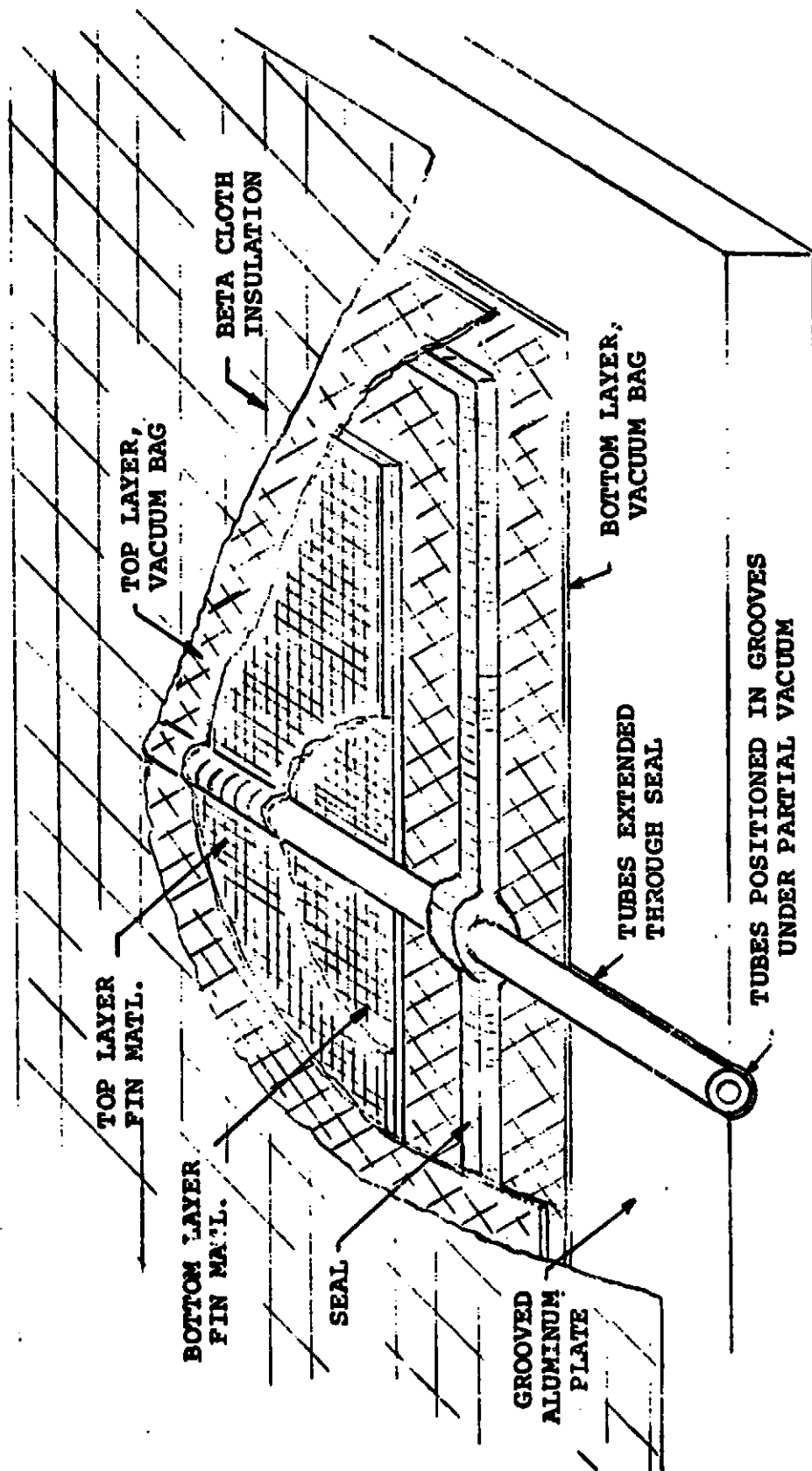
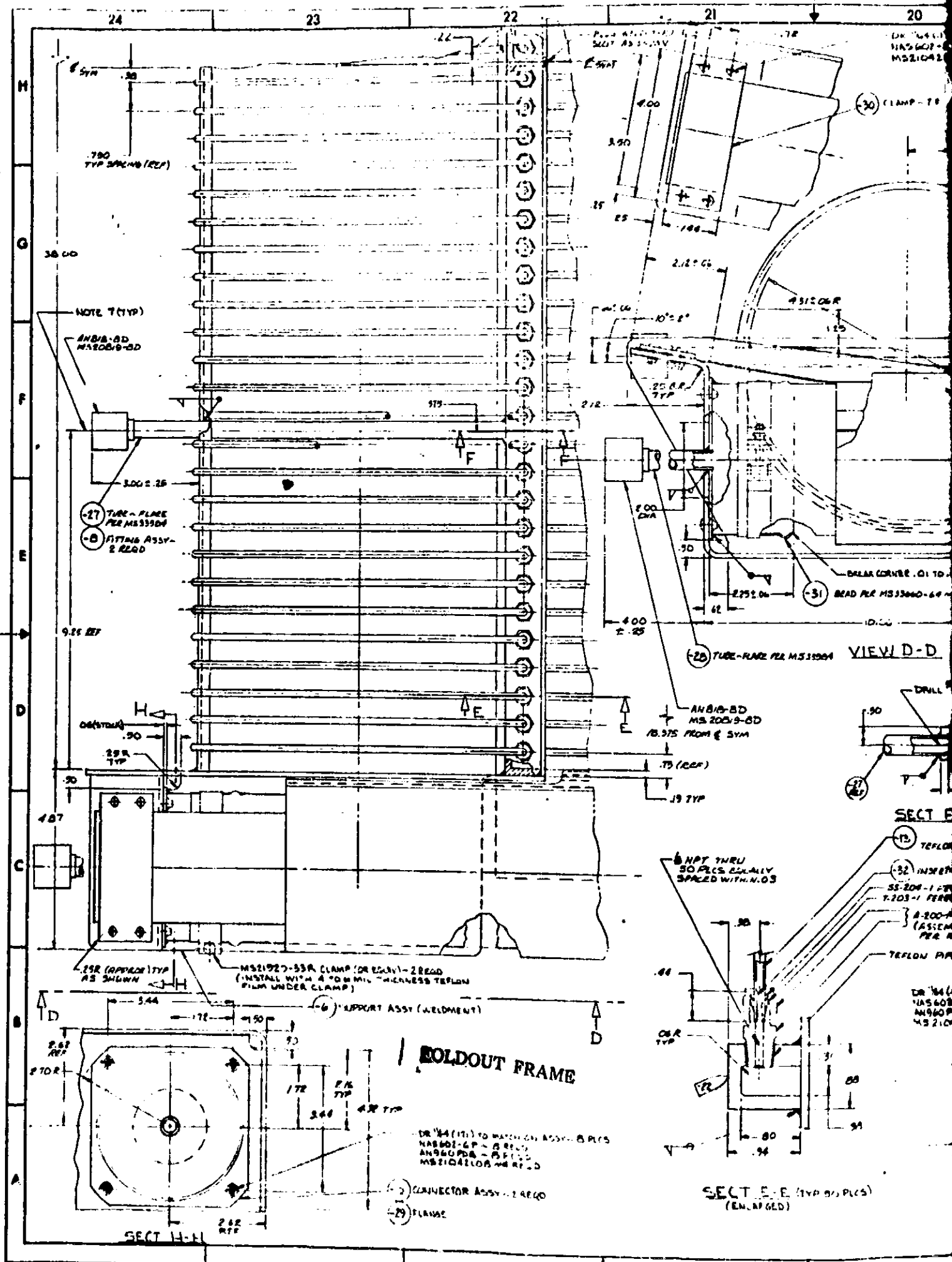
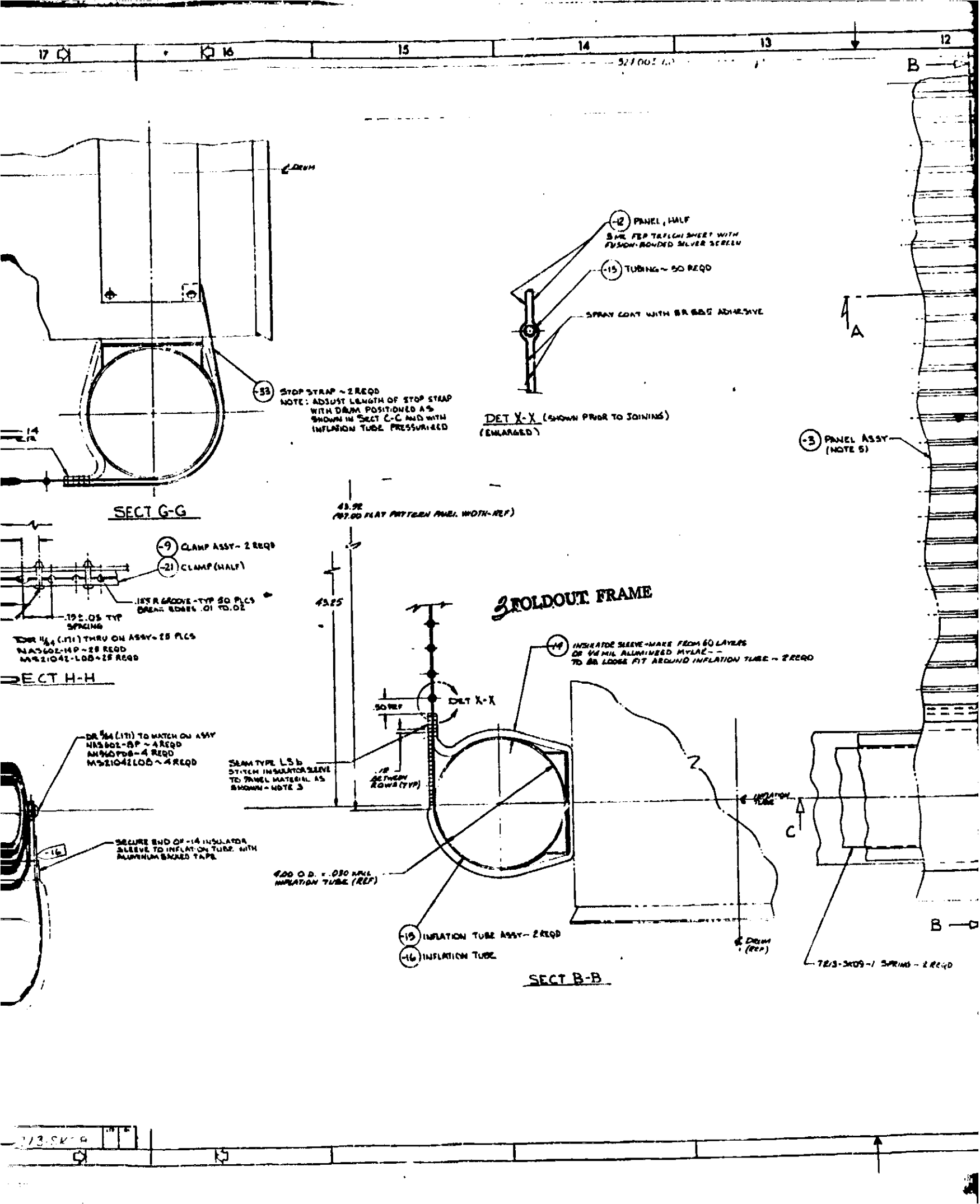


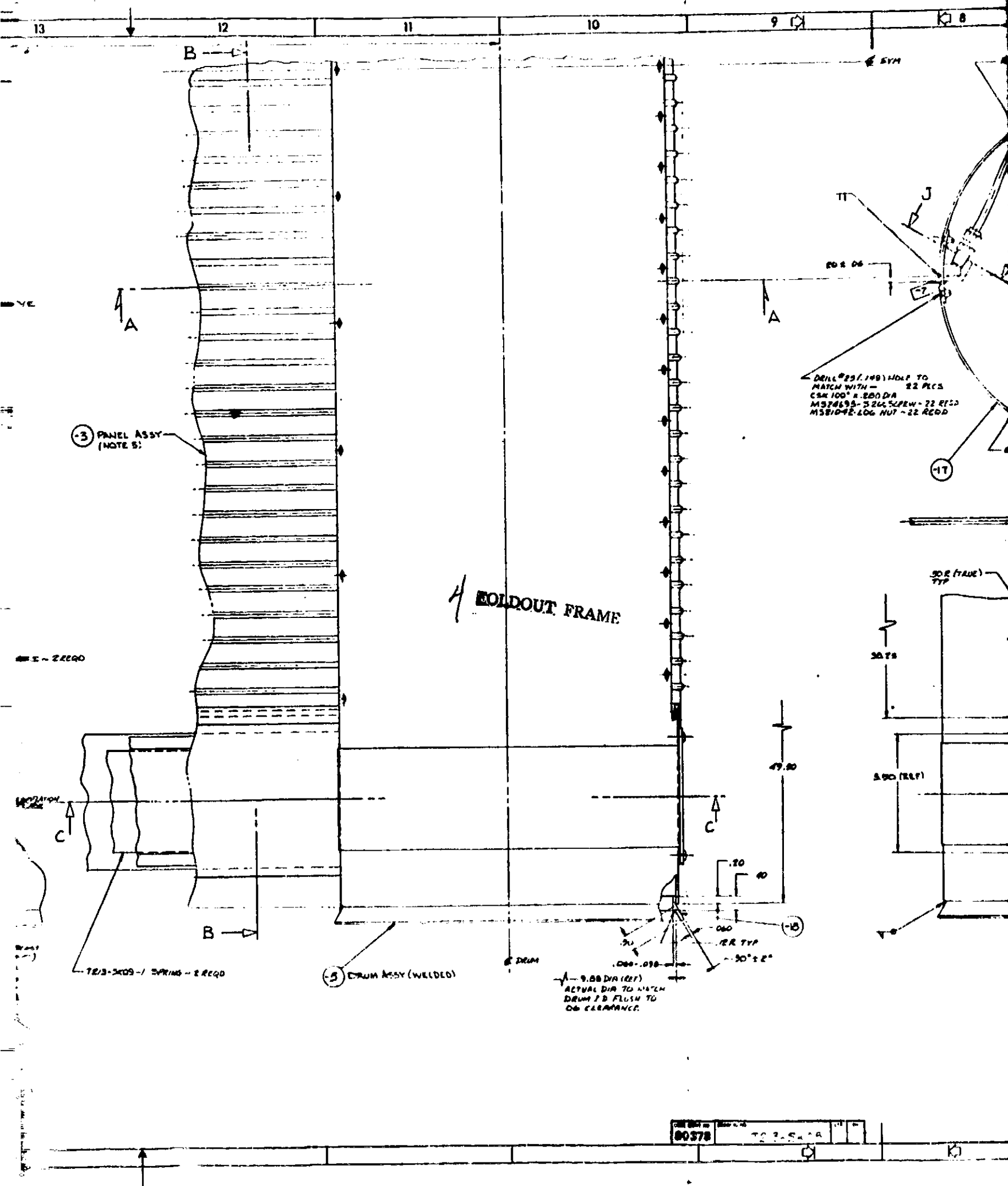
FIGURE 9 ASSEMBLY FOR FUSION BONDING RADIATOR

5.0 RADIATOR PANEL TESTING

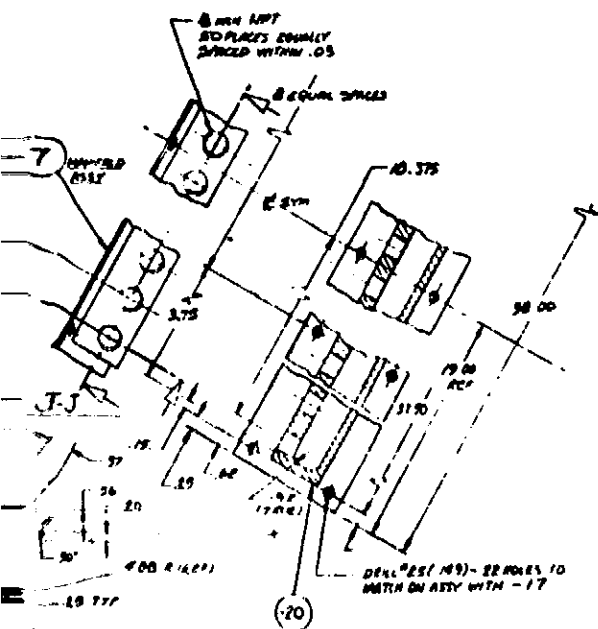
Testing of the flexible radiator panel consisted of a room ambient deployment/retraction test and a thermal vacuum solar exposure test. The deployment test was performed at Vought in May 1978 and the solar exposure test was performed at NASA-JSC in November 1978. Successful deployment and retraction of the panel was witnessed by the NASA contract technical monitor and recorded on 16 mm movie film. The purpose of the solar exposure test was to evaluate radiator performance degradation due to radiation near the solar wavelength. The panel optical properties and mechanical strength were checked carefully after 100 hours of solar exposure and no degradation was detected. Panel heat rejection also corroborated the conclusion of no measurable thermal performance degradation.







1. BREAK ALL SHARP EDGES
2. FURNISH WELD PER SPEC. ENVI-112
3. SWITCHING TO BE PER FSD STD 78
4. ATTACH NOTER TUBE CONNECTIONS AS FOLLOWS:
 - A. INSTALL UNIONS IN MANIFOLDS WITH TIGHTENING TORQUE TO 25-30 LB-FT
 - B. AFTER TUBES ARE CUT TO MIN. LENGTH, STEW TUBE ENDS APPROX 1/2" WITH STEERING MOUNTING ITEM (BUSH OR EQUIV).
 - C. PLACE CONNECTOR WITH 1/2" BUSH OVER TUBE ENDS.
 - D. LIGHTLY COAT STEWED TUBE ENDS AND THE FRONT FERRULE (1) WITH E-3111 ADHESIVE AND SLIDE SERREUSE OVER TUBES.
 - E. THREAD NUT TO CONNECTOR UNION AND TORQUE 1/4 TO 1 TURN AFTER FULLY TIGHT.
5. THE -3 PANEL BODY SHALL BE FABRICATED USING VACUUM FORMING PLATE 721-3807
6. ANOTHER NOTED ITEMS PER SPEC. 1/4-4 TYPE A
7. ATTACH TEMPERATURE INSTRUMENTATION AS REQUIRED IN CHANNING 721-3808 SHEET 2.



FOLDOUT FRAME

FLYING 10

[illegible]

APPENDIX A

PROGRAM PROGRESS REPORTS 1-25
(7 June 1976 thru 31 December 1978)

DEVELOPMENT OF A PROTOTYPE FLEXIBLE RADIATOR SYSTEM

PROGRESS REPORT NO. 1

7 JUNE through 31 JULY 1976

11 August 1976

CONTRACT NO. NAS9-14776
DRL: T-1213, LINE ITEM 2
DRD: MA-182TD

Submitted To:
THE NATIONAL AERONAUTICS AND SPACE ADMINISTRATION
JOHNSON SPACE CENTER
HOUSTON, TEXAS

BY

VOUGHT CORPORATION
SYSTEMS DIVISION
DALLAS, TEXAS 75222

PREPARED BY:

CHECKED BY:

APPROVED BY:

J. W. Leach
J. W. Leach

J. A. Oren
J. A. Oren

R. L. Cox
R. L. Cox

TABLE OF CONTENTS

		<u>PAGE</u>
1.0	OVERALL PROGRESS	1
2.0	DESIGN REQUIREMENTS ANALYSES	2
	2.1 Micrometeoroid Damage Studies	2
	2.2 Temperature/Pressure Test of Polyurethane Tubing . .	8
	2.3 Thermal Modeling and Performance/Optimization Analyses	14
	2.4 Assessment of Two Layers Wire Mesh Construction . . .	26
	2.5 Inflation Tubing Requirements	29
	2.6 Extendible Boom Analysis	37
3.0	PROGRESS ON MAJOR END ITEMS	38
4.0	WORK SCHEDULED DURING THE NEXT REPORTING PERIOD	38
5.0	REFERENCES	39

MONTHLY PROGRESS REPORT NO. 1
DEVELOPMENT OF A PROTOTYPE FLEXIBLE RADIATOR SYSTEM

1.0 OVERALL PROGRESS

Work during the first reporting period has been concentrated on the design requirements for the prototype flexible radiator system, and has included analyses, element tests, and surveys of manufacturers capabilities relevant to the design and fabrication of the system which will follow in subsequent reporting periods. The studies of the initial period follow the outline of the statement of work of ref. (1), and address the following subjects:

- 1) Loading requirements and performance data for tubular extendible space booms.
- 2) Alternate fabrication techniques for improving the fin material construction and radiator panel assembly.
- 3) Computer modeling and performance/optimization analyses.
- 4) Inflation tubing deployment/retraction system performance requirements.
- 5) Assessment of alternate fin layup with two layers silver wire mesh.
- 6) Micrometeoroid protection requirements and impact on tubing size.
- 7) Tests of transport tubing and fittings.

A briefing has been scheduled at NASA-JSC during the next reporting period to discuss the findings of the design requirements studies and to obtain NASA inputs prior to initiating the design phase of the program.

2.0 DESIGN REQUIREMENTS STUDIES

This section summarizes the results of individual design requirements studies conducted to obtain data for designing and fabricating the flexible radiator system.

2.1 Micrometeoroid Damage Studies

The literature on micrometeoroid penetration of plastic materials was surveyed to determine whether experimental data or analytical methods exist for sizing the tube wall thickness of the flexible radiator. The limited data available indicates that plastics are more effective for resisting micrometeoroid penetration than had been predicted from data for metals. An equation given in reference (2) predicts depth of penetration conservatively for polyethylene. The equation is

$$t = 0.65 \left(\frac{1}{\epsilon_t} \right)^{1/8} \left(\frac{\rho_m}{\rho_t} \right)^{1/2} (V_m)^{7/8} (d_m)^{19/8} \quad (1)$$

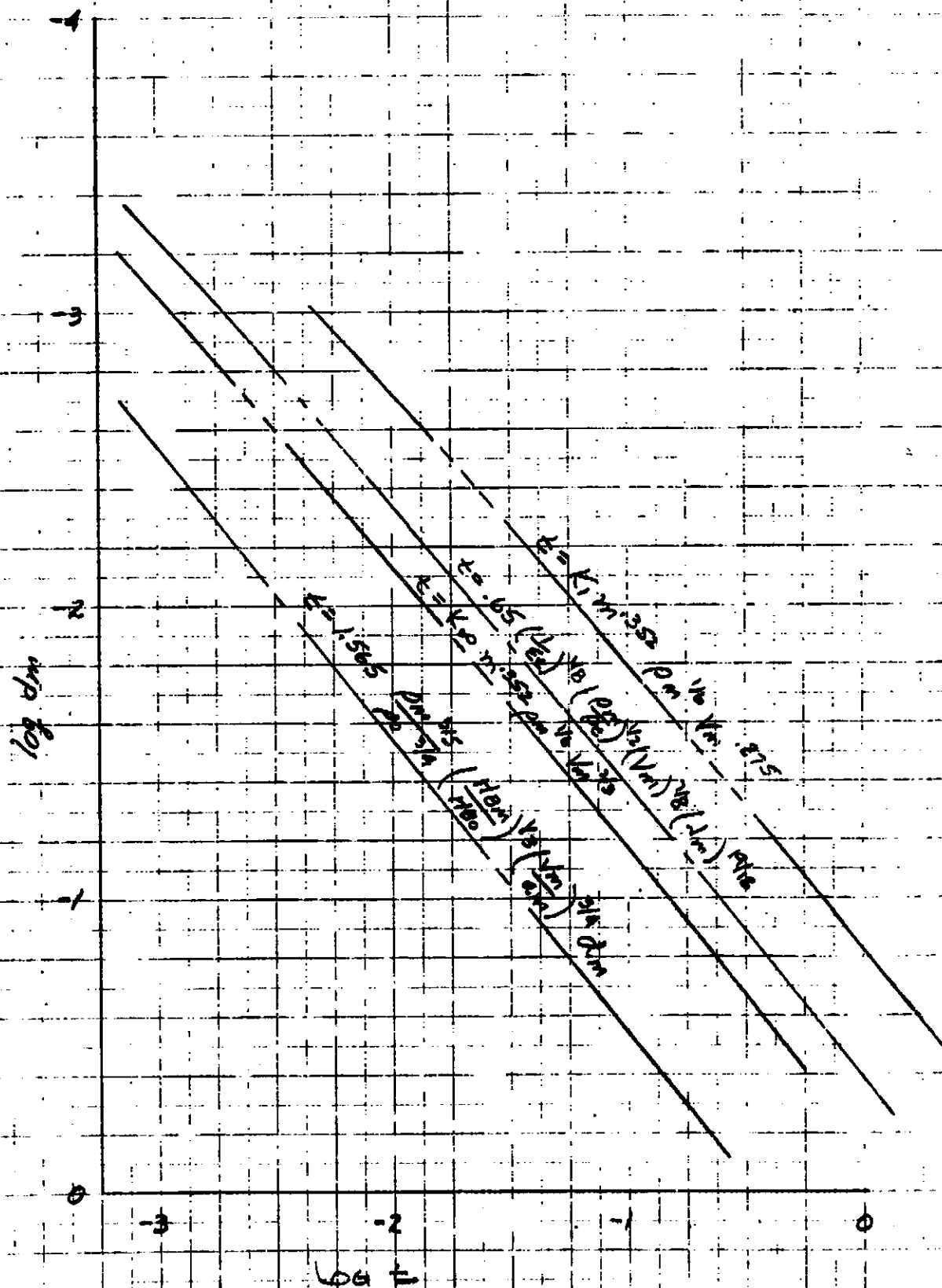
where:

- t = thickness of target material penetrated
- ϵ_t = percentage elongation of sheet material
- ρ_t = mass density of sheet material
- ρ_m = mass density of meteoroid
- V_m = normal impact velocity
- d_m = meteoroid diameter

Figure 1 compares the depth of penetration predictions for 2024-T6 aluminum with those of other equations developed for metals.

The elongation term in Eq. 1 is much larger for plastics ($\epsilon \approx 300$) than for metals ($\epsilon \approx 3$), and has a significant impact on the design of flexible radiators. For example, the wall thickness computed from Fig. 1 for 30 days lifetime for polyurethane tubing is 0.032". If the elongation term were assumed to be that of a metal, the required wall thickness is 0.058".

Figure 2 compares predicted and experimental depths of penetration for polyethylene ($\rho = .9$, $\epsilon \approx 500$)



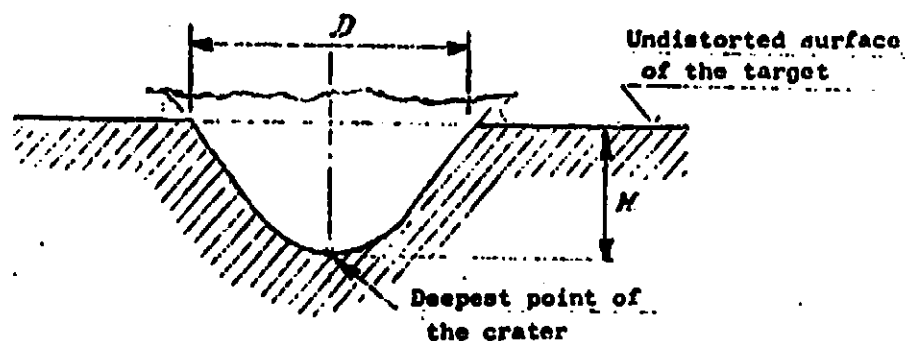


Figure 1. method of crater measurement

EQUATION 1

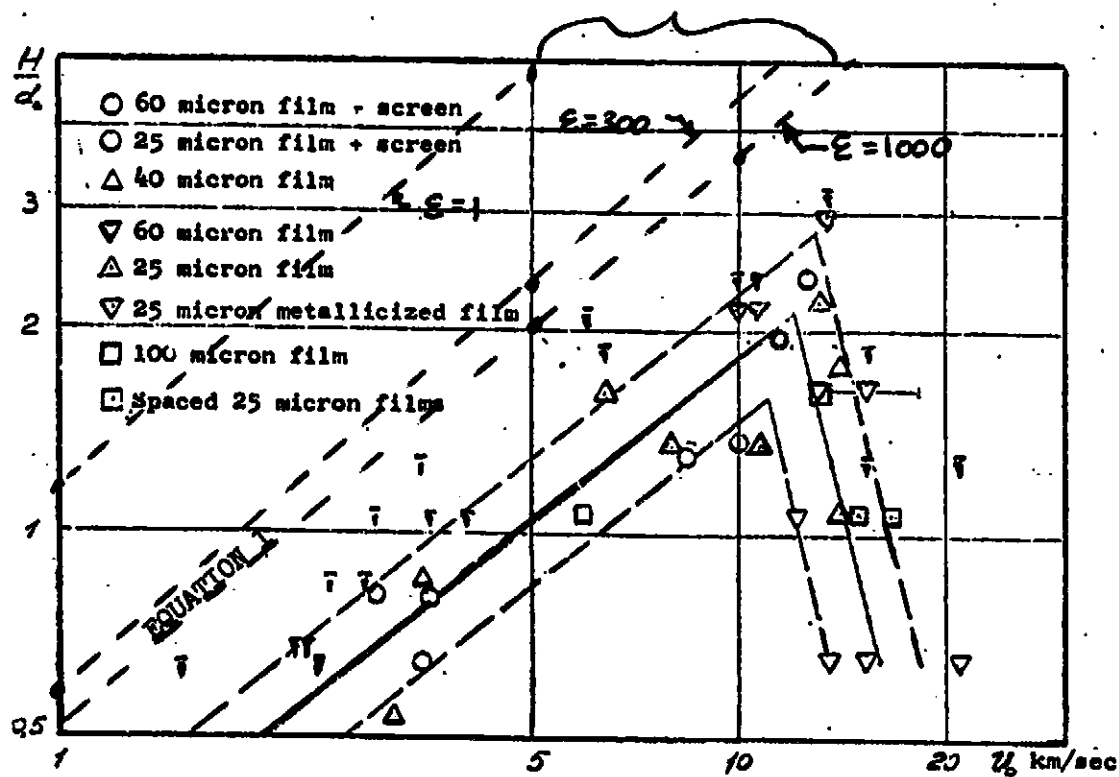


Figure 2. results of the bombardment of polyethylene films by glass beads 85-250 microns in size

The equation follows the trend of the data from ref. (3) for low velocities, but predicts much greater depths of penetration than actually occur at velocities typical of micrometeoroids (20 km/sec.). Thus based on the data for polyethylene, Eq. (1) appears to give a conservative estimate of the wall thickness required to prevent penetration. Qualitative experimental data for plexiglas and polycarbonate in ref. (4) shows that polycarbonate ($\rho = 1.2$, $\epsilon = 115$) is superior to plexiglas ($\rho = 1.2$, $\epsilon = 5$) for retarding meteoroids. This also reflects the importance of elongation in the penetration equation. No additional experimental data on plastics was found in the literature. A complete list of the literature surveyed is given in Appendix A. An attempt was made to locate existing facilities for testing penetration resistance of the tubing materials. Texas A&M University has one of the few active facilities suitable for the tests. Their preliminary estimate of the cost is \$6000 for a 6 month program.

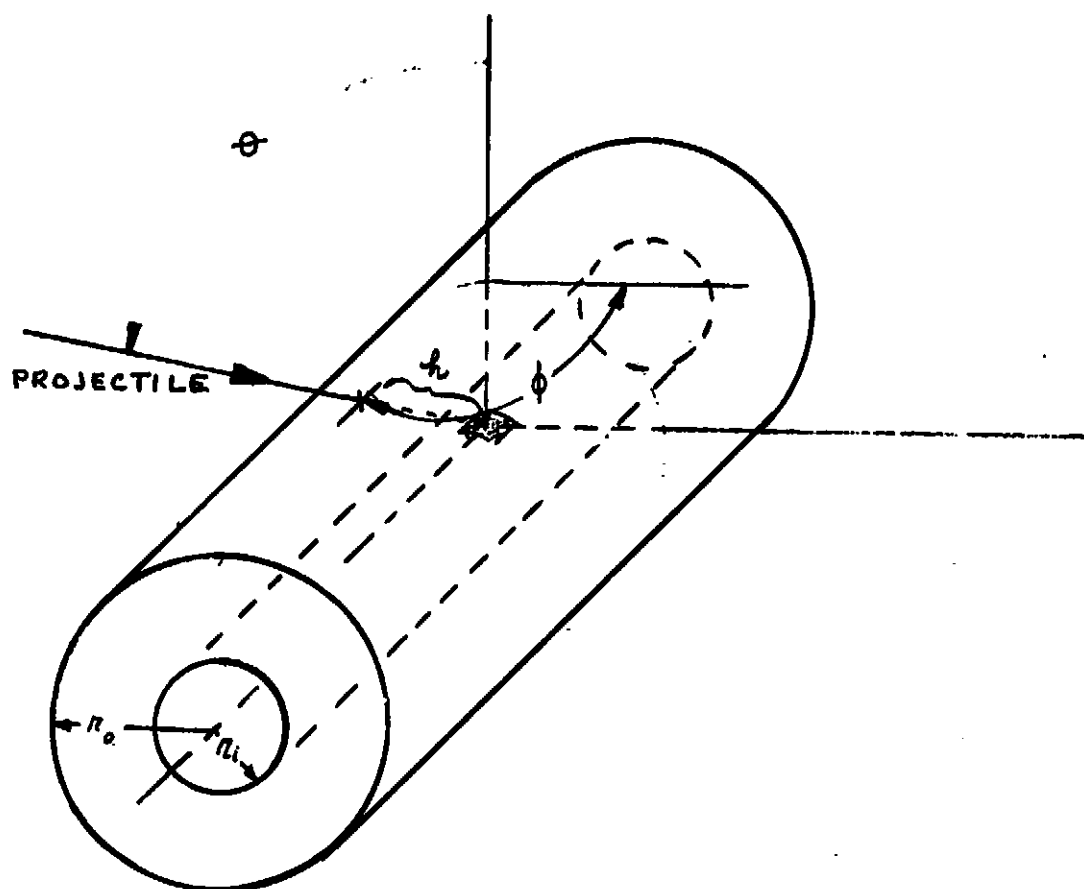
It is recommended that until additional data are available, the radiator tube wall thickness be sized from Eq. 1.

Analyses were made to determine the average depth that a meteoroid must penetrate to puncture a tube. The average depth is greater than the tube wall thickness because most meteoroids do not strike the tubing from a direction which is normal to the surface. Figure 3 shows a typical trajectory of a meteoroid which is directed towards an element on the interior tube wall. The depth that the meteoroid must penetrate to reach the interior wall is

$$h = \frac{-r_i + \sqrt{(r_o^2 - r_i^2)(1 + \cos^2 \phi \tan^2 \theta) + r_i^2}}{\cos \theta [1 + \cos^2 \phi \tan^2 \theta]} \quad (2)$$

The number of meteoroids which strike the surface from the θ, ϕ direction with velocity v and mass sufficient to penetrate the depth h is

$$d^2 n_{\theta, \phi} = \frac{N}{\pi} \sin \theta \cos \phi d\theta d\phi \quad (3)$$



$$h = \frac{-r_i + \sqrt{(r_o^2 - r_i^2)(1 + \cos^2 \phi \tan^2 \theta) + r_i^2}}{\cos \theta [1 + \cos^2 \phi \tan^2 \theta]}$$

FIGURE 3 EFFECTIVE WALL THICKNESS
FOR METEOROID PENETRATION OF
FLEXIBLE RADIATOR TUBING

where N is the cumulative flux of meteoroids, per unit area per unit time given as a function of meteoroid mass in meteoroid environment models. For the meteoroids of interest in this work

$$\log_{10} N = -14.37 - 1.213 \log_{10} M \quad (4)$$

The total number of meteoroids which strike the element which are capable of penetrating the tubing is obtained by integrating

$$\bar{N} = \frac{4}{\pi} \int_{\phi=0}^{\pi/2} \int_{\theta=0}^{\pi/2} N \sin \theta \cos \phi d\theta d\phi \quad (5)$$

N is computed from Eq. 4 for each angle after the mass required to penetrate the depth $h(\theta, \phi)$ is computed from Eq. 1. The integral in Eq. (5) is then evaluated numerically.

The probability of no penetration is given by

$$P_0 = e^{-SNA\tau} \quad (6)$$

where S is the shielding factor

A is the exposed area

τ is the time of exposure

The shielding factor accounts for meteoroid blockage by the earth, the orbiting payload, and by the radiator itself. In this analysis, only the earth shielding factor is taken into consideration. For a 200 n.m. orbit $S = 0.685$. Because of shielding by other factors, the actual shielding factor will be less, and the radiator will have a higher probability of success than is computed from Eq. (6).

Analyses were made to determine the additional wall thickness required to prevent leakage after a meteoroid has penetrated to the depth computed from Eq. 1. The tube wall thickness must be increased by this amount to prevent failure even though the meteoroid does not actually penetrate the tubing. Calculations showed that the additional wall thickness is approximately 0.002 inch for polyurethane tubing, and 0.004 inch for teflon tubing.

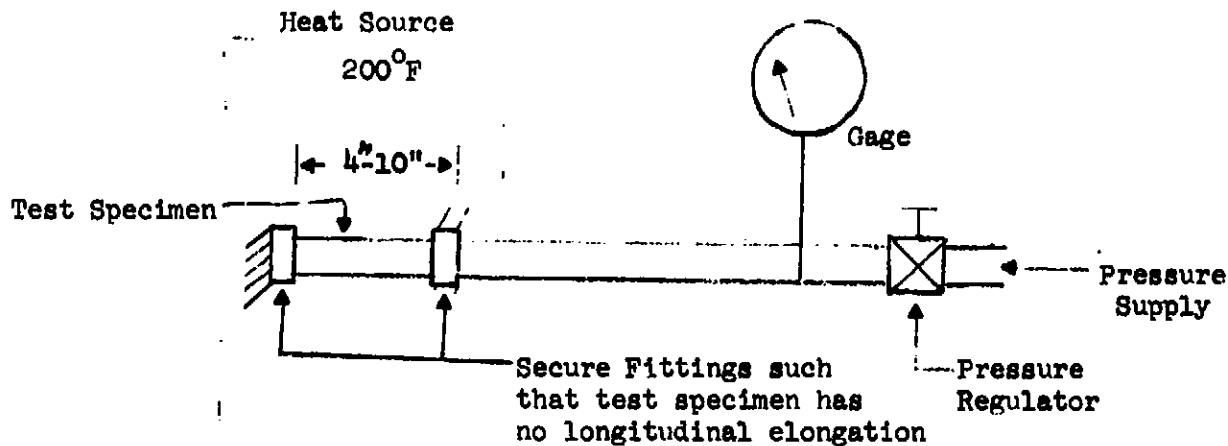
For the total radiator system to have a 90% survivability, the transport tubing and the inflation tubing must independently have higher probabilities of success. Thus, the inflation tubing was designed for 96% survivability (wall thickness = 0.044 inch for 4" O.D. tubing). The polyurethane tubing was selected so that the outside diameter is a standard dimension (0.1875" for polyurethane tubing and 0.125" for teflon tubing). For the optimum inside wall diameters the wall thickness for polyurethane is 0.0488 inch and the wall thickness for teflon is 0.0325 inch. Subtracting the thickness required for pressure retention, the thickness left for meteoroid protection is 0.0468 inch for polyurethane and 0.0285 for teflon. Treating the tubing as a thin sheet (not accounting for variable h as given by Eq. 2) the probabilities for surviving 90 days are 0.965 for polyurethane and 0.940 for teflon. If the variable h is taken into account, the probabilities are 0.983 for polyurethane and 0.974 for teflon. The combined probabilities of survivability for the inflation tubing and the transport tubing exceeds 90%.

2.2 Temperature/Pressure Test of Polyurethane Tubing

Small sections of polyurethane tubing were pressurized and maintained at constant temperature for extended periods of time to test for leakage at the fittings, and to determine whether plastic flow of the material is a significant problem at elevated temperatures. Figure 4 describes the test apparatus and procedure. The tubing size is 0.250 in. O.D. x 0.125 in. I.D. This is standard tubing which is similar to the 0.205 in. O.D. x 0.090 in. I.D. tubing specified in the baseline design. The stress levels at 50 psi are approximately the same for the standard and non-standard tubing. The first sample of tubing was tested at 200°F and 50 psi. The tube O.D. was measured at three sections as a function of time and the sample was submerged in water so that any leakage would be detected. The tubing was filled with Coolanol 15 and the system was pressurized with nitrogen. The measured tube O.D. is given as a function of time in Fig. 5. The tube ruptured after approximately 30 hours of testing. Standard Swagelok fittings were used with inserts made from 0.125 inch O.D. aluminum tubing. No leakage was observed

FIGURE 4
POLYURETHANE TUBE PRESSURE CREEP TEST

Approximate Test Setup -



Specimen -

- o 4" - 10" Long
- o 1/4" OD
- o 1/8" ID
- o Fittings: Swagelok with alum. ferrules. One end 1/8 OD SS tube insert; other end no insert.

Procedures -

- o Pressurize specimen to 52.1 psig (\pm 1psig)
- o Measure tube OD in three locations
- o Check end fittings for leaks, correct as required
- o Heat to 200°F
- o Measure tube OD in same three locations and check end fittings for leaks in the following increments:
 - 1 hr
 - 4 hrs
 - 24 hrs
 - 48 hrs
 - 72 hrs
- o Also check for tube rupture, terminate test upon rupture

Report - None Required

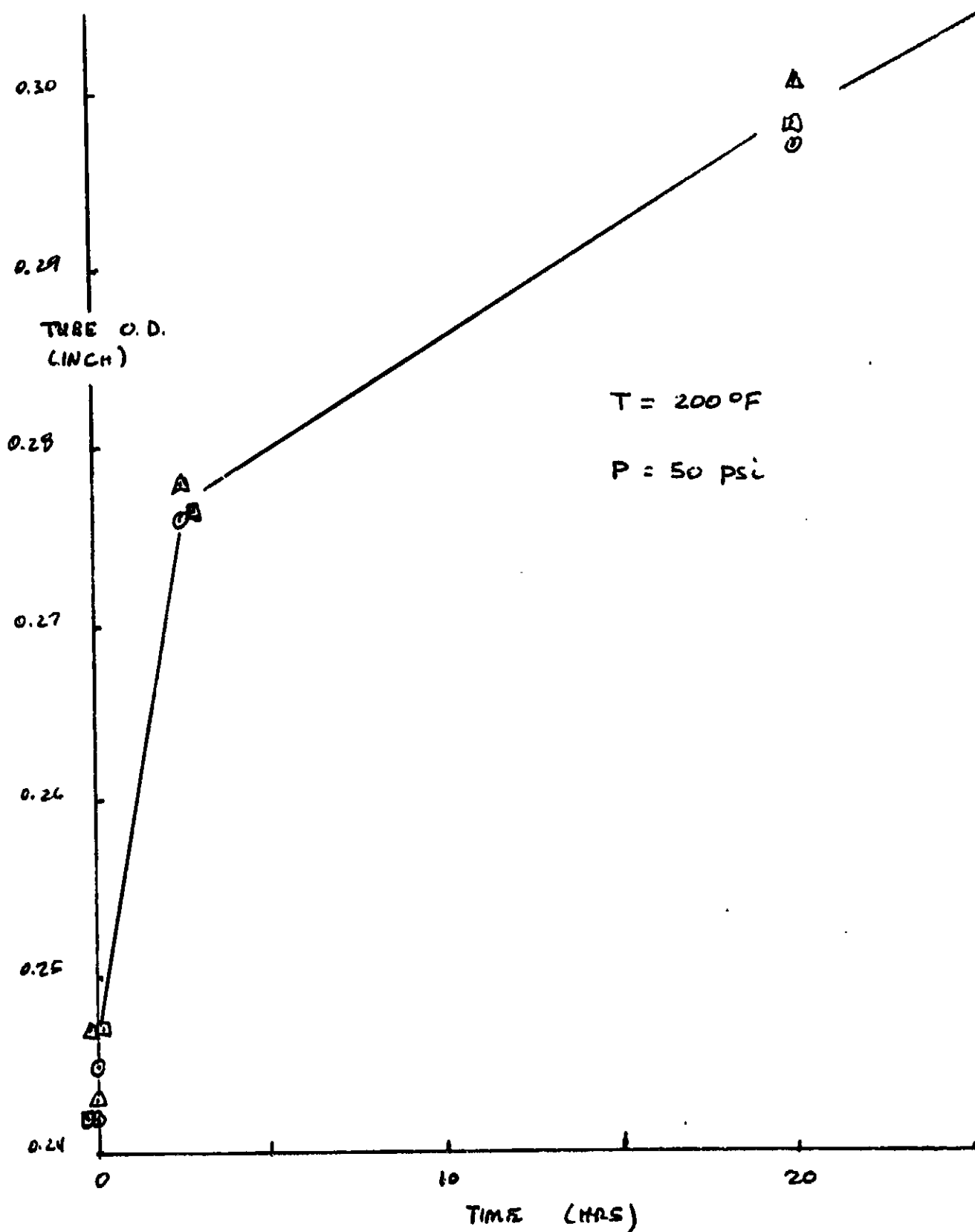


FIGURE 5 TEST OF POLYURETHANE TUBING AT 200°F

during the test sequence. A second section of tubing was tested at 175°F and 50 psi. The apparatus and procedure were the same as for the first sample except that the 0.125" O.D. insert was removed from the tubing at the fittings. Figure 6 shows the tube diameters measured at three sections as a function of time. The tube slipped out of the fitting after approximately 100 hours of testing. This verifies that inserts are required with polyurethane tubing. The tubing did not rupture during the first 100 hours. However, the diameter was increasing at a fairly steady rate so that failure would probably have occurred within the next 100 or 200 hours. Additional testing is planned with fitting inserts at lower temperatures to establish a safe operating range for polyurethane tubing.

The experimental results at 200°F are not consistent with published vendor data for polyurethane. Figure 7 from Ref. (5) shows that the published ultimate strength at 200°F is 2000 psi. The stress in the tube is given by

$$\sigma = \frac{P d_i}{2 t} \quad (7)$$

The tube wall thickness for a stressed tube is given approximately by

$$t = \frac{\bar{d}_{init} t_{init}}{\bar{d}} = \frac{(0.1875)(.0625)}{\bar{d}} \quad (8)$$

where \bar{d} is the average of the inside and outside diameters. The inside diameter in Eq. 7 is

$$d_i = \bar{d} - t = \bar{d} - \frac{.0078125}{\bar{d}} \quad (9)$$

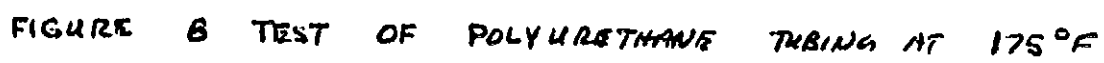
Equation (7) becomes

$$\sigma = 3200 (\bar{d}^2 - .0078125) \quad (10)$$

for

$\sigma_{max} = 2000 \text{ psi}$, Eq 10 gives

$$\bar{d} = 0.795 \text{ inch}$$



Hi-TUFF polyurethane thin gauge sheeting and film

Hi-TUFF Polyurethane sheeting out-performs all other plastic film and thin-gauge rubber sheeting where product applications require superior toughness, abrasion resistance, tear strength, flex-life, low temperature flexibility, oil and gasoline resistance, and longer aging properties. Hi-TUFF Sheeting can be vacuum formed, dielectrically sealed, blow-molded and solvent or heat-bonded to substrates.

Typical Applications:

Fluid Containers
Dust Boots and Bellows
Protective Covers
Packaging
Conveyor Belting
Overlays
Cable Jacketing
(slit and spiral wrapped)

Diaphragms
Furniture
Skin Covering for Foams
and Sponge
Bag-in-Box Packaging
Oil and Grease Pouches
Bearing and Tool Packaging

Lamination to Fabrics
Gaskets
Seals
Noise/Vibration Damper
Moisture/Vapor Barrier
Flexible Fuel Tanks
Dry Chemical Packaging

Available: MP-1880, MP-1885, MP-1890, Natural or Black colors on special order. Thickness from .010" to .090" in 18" wide rolls. Tolerances: .010" to .025" \pm 2 mil.; .026" to .090" \pm 3 mil. MP-2080 natural and black, colors on special order. Thickness from .005" to .125" in 36" wide rolls. Tolerances: .005" to .040" \pm 2 mil. .041" to .062" \pm 3 mil.; .063" to .090" \pm 4 mil.; .091" to .125" \pm 6 mil.

Length — Continuous rolls/bulk pack

Hi-TUFF polyurethane extruded sheeting and film

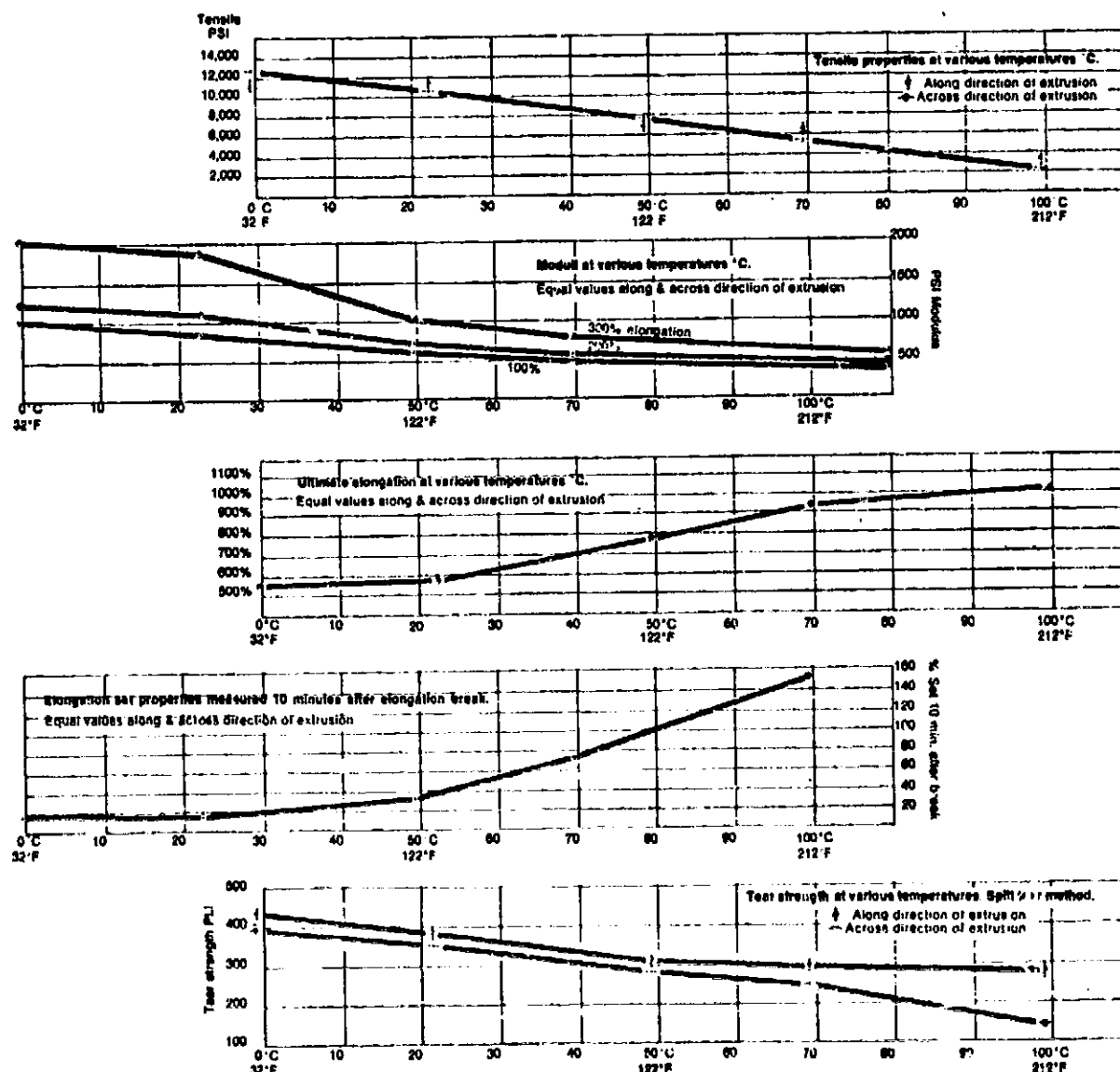


FIGURE 7 MANUFACTURERS DATA FOR POLYURETHANE

This should correspond to the measured tube wall thickness prior to failure. Since the tube failed at a diameter of approximately 0.30 inch, the effective ultimate strength is approximately 260 psi.

2.3 Thermal Modeling and Performance/Optimization Analyses

A two dimensional flow computer model was constructed to determine the effects of cross conduction between the hot fluid entering the radiator and the cooler fluid leaving the radiator through adjacent transport tubing. Figure 8 shows the flow path routing in the baseline design. Figures 9, 10, and 11 identify the nodes and conductors of the thermal model. The incoming and outgoing tubes of the computer model may be thermally isolated by equating the center conductor to zero. Figure 12 shows typical temperature profiles for configurations with and without cross conduction. The results show that with regeneration the average temperature in the mid sections of the radiator is lower than when the cross conduction is eliminated. Because of the lower average temperatures, heat rejection is reduced by approximately 8%. To reduce the effects of regeneration, it is recommended that the radiator be designed so that the incoming and outgoing tubes are separated. This requires a manifold at the free end of the radiator so that the outgoing tubes may be located on one half of the radiator, and the return tubes located on the opposing half.

Analyses were made to determine optimum tube spacing and diameters. The projected radiator surface area is given by

$$A = \frac{Q}{\eta \bar{\epsilon} \sigma (T_{IN} - T_{OUT})} \int_{T_{OUT}}^{T_{IN}} \frac{(1 + 4\eta S \bar{\epsilon} \sigma R T^3) dT}{\left[1 + \frac{6(\eta S \bar{\epsilon} \sigma R T^3)^2 (1 - T_{\infty}/T)^4}{(1 + 4\eta S \bar{\epsilon} \sigma R T^3)^2} \right] [T^4 - T_{\infty}^4]} \quad (11)$$

where η = radiator fin efficiency

S = tube spacing

$\bar{\epsilon}$ = effective surface emissivity ($\bar{\epsilon} = 2$ for two sided radiators)

R = thermal resistance from the fluid to the base of the radiator fin

T_{IN} = fluid inlet temperatures

T_{OUT} = fluid outlet temperature

ANALYSIS OF REGENERATION IN FLEXIBLE RADIATORS

TYPICAL FLOW PATHS

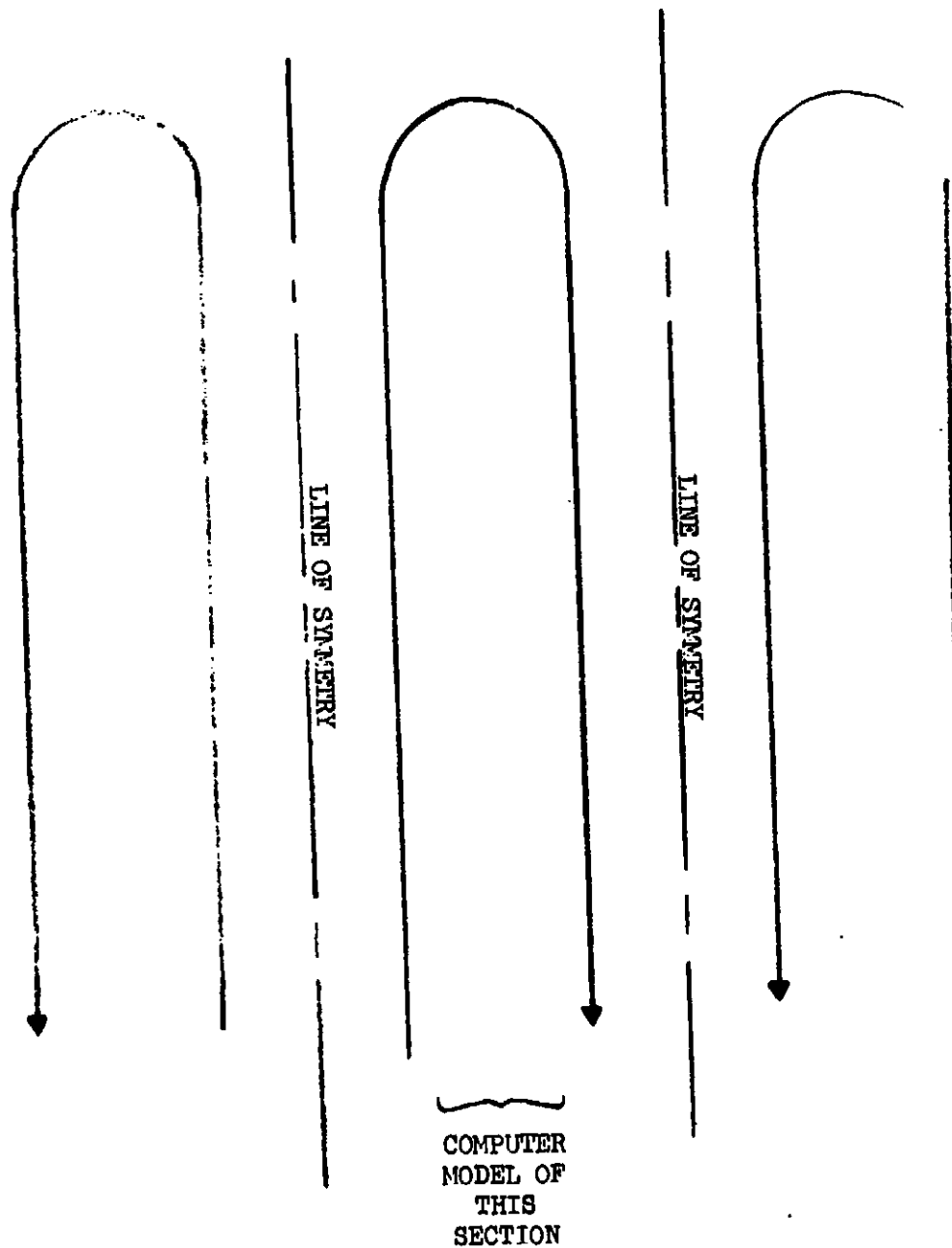


FIGURE 8

PARALLEL FLOW PATHS ARE ARRANGED TO MINIMIZE REGENERATION. COMPUTER MODEL SHOWS EFFECT OF REGENERATION ON RADIATOR PERFORMANCE.

MODEL DEFINITION, INFLATABLE RADIATOR REGENERATION EFFECTS

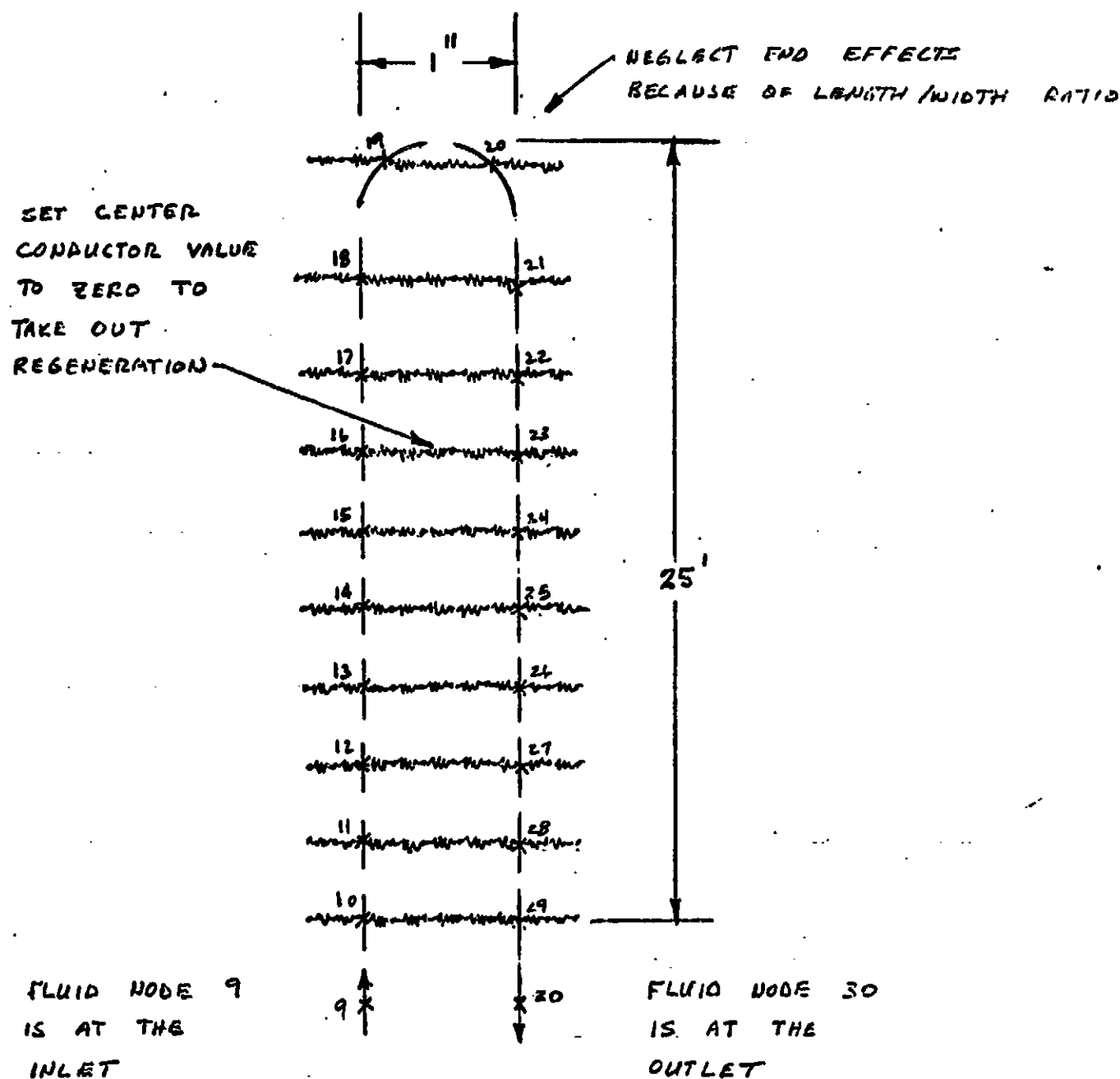
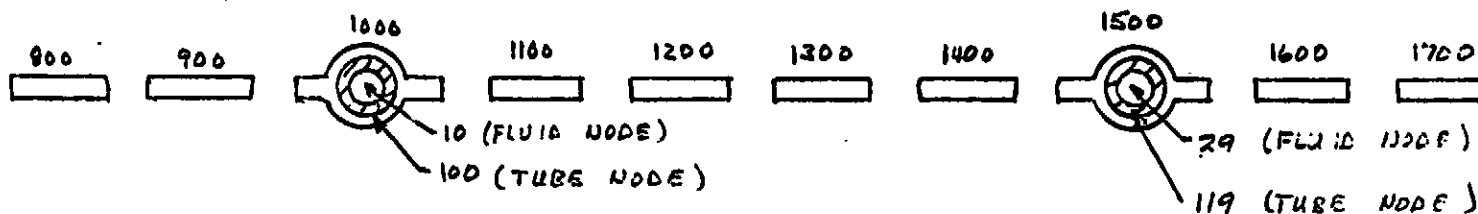


FIGURE 9

NODE IDENTIFICATION, TYPICAL CROSS SECTION



CONDUCTOR IDENTIFICATION, TYPICAL CROSS SECTION

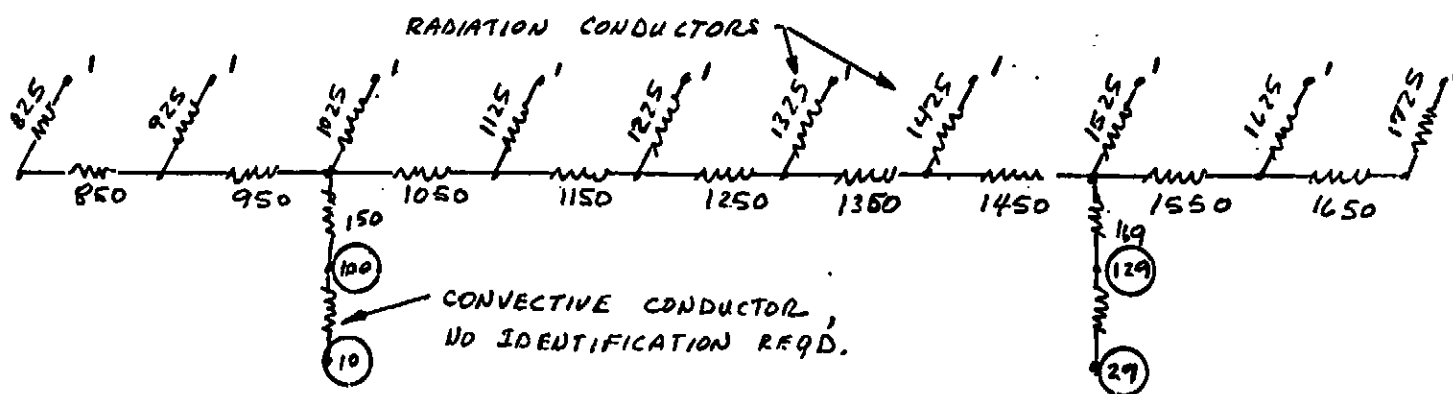
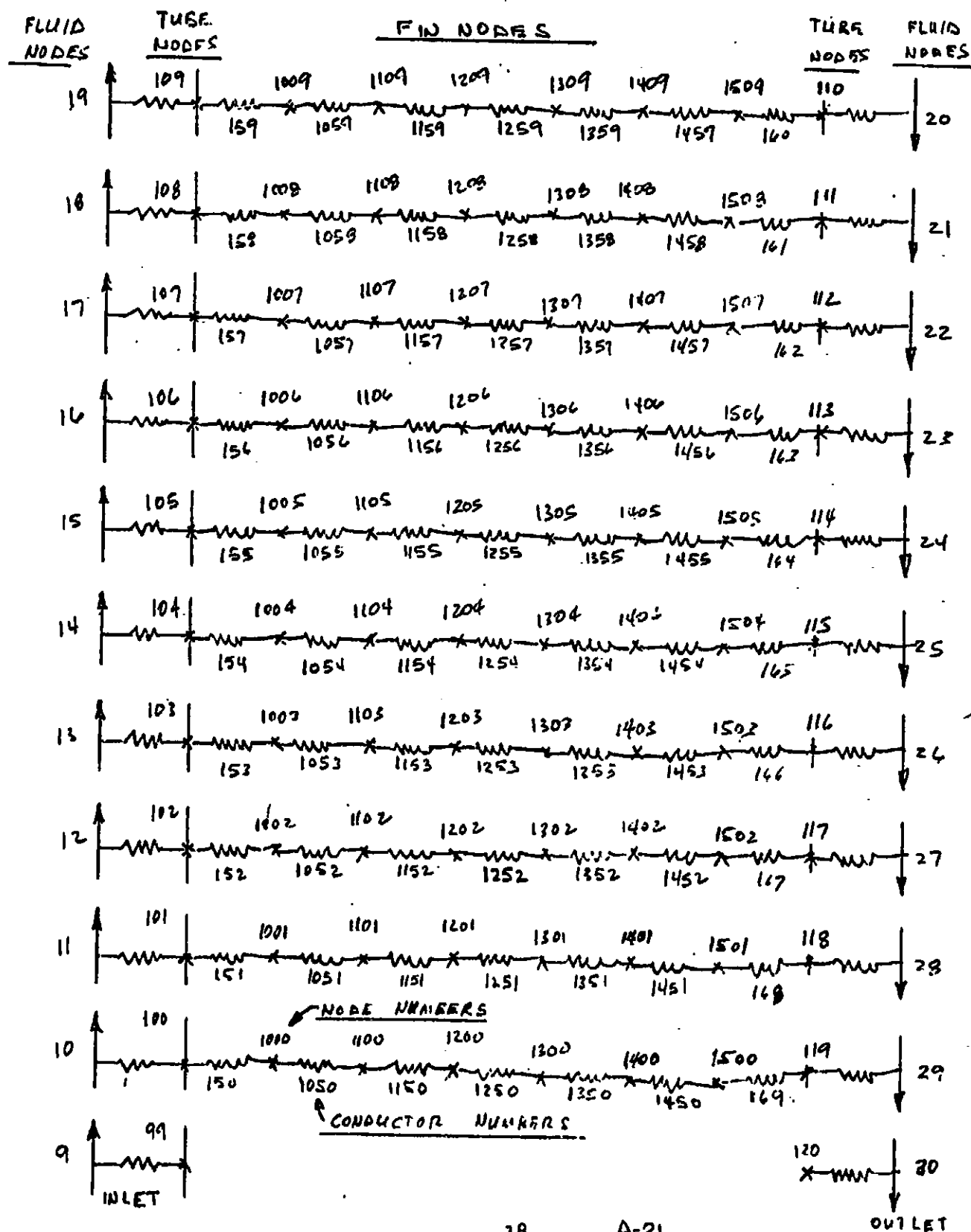


FIGURE 10

FIGURE 11
NODE AND CONDUCTOR IDENTIFICATION FOR FLEXIBLE
RADIATOR SINDA MODEL (INTERIOR NODES ONLY)



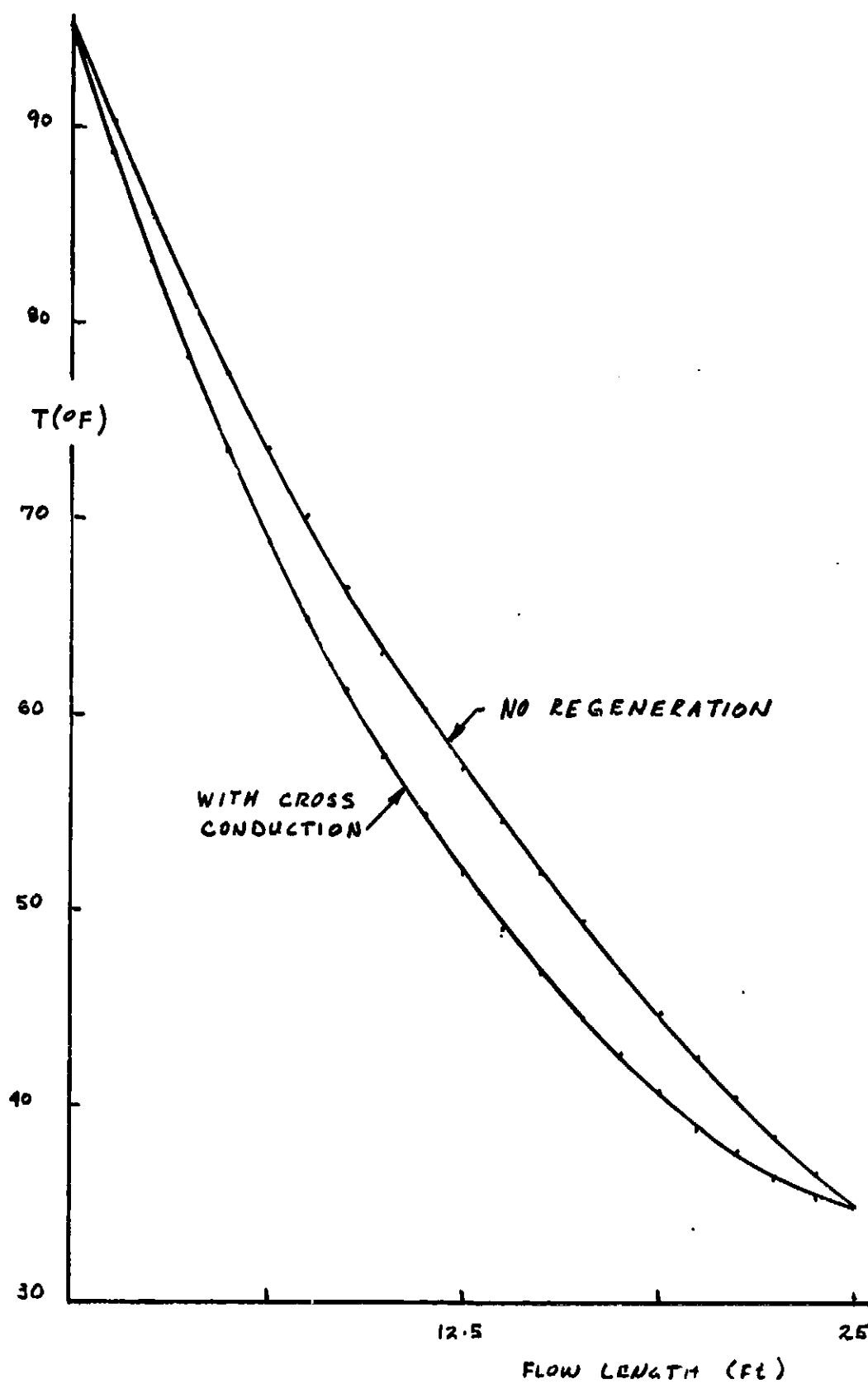


FIGURE 12 EFFECT OF REGENERATION ON FLUID TEMPERATURE

The surface area computed from Eq. 11 is given as a function of the parameter $n\bar{S}\bar{E}OR$ in Figure 13. The thermal resistance at the tube wall for the baseline design was computed from the two dimensional math model shown in Figure 14. For laminar flow the resistance computed from steady state analyses is

$$R = 5.40 \text{ } ^\circ\text{F} \cdot \text{HR} \cdot \text{Ft} / \text{BTU} \quad (12)$$

For the alternate construction with silver wire mesh on both sides of the tubing, the thermal resistance is

$$R = 2.29 \text{ } ^\circ\text{F} \cdot \text{HR} \cdot \text{Ft} / \text{BTU} \quad (13)$$

The radiator fin efficiency is given as a function of tube spacing in Table I.

TABLE I RADIATOR FIN EFFICIENCY FOR FLEXIBLE RADIATOR

Radiator Construction	S (inch)	η
One Layer Screen Wire, $K = 0.0057$, $\bar{E} = 1.42$	0.5	0.947
	1.0	0.867
	1.5	0.767
Two Layers Screen Wire, $K = 0.0112$, $\bar{E} = 1.50$	0.5	0.962
	1.0	0.917
	1.5	0.853

The weight of the radiator to be minimized in this analysis includes manifolds, the deployment drum, retraction springs, transport tubing, radiator fin material, transport fluid, tube fittings, and weight penalty for pumping power.

$$\text{wt} = \text{wt (manifolds)} + \text{wt (Drum)} + \text{wt (springs)} + \text{wt (tubes)} + \text{wt (fins)} + \text{wt (fluid)} \\ + \text{wt (fittings)} + \text{wt } (\Delta P) \quad (14)$$

For the baseline design with one layer of wire mesh

$$\text{wt} = 0.0354 W + 0.01948 DW + 12.15 tL + 4.7 \frac{A}{S} (d_o^2 - d_i^2) \\ + [0.107 + 0.049 \frac{d_o}{S}] A + 3.64 \frac{A}{S} d_i^2 + 0.032 \frac{W}{S} \\ + 5.34 \cdot 10^{-4} \left(\frac{SL}{W d_i^4} \right) \quad (15)$$

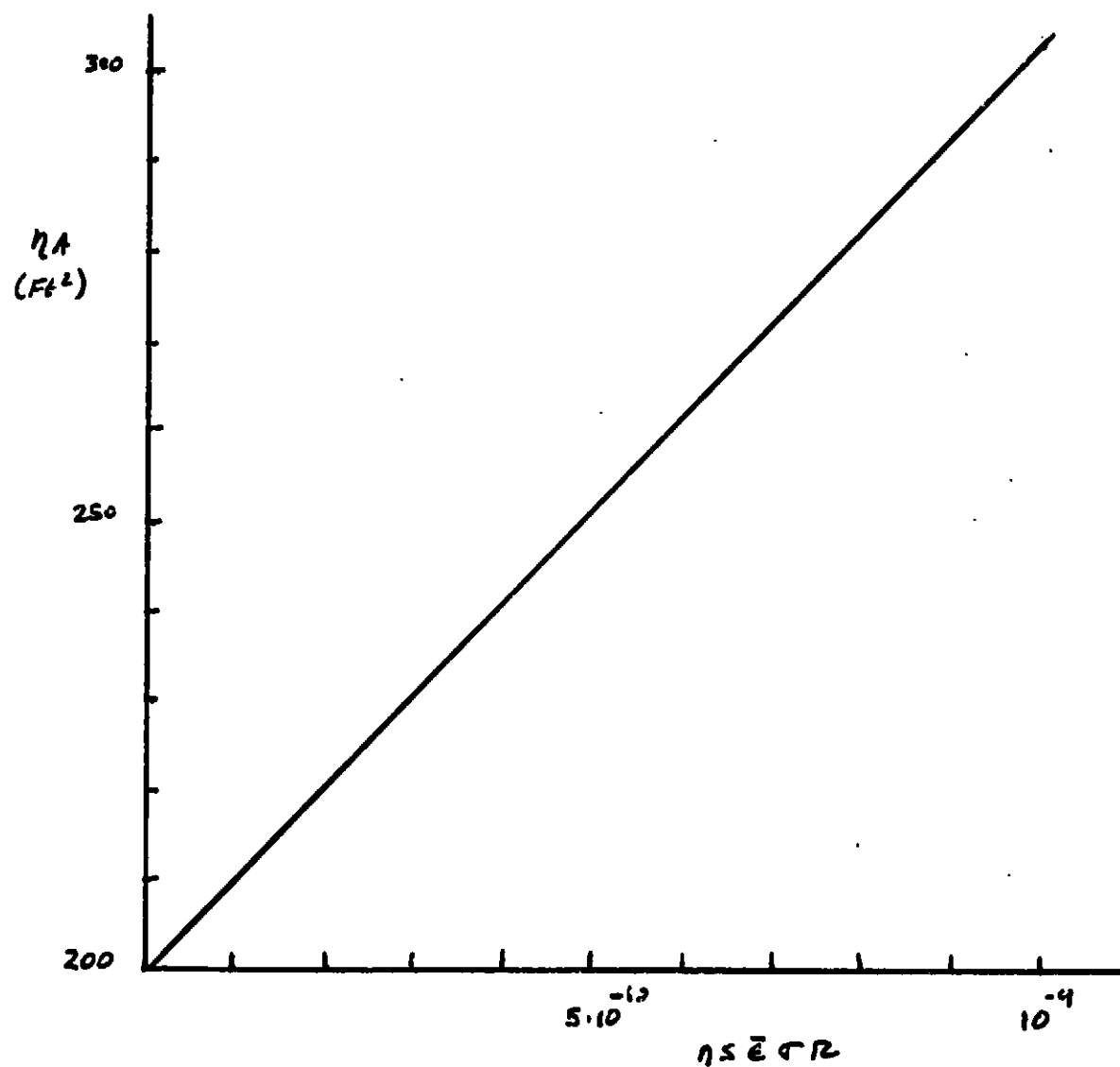


FIGURE 13 SURFACE AREA REQUIREMENTS FOR 4 KW
HEAT REJECTION , $T_{IN} = 95^{\circ}\text{F}$, $T_{OUT} = 35^{\circ}\text{F}$

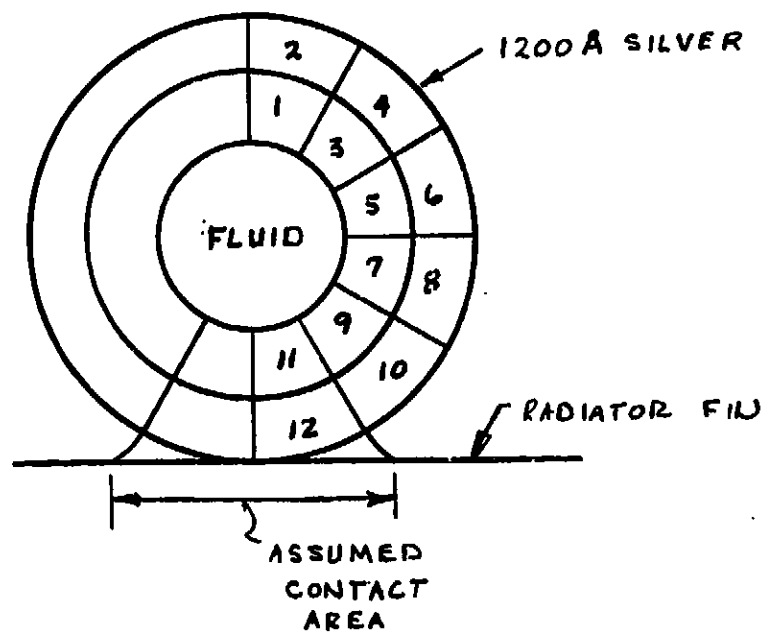


FIGURE 14 MATH MODEL FOR COMPUTING THERMAL
RESISTANCE AT THE TUBE WALL

where

- W = the width of the radiator (inch)
- D = diameter of deployment drum (inch)
- t = thickness of retraction spring (inch)
- L = length of radiator panel (ft.)
- A = area of radiator panel (ft.²)
- S = tube spacing (inch)
- d_o = outside tube diameter (inch)
- d_i = inside tube diameter (inch)
- W_t = weight of one radiator panel (lbs)

For the alternate design with two layers of wire mesh the term representing the weight of the radiator fins is replaced by

$$W_t(FIN) = [0.1397 + 0.080 \frac{d_o}{S}] A \quad (16)$$

For freon 21 transport fluid, the flow is turbulent and the pressure drop weight penalty is computed from

$$W_t(\Delta P) = 7.65 \cdot 10^{-4} \left(\frac{S}{W d_i} \right)^{1.8} \frac{L}{d_i^3} \quad (17)$$

The thermal resistance at the tube wall is given approximately by

$$R = 1.25 \text{ } ^\circ\text{F} - \text{HR} - \text{Ft} / \text{BTU} \quad (18)$$

Table II compares the dimensions and weights of candidate radiator constructions for various tube spacings for a system heat rejection of 4 kw. The tube diameters were selected to provide micrometeoroid protection and to be compatible with standard tube fittings. Table III shows the effect of varying the tube diameters on radiator weight. The results show that near minimum weights are possible with standard tube diameters. The analyses assume that the wall thickness required for meteoroid protection is independent of the tube spacing. This is not exactly true because the exposed area increases as the tube spacing decreases. Thus, the exposed area for a tube spacing of 0.5 inch is approximately twice the area for 1 inch spacing. The wall thickness required for constant probability of no penetration is

TABLE II COMPARISON OF RADIATOR DIMENSIONS AND WEIGHT
FOR ALTERNATE PANEL CONSTRUCTIONS

TYPE OF CONSTRUCTION	TUBE SPACE (INCH)	η	M (IN-LB)	W (INCH)	NO. TUBES	A ₂ (FT ²)	L (FT)	WT (LB)
1 LAYER WIRE MESH, POLYURETHANE TUBING (ID = .090", OD = 0.1875")	.50	0.947	40.3	42	84	88.7	25.3	61.3
	.75	0.907	26.9	42	56	101.4	28.9	57.9
	1.00	0.867	20.2	42	42	114.2	32.6	58.7
	1.50	0.767	13.4	42	28	143.4	41.0	67.0
2 LAYERS WIRE MESH, POLYURETHANE TUBING (ID = .090", OD = 0.1875")	.50	0.960	28.0	34.6	68	73.3	25.4	57.3
	0.75	0.930	19.8	36.8	48	79.4	25.9	51.6
	1.00	0.917	15.7	37.9	38	84.0	26.6	50.0
	1.50	0.853	10.7	39.2	26	96.9	29.7	53.0
2 LAYERS WIRE MESH, TEFLON TUBING (ID = 0.062", OD = 0.125")	0.50	0.960	20.7	36.7	72	69.0	22.5	42.7
	0.75	0.930	14.9	38.8	52	74.0	23.1	44.5
	1.00	0.917	11.5	39.2	40	77.1	23.6	49.0
	1.50	0.853	7.5	40.1	26	86.6	25.9	66.9

TABLE III EFFECT OF TUBE DIAVETER ON WEIGHT
FOR ALTERNATE PANEL CONSTRUCTION

<u>TYPE OF CONSTRUCTION</u>	<u>TUBE ID (INCH)</u>	<u>TUBE OD (INCH)</u>	<u>SPACING (INCH)</u>	<u>WT. (LB)</u>
1 LAYER WIRE MESH, POLYURETHANE	.090	.1875	0.50	61.3
	.090	.1875	0.75	57.9
	.090	.1875	1.00	58.7
	.090	.1875	1.50	67.0
	.080	.1775	0.50	60.0
	.080	.1775	0.75	58.4
	.080	.1775	1.00	60.9
	.100	.1975	0.50	63.4
	.100	.1975	0.75	58.8
	.100	.1975	1.00	58.6
2 LAYERS WIRE MESH, POLYURETHANE	.090	.1875	0.50	57.3
	.090	.1875	0.75	51.6
	.090	.1875	1.00	50.0
	.080	.1775	0.50	55.8
	.080	.1775	0.75	52.3
	.080	.1775	1.00	51.9
	.100	.1975	0.50	57.9
	.100	.1975	0.75	53.8
	.100	.1975	1.00	49.5
2 LAYERS WIRE MESH, TEFLON	.0625	.125	0.50	42.7
	.0625	.125	0.75	44.5
	.0625	.125	1.00	49.0
	.0525	.115	0.50	46.8
	.0525	.115	0.75	54.8
	.0525	.115	1.00	66.9
	.0725	.135	0.50	42.0
	.0725	.135	0.75	41.1
	.0725	.135	1.00	42.5

related to area through the following equation.

$$t = C A^{0.290} \quad (19)$$

Thus, if the area doubles, the required wall thickness increases by 22.3% or approximately 0.010 inch. This reduces some of the weight advantage indicated for close tube spacing in Table II. Radiator stiffness, producability and cost also favor wider tube spacing. However, the required surface area increases rapidly with tube spacing. Because of this, 0.625" spacing is recommended for construction with one layer of wire mesh, and 0.750 spacing is recommended for two layers of wire mesh.

2.4 Assessment of Two Layers Wire Mesh Construction

The computations in Section 2.3 show that the radiator weight and size are reduced when the fin material is constructed with two layers of wire mesh. However, stiffness and fabricability must also be considered when evaluating the merits of the alternate radiator constructions.

Stiffness is important because of its impact on the deployment/retraction system. The bending moment required to roll the radiator panel around the deployment drum depends on the cumulative EI product of the transport tubing, the fin material, and the inflation tubing. The major part of the bending moment is associated with the transport tubing. The equation for the moment required to bend a tube about a constant radius of curvature is

$$M = \frac{EI}{R} \quad (20)$$

Where R is the radius of curvature, as in the case of the flexible radiator, the radius of the deployment drum. Stiffness tests were conducted with 1 sq. ft. elements of radiator panel at ambient conditions and in cold environment to verify that Eq. 20 provides a reliable method for computing the stiffness of the proposed prototype radiator. It was determined that the EI product in Eq. (20) could be computed by summing the terms for the transport tubing and the thin shell of radiator fin material which encompasses the transport tubing ;

$$EI = \frac{\pi E(TUBE)}{64} (d_o^4 - d_i^4) + \frac{\pi E(FIN)}{64} [(d_o + 2t)^4 - d_o^4] \quad (21)$$

This assumes that the tubing bends about its own neutral axis, and that the fin material forms a separate tube which surrounds the transport tubing. One of the elements tested contained 12 polyurethane tubes with thick silver backed teflon fin material. The bending moment computed for the tubing and the fin materials are 0.047 in-lb and 0.473 in-lb respectively for a total of 0.52 in-lb. This compares to the experimentally determined value of 0.46 in-lb at ambient conditions. The second element was constructed from teflon tubing and thick silver backed teflon film. The predicted values for the tubing and fin are 1.025 in-lb and 0.261 in-lb for a total of 1.286 in-lb. The experimental value is 1.8 in-lb. The elements were also tested at 0°F. For the cold environment the experimental bending moment for the element with polyurethane tubing increased to 0.57 in-lb, whereas the moment for the teflon tube element remained approximately the same as for ambient conditions.

The element tests showed that equation 20 provides an approximate method for computing the required bending moment but that a factor of safety should be included to allow for unknowns in the analysis.

Equation (20) was applied to estimate the spring sizes required for the prototype radiator. The results for the alternate radiator construction are compared in Table IV. For the construction with one layer of wire mesh, the neutral axis was assumed to coincide with the silver wire mesh. This causes the computed stiffness with one layer of wire mesh to be almost as great as that for two layers. Actually the neutral axis will be positioned between the layer of wire mesh and the center of the tubes so that the panel should not be as stiff as calculated. With two layers of wire mesh the radiator is stiffer with polyurethane tubing than with teflon tubing. The reason is that the smaller diameter of the teflon tubes reduces the moment of inertia of the screen wire fin material enough to offset the added stiffness of the teflon tubes. It is recommended that a factor of safety of at least 2.0 be applied to the results of Table 4 when sizing the springs for the retraction mechanism. This will insure that the radiator will wrap tightly about the deployment drum upon retraction.

TABLE IV COMPARISON OF STIFFNESS IN ALTERNATE RADIATOR CONSTRUCTIONS

<u>TYPE OF CONSTRUCTION</u>	<u>K' (TUBING)</u> <u>INCH - LB</u>	<u>K' (FIN)</u> <u>INCH - LB</u>	<u>K' (TOTAL)</u> <u>INCH - LB</u>
1 LAYER SCREEN WIRE MESH, POLYURETHANE TUBING (ID = .090, OD = .1875, 40 TUBES)	2.44	16.71	19.2
2 LAYERS SCREEN WIRE MESH, POLYURETHANE TUBING (ID = .090, OD = .1875, 50 TUBES)	0.70	19.9	20.6
2 LAYERS SCREEN WIRE MESH, TEFLON TUBING (ID = .0625, OD = .125, 52 TUBES)	8.74	6.14	14.9

Thus, with regard to stiffness, the construction with two layers of wire mesh are comparable or superior to the construction with one layer.

A small element was fabricated with two layers of screen wire and teflon tubing to determine whether the problems will occur in laminating the radiator.

Sheldahl Advanced Products Division stated that they will not be able to fabricate the radiator with two layers of screen wire without extensive revisions of their roll laminating machines. Therefore, it will be necessary to develop alternate procedures for fabricating the panel. To construct the element, an aluminum die was made with machined grooves for accommodating the transport tubing. Vacuum holes were drilled periodically at the bottom of the grooves to hold the fin material in place while the tubing is being positioned. The tubes are bonded to one-half of the radiator which is held in position by means of the vacuum holes. Subsequently, the opposing half of the radiator is held in the die and the mating half with attached tubing is placed in position. The two halves of the radiator are then removed from the die and placed in vacuum bags for curing at elevated temperature. The element constructed in this manner appears to be of excellent quality. Application of the aluminum die should make it possible to produce a prototype radiator which is straight and uniform in cross section.

Therefore, since the construction having two layers of wire mesh have performance and weight advantages, are comparable in stiffness to those having one layer, and appear to be manufacturable with proper tooling, it is recommended that the prototype radiator be made with the double layer of screen wire.

2.5 Inflation Tubing Requirements

Numerous ambient tests were conducted with inflation tubing and retraction springs to determine the best method of attaching the tubing to the springs, and to obtain deflection data for sizing the inflation tubing for the prototype radiator. The tests showed that the springs must be attached to the

tubing as shown in Fig. 15. For this method of attachment, the spring tends to stretch the inflation tubing while the inflation tubing tries to compress the spring. This type of loading causes the system to deploy and retract with a linear motion, whereas for other methods of attachment the tip of the radiator extends in a curved trajectory with the spring and inflation tubing forming a spiral as shown in Fig. 16. With the correct method of attachment, the spring and inflation tubing remain reasonably straight until they contact the deployment drum. Then they roll around the drum with a radius of curvature slightly larger than that of the drum. Apparently there is a buckling phenomenon which occurs as the tubing contacts the drum. At sections removed from the drum the tubing remains inflated and is stiff enough to straighten the spring. As the tubing contacts the drum it buckles and the spring is able to wrap it around the drum.

A slight curvature exists over the entire length of the inflation tubing. The tubing acts as a beam with a prescribed stiffness which is subjected to a constant bending moment induced by the spring. It, therefore, seeks an equilibrium position which is described by a constant radius of curvature. The radius of curvature and bending moment are related by

$$R = \frac{EI}{M} \quad (22)$$

Sections of inflation tubing were pressurized and loaded to establish the effective EI experimentally. E was then measured separately in a tensile test machine so that I could be determined and compared with theoretical predictions. The tubing tested in this manner has a non uniform cross section as shown in Fig. 17. Because of the overlapped joint the moment of inertia is much larger about the x-x axis than about the y-y axis. The effective moment about each axis was determined experimentally by loading the tubing as a cantilevered beam as shown in Fig. 18. The deflection at the end of the beam is given by

$$\Delta = \frac{F l^3}{3EI} \quad (23)$$

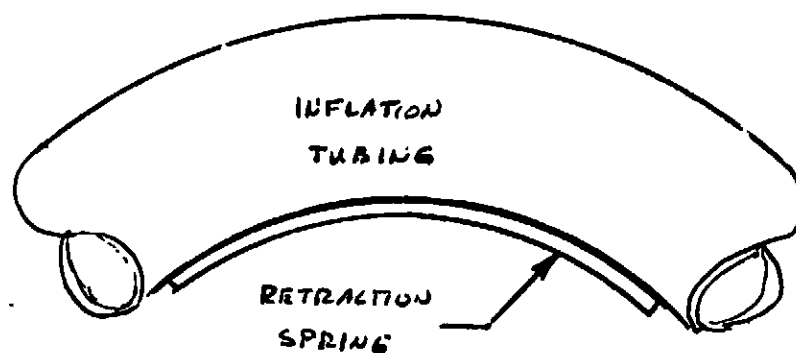


FIGURE 15 ATTACHMENT OF RETRACTION SPRING
TO INFLATION TUBING

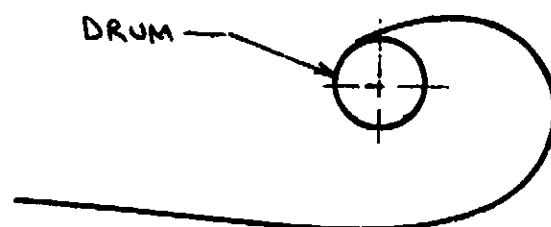


FIGURE 16 SHAPE OF INFLATION TUBING WITH
INCORRECT SPRING ATTACHMENT

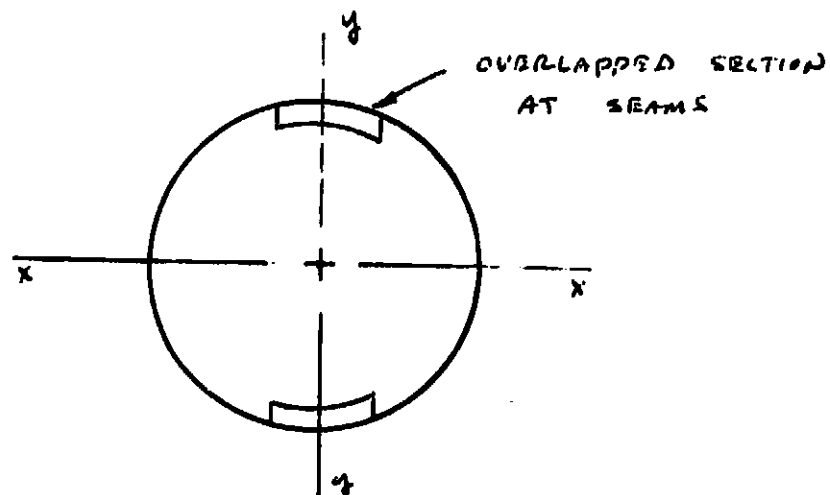


FIGURE 17 TYPICAL CROSS SECTION OF INFLATION TUBING

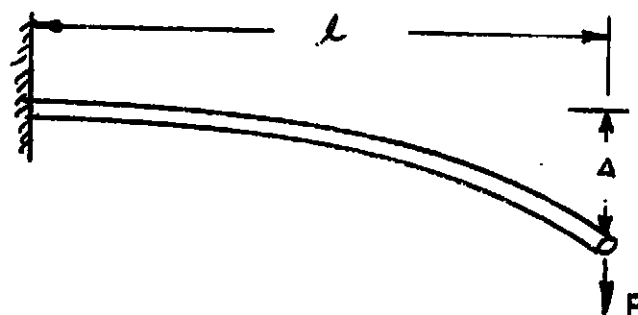


FIGURE 18 STIFFNESS TEST OF INFLATION TUBING

Thus, EI could be determined by measuring the deflection as a function of loading

$$EI = \frac{F l^3}{3 \Delta} \quad (24)$$

Table V compares the EI values computed from Eq. 24 using experimental values of F and D with the EI values computed from geometric measurements of the tube wall thickness and diameter. The results show that the experimental measurements do not correlate with the values predicted for a hollow tube. The measured moment of inertia is relatively insensitive to the loading axis, and can be computed approximately by treating the tube as having a uniform wall thickness equal to the average wall thickness

TABLE V EFFECTIVE EI FOR INFLATION TUBING

Pressure (psi)	Load Axis	EI - Experimental (lb-in ²)	EI - Predicted (lb-in ²)
5	y-y	5670	10,275
10	y-y	7290	
15	y-y	7290	
5	x-x	6745	5,130
10	x-x	8993	
15	x-x	9810	

of the inflation tubing. The average EI computed by this method is 7296. This compares reasonably well with the experimental values in Table V.

Figure 19 shows the position of the tip of the inflation tubing as a function of the radius of curvature in Eq. 22. As a design goal it is recommended that a radius of at least 250 ft. be selected. The EI required from Eq. 22 is

$$EI = (250) (12) M$$

Assuming a factor of safety of 2.0 in Table 4 the bending moment required in each inflation tube is approximately 20 in-lb. The modulus of the inflation tube material is approximately 80,000 psi. Thus

$$I = \frac{(250) (12) (20)}{80,000} = 0.75 \text{ in}^4$$

For 4" diameter inflation tubing the wall thickness required is 0.030 inch. No factor of safety is required in this case because unknowns in the analyses will only change the radius of curvature of the tubing. Figure 19 shows that the end coordinates of the tubing are not sensitive to small variations in R for the design goal of 250.

An equation for buckling of the inflation tubing was derived by assuming that the energy for bending is absorbed in deforming the material and in compressing the gas in the inflation tubing.

$$M = \frac{\pi}{R} E t r^2 \left(r - \frac{7}{3} \Delta \right) + 2.696 P R \Delta \left(r + \frac{4}{3} \Delta \right) \quad (25)$$

where r = the radius of the inflation tubing

t = thickness of inflation tubing

Δ = deflection of the wall of the inflation tubing with bending

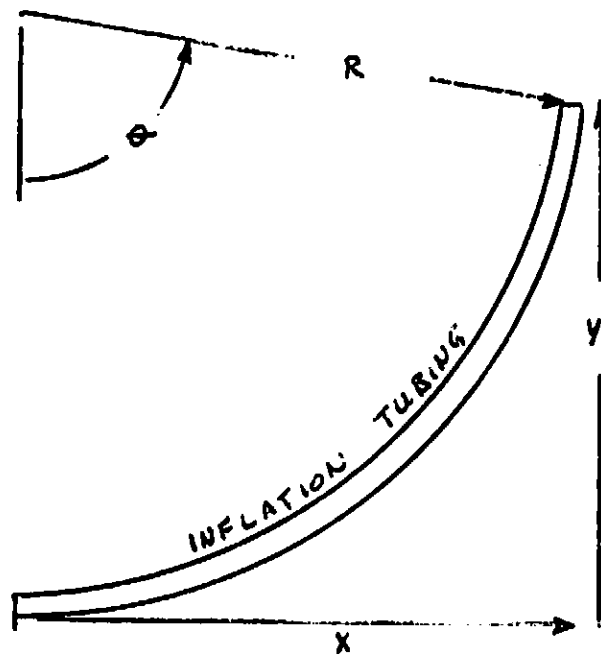
E = modulus of inflation tubing

R = radius of curvature

P = internal pressure

Castigliano's theorem was applied to compute Δ in Eq. (25). The result is

$$\Delta = \frac{22.44 r^5}{D^2 t^2 \left[1 + 1.229 \frac{r^4}{D^2 t^2} + 5.609 \frac{P r^3}{E t^2} \right]} \quad (26)$$



$$L = R\theta \quad x = R \sin \theta \quad y = R(1 - \cos \theta)$$

<u>R</u>	<u>x (L=30')</u>	<u>y (L=30')</u>
5	-1.4	9.95
50	28.3	8.70
100	24.5	4.46
250	29.9	1.80
500	30.0	0.90

FIGURE 19 Displacement of inflation Tubing

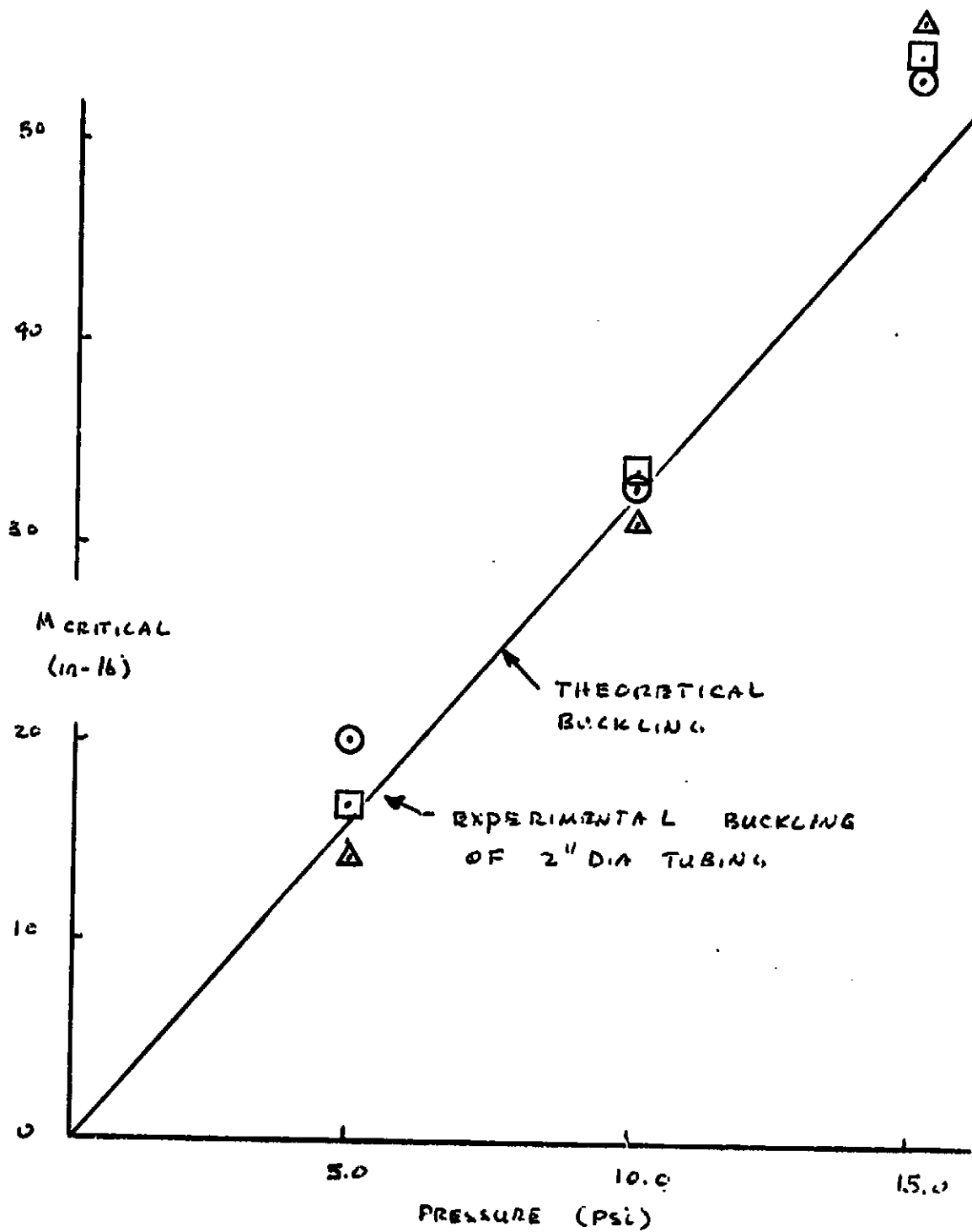


FIGURE 20 BUCKLING OF INFLATION TUBING

To determine the limits for buckling it is assumed that the walls of the inflation tubing will not withstand a compressive load. Thus when the compressive stress in the wall associated with bending exceeds the tensile stress caused by the internal pressure of the gas the tube will buckle. The compressive stress in the wall caused by bending is

$$\sigma = [M - 2.696 PR \Delta r] \frac{c}{I} \quad (27)$$

The tensile stress caused by the internal pressure is

$$\sigma = \frac{Pd}{4t} \quad (28)$$

Equating the stress in Eqs. (27) and (28) with Δ computed from Eq. (26) defines the limits for buckling. The critical bending moment for the existing 2" diameter inflation was determined experimentally to test the accuracy of the theoretical method. The experimental and theoretical results are compared in Figure 20.

The minimum pressure required to prevent buckling of the inflation tubing was computed for a bending moment of 20 in-lb and a diameter of 4 inches. The analysis shows that the pressure required is only 0.86 psi.

2.6 Extendible Boom Analysis

With a general lack of material and section property data, certain assumptions, tests, and analysis methods were used to determine the allowable compressive load carrying capability of the boom. Based on some section property, and ultimate bending moment data obtained from Fairchild through a telecon, some basic assumptions were made as to the material properties and the other section properties.

Preliminary analysis based on a simple support beam column indicated that the critical buckling load was approximately 2 lbs. on earth and 32 lbs. in a zero-g environment. Test results of a simple experiment conducted at Vought indicated that either the stiffness data provided by Fairchild, material property assumptions, and/or end-fixity assumptions were in error. By continuing to assume the validity of the Fairchild data, material and section property data was altered and the coefficient of end fixity established. The

coefficient of end fixity agreed very closely with that of a beam column fixed at both ends.

By applying the appropriate buckling equations, it was determined that the critical buckling load on earth was approximately 127 lbs. and 417 lbs. in a zero-g environment.

The analysis to date is incomplete and further tests, review and analysis are required to either support or refine this the simplified analysis and its associated assumptions.

3.0 PROGRESS ON MAJOR END ITEMS

The design requirements phase is essentially complete. Additional analyses and tests are required to establish the operating temperature limits of the transport tubing and fittings. Additional ambient tests are planned for the prototype inflation tubing and retraction springs. The space deployable boom will be loaded axially to insure that it will not buckle in a 1-g test environment. Experimental data is needed concerning micrometeoroid penetration of polyurethane and Teflon. The thermal analyses showed significant weight and performance advantages for two layers of screen wire mesh. An element was fabricated with the double layer construction to establish fabrication techniques.

The program is on schedule, and no major technical problems have occurred.

4.0 WORK SCHEDULED DURING THE NEXT REPORTING PERIOD

Work during the next monthly reporting period will be directed towards finalizing the design requirements studies and initiating the detailed design drawings for fabricating the system. Vendors will be contracted to begin fabrication of the fin material. Retraction springs, inflation tubing, transport tubing, and additional materials will be purchased for fabricating the prototype system.

5.0 REFERENCES

- 1) Statement of Work for Development of A Prototype Flexible Deployable/Retractable Radiator System, NASA/JSC Contract NAS9-14476, June 1976
- 2) Rittenhouse, J. B., "Meteoroids", Space Materials Handbook - Third Edition, July 1968.
- 3) Leont'ev, L. V., "Some Results of Research on High Velocity Impacts", NASA TT F-13,740, August 1971
- 4) Di Battista, "Correlation of Data In Multilayer Lamination Plates", November 1972
- 5) "Solid Polyurethane Technical Specifications", J. P. Stephens, Co., Inc., East Hampton, Mass. February 1974.

APPENDIX A REFERENCES ON MICROMETEORIDS

1. "Investigation of Stress Waves and Effects of Hypervelocity Impact", Final Report, Principal Investigator Ray Kinslow; NASA Grant #NGR-43-003-007, Supplement 2; Final Report, #N71-37953; July 1, 1969-November 30, 1970.
2. "NASA Space Vehicle Design Criteria (Environment)", Meteoroid Environmental Model, (Near Earth to Lunar Surface); Prepared by B. G. Courpalais - NASA; March 1969.
3. Symposium on Reuseable Surface Insulation for Space Shuttle exert 1.1, "Simulatic Meteoroid Penetration of Reuseable Surface Insulation"; by J. K. Lehman and H. E. Christensen, McDonnell Douglas Astronautics Co.; Pg 731; September 1972.
4. NASA Space Vehicle Design Criteria - (Structures)", Meteoroid Damage Assessment; Author, V. C. Frost, Aerospace Corp.; May 1970.
5. "Multimaterial Lamination as a Means of Retarding Penetration and Spallation Failures in Plates", #NASA TN D-6989; Prepared by John D. DiBattista and Donald H. Humes, Langley Research Center; November 1972.
6. "Development of Materials and Materials Application Concepts for Joint Use as Cryogenic Insulation and Micrometeorite Bumpers", Annual Summary Report; Goodyear Aerospace Corp. #GER 11676 S/24; Reproduction; Section VII pg 117; June 30, 1976.
7. "Phenomena After Meteoroid Penetration of a Bumper Plate", Final Report; by F. C. Todd; #N73-17894; November 1, 1971-January 1, 1972.
8. "A Guide to Using Meteoroid - Environment Models for Experiment and Spacecraft Design Applications"; by Donald J. Kessler, NASA; #NASA TN D-6596; March 1972.
9. "Hypervelocity Impacts into Stainless-Steel Tubes Armored with Reinforced Beryllium"; by A. R. McMillan, General Motors Corporation; #NASA-TN-D-3512; August 1966.
10. "Final Report Meteoroid - Bumper Interactions Program"; by P. S. Gough; #NASA CR-72800 SRI-R-59; November 1970.
11. "Dustwall Meteoroid Shielding"; by Carl N. Klahr and Sylven Cutter; Technical Report AFFDL-TR-65-67; September 1965.
12. "Simplified Ballistic - Limit Expressions for Thin Sheets"; by Deene J. Weidman; #NASA TN D-5556; November 1969.
13. "Thermal Design of Explorer XII Micro Meteoroid Satellite"; by Earl C. Hastings, Jr., Richard E. Turner, and Katherine C. Speegle; #NASA TN D-1001; May 1962.

14. NASA Technical Memorandum "Hypervelocity Impact Testing of L-Band Truss Cable Meteoroid Shielding on Skylab"; by David W. Jex; #NASA TMX-64743; February 23, 1973.
15. "Meteoroid Damage Assessment", Distributed by National Technical Information Service #N71-25070; May 1970.
16. "Some Results of Research of High Velocity Impacts"; by L. V. Leont'ev, A. V. Tarasov, I. A. Tereshkin; NASA Technical Translation; #NASA TT-13,740; 1971.
17. "Development of Meteoroid Simulators for Hypervelocity Impact Studies"; by R. L. Woodall and E. R. Berus; #N71-12664; October 1970.
18. "A Guide to Using Meteoroid - Environment Models for Experiment and Spacecraft Design Applications"; by Donald J. Kessler; NASA TN D-6596; March 1972.
19. "Hypervelocity Research Program", Final Report; by H. W. Gemon; General Electric Co.; R63SD19; February 1963.
20. "Investigation of High-Speed Phenomena", Final Report; by D. G. Becker and J. C. Slattery; December 1972.
21. "Meteor Research Program"; by A. F. Cook, M. R. Flannery, H. Levy II, R. E. McCrosby, Z. Sekanina, C. Y. Shao, R. B. Southworth, and J. T. Williams; NASA CR-2109; September 1972.
22. "Bumper-Protected Laminated Spacecraft Mainwalls"; by Ray Kinslow; NASA CR-2262; May 1971.
23. "A Discussion of the Modes of Failure of Bumper-Hull Structures with Application to the Meteoroid Hazard"; by C. Robert Nysmith; #NASA TN D-6039; October 1970.
24. "Meteoroids"; J. B. Rittenhouse, Space Materials Handbook - Third Edition; July 1968.
25. "Study of Hypervelocity Meteoroid Impact on Orbital Space Stations", Final Report; by K. R. Leimback and R. J. Prozan; #N73 23841; April 1973.
26. "Performance of Solar Shields"; by Robert J. Schwinghammer, NASA Technical Memorandum; #NASA TM X-64901; October 1974.

DEVELOPMENT OF A PROTOTYPE FLEXIBLE RADIATOR SYSTEM

PROGRESS REPORT NO. 2

1 August through 31 August 1976

10 September 1976

CONTRACT NO. NAS9-14776
DRL: T-1213, LINE ITEM 2
DRD: MA-182TD

Submitted to:

THE NATIONAL AERONAUTICS AND SPACE ADMINISTRATION
JOHNSON SPACE CENTER
HOUSTON, TEXAS

BY

VOUGHT CORPORATION
SYSTEMS DIVISION
DALLAS, TEXAS 75222

PREPARED BY:

CHECKED BY:

APPROVED BY:

J. W. Leach
J. W. Leach

J. A. Oren
J. A. Oren

R. L. Cox
R. L. Cox

Monthly Progress Report No. 2

Development of a Prototype Flexible Radiator System

1.0 Overall Progress

Work during the second reporting period has been concentrated on design requirements for the prototype flexible radiator system, and has included analyses, element tests, and surveys of manufacturers' capabilities relevant to the design and fabrication of the system which will follow in subsequent reporting periods. The studies of the second reporting period follow the outline of the statement of work of reference (1) and address the following subjects.

- 1) evaluation of effect of curvature of the soft tube radiator panel on radiator performance
- 2) evaluation of methods for fabricating the prototype panel
- 3) permeability of plastic and elastomeric transport tubing.

A briefing was held at NASA-JSC on 12 August to discuss findings of studies documented in reference (2) and to obtain NASA inputs prior to initiating the design phase of the program. The design requirements studies showed that significant performance advantages are possible if two layers of screen wire mesh are incorporated into the radiator fin construction. The performance is also improved if Teflon tubing and Freon 21 transport fluid are used instead of the proposed polyurethane tubing and Coolanol 15 transport fluid. NASA and Vought agreed that the radiator would be constructed with a dual layer of wire mesh and that additional tests and analyses would be conducted to evaluate and attempt to resolve potential problems with the Teflon/Freon 21 system. It was also agreed that tests and analyses of the tubular extendible boom deployment system would be delayed until after the inflation tubing deployment system is checked out on the full scale radiator panel. The inflation tubing system was demonstrated successfully on the smaller engineering model radiator during the initial reporting period. Additional design studies were planned to develop a fabrication technique for constructing the prototype panel, to establish operating limits of transport tubing, and to evaluate the effects of radiator panel curvature on thermal performance.

2.0 Design Requirement Studies

This section describes the results of individual design requirements studies conducted to obtain data for designing and fabricating the flexible radiator system.

2.1 Effects of Radiator Panel Curvature on Thermal Performance

The retraction spring of the inflation tube deployment/retraction system cause the radiator panel to be slightly curved. This influences the effective environment of the panel because part of the thermal radiation emitted from an element on the panel is absorbed at adjacent surfaces. The view factor between two elements on the panel shown in Figure 1 is:

$$F_{1,2} = \frac{\cos^2 \phi \, dA_2}{\pi R^2} \quad (1)$$

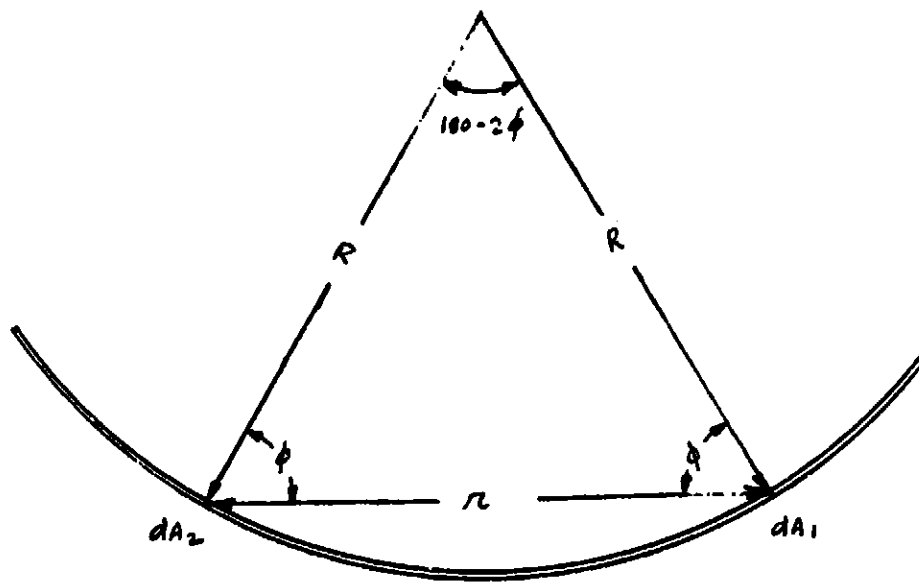


FIGURE 1 GEOMETRY OF CURVED RADIATOR PANEL

where

$$R = R \sin 2\phi / \sin \phi$$

(2)

The view factor from the panel to itself is obtained by integrating. For a two sided radiator

$$F_{\text{PANEL-PANEL}} = \frac{A}{8\pi R^2}$$

(3)

The radiosity leaving the panel is

$$J = \epsilon \sigma T^4 + \rho G$$

(4)

where

$$G = \epsilon \sigma T_\infty^4 + F_{\text{PANEL-PANEL}} J$$

(5)

The net heat transfer from the panel is

$$q = \frac{\epsilon A (1 - F_{\text{PANEL-PANEL}}) \sigma (T^4 - T_\infty^4)}{(1 - \rho F_{\text{PANEL-PANEL}})}$$

(6)

The ratio of the heat rejection for a curved panel to the heat rejection for a straight panel is

$$\frac{q(\text{CURVED})}{q(\text{STRAIGHT})} = \frac{1 - \frac{A}{8\pi R^2}}{1 - \frac{\rho A}{8\pi R^2}}$$

(7)

Table I gives the ratio computed from Equation 7 as a function of the radius of curvature of the panel.

TABLE I Effects of Panel Curvature

R(Ft)	$\frac{q(\text{curved})}{q(\text{straight})}$
50	.9980
100	.9995
200	.9999

The results show that there is little reduction in radiator performance caused by panel curvature.

2.2 Evaluation of Methods for Fabricating the Prototype Radiator Panel

A method is being developed for laminating the radiator with the transport tubing sandwiched between the two opposing halves of the panel. The method employs dies made from aluminum plates. The plates have grooves machined on one side as shown in Figure 2 to accommodate the transport tubing. Vacuum holes are drilled at the bottom of the grooves to provide a means for holding the panel in position during the fabrication process. To laminate the radiator, one half of the fin material is positioned on the plate, and adhesive is applied to the exposed surface in the form of a fine mist spray. Several thin coats are required to prevent the adhesive from collecting in puddles and leaving bare spots on the panel. The tubing is then placed in the grooves and is held in position by the adhesive. The tubing will have been connected to manifolds and checked for leaks prior to lamination. The vacuum is then released and half of the radiator removed from the mold. Subsequently the opposing half is placed in the mold and coated with adhesive. The two halves are then carefully joined together and the assembly including the mold is placed in an autoclave to cure the adhesive. Pressure is maintained on the panel during the cure cycle by means of a vacuum bag. A small section of the panel was fabricated using this method to determine whether problems are likely to occur. The section laminated by this procedure is straight and uniform in cross section. It is probable that the prototype panel can be fabricated successfully with this technique.

2.3 Permeability of Plastic and Elastomeric Transport Tubing

A study was conducted to determine potential problem areas for an alternate radiator transport loop system consisting of Teflon tubing with Freon 21 transport fluid. DuPont was contacted to obtain information relevant to obtaining leak free connections between Teflon tubing and manifolds. Work under previous contracts had shown that because of cold flow of the Teflon, leaks develop at the connectors during operation which require repeated tightening of the fittings. DuPont's representative (Mr. J. Ferrin) could not recommend a solution, but suggested that part of the leakage could be a result of the permeability of the transport tubing. No permeability data was available for Freon 21 but data for Freon 22 and Freon 12 indicate relatively high leakage rates may occur.

The test apparatus shown in Figure 3 was constructed to measure permeability. The apparatus contains a 15 ft. length of 3/16" OD x 1/8" ID FEP Teflon tubing which is arranged as a U-tube, filled to near the ends, and pressurized with nitrogen gas. The meniscus level is monitored as a function of time to determine permeability. Tests were conducted with the tubing exposed to ambient air and immersed in hot water to observe temperature effects. The apparatus was arranged so that the liquid Freon was not exposed to a fitting, thus eliminating the possibility of leakage at the connectors. Any potential leakage could be detected by observing a decay in pressure of the nitrogen gas or by employing a Halogen leak detector. A G.E. model R-10 leak detector indicated leakage along the entire length of tubing, confirming that the tubing is permeable to Freon 21. The measurements given in Figure 4 shows that permeability increases markedly at higher temperatures.

To show the impact of the tubing permeability on the operation of flexible radiators the total leakage rate from a three panel system is computed below. From Figure 4, the permeability at a nominal temperature of 80°F is

$$P = 9.5 \frac{\text{gm} \cdot \text{mil}}{\text{day} \cdot \text{ATM} \cdot \text{sq in}^2} = 1.42 \cdot 10^{-5} \frac{\text{lbm}}{\text{day} \cdot \text{in} \cdot \text{psi}}$$

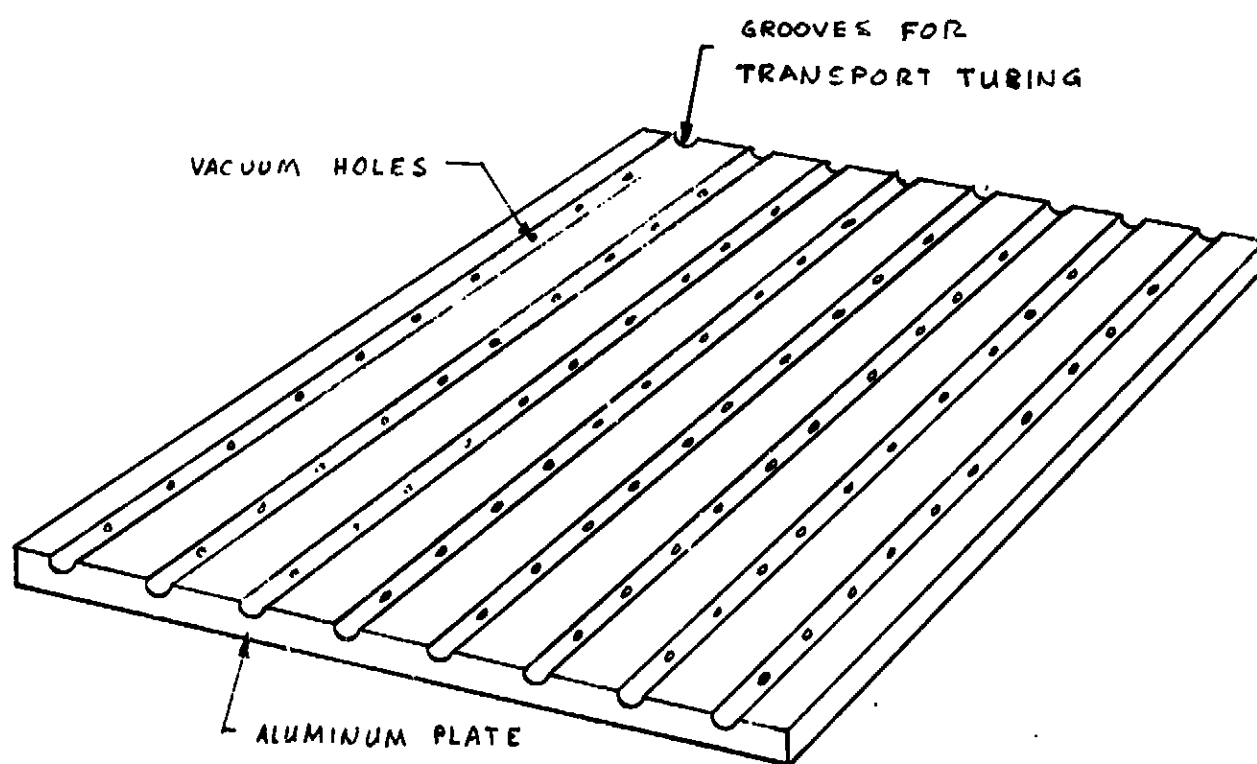
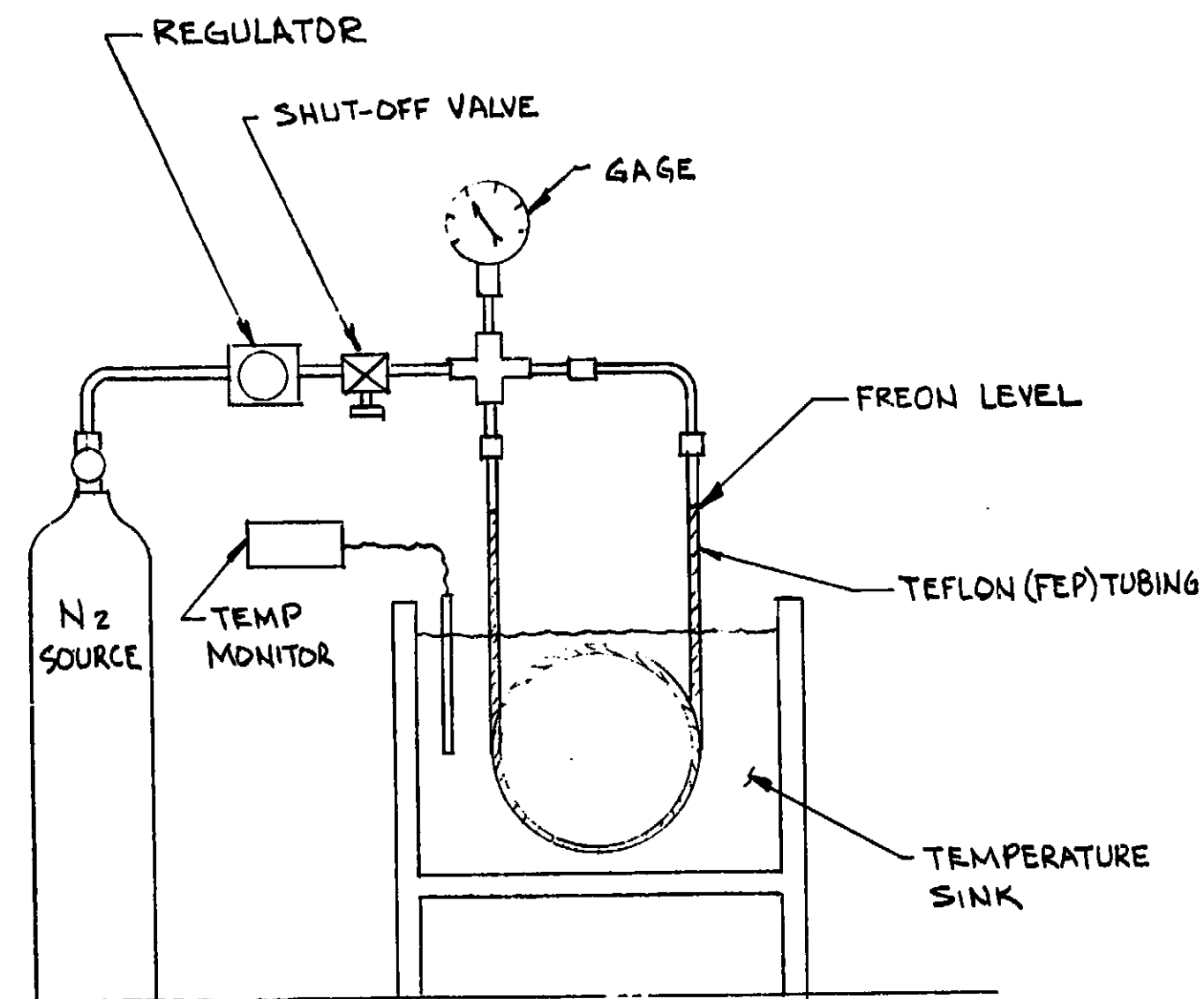
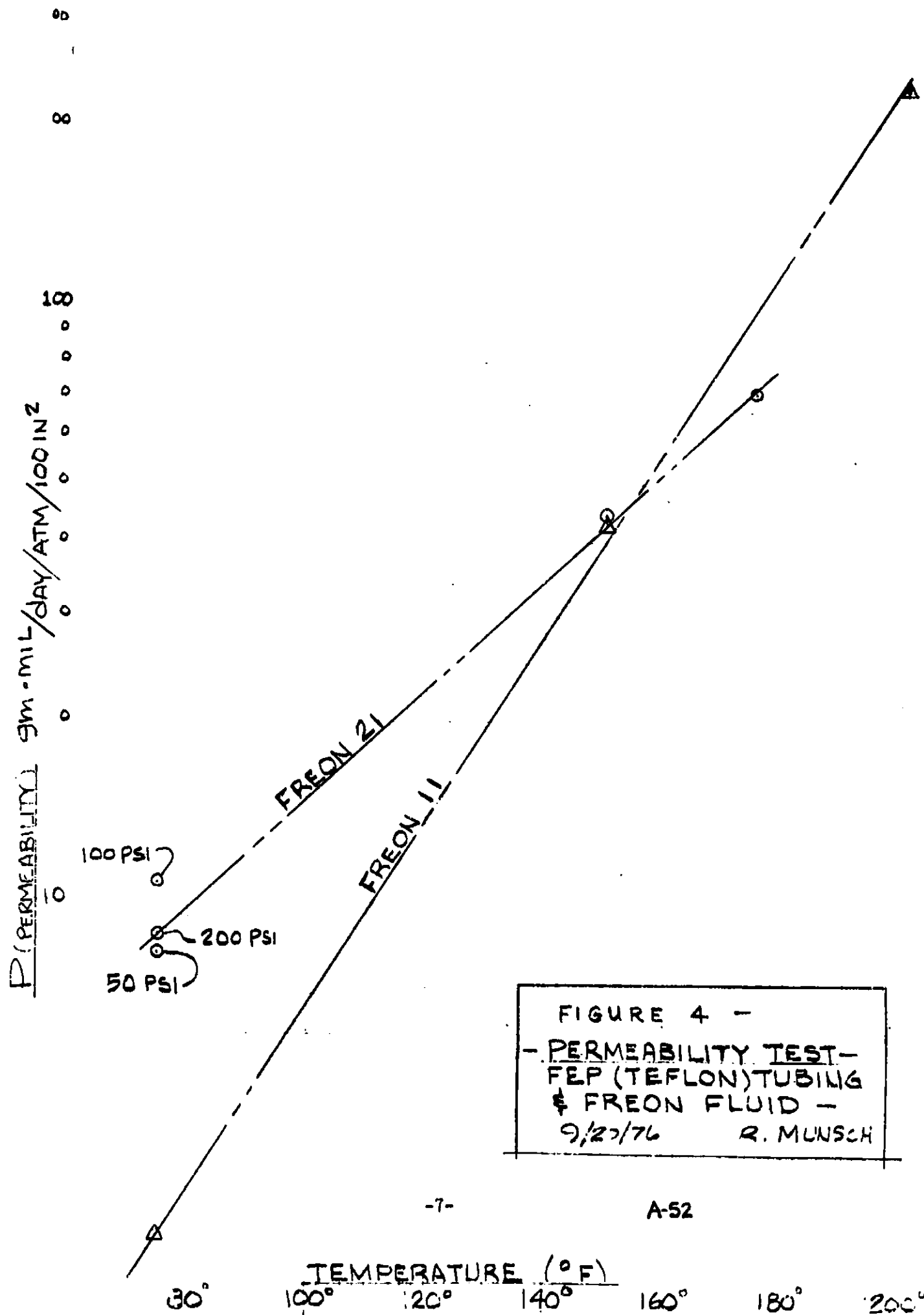


FIGURE 2 MOLD FOR LAMINATING FLEXIBLE RADIATOR PANEL



PERMEABILITY TEST
SET-UP

FIGURE 3 PERMEABILITY TEST



The leakage rate through a section of tubing is given by

$$\dot{m} = \frac{2\pi G L \Delta P}{\ln(p_o/p_i)}$$

For .0625" ID X .125" OD tubing, 48 tubes/panel, $l = 25'$, $P = 100$ psi, the leakage rate is

$$\dot{m} = (3)(48)(25)(12)(2)(\pi)(1.42 \cdot 10^{-8})(100) / \ln(2)$$

$$\dot{m} = 0.556 \text{ lbm / day}$$

This leakage rate would result in a loss of approximately 17 lb_m of Freon 21 in a thirty day mission. There is also a potential problem that the transport fluid leaking through the tubing would attack the adhesive used to bond the two halves of the radiator panel.

Mr. J. Lann of DuPont Fluorocarbon Division was contacted for suggestions on a possible substitute fluid. He recommended that we test Freon 11. The results given in Figure 4 show that the permeability of Teflon to Freon 11 is substantially lower than for Freon 21 at low temperatures, but exceeds that of Freon 21 above 150°F. The leakage rates for Freon 11 are probably acceptable for missions where the average fluid temperature is around 70°F. Freon 11 is more likely to be compatible with surrounding materials than is Freon 21.

Permeability tests were also conducted with Coolanol 15 transport fluid. No leakage was detected at temperatures to 200°F Teflon or Polyurethane tubing.

3.0 Progress on Major End Items

Additional analyses and tests are required in the design requirements phase. Alternate materials need to be evaluated to obtain maximum thermal performance, operating temperature range, and reliability of operation. Experimental data is needed concerning micrometeoroid penetration of the transport tubing. Tests should be conducted to develop reliable methods for connecting the tubing to the manifolds.

The program is on schedule. Permeability of Teflon to Freons and low strength of Polyurethane at high temperature are problems which were not anticipated. Therefore, unscheduled work is required to evaluate alternate materials. The program could fall behind schedule if long delivery times are required to obtain materials for testing.

4.0 Work Scheduled During the Next Reporting Period

Work during the next monthly reporting period will be directed towards finalizing the design requirements studies and initiating the detailed design drawings for fabricating the system.

DEVELOPMENT OF A PROTOTYPE FLEXIBLE RADIATOR SYSTEM

PROGRESS REPORT NO. 3

1 SEPTEMBER through 30 SEPTEMBER 1976

13 OCTOBER 1976

CONTRACT NO. KAS9-14776
DRL: T-1213, LINE ITEM 2
DRD: MA-182TD

Submitted To:

THE NATIONAL AERONAUTICS AND SPACE ADMINISTRATION
JOHNSON SPACE CENTER
HOUSTON, TEXAS

BY

VOUGHT CORPORATION
SYSTEMS DIVISION
DALLAS, TEXAS 75222

PREPARED BY:

CHECKED BY:

APPROVED BY:

J. W. Leach
J. W. Leach

J. A. Oren
J. A. Oren

R. L. Cox
R. L. Cox

Monthly Progress Report No. 3

DEVELOPMENT OF A PROTOTYPE FLEXIBLE RADIATOR SYSTEM

1.0 Overall Progress

Work during the third reporting period has been concentrated on the design requirements for the prototype flexible radiator system and addresses the following subjects:

- 1) Transport fluid evaluation
- 2) Transport tubing evaluation
- 3) Tubing/manifold connector tests
- 4) Micrometeoroid impact simulation test
- 5) Copper/silver backed Teflon fin material test.

The studies identified two fluids, Freon 11 and Coolanol 15, and two tubing materials, Hytrel and FEP Teflon, for use in the flexible radiator system. Several variations of tubing/manifold connectors combining epoxy and compression type fittings were tested successfully in the temperature range -50°F to $+200^{\circ}\text{F}$. A purchase order was released to Texas A&M University to conduct micrometeoroid impact simulation tests. Copper/silver backed Teflon was tested as a possible lower cost substitute for Inconel/silver backed Teflon fin material. The tests showed the copper/silver combination is unacceptable because the copper diffuses into the silver at temperatures which will be experienced at extreme operating conditions.

The design requirements phase is nearing completion, and satisfactory solutions have been achieved for all foreseeable problems. The design phase will begin during the next reporting period.

2.0 Design Requirements Studies

This section summarizes the results of individual design requirements studies conducted to obtain data for designing and fabricating the flexible radiator system.

2.1 Fluid Selection Studies

Published data on transport fluids were analyzed, and compatibility/permeability tests were conducted to evaluate and select fluids for optimum performance and operating range. Table I gives transport property data of candidate fluids at 77°F . This temperature is representative of the operating conditions of flexible radiators. The radiator panel area requirements for the candidate fluids are given in Fig. 1. The minimum area in Figure 1 assumes no thermal resistance between the fluid and the base of the radiator fin. This would be approached for the case of a fluid with very high thermal conductivity in aluminum tubing. The actual area requirements are based on the various candidate fluid conductivities with 0.035" wall thickness FEP Teflon tubing. The radiator tube spacing is assumed to be 0.75", and the fluid flow rates are computed from the specific heat data in Table I for a 4 KW - 60°F Delta T - three panel system. The discontinuities in the curves for FC-88, E-1, Freon 11, and Freon 21 indicate transition from laminar to turbulent flow. Pressure drop data computed for the candidate fluids is given in Fig. 2. The flow length is assumed to be 50' for a 25' radiator panel, and the flow per tube is computed assuming twenty parallel flow tubes per panel. Pumping power weight penalties for the fluids is given in Fig. 3. The weight penalty

PROPERTIES OF CANDIDATE FLUIDS FOR FLEXIBLE RADIATORS

FLUID	P _v (PSIA)	P (lbm/ft ³)	C _p (BTU/lb-°F)	μ (lb/ft-sec)	κ (BTU/lb-°F)	Pow Pt. (°F)	Flash Pt. (°F)
ORONITE FC-100	<.1	56.0	0.45	6.1	.057	-100	220
ORONITE 70	<.1	59.5	0.37	72.6	.080	-100	430
DOW CORNING DC 331	<.1	58.6	0.36	24.2	.050	-130	420
GENERAL ELECTRIC SF 96	<.1	57.1	0.36	12.1	.067	-120	275
GENERAL ELECTRIC SF 81	<.1	60.6	0.36	120	.087	-120	NONE
ETHYLENE GLYCOL-WATER (RS-89a)	0.3	67.1	0.73	11.8	.219	-80	240
Du Pont FREON 21	25	85.3	0.25	0.83	.071	-211	NONE
Du Pont FREON 11	14	92.1	0.208	1.01	.050	-168	NONE
Du Pont FREON E-1	8	96	0.245	1.2	.036	-246	NONE
Du Pont FREON E-2	0'	105	0.240	2.1	.041	-195	NONE
3-M FC-88	4.4	101	0.244	1.19	.037	-150	NONE
3-M FC-75	0.5	111	0.24	3.6	.079	-135	NONE
3-M FC-77	0.8	113	0.24	3.6	.038	-150	NONE
MONSANTO COOLANDOL 15	<.1	56.0	0.43	4.5	.062	-140	170

461510

USE IN THE PROCEEDINGS OF THE
NATIONAL ACADEMY OF SCIENCES

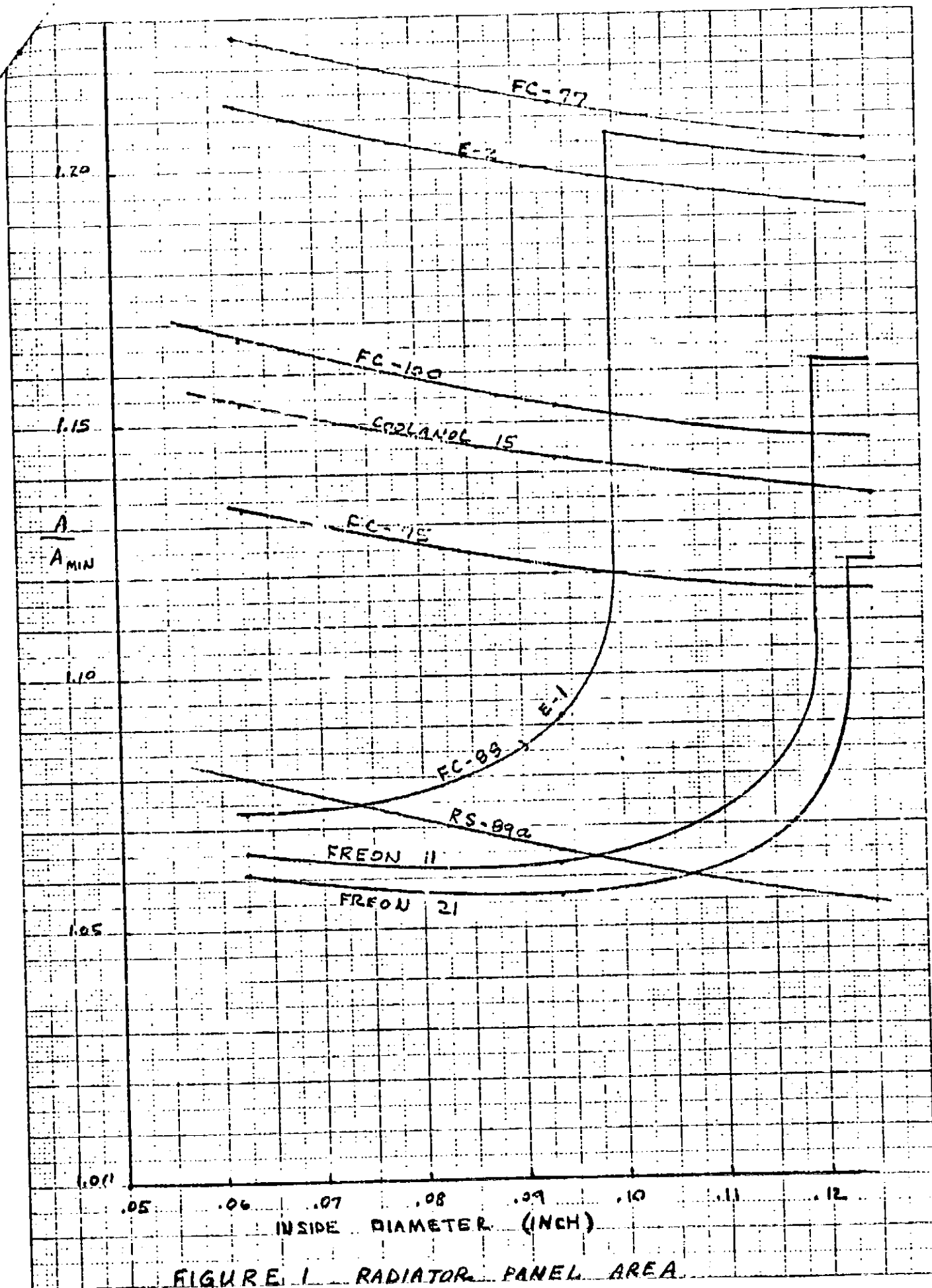
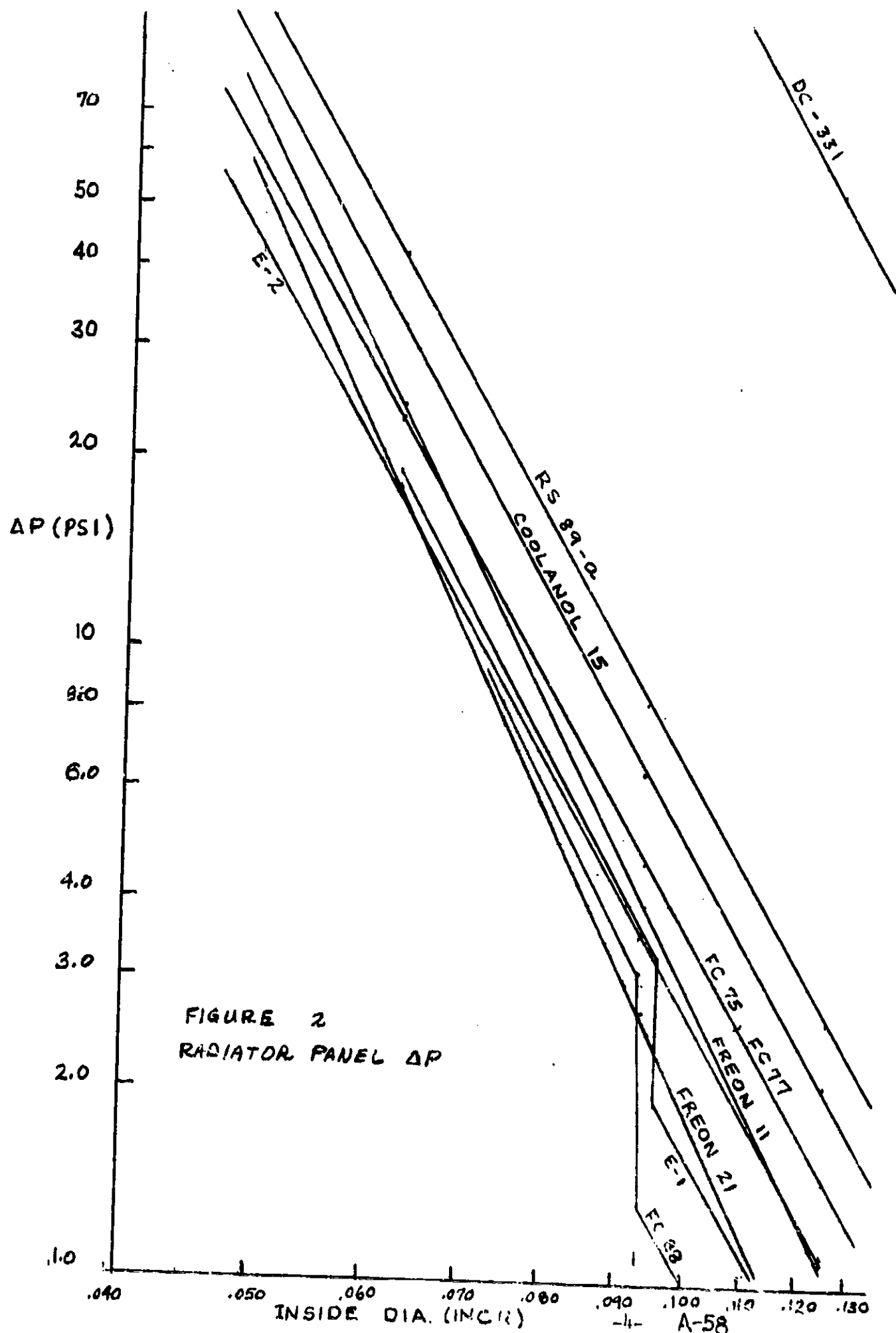


FIGURE 1 RADIATOR PANEL AREA



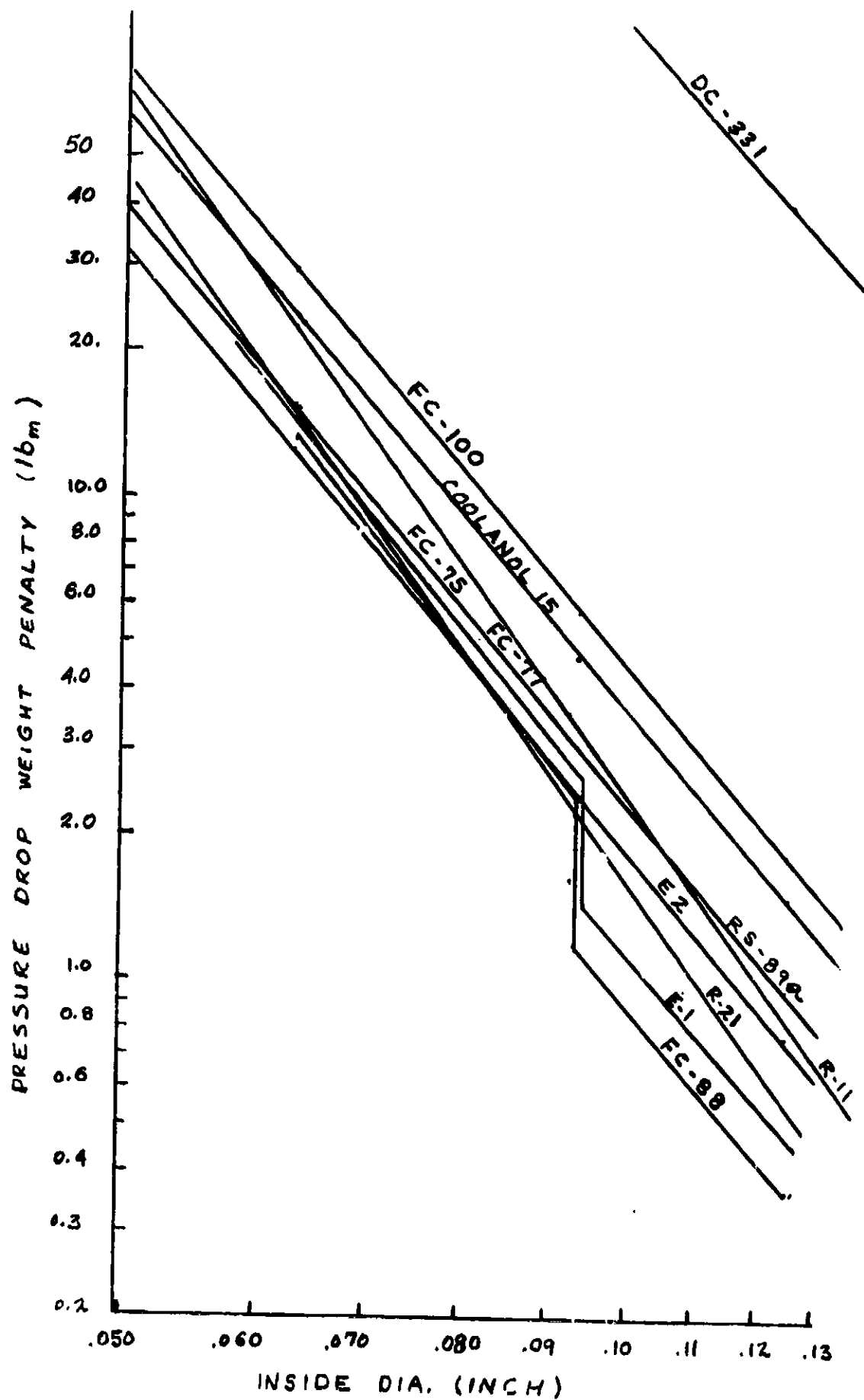


FIGURE 3 PRESSURE DROP WEIGHT PENALTY

is assessed at 540 lb_m/KW assuming a 13% pump/motor efficiency. Fluid weight given in Fig. 4 is computed from the fluid densities assuming that the total volume of fluid required is double the volume contained in the radiator. This is probably less than the actual requirements, which will depend on the length of connecting lines, the volume of the system accumulator, etc. For comparison purposes, example computations were made for the weight of fluid in a 25' length of 0.375" ID connecting line. The weight ranges from 1.1 lb_m for Coolanol 15 to 2.3 lb_m for FC-77.

The total fluid system weight for a 4' width x 25' length radiator containing 40 parallel tubes is given in Fig. 5. The tube wall thickness is assumed to be .035", and the tube material density is taken to be that of Teflon ($\rho = 135 \text{ lb}_m/\text{ft}^3$). The figure shows that an optimum tube diameter exists for each fluid for which the weight of the radiator is minimized. The difference in the minimum unit weight for the candidate fluids is not large enough to be a decisive factor influencing the selection of the optimum flexible radiator fluid. The diameter for which the minimum weight occurs is important because the tube diameter affects the stiffness of the radiator and the weight of the deployment/retraction system. The area requirements also impact the deployment system and the panel weight. Operating temperature range, and materials compatibility are additional factors which must be considered in selecting a fluid.

Fluid system weight and radiator panel areas are given relative to Freon 21 in Table II. The adjusted weight accounts for effects of differences in area requirements on fluid system weight, but does not account for weight of the fin material or weight of the deployment system. Thus Table II does not give a complete account of the weight penalties for the candidate fluids. However, the data is sufficient for quantitative evaluation of the fluids. More detailed analyses will be conducted for the fluids selected for potential use in the flexible radiator system. Based on area requirements and fluid system weight in Table II, Oronite FC-100, Freon E-2, and FC-77 may be eliminated from the list of candidates.

For spaceradiator applications the lower operating temperature limit of a fluid is restricted by the onset of flow instabilities which occur when viscosity increases as the fluid is cooled within the parallel flow passages of the radiator. The instabilities adversely affect the distribution of flow in the parallel network. An equation is developed in Ref. (1) for computing the limits of stable operation. Figure 6 compares the minimum stable operating temperatures computed for the remaining fluids for which low temperature viscosity data are available. RS-89a* is unacceptable for very low temperature applications because of flow stability problems. It is expected that the FC fluids which could not be analyzed would be acceptable.

High temperature operation is limited by permeability and strength of transport tubing. Fluids with high permeability coefficients and high vapor pressure require unacceptable tube wall thickness. Permeability tests discussed in Ref. (2) show that leakage rates for Freon 21 are too high except at very low temperatures, and that Freon 11 and Freon E-1 are acceptable only for temperatures below 100°F. Samples of the FC fluids have been ordered for testing. It is expected that the permeability of these fluids will be similar to that of the Freons. However, no decisions should be made with regard to fluid selection until the FC fluids can be tested. FC-88 is attractive as a candidate fluid because of its thermal performance characteristics and tube diameter requirements. Of the fluids tested Coolanol 15 and Freon 11 have the more desirable properties for flexible radiators. RS-89-a is the optimum fluid for applications where the minimum fluid outlet temperature does not drop below the stable operating limit. Because of the way that the manifolds are arranged in the prototype radiator, the flow network actually is comprised of two series connected parallel banks of tubing. This extends the limits of stable operation. Figure 6-a gives the approximate stable region of operation for RS-89a in the prototype radiator.

*RS89a - Ethylene Glycol - water

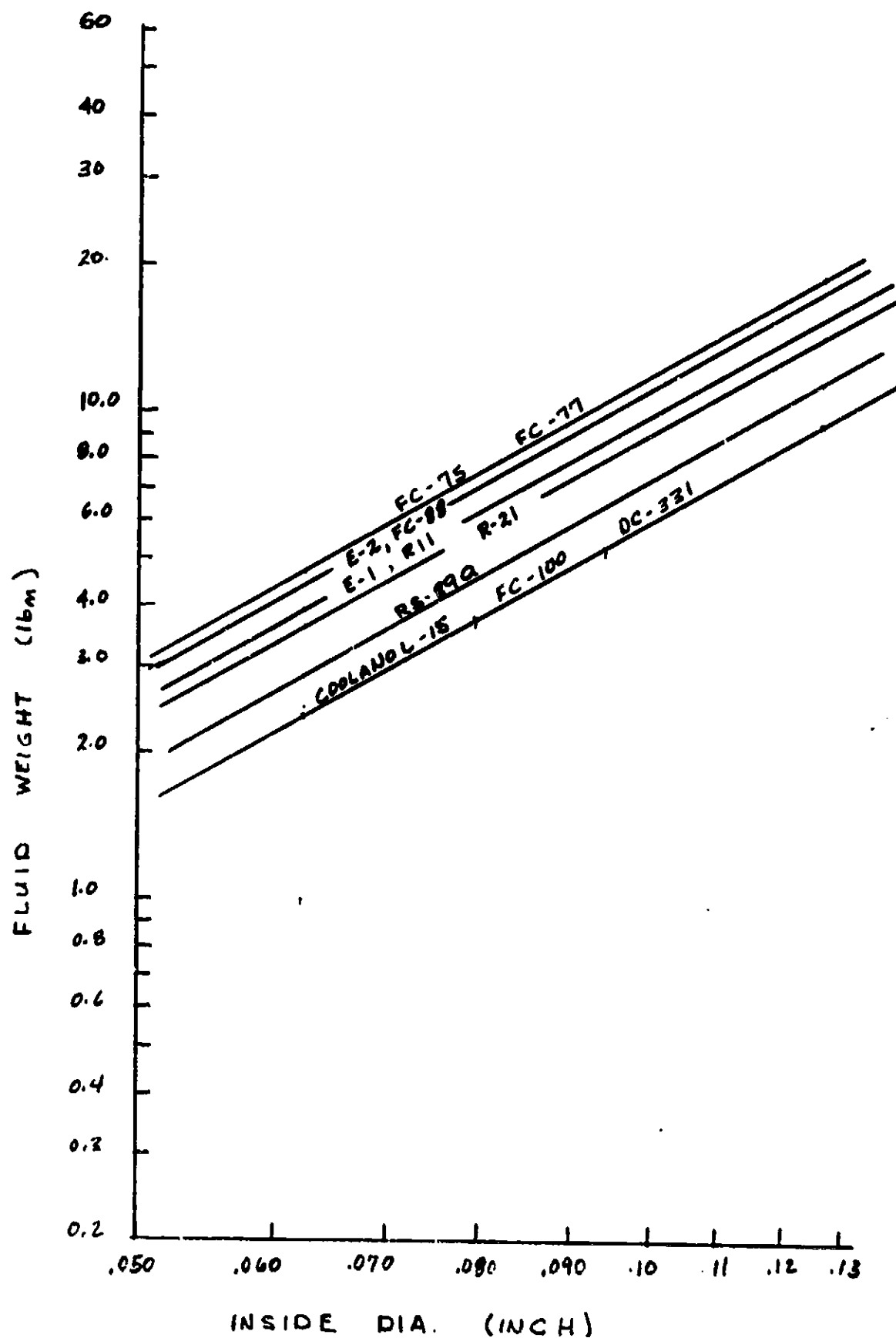


FIGURE 4 FLUID WEIGHT

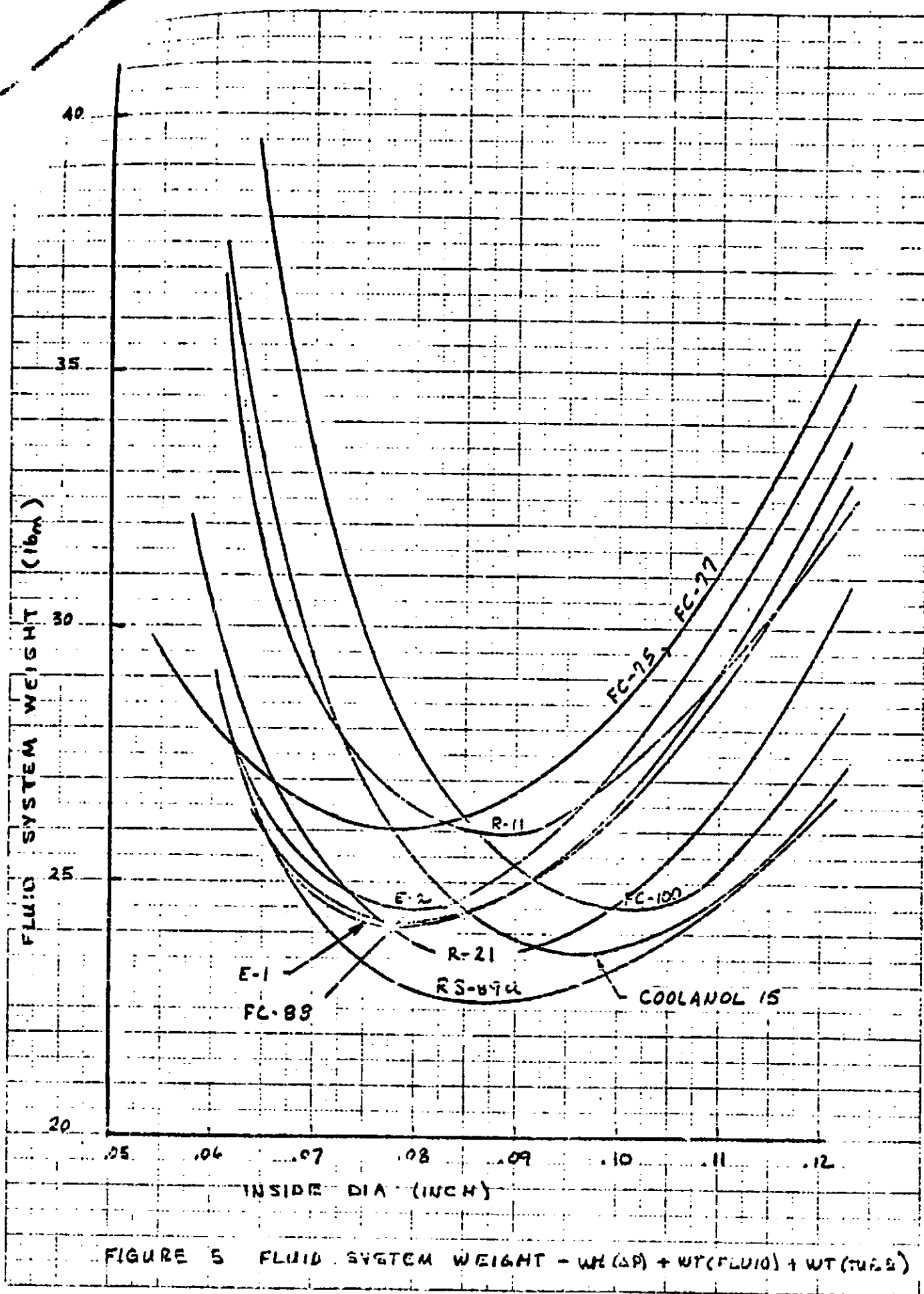


FIGURE 5 FLUID SYSTEM WEIGHT - WT (AP) + WT (FLUID) + WT (TUBES)

COMPARISON OF CANDIDATE FLUIDS

FLUID	OPT. DIA. (INCH)	OPT. NT (LB)	A/RMIN	ADJUSTED WT. (LB)	DELTA /R-21 (LB)	A A(R-21)
ORONITE FC-100	.100	24.5	1.151	28.2	3.4	1.090
ETHYLENE GLYCOL WATER (RS-89a)	.085	22.7	1.069	24.3	-0.5	1.012
FREON 21	.085	23.5	1.056	24.9	0	1.000
FREON 11	.090	26.0	1.062	27.6	2.8	1.006
FREON E-1	.075	24.0	1.075	25.8	1.0	1.018
FREON E-2	.080	24.4	1.204	29.4	4.6	1.140
FC - 88	.075	24.0	1.075	25.9	1.0	1.018
FC - 75	.075	26.0	1.128	29.3	4.5	1.068
FC - 77	.075	26.6	1.220	31.7	6.9	1.155
COOLANT 15	.075	23.6	1.143	27.0	2.2	1.082

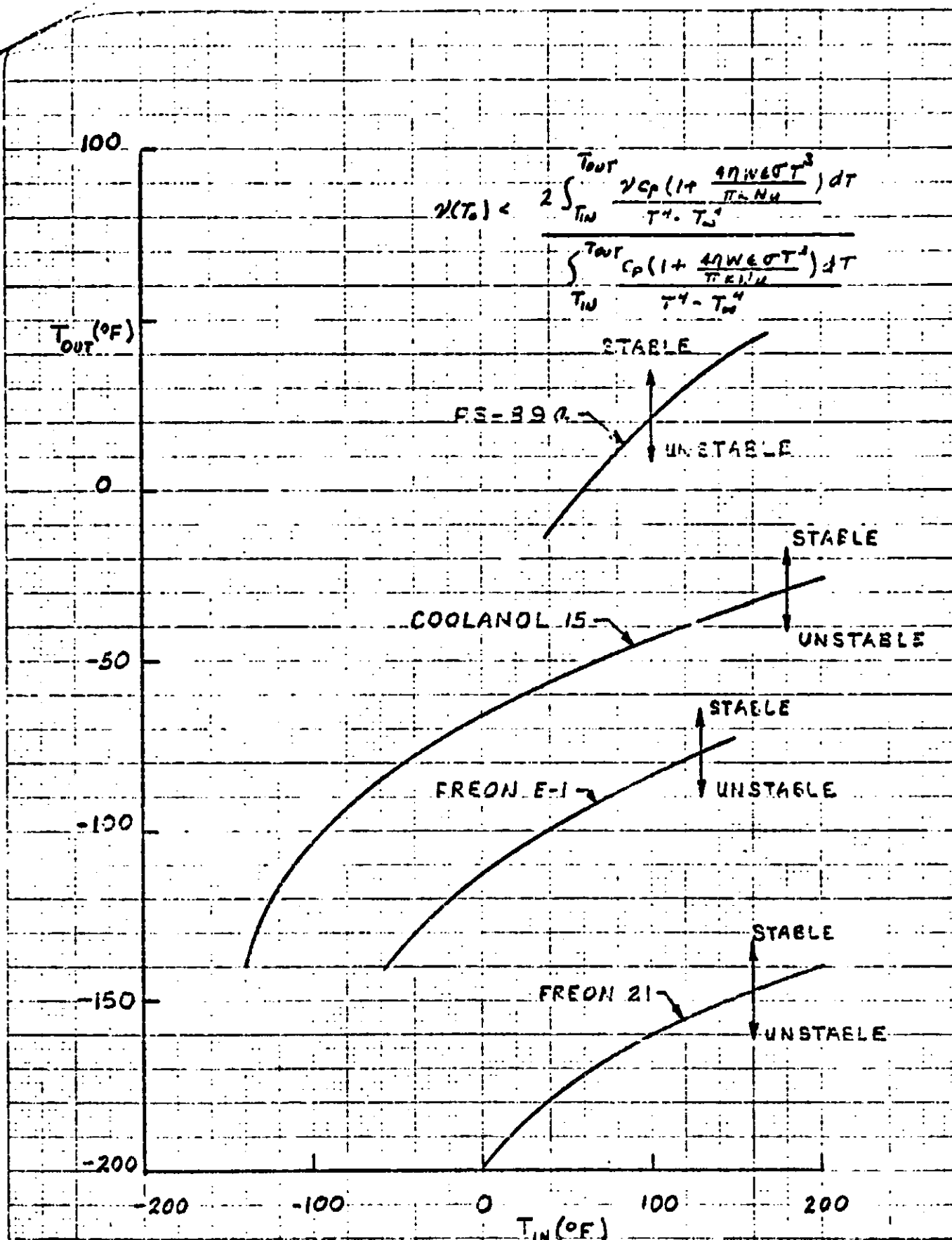


FIGURE 6
 APPROXIMATE STABILITY CURVES FOR CANDIDATE
 INFLATABLE RADIATOR FLUIDS

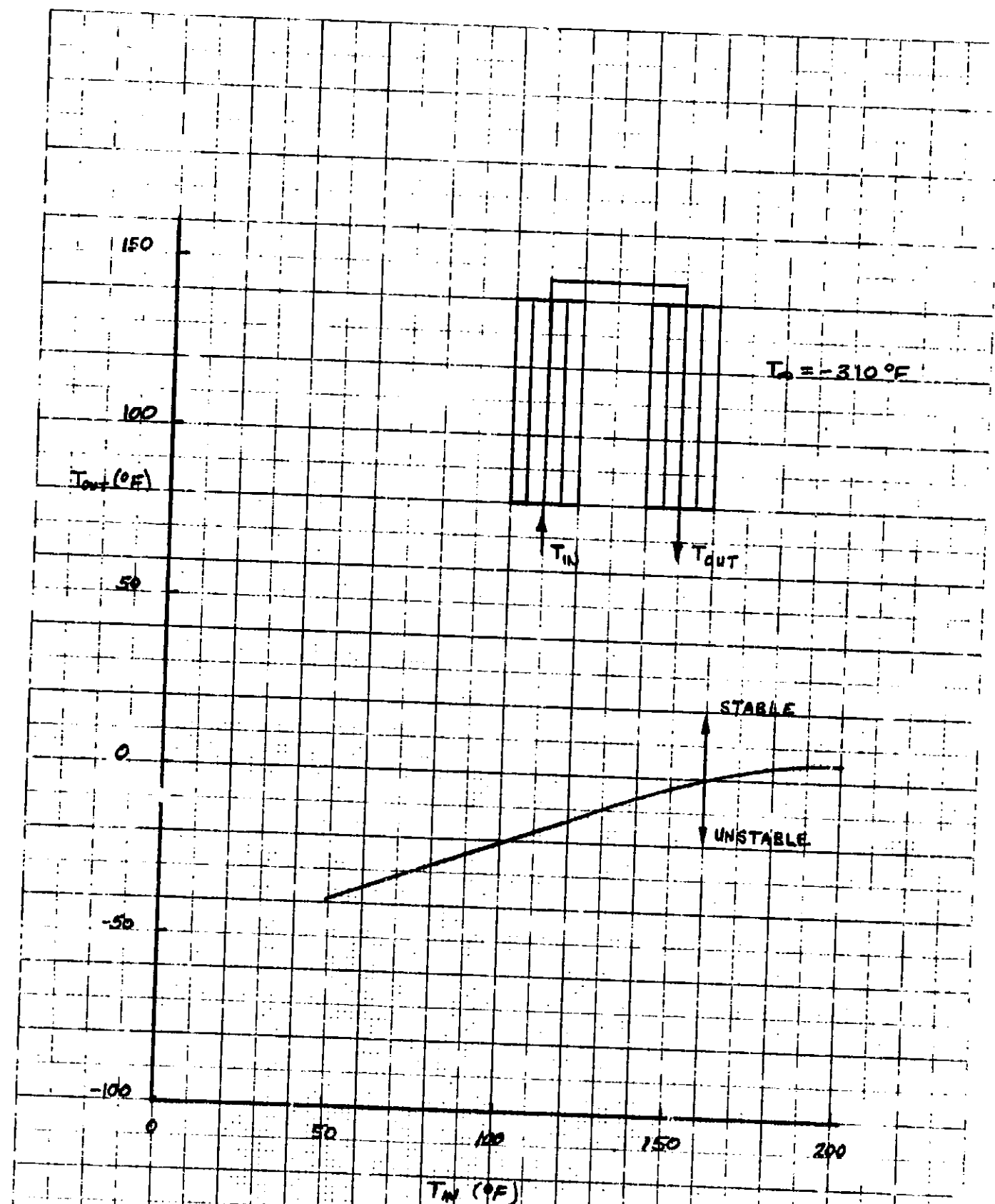


FIGURE 6-2
APPROXIMATE STABILITY CURVE FOR
60% ETHYLENE GLYCOL - 40% WATER

2.2 Tubing Selection Studies

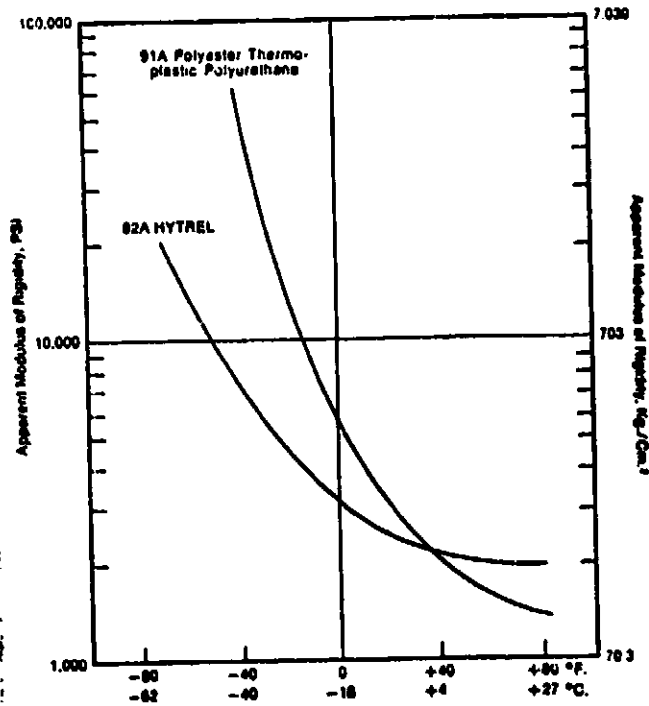
An extensive materials evaluation survey documented in Ref. (3) compared data on twenty-eight tubing materials. The study identified polyurethane and FEP Teflon as having desirable properties for use in flexible radiators. Two additional materials were tested during this reporting period as possible alternates. Flexite FN Nylon was selected for further evaluation at NASA's request because of its compatibility with Freons. A sample of tubing was obtained and tested for flexibility. The sample was extremely stiff at low temperatures and shattered upon bending at -75°F . Hytrel tubing was also obtained and tested as a possible substitute for polyurethane. Compatibility tests at 200°F showed no effects of exposure to Coolanol 15 and Freon E-1 after 24 hours. The Hytrel did swell by approximately 30% in the presence of Freon 11, and deteriorated with exposure to Freon 21. Vendor data given in Fig. 7 indicates that the Hytrel is more flexible than Polyurethane at low temperature, and is stronger at high temperatures. Creep data given in Fig. 8 shows that the high temperature strength is sufficient for flexible radiator applications when the wall stress does not exceed 500 psi. This is well within the limits expected for the fluids identified in Section 2.1. Vought tests showed the material to be compatible with Coolanol 15. Additional tests are planned for compatibility with the FC fluids.

2.3 Tubing/Manifold Connector Tests

An apparatus was designed to test methods for connecting Teflon transport tubing to a manifold. Work under previous contracts has shown that leaks develop at the manifold fittings because of cold flow of the Teflon. Therefore, several unusual types of connectors designed to resist leakage caused by cold flow were tested. A manifold was constructed, as shown in Fig. 9, so that several concepts could be tested simultaneously. The test sequence consisted of alternate exposures to hot and cold environments with the system pressurized to 200 psig. The tubing was charged with Coolanol 15 to test compatibility between the transport fluid and materials used in the connectors. The system was submerged in a 200°F bath for periods of approximately two days followed by short exposures of approximately 10 minutes duration to a dry ice bath at -75°F . The system was then checked for leaks and re-immersed in the hot bath. Very small leaks were easily detectable following the cold exposure because the leaking transport fluid would melt and discolor frost accumulating on the system. Leakage was also monitored by measuring the level of the Meniscus of the extrapped transport fluid which was observable through a 0.25" dia. sight glass. Table III lists the types of fittings tested and gives the results after 24 days of testing. The test sequence is scheduled to continue for 30 days. The Swagelok fittings listed in Table III contain two compression ferrules that squeeze the tubing as the fitting is tightened. The aluminum-aluminum designation for test specimen No. 1 indicates that both ferrules are aluminum. For specimen No. 4, the back ferrule is stainless steel and the front ferrule is Teflon. The threaded nut of all swagelok fittings tested is aluminum. Inserts made from stainless steel tubing (.062" OD x .006" wall) were installed inside the 1/8" OD x 1/16" ID Teflon tubing to restrain the deflection of tubing as the fittings were tightened. Similar inserts were used in the non-compression type glued connectors. In this case the Teflon tubing is glued to the inside of a larger tube as shown in Fig. 10. This type of fitting is not susceptible to cold flow of Teflon as occurs in compression type connectors. The inserts were used in this case to force the tubing cross section to be circular, and insure a sound, close tolerance glue joint.

The results in Table III show that all of the pure compression type fittings leaked at some point in the test. These fittings did not leak after every cold soak, but some leakage did occur at each fitting at least once during the 24 day test. The connector with stainless steel back ferrule and Teflon front ferrule leaked less than the other

Figure 7
Low Temperature Moduli
of 92A HYTREL
ASTM D-1043 (Clash Berg)



High Temperature Tensile
Properties of 55D HYTREL

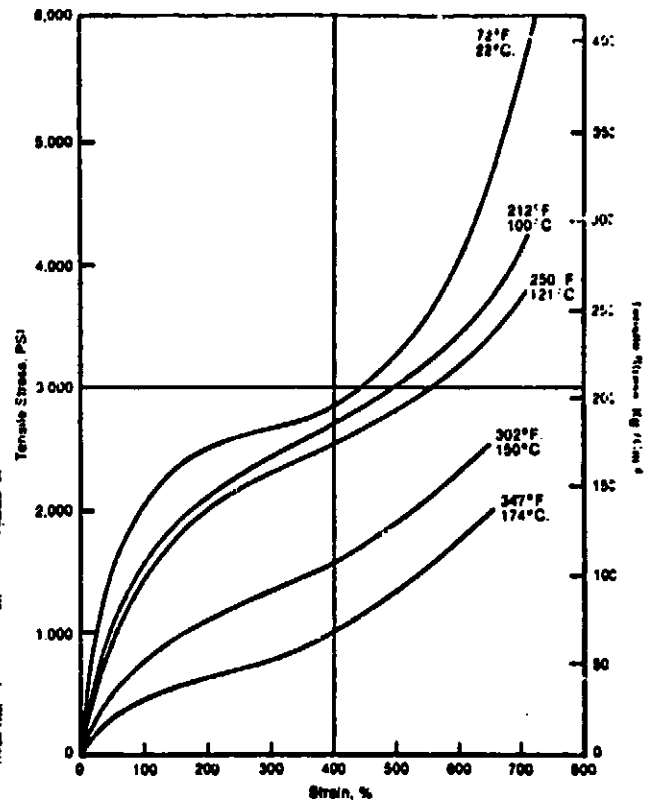
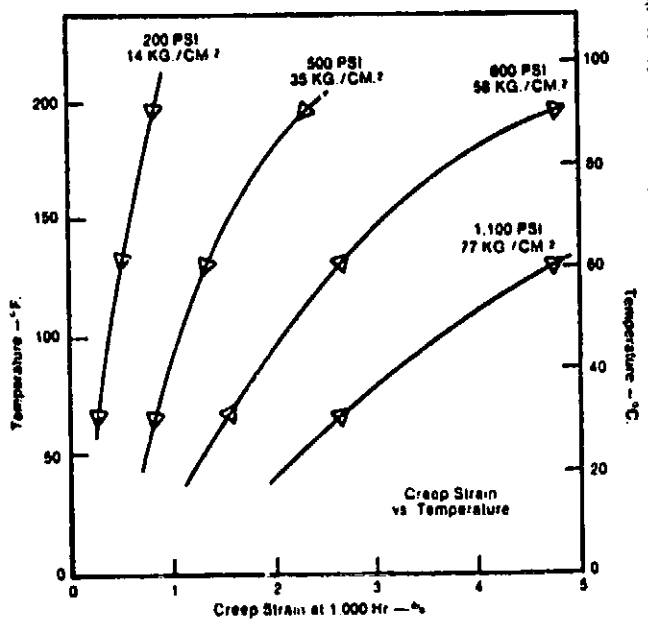
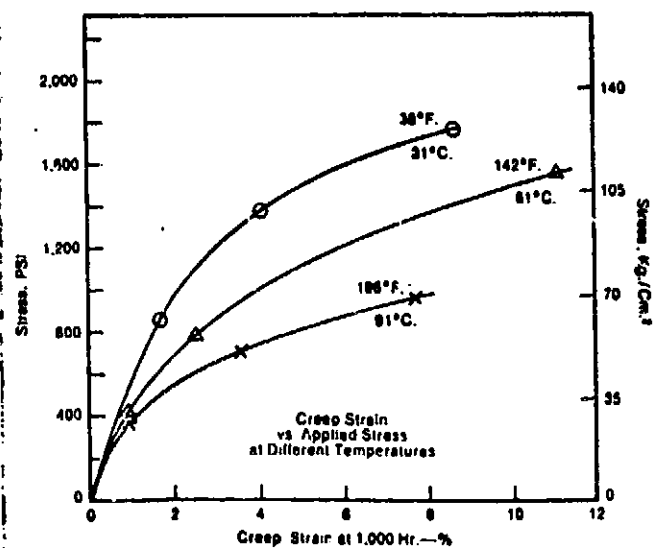


Figure 8
1,000 Hr. Creep—HYTREL (55D)



1,000 Hr. Creep—HYTREL (55D)



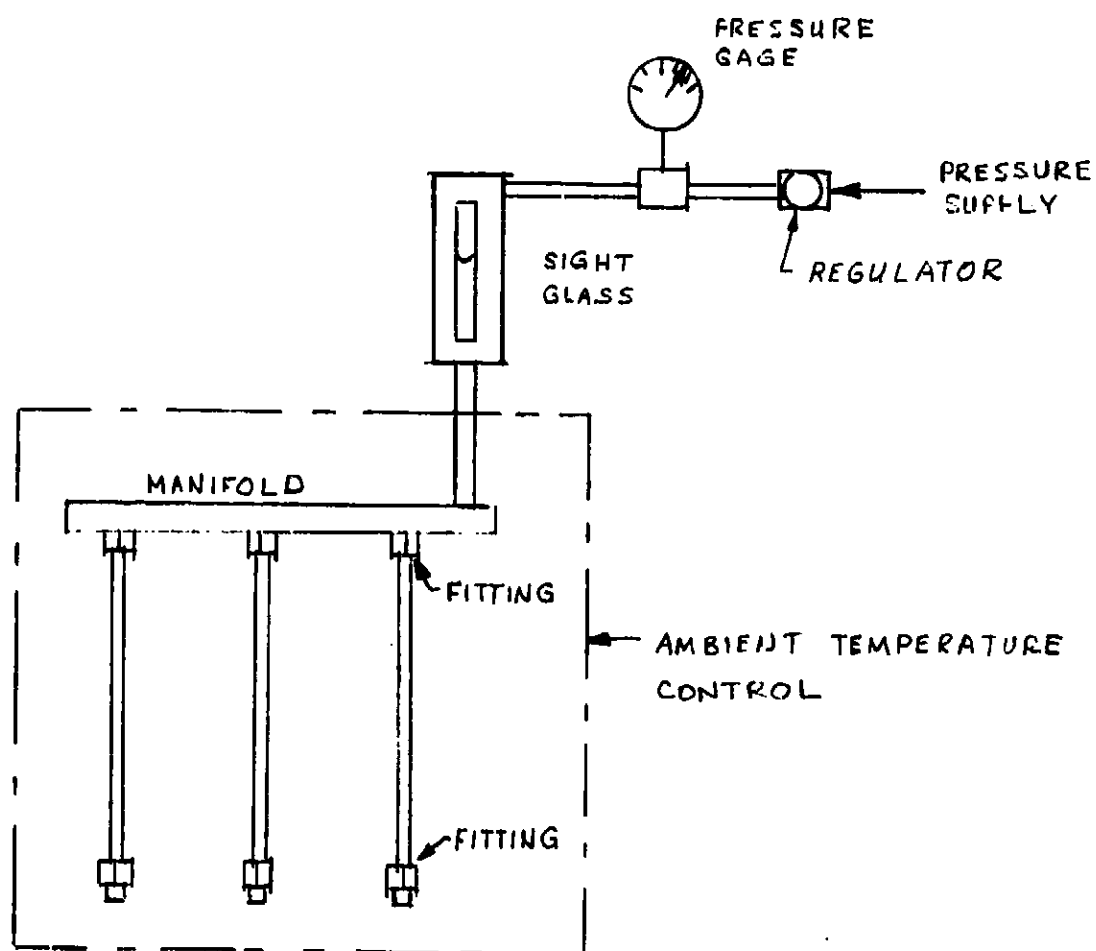


FIGURE 9 MANIFOLD FITTING TEST APPARATUS

TABLE III MANIFOLD FITTING TEST SEQUENCE

<u>TEST SPECIMEN</u>	<u>DESCRIPTION</u>	<u>RESULTS</u>
1	Swagelok, Aluminum-aluminum	Usually leaks after cold soak
2	Swagelok, S.S.-S.S.	Usually leaks after cold soak
3	Swagelok, Teflon-Teflon	Sometimes leaks after cold soak
4	Swagelok, S.S.-Teflon	Sometimes leaks after cold soak
5	Swagelok, Al-Al-EC2216	No measured leakage
6	Swagelok, SS-SS-EC2216	No measured leakage
7	Swagelok, Teflon-Teflon-EC2216	No measured leakage
8	Swagelok, S.S.-Teflon	No measured leakage
9	Aluminum tube - EC2216	Immediate leakage
10	Teflon tube - EC2216	Some specimens leaked
11	Teflon tube - Aremco Bond 526	Immediate leakage

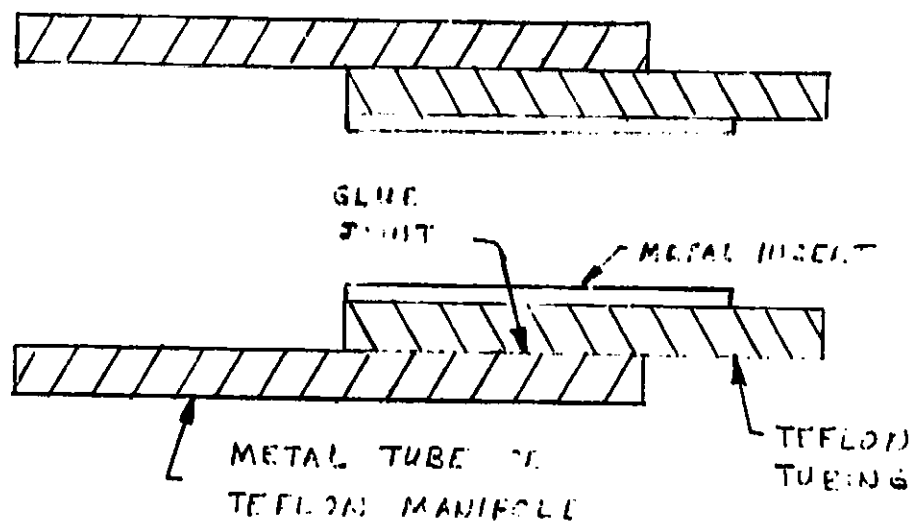


FIGURE 10 OVERLAPPING TUBE GLUE JOINT

compression fittings. None of the compression type fittings with glued ferrules leaked. These fittings were prepared by etching the outside diameter of the Teflon tubing and coating it with 3-M EC-2216 epoxy. The fitting was then assembled and tightened before the adhesive was cured. Most of the overlapping tube glued joint connections developed leaks during the test. Apparently it is more difficult to obtain a thin uniform layer of glue with this method than in the compression type fittings. This is important because vapors form inside the adhesive during the cure cycle and create leak paths for the transport fluid. It is, therefore, essential to maintain pressure at the joint during the cure process to keep the glue thickness at a minimum and retard the formation of leak paths. It is possible that methods could be developed for making this type of joint effective. However, because of the success of the compression type glued joint, no further work is planned in this area under the present contract. Two types of Epoxy, 3M-EC2216 and Aremco-Bond 526 were tested. The EC-2216 adhesive proved satisfactory for the compression joint as described above. However, the Aremco-Bond 526 adhesive is unacceptable for this application because it expands to approximately double its original volume during the cure cycle, and is very porous in the cured state.

2.4 Micrometeoroid Impact Simulation Tests

Texas A&M University has been contracted to perform micrometeoroid impact simulation tests on Teflon and Polyurethane. A \$750 fixed price, best effort contract was issued. The work will be carried out by student labor under the supervision of Dr. J. L. Rand, Space Technology Division, Texas Engineering Experiment Station, Texas, A&M University. The work will be completed before 20 December 1976. An unspecified number of 0.080 inch projectiles will be fired at various velocities up to 6 kilometers/sec using a light gas gun. FEP Teflon sheet and Polyurethane tubing were supplied by Vought. The test will be designed to verify or establish equations used to size the tube wall thickness of the flexible radiator.

2.5 Evaluation of Copper/Silver backed Teflon

Sheldahl Advanced Products Division, who manufactures Inconel/Silver backed Teflon used in the fin material of flexible radiators, suggested that the Inconel film normally used in conjunction with silver might be replaced by copper. The purpose of the Inconel film is to protect the silver from corrosion. Sheldahl has recently successfully replaced this film with copper on materials used in solar collectors. If copper is used, the cost of fabricating the fin material is reduced by more than \$5,000, and the material can be produced in continuous rolls rather than in 10' lengths. Sheldahl shipped samples of copper/silver backed Teflon to Vought for preliminary testing. Small sections of the material were glued together to test compatibility of the copper and the adhesive previously selected for laminating the Prototype flexible radiator. When the sample was examined after it had been heated to 300°F to cure the adhesive, it was discovered that the silver fin had become discolored. A second sample was prepared without adhesive and placed in an oven at 200°F. It also became discolored after a few hours exposure. This indicated that the copper had diffused into the silver at high temperature. Sheldahl was contacted, and they subsequently performed similar tests at their facility. They confirmed Vought's conclusions. Sheldahl measured the solar absorptivity prior to and subsequent to heating. This measurement showed that the absorptivity had doubled. The higher value of solar absorptivity is unacceptable for flexible radiators. Thus copper/silver backed Teflon was rejected for use in this application.

3.0 Progress on Major End Items

The design requirements phase is nearing completion. One transport fluid, FC88, remains to be tested for compatibility and permeability in Hytrel and FEP Teflon tubing.

These tests should be completed within the next two weeks. Meteoroid penetration tests are in progress, but final results will not be available in time to influence the design of the prototype radiator system. Preliminary results will be available to verify equations used in the design, and could impact the program if major discrepancies are observed. Design drawings are being prepared for tooling to laminate the radiator, and for components such as the deployment drum which are not affected by the unresolved items in the design requirement phase. Sheldahl Advanced Products Division has been contracted to fabricate the fin material for the radiator, and delivery is expected by 30 November 1976.

4.0 Work Scheduled During the Next Reporting Period

Work during the next monthly reporting period will be directed towards finalizing the design requirements studies and initiating the detailed design drawings for fabricating the system.

References

1. Leach, J. W., "Flow Instabilities in Spacecraft Radiators", Vought Report No. T 169-56, 20 November 1974.
2. Leach, J. W., "Development of a Prototype Flexible Radiator System, Progress Report No. 2", NASA Contract No. NAS9-14776, DRL: T-1213, Line Item 2, DRD: MA-182TD, 10 September 1976.
3. Leach, J. W., "Development of an Inflatable Radiator System, Final Report", Vought Report No. 2-53002/6R-51338, 28 May 1976.

DEVELOPMENT OF A PROTOTYPE FLEXIBLE RADIATOR SYSTEM

PROGRESS REPORT NO. 4

1 October through 31 October 1976

19 NOVEMBER 1976

CONTRACT NO. FAS9-14776
DRL: T-1213, LINE ITEM 2
DRD: MA-182TD

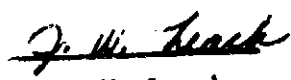
Submitted to:

THE NATIONAL AERONAUTICS AND SPACE ADMINISTRATION
JOHNSON SPACE CENTER
HOUSTON, TEXAS

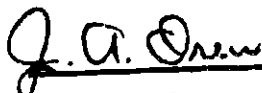
BY

VOUGHT CORPORATION
SYSTEMS DIVISION
DALLAS, TEXAS 75222

PREPARED BY:


J. W. Leach

CHECKED BY:


J. A. Oren

APPROVED BY:


R. L. Cox

1.0 Overall Progress

Work during the fourth reporting period has been concentrated on the design requirements and design phases of the program, and addresses the following subjects:

- 1) transport fluid evaluation
- 2) transport tubing evaluation
- 3) U.V. degradation of flexible radiator adhesives
- 4) fabrication tooling design
- 5) detail design drawing

Studies documented in previous reporting periods have established a basis for designing the system. The purpose of the design requirements studies of this reporting period have been to reduce cost and improve the radiator performance. The search for better fluids and tubing during the last reporting period has eliminated several possible candidate materials but has not lead to improvements in the system design. U.V. degradation tests on adhesives are being conducted at NASA Langley Research Center to determine whether it is possible to delete the Silver/Inconel vacuum deposited coating currently being employed to protect the adhesives from solar exposure. There is a potential for significant cost reduction if it is determined that the glue is not vulnerable to U.V. radiation and therefore does not require the protective Silver/Inconel coating.

Tooling for fabricating the radiator panel will be produced during the next reporting period, and the fin material will be laminated at Sheldahl Advanced Products Division. This will initiate the fabrication phase of the program.

2.0 Progress on Individual Major Areas.

2.1 Transport fluid/tubing evaluation: Fluid/tubing compatibility and permeability tests were conducted with 3M fluids FC 77 and FC88 and transport tubing constructed from Dupont Hytrel and FEP Teflon. The tests showed that the fluids permeate the Teflon tubing at unacceptable rates, and weaken the Hytrel tubing to such an extent that it cannot withstand the required internal fluid pressure. Permeability does not appear to be significant for the Hytrel tubing. However, at temperatures above 150°F the material creeps at a prohibitive rate when exposed to the FC fluids at operating pressures. The tubing does not creep when it is pressurized with N₂ gas at 200°F.

2.2 Adhesives Tests: Small samples consisting of films of adhesive coated on 1" diameter aluminum disks were prepared and shipped to NASA Langley Research

Center for U.V. degradation testing. The samples completed at the time of this report were prepared with General Electric SR-585 and SR-574 adhesives. Two types of samples were made with SR-585 adhesive. One has the adhesive film exposed directly to a vacuum-U.V. environment. The second has the adhesive covered with a film of Teflon/Silver wire mesh radiator fin material. A single sample was constructed with SR-574 adhesive exposed directly to the vacuum-U.V. environment. Materials have been ordered to prepare additional samples with SR-574 and 573 adhesives. The exposure tests will last approximately 30 days. The purpose of the tests is to determine whether a layer of Silver/Inconel is required in the flexible radiator fin material to protect the adhesive from the solar flux. Additional samples are being constructed to determine the peel strength of the adhesives.

2.3 Design: Design drawings were produced for a tooling plate to be used in fabricating the radiator panel. A conceptual sketch of the plate is given in Progress Report No. 2. Materials for the tooling plate have been ordered, and fabrication will occur during the next reporting period. Work continues on the design drawings for the flexible radiator panel and deployment/retraction system.

3.0 Progress on Major End Items

The program is on schedule. The design requirements phase has been completed, and work is in progress in the design phase.

4.0 Work Scheduled During the Next Reporting Period

The fabrication phase will begin during the next reporting period. Tooling plates will be fabricated at Vought, and the radiator fin material will be laminated at Sheldahl Advanced Products Division. A meeting will be scheduled with NASA JSC to review the design phase effort.

DEVELOPMENT OF A PROTOTYPE FLEXIBLE RADIATOR SYSTEM

PROGRESS REPORT NO. 5

1 NOVEMBER through 30 NOVEMBER 1976

10 DECEMBER 1976

CONTRACT NO. NAS9-14776
DRL: T-1213, LINE ITEM 2
DRD: MA-182TD

Submitted To:

THE NATIONAL AERONAUTICS AND SPACE ADMINISTRATION
JOHNSON SPACE CENTER
HOUSTON, TEXAS

BY

VOUGHT CORPORATION
SYSTEMS DIVISION
DALLAS, TEXAS 75222

PREPARED BY:

J. W. Leach
J. W. Leach

CHECKED BY:

J. A. Oren
J. A. Oren

APPROVED BY:

R. L. Cox
R. L. Cox

Monthly Progress Report No. 5

Development of a Prototype Flexible Radiator System

1.0 Overall Progress

Work during the fifth reporting period has been concentrated on the design and fabrication phases of the flexible radiator development program and addresses the following subjects:

- 1) radiator design for selected transport fluids
- 2) UV degradation of flexible radiator adhesives
- 3) lamination of radiator fin materials
- 4) machining of tooling plates for fabricating the radiator panel assembly.

The optimum weight and dimensions of the radiator panel were determined for Coolanol 15 and Ethylene Glycol-Water transport fluids. Ultraviolet degradation tests are being conducted at NASA Langley Research Center to determine whether it is possible to delete the Silver/Inconel vacuum deposited coating currently being employed to protect the adhesives from solar exposure. The composite radiator fin material consisting of silver wire mesh and FEP Teflon was fabricated successfully at Sheldahl Advanced Products Division. A tooling plate for laminating the fin materials to transport tubing is being produced by the Vought SES Laboratory.

2.0 Progress on Individual Major Areas

2.1 Radiator Design for Selected Transport Fluids. Calculations were made to determine the radiator panel and deployment system size, weight and operating limits for Coolanol 15 and RS-89a transport fluids. As discussed in Progress Report No. 3, these fluids have acceptable thermal properties and have very low rates of permeation through the flexible transport tubing. FEP Teflon and Hytrel tubing are compatible with these fluids, and have sufficient strength and flexibility at high and low temperatures. Table I summarizes the radiator design parameters which result from optimizing the system based on the thermodynamic properties of the two fluids. The table shows that the system weight and size are reduced if RS-89a is selected over Coolanol 15. However, the minimum stable fluid outlet temperature is lower for Coolanol 15. Figure 1 gives the stability curves of the two fluids for the series connected banks of parallel tubes of the flexible radiator. The data in Fig. 1 are determined by methods described in reference (1). They show that the minimum stable outlet temperature for Coolanol 15 is from 25°F to 75°F lower than for RS-89a. This is probably more significant than the advantage of weight and size for RS-89a. However, the stable range of operation for either fluid is too narrow for most space applications where the mixed fluid outlet temperature is regulated by means of a typical by-pass valve type controller. The disadvantage of a narrow stable operating band can be off-set by employing a controller which adjusts the extent of deployment of radiator panel to prevent the fluid outlet temperature from becoming too cold during low-load conditions. If

TABLE I
COMPARISON OF FLEXIBLE RADIATOR DESIGNS

<u>DESIGN VARIABLE</u>	<u>RS-89A</u>	<u>COOLANOL 15</u>
Radiator Panel Length	24.1'	25.7'
Radiator Panel Area	76.9 Ft ²	82.0 Ft ²
Radiator Panel Width	38"	38"
Number of Tubes	50	50
Tube Spacing	0.75"	0.75"
Tube Outside Diameter	0.125"	0.125"
Tube Inside Diameter	0.0625"	0.0625"
Relative Weight *	51.3 lb	58.3 lb
Pressure Drop	33.0 psi	25.5 psi
Bending Moment for 10" Dia Drum	14 in-lb	14 in-lb
Minimum Outlet Temp. (100°F Inlet)	-20°F	-70°F
Radiator Fin Emissivity	0.71	0.71
Radiator Fin Efficiency	0.943	0.943
Spring Dimensions (5" Dia Mandrel)	.0167" x 3" x 29'	.0167" x 3" x 31'

*The relative weight includes manifolds, the deployment drum, retraction springs, transport tubing and fittings, transport fluid, radiator fins, and the weight penalty for fluid pressure drop.

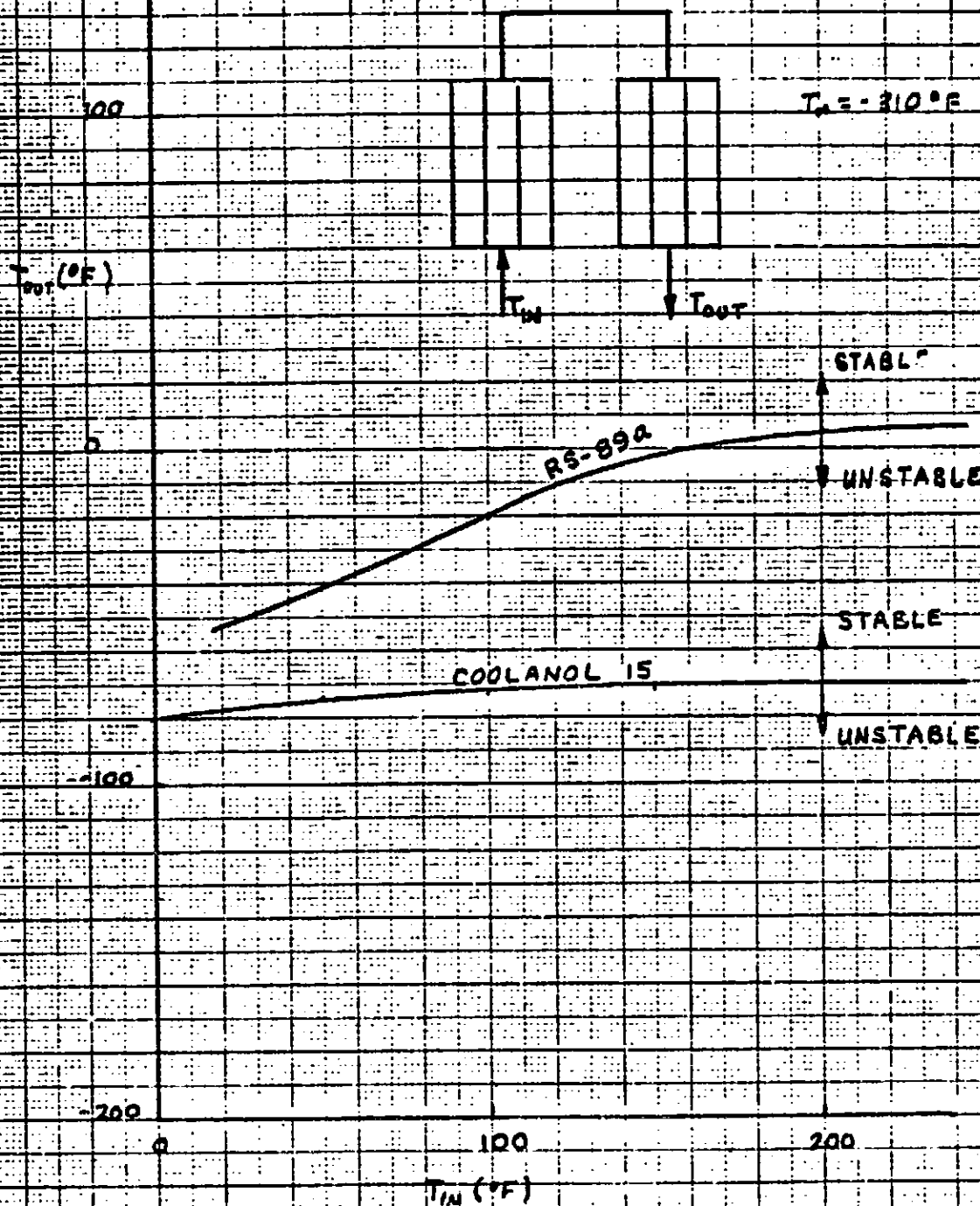


FIG. 1 APPROXIMATE STABILITY CURVES FOR
CANDIDATE FLEXIBLE RADIATOR FLUIDS

this is done, the limits of stable operation will influence the design of the controller, but the magnitude of the effect is unknown at the present time. A Vought funded study is being conducted to establish a preliminary controller design for flexible radiators.

The availability of Coolanol 15 for future flexible radiator applications is questionable. There are currently only 441 gallons in existence, and the manufacturer (Monsanto) does not plan to continue production. The minimum order required to re-open production is 7000 gallons at the current price of approximately \$110 per gallon.

The radiator designs summarized in Table I are based on results given in Figures 2-10. Figure 2 gives the bending moment which must be supplied by retraction springs to wrap the radiator panel around a 10" dia. deployment drum for various tubing diameters and spacing. Since the tubing must be connected to manifolds with standard sized fittings, only two diameters, .0625" and .125", given on the abscissa of Fig. 2 are actually practical for the prototype test article. The weight and size of the deployment system required to support the bending moment associated with the 0.125" ID tubing is much greater than for the 0.0625" ID tubing.

Figures 3-6 show the effect of tube spacing and diameter on required radiator panel area and length for the two transport fluids. The figures show that the panel size is relatively sensitive to tube spacing and is smallest for close tube spacing. Tube spacing less than 0.75" is not practical because of weight considerations and associated problems in fabricating the radiator panel.

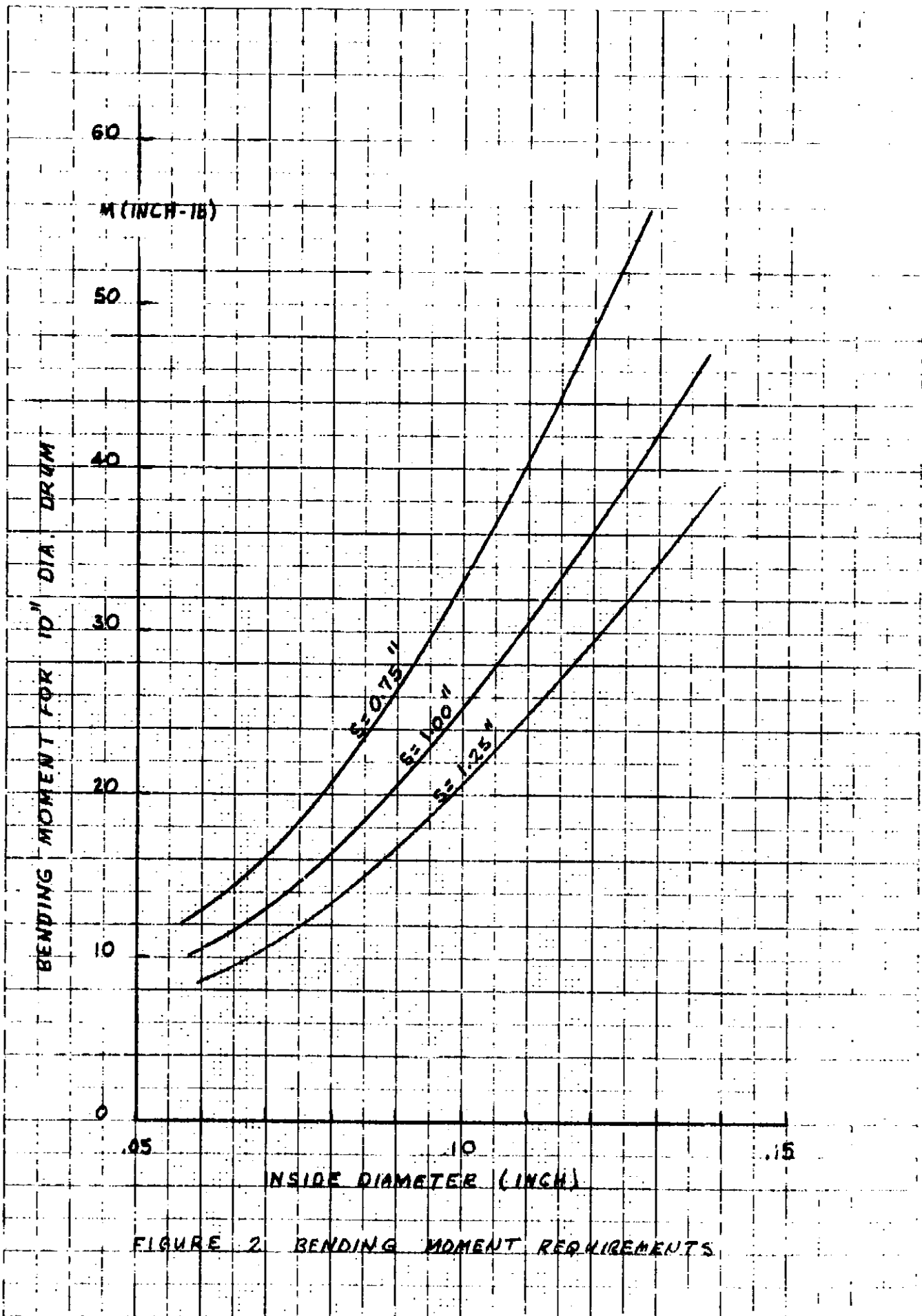
Figures 7 and 8 give the system wet weight as a function of tube diameter and spacing. The curves show that the minimum weight occurs at diameters intermediate to the two practical values of .0625" and 0.125". However, the weight obtained for .0625" ID and 0.75" spacing is only a few pounds greater than the minimum possible value. The system weight given in Figs. 7 and 8 includes a weight penalty for pumping power which is assessed assuming a penalty factor of 540 lb./kw and a combined pump/motor efficiency of 13%. It does not include the weight of a deployment box or of other hardware which is independent of the radiator panel configuration.

For reference purposes, the pressure drop across the radiator panel is given in Figs. 9 and 10. The data given in the figures includes the pressure losses in the manifolds, and minor losses at the tube fittings.

Considering radiator panel stiffness, weight, and area, and the practicality of standard tube sizing; a tube spacing of 0.75" and tubing ID of 0.0625" is recommended. The required tubing OD for 90% survivability for a 30 day mission in a micrometeoroid environment is 0.125". This leads to the radiator design summarized in Table I. Coolanol 15 is better suited for this application than RS-89a because of low temperature operating characteristics. However, because of the possibility of Coolanol 15 being unavailable for future applications, it is recommended that the prototype radiator be tested with RS-89a.

2.2 Ultraviolet Degradation of Flexible Radiator Adhesives

A 30 day solar exposure test of General Electric SR 585 adhesive is in progress at NASA Langley Research Center. The test sample consists of a small section of flexible radiator fin material bonded to a polished aluminum test fixture with SR 585 adhesive. The sample is tested in a vacuum environment with the ultraviolet flux directed on the adhesive through the transparent fin material. This approximates the shielding of the adhesive by the fin material that would actually occur in a solar oriented space application of the flexible radiator. However, the presence of the aluminum test fixture could have an undesirable effect on the test results. The fin material and



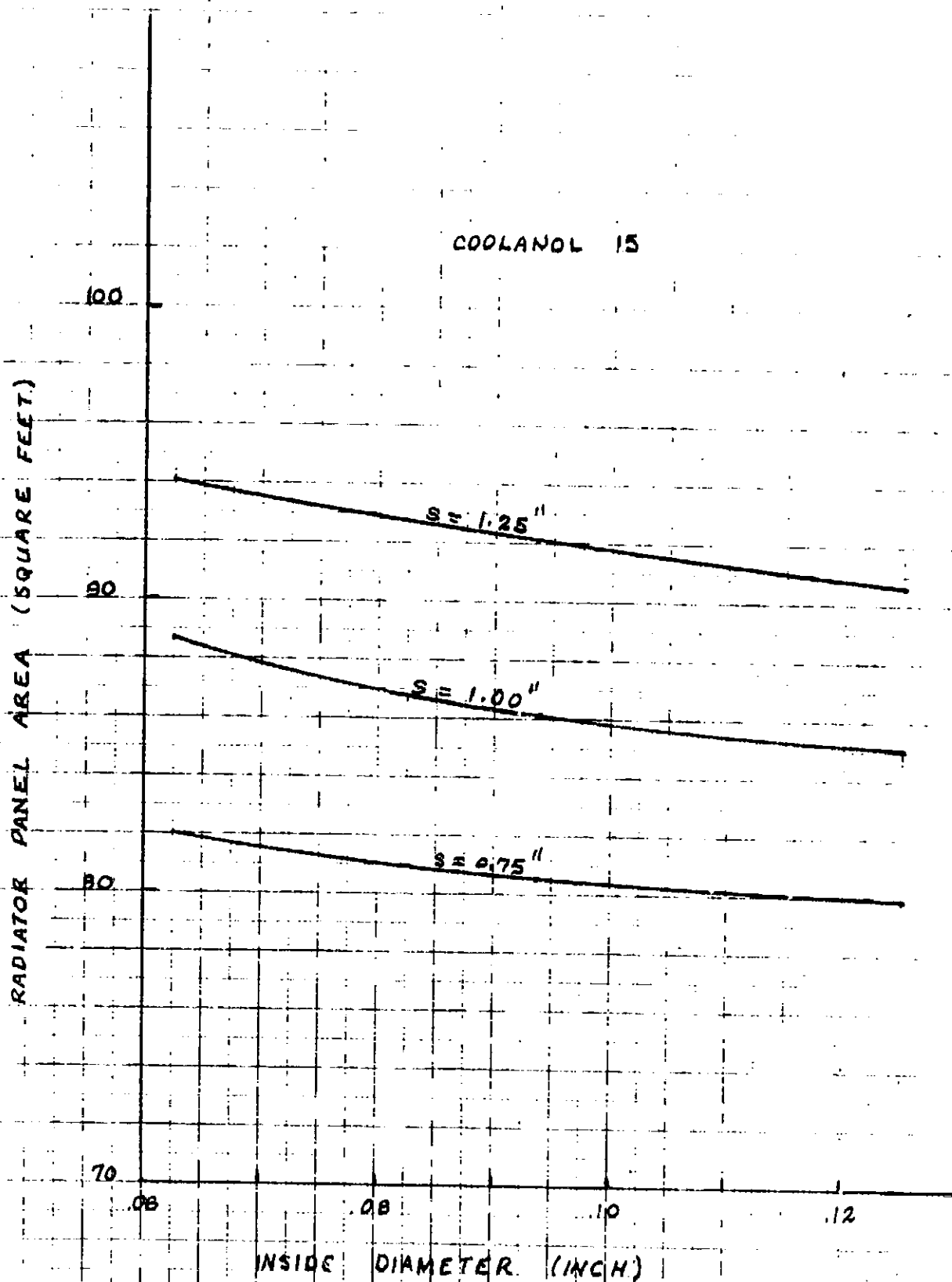


FIGURE 3 RADIATOR AREA REQUIREMENTS FOR COOLANOL 15

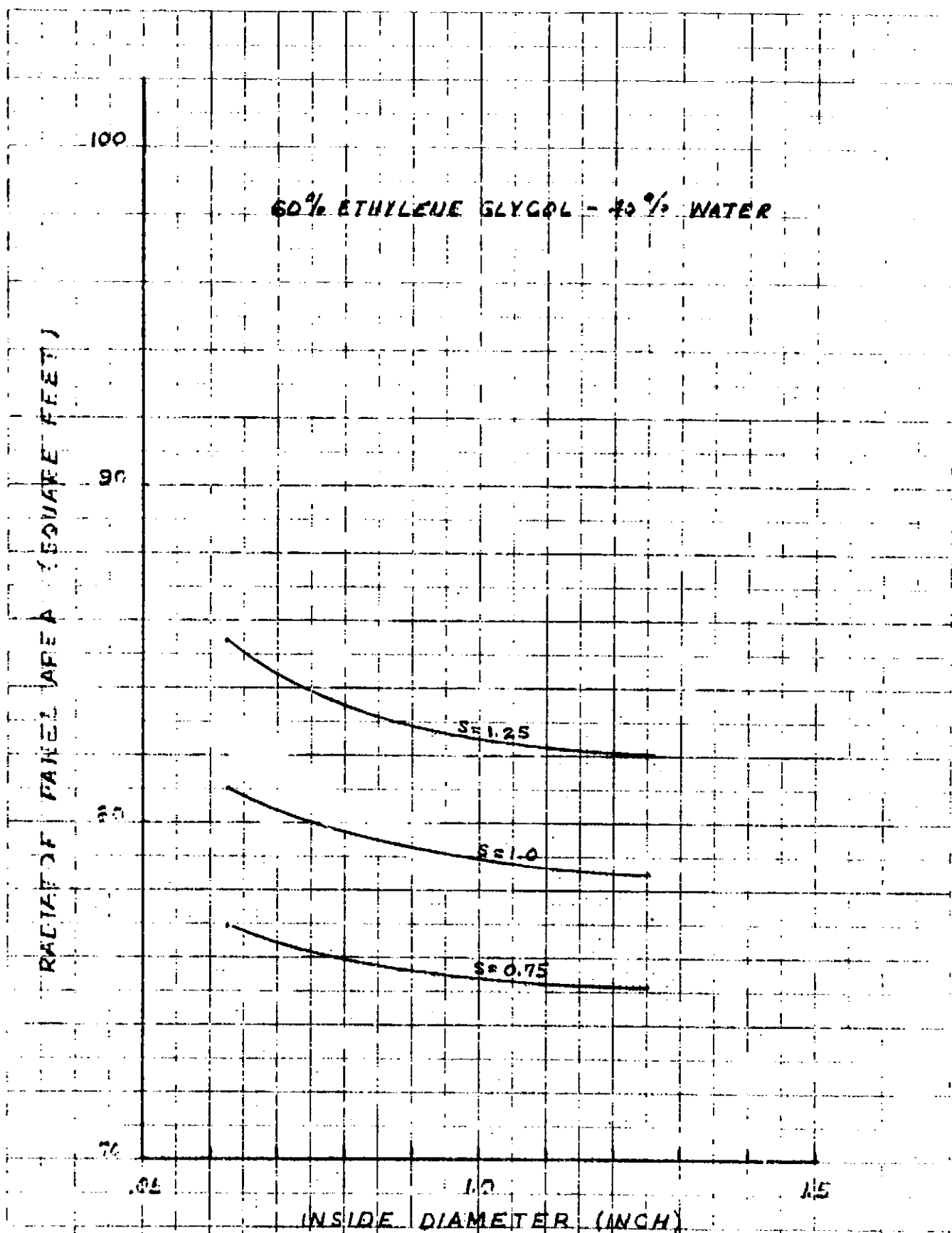


FIGURE 4 RADIATOR AREA REQUIREMENTS FOR RS-89 a

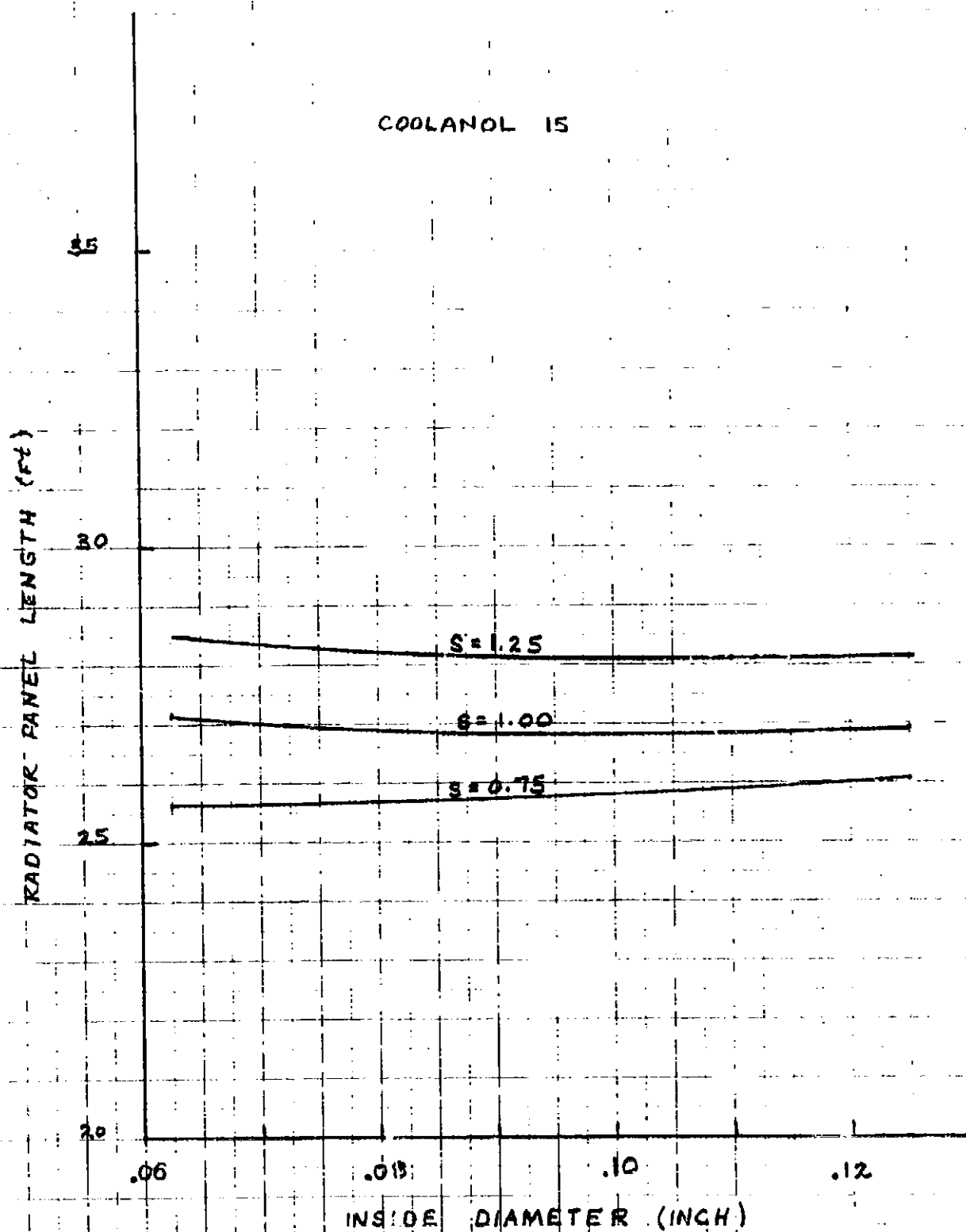


FIGURE 5. RADIATOR LENGTH REQUIREMENTS FOR COOLANOL 15

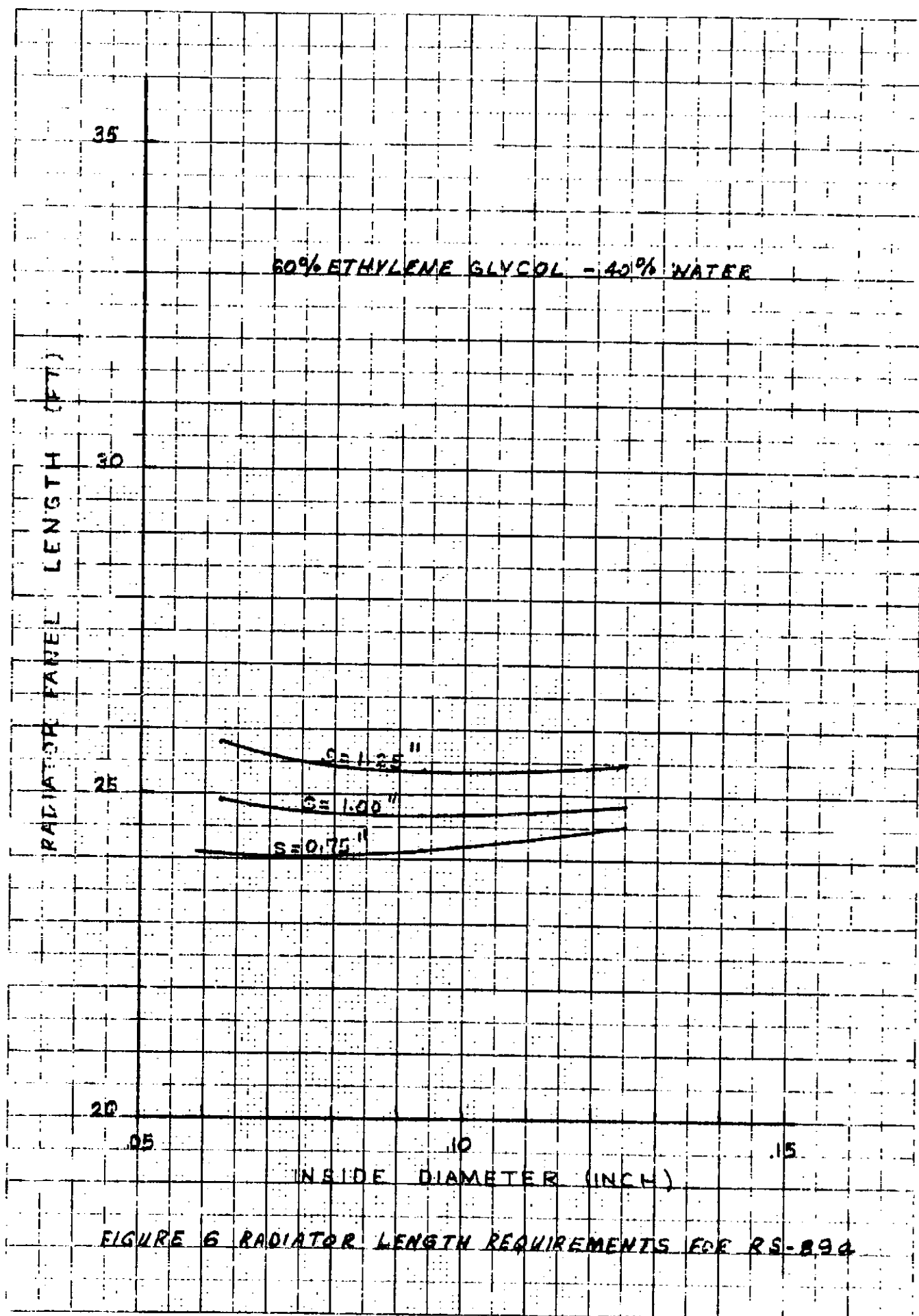
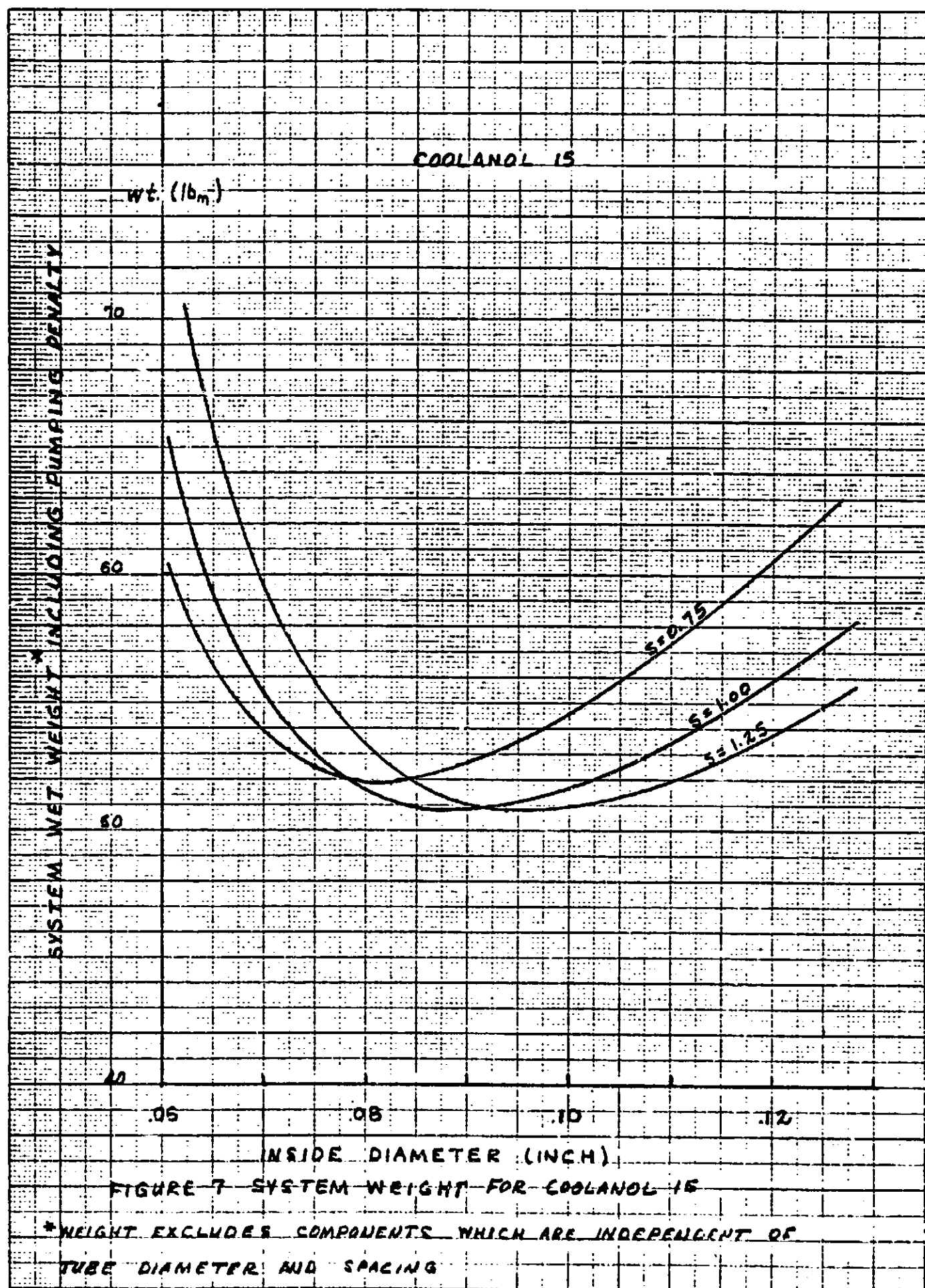
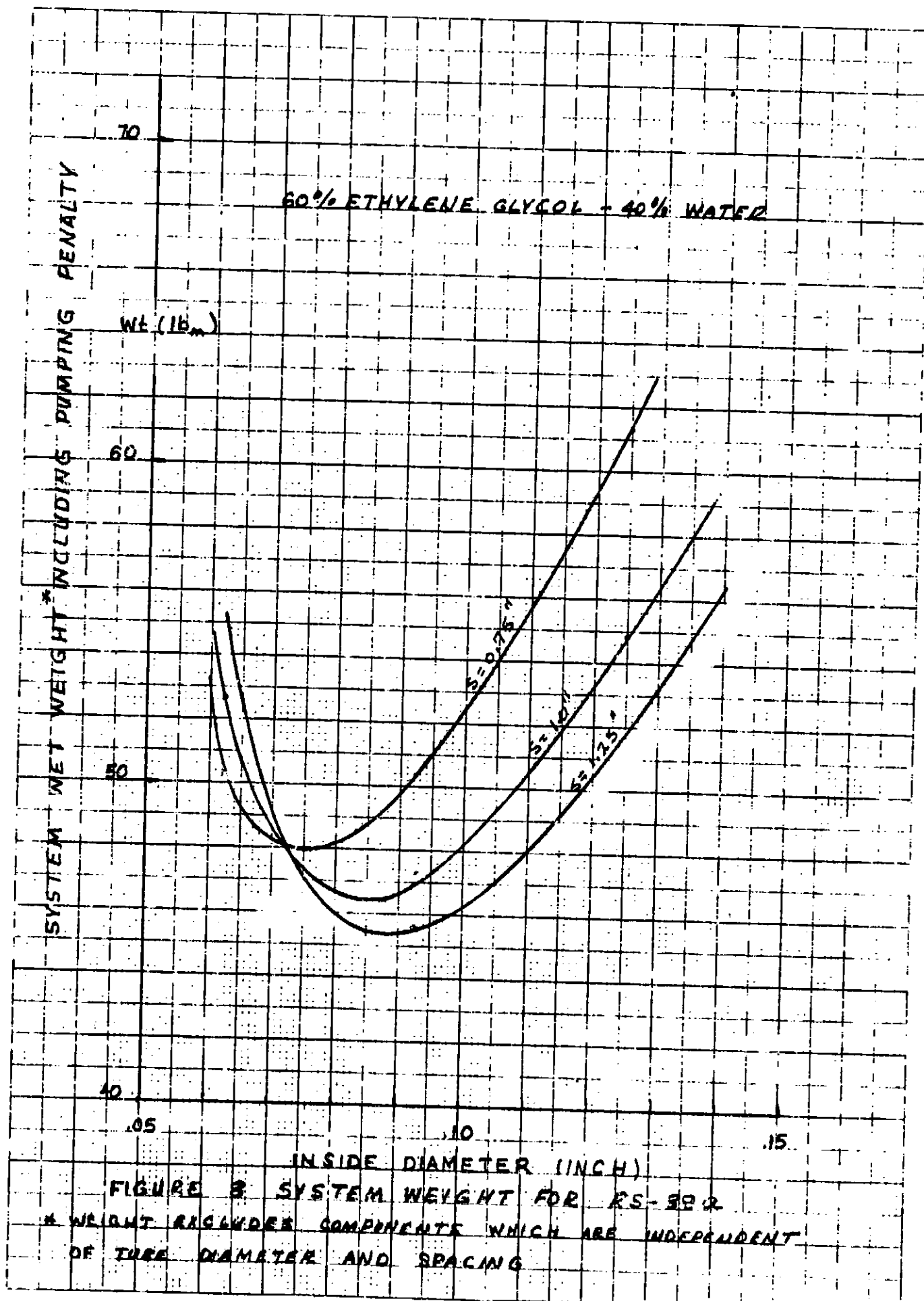


FIGURE 6 RADIATOR LENGTH REQUIREMENTS FOR RS-894

461510

K-E 10 X 10 TO THE CENTIMETER 10 X 25 CM
KUPFER & ESSER CO. MADE IN U.S.A.



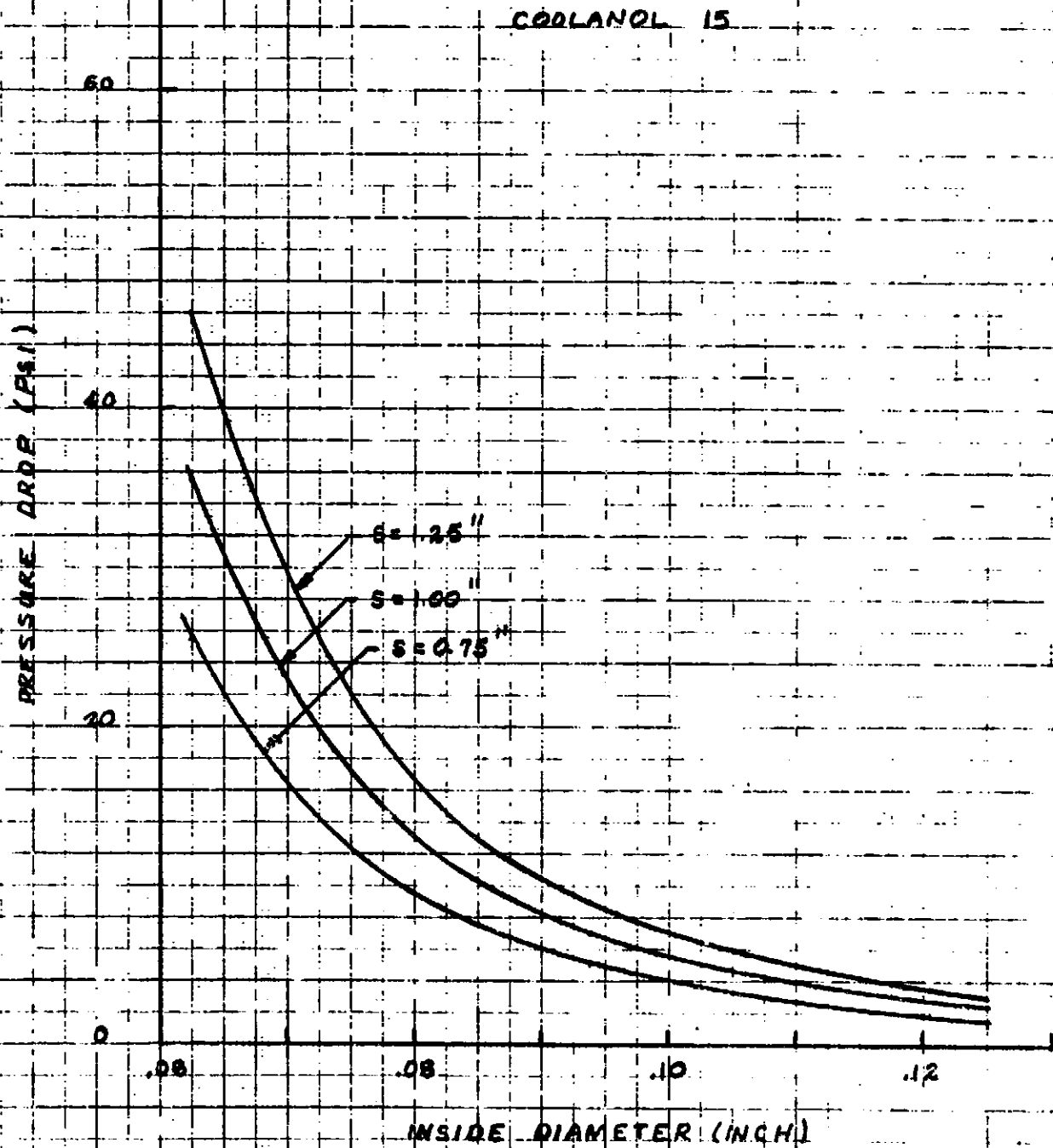
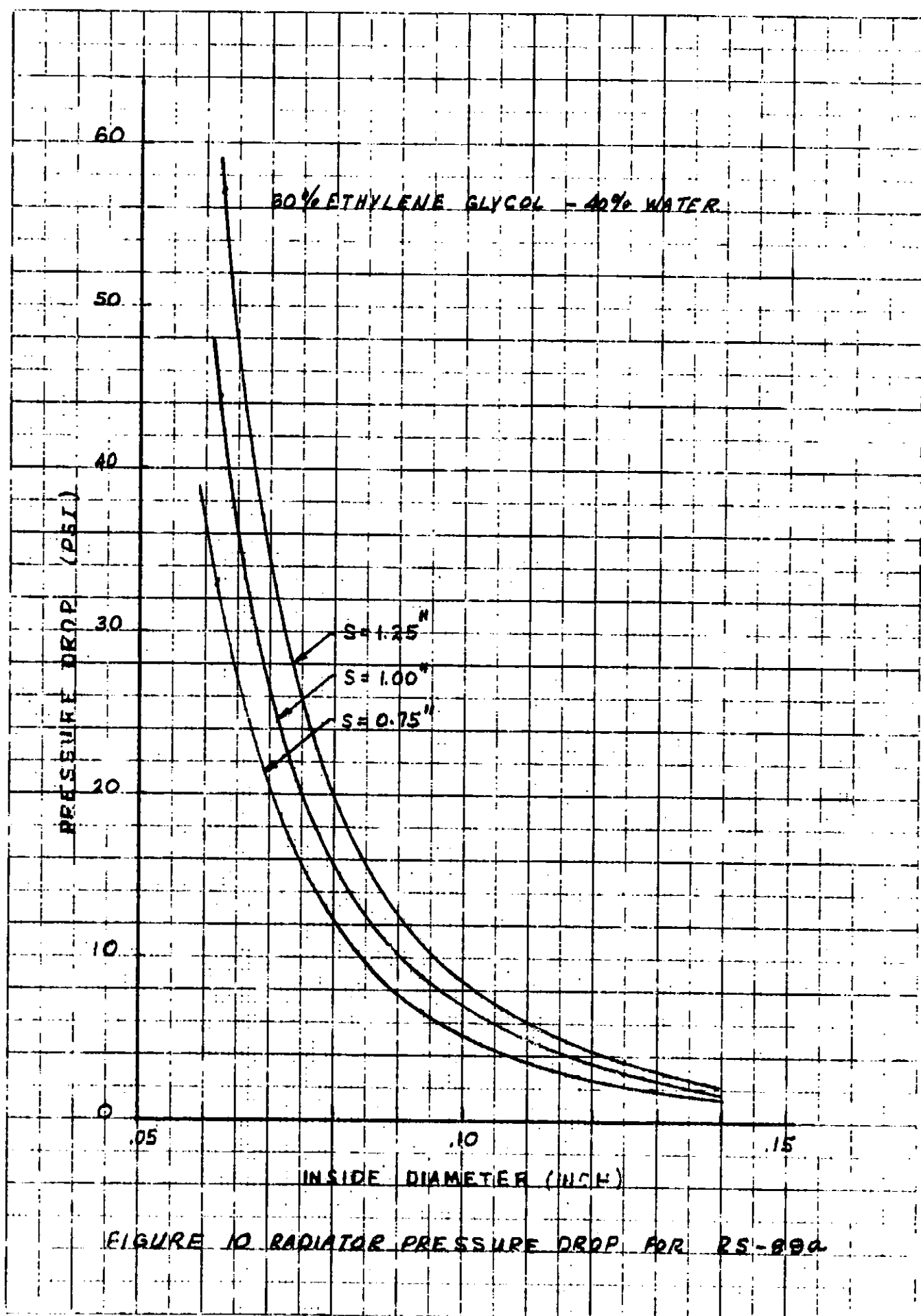


FIGURE 9 RADIATOR PRESSURE DROP FOR COOLANT 15



adhesive are transparent so that the aluminum mounting fixture is visible through the test specimen. Thus the emittance and absorptance measurements made for the test sample include the properties of the aluminum fixture. If the adhesive reacts with the test fixture such that it changes the aluminum surface properties, the effects of the degraded aluminum properties will be indistinguishable from those which would be associated with the degradation of the adhesive. Also, since the solar absorptance of the aluminum is relatively high, the equilibrium temperature of the test sample is higher than the normal operating temperature of the radiator. Data for the first week of testing show that the measured solar absorptivity of the test sample is increasing as a result of the UV exposure. This could mean that the adhesive is degrading and would thus require protection from solar exposure. The present plans are to continue the current test to see if the early trends continue, and to try to devise an alternate test which better simulates the actual radiator operating conditions.

2.3 Lamination of Radiator Fin Material

Sheldahl Advanced Products Division fusion bonded silver wire mesh to Teflon film to produce the fin material to be used in the flexible radiator. The fin material is produced on a roll laminating machine which employs matched heated rollers to increase the temperature of the Teflon to the melting point and to press the silver screen into the molten film. This is an unusual laminating process which required modification and adjustment of the roll laminating equipment. Sheldahl had requested that Vought supply three times the quantity of materials actually required. They actually needed only twice the required amount and thus were able to produce more fin material than is needed to fabricate the radiator. However, the silver wire mesh (purchased from Newark Wire and Cloth Company) is relatively non-uniform, and as a result, not all of the fin material produced is usable. The excess fin material not used in the prototype radiator will be stored and eventually used to make smaller sections of radiator for element tests and demonstration purposes.

Because of the high cost and relatively poor quality of the silver wire mesh, alternate vendors or materials such as expanded silver metal foil should be considered. The mesh used in the prototype radiator contained several small void areas where wires had been skipped in the weaving process; and large sections were severely distorted, apparently as a result of stretching the wire when stowing it for shipment. The small diameter wire is very flimsy and easily damaged.

2.4 Machining of Tooling Plates for Fabricating the Radiator Panel Assembly

The tooling plate described in the Progress Report No. 2 is being fabricated in the Vought SES Laboratory. The fabrication of the plate should be completed during the next reporting period.

3.0 Progress on Major End Items

The program is on schedule. Work is in progress in the design and fabrication phases.

4.0 Work Scheduled During the Next Reporting Period

The UV degradation tests of adhesives at NASA Langley Research Center and the fabrication of tooling plates in the SES laboratory will continue. Otherwise very little activity is scheduled during December 1976. The next fabrication phase activities depend on the outcome of the adhesives tests. Vought funded Research and Development will be conducted during December 1976 to prepare for future bid opportunities on long life flexible radiators and to develop a control system for the prototype radiator.

References

- (1) Leach, J.W., "Flow Instabilities in Spacecraft Radiators", Vought Report No. 169-56, 20 Nov. 1974.

DEVELOPMENT OF A PROTOTYPE FLEXIBLE RADIATOR SYSTEM

PROGRESS REPORT NO. 6

1 DECEMBER through 31 DECEMBER 1976

3 JANUARY 1977

CONTRACT NO. NAS9-14776
DRL: T-1213, LINE ITEM 2
DRD: MA-182TD

Submitted to:

THE NATIONAL AERONAUTICS AND SPACE ADMINISTRATION
JOHNSON SPACE CENTER
HOUSTON, TEXAS

BY

VOUGHT CORPORATION
An LTV Company
Dallas, Texas 75222

PREPARED BY:

J. W. Leach
J. W. Leach

CHECKED BY:

J. A. Oren
J. A. Oren

APPROVED BY:

R. L. Cox
R. L. Cox

MONTHLY PROGRESS REPORT NO. 6

DEVELOPMENT OF A PROTOTYPE FLEXIBLE RADIATOR SYSTEM

1.0 Overall Progress

Work during the sixth reporting period has been concentrated on the design and fabrication phases of the flexible radiator development program and addresses the following subjects:

- 1) Ultraviolet degradation of flexible radiator adhesives
- 2) Machining of tooling plates for fabricating the radiator panel assembly.

Ultraviolet degradation tests are being conducted at NASA Langley Research Center to determine whether it is possible to delete the Silver/Inconel vacuum deposited coating currently being employed to protect the adhesives from solar exposure. A tooling plate for laminating the composite flexible radiator fin material to transport tubing is being produced by the Vought SES laboratory.

2.0 Progress on Individual Major Areas

2.1 Ultraviolet Radiation Degradation of Flexible Radiator Adhesives.

The vacuum/solar degradation test of General Electric SR 585 adhesive at NASA Langley Research Center was terminated after two weeks exposure. The solar absorptivity data collected during the test and presented in Table I show that the properties of the adhesive did change appreciably as a result of the vacuum/ultraviolet radiation exposure.

TABLE I VACUUM Ultraviolet Radiation Degradation of
General Electric SR 585 Adhesive

<u>Test Condition</u>	<u>Solar Absorptivity</u>
Ambient Air	0.260
Vacuum	0.273
After 5 days in vacuum	0.282
After 42 hrs vacuum/UV exposure	0.291
After 68 hrs vacuum/UV exposure	0.302
After 159 hrs vacuum/UV exposure	0.312
After 325 hrs vacuum/UV exposure	0.354

The adhesive sample was examined under a microscope following the test to determine whether the absorptivity measurements actually reflect physical degradation of the adhesive. As described in Progress Report No. 5, there was some concern that the aluminum test fixture to which the adhesive was attached might influence the test results. However, the post test examination revealed that the adhesive had darkened, and therefore, would necessarily have a higher absorptivity than it initially had as a transparent film. Small sections were observed where the adhesive was not in contact with the aluminum test fixture. These sections had the same appearance and color as the sections which were in contact with the aluminum. This indicates that the adhesive had degraded independently of the test fixture, and that the changes in the solar absorptivity measurements are tied directly to the physical degradation of the adhesive. Because of the magnitude of the absorptivity increase in Table I, the SR-585 adhesive is unacceptable for the flexible radiator application unless it is protected from solar exposure.

A second test specimen was prepared with SR 573 adhesive and shipped to NASA Langley for testing. If this sample does not degrade, SR 573 will be used to fabricate the radiator. If the adhesive does degrade, the radiator will be fabricated with either SR-585 or SR-573 adhesive, and a protective coating of Silver/Inconel will be provided as originally planned. The tests at NASA Langley will be terminated in January 1977.

2.2 Machining of Tooling Plates for Fabricating the Radiator Panel Assembly

The Vought SES Laboratory completed work on the Flexible Radiator tooling plate. A plumbing system is being fabricated to connect the plate to the Vought 12' diameter vacuum chamber. The vacuum equipped plate will be used to hold the radiator panel and tubing in position for lamination. The radiator will be laminated during February 1977.

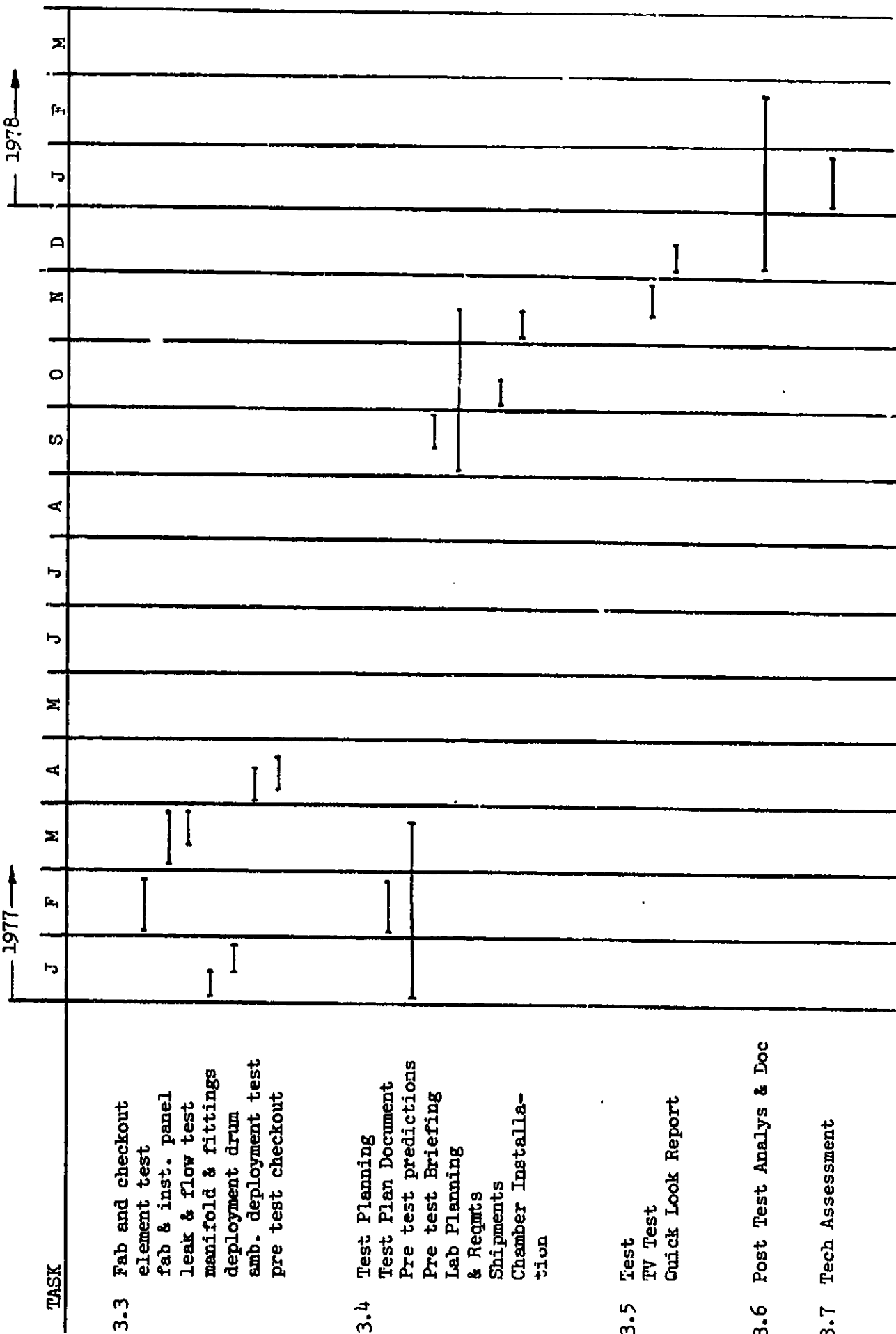
3.0 Progress on Major End Items

The Flexible Radiator thermal vacuum test at NASA-JSC has been rescheduled for November 1977 to coincide with the availability of the NASA-JSC vacuum chamber. The revised Flexible Radiator development program schedule is given in Fig. 1. The design phase of the program is essentially complete. Work is in progress on the fabrication phase.

..0 Work Scheduled During the Next Reporting Period

The ultraviolet degradation tests of adhesives at NASA Langley Research Center will continue during January 1977. The flexible radiator deployment drum, manifolds, and fittings will be fabricated in the Vought SES Laboratories.

FIGURE 1 REVISED FLEXIBLE RADIATOR PROTOTYPE DEVELOPMENT PROGRAM SCHEDULE



DEVELOPMENT OF A PROTOTYPE FLEXIBLE RADIATOR SYSTEM

PROGRESS REPORT NO. 7

1 JANUARY through 31 JANUARY 1977

9 FEBRUARY 1977

CONTRACT NO. NAS9-14776
DRL: T-1213, LINE ITEM 2
DRD: MA-182TD

Submitted to:

THE NATIONAL AERONAUTICS AND SPACE ADMINISTRATION
JOHNSON SPACE CENTER
HOUSTON, TEXAS

BY

VOUGHT CORPORATION
An LTV Company
Dallas, Texas 75222

PREPARED BY:

J. W. Leach
J. W. Leach

CHECKED BY:

J. A. Oren
J. A. Oren

APPROVED BY:

R. L. Cox
R. L. Cox

MONTHLY PROGRESS REPORT NO. 7

DEVELOPMENT OF A PROTOTYPE FLEXIBLE RADIATOR SYSTEM

1.0 OVERALL PROGRESS

Work during the seventh reporting period has been concentrated on the fabrication and test planning phases of the flexible radiator development program and addresses the following subjects.

1. Ultraviolet degradation of flexible radiator adhesives
2. Fabrication of manifolds and the deployment drum
3. Computer math models for pre-test predictions
4. Selection of time and place for thermal vacuum testing
5. Hypervelocity impact testing

2.0 PROGRESS ON INDIVIDUAL MAJOR AREAS

2.1 Ultraviolet Radiation Degradation of Flexible Radiator Adhesives

Two samples of flexible radiator adhesives were tested at NASA-Langley Research Center. The first sample consists of General Electric SR-585 adhesive sprayed on an aluminum test fixture. The solar absorptivity increased from 0.155 to 0.215 during 583 hours of exposure. Although this rate of degradation is not as severe as was measured for a previous sample of SR-585 adhesive covered with flexible radiator fin material, it is still unacceptable for this flexible radiator application. The second sample consists of a section of flexible radiator fin material glued to an aluminum test fixture with SR-573 adhesive. The solar absorptivity measurements for the sample are given in Table I.

TABLE I
UV EXPOSURE DATA FOR GE SR-585 ADHESIVE

<u>Test Conditions</u>	<u>α</u>
In air before exposure to vacuum	0.230
In vacuum prior to UV exposure	0.233
In vacuum after 19 hours UV exposure	0.256
In vacuum after 66 hours UV exposure	0.261
In vacuum after 180 hours UV exposure	0.279

The results show that the rate of degradation for SR-573 is too great for the flexible radiator requirements. NASA-Langley has requested a second SR-573 adhesive sample without radiator fin material. This sample is being prepared

by Vought. However, because of schedule commitments it is not possible to delay the fabrication of the radiator panel to obtain data from this test. Because of the increase in solar absorptivity measured for the other samples a decision was made jointly by NASA/JSC and Vought to provide UV protection for the flexible radiator adhesive. This requires that the radiator fin be coated with silver/Inconel prior to the application of the adhesive.

2.2 Fabrication of Manifolds and Deployment Drum

The Vought SES Laboratory is manufacturing the manifolds and deployment drum for the prototype radiator. The manifold is 0.50 inch I.D. x 0.75 inch O.D. 6061-T6 aluminum. Swagelok compression type fittings are being welded into holes drilled through the 0.125 inch thick tube stock on 0.75 inch centers. The Swagelok forgings to be welded into the manifold are 2014 aluminum. Special order anodized swagelok nuts are being purchased in place of the standard swagelok nuts which are cadmium plated 2017 aluminum. The deployment drum is being rolled formed from 0.0625 inch thick 6061-T6 aluminum sheets.

2.3 Computer Math Model

Two SINDA thermal math models are being prepared to perform pre-test predictions for the flexible radiator thermal vacuum test. The first model is designed to expedite the development of a method for controlling the fluid outlet temperature by regulating the extent of deployment of the radiator panel. It models a typical flow path rather than a bank of parallel flow passages. It accounts for fluid lag time in the manifolds and also models the thermal interactions between adjacent elements of the radiator panel as the radiator is rolled or unrolled from the deployment drum. This model will be employed to test candidate methods for controlling the system, and will not require excessive computation time. The second computer model being developed is much more complex, and simulates thermal interactions such as the heat transfer between adjacent tubes which are not accounted for in the first model. It will be employed to make the final pre-test predictions after a method of control has been established from the simpler model.

2.4 Selection of Time and Place For Thermal Vacuum Testing

NASA/JSC decided that the test would be performed at their facility during July 1977. The decision to test at NASA rather than at Vought was made primarily because NASA has the capability to simulate solar exposures whereas Vought can provide only infrared environments for large test articles. The July time period was selected in accordance with the availability of the NASA Chamber B and the schedule of the Flexible Radiator Development Program.

2.5 Hypervelocity Impact Test Results

Meteoroid impact simulation tests at Texas A&M University were concluded in December 1976. The test report is enclosed as Appendix A. The results indicate that the ballistic equation described in Progress Report No. 1

provides an accurate means for computing the depth of penetration of hypervelocity projectiles in Teflon transport tubing material. This equation has been used as a basis for determining the tube wall thickness required for survival in the near earth micrometeoroid environment. Therefore, no design changes are required as a result of the Texas A&M study.

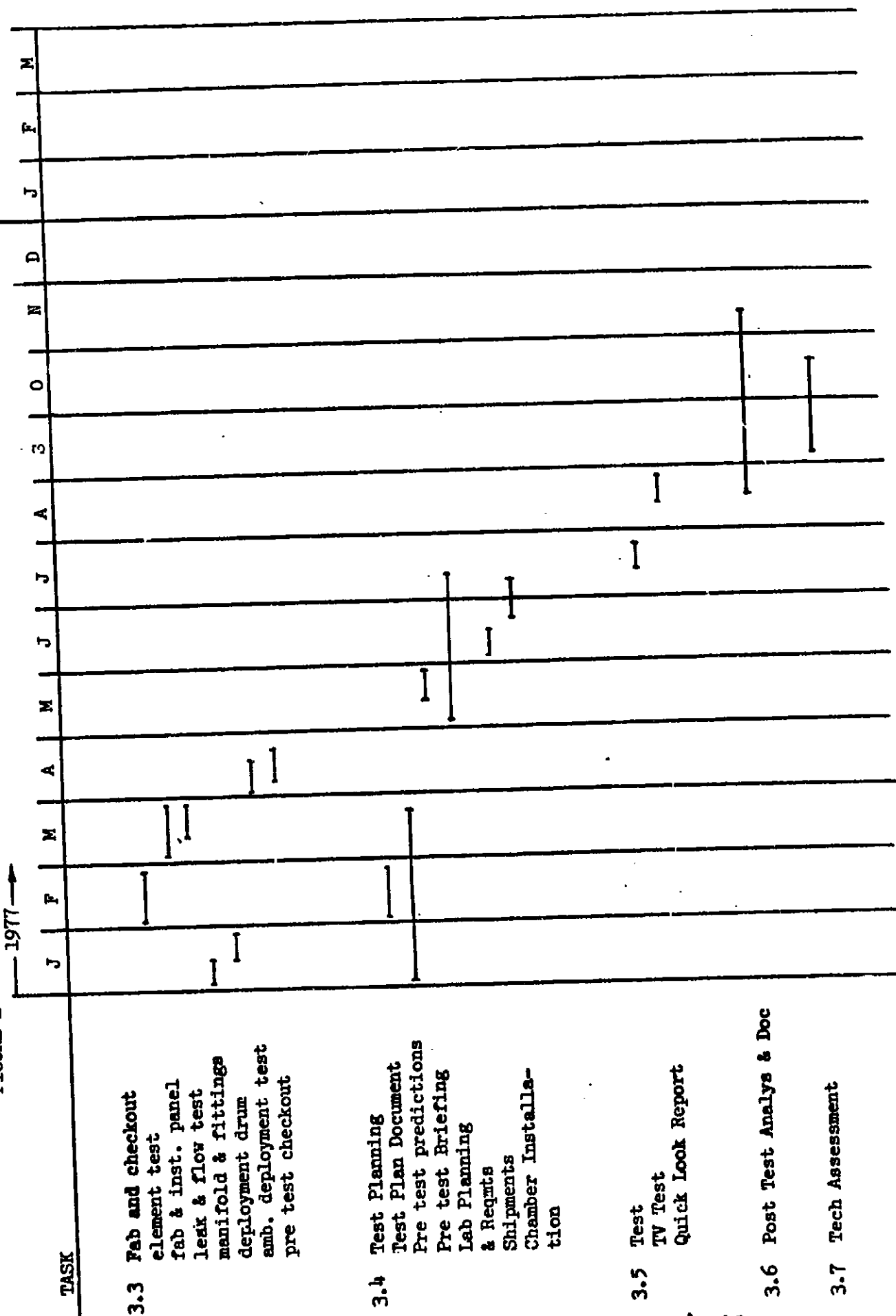
3.0 PROGRESS ON MAJOR END ITEMS

The Flexible Radiator thermal vacuum test at NASA/JSC has been rescheduled for July 1977. The revised Flexible Radiator development program is given in Figure 1. The design phase of the program is essentially complete. Work is in progress in the fabrication and test planning phases.

4.0 WORK SCHEDULED DURING THE NEXT REPORTING PERIOD

Work will continue in the fabrication and test planning phases of the program as shown in Figure 1.

FIGURE 1 REVISED 1977 FLEXIBLE RADIATOR PROTOTYPE DEVELOPMENT PROGRAM SCHEDULE 1978



DEVELOPMENT OF A PROTOTYPE FLEXIBLE RADIATOR SYSTEM

PROGRESS REPORT NO. 8

1 FEBRUARY through 28 FEBRUARY 1977

8 MARCH 1977

CONTRACT NO. NAS9-14776
DRL: T-1213, LINE ITEM 2
DRD: MA-182TD

Submitted to:

THE NATIONAL AERONAUTICS AND SPACE ADMINISTRATION
JOHNSON SPACE CENTER
HOUSTON, TEXAS

BY

VOUGHT CORPORATION
An LTV Company
Dallas, Texas 75222


PREPARED BY:


J. W. Leach

CHECKED BY:


J. A. Oren

APPROVED BY:


R. L. Cox

MONTHLY PROGRESS REPORT NO. 8

DEVELOPMENT OF A PROTOTYPE FLEXIBLE RADIATOR SYSTEM

1.0 OVERALL PROGRESS

Work during the eighth reporting period has been concentrated on the fabrication and test planning phases of the flexible radiator development program and addresses the following subjects.

1. Silver/Inconel coating of fin material
2. Computer math models for pre-test predictions
3. Design of Table for 1-g deployment of radiator
4. Preliminary test sequence and requirements list

2.0 PROGRESS ON INDIVIDUAL MAJOR AREAS

2.1 Silver/Inconel Coating of Fin Material

Sheldahl Advanced Products Division is upgrading their vacuum deposition facilities so that they will be able to coat the flexible radiator fin material in a continuous section. Previously they have had the capabilities to coat 4' x 8' sheets, but have not been able to vacuum deposit silver/inconel on continuous rolls of material. This is significant because it will remove the requirement for having to cut the panel into sections to apply the coating, and subsequently to reconnect it to form 30' lengths.

2.2 Computer Math Model

Two SINDA thermal math models are being prepared to perform pre-test predictions for the flexible radiator thermal vacuum test. The first model is designed to expedite the development of a method for controlling the fluid outlet temperature by regulating the extent of deployment of the radiator panel. It models a typical flow path rather than a bank of parallel flow passages. It accounts for fluid lag time in the manifolds and also models the thermal interactions between adjacent elements of the radiator panel as the radiator is rolled or unrolled from the deployment drum. This model will be employed to test candidate methods for controlling the system, and will not require excessive computation time. The second computer model being developed is much more complex, and simulates thermal interactions such as the heat transfer between adjacent tubes which are not accounted for in the first model. It will be employed to make the final pre-test predictions after a method of control has been established from the simpler model.

2.3 Design of Table for 1-g Deployment of Radiator

Preliminary sketches were prepared for fabricating a deployment table to be used in thermal vacuum tests at NASA/JSC. The table will be

fabricated by NASA-JSC. Ambient deployment tests will be conducted at Vought on an existing table to confirm the design principles of the new table prior to fabrication. The existing table is unsuitable for the thermal vacuum tests. Ambient tests will also be performed with the new table at NASA prior to thermal vacuum testing.

2.4 Preparation for Thermal Vacuum Testing

A preliminary list of instrumentation and NASA-SESL support equipment requirements was prepared and submitted to NASA-JSC. A preliminary test sequence which describes a recommended approach for measuring the flexible radiator performance is enclosed in Appendix A. Analysis pertaining to the optimum spacing and power requirements for IR lamps is given in Appendix B. A detailed test schedule which includes the dates that all test documentation will be submitted to NASA JSC is being prepared by M. L. Fleming.

3.0 PROGRESS MAJOR END ITEMS

The design phase of the program is essentially complete. Work is in progress in the fabrication and test planning phases.

4.0 WORK PLANNED DURING THE NEXT REPORTING PERIOD

Work will continue in the fabrication and test planning phases.

22 Feb 1977

APPENDIX - A

PRELIMINARY FLEXIBLE RADIATOR TEST SEQUENCE

A. SOLAR AND INFRARED ENVIRONMENT, $T = 0^{\circ}\text{F}$

0. Measure α , ϵ

1. Deployment, $T_{\text{IN}} = 100^{\circ}\text{F}$, $\dot{W} = 176 \text{ \#/hr}$
2. Steady State Heat Rejection, $T_{\text{IN}} = 100^{\circ}\text{F}$, $T_{\text{OUT}} = 40^{\circ}\text{F}$, $\dot{W} = 176 \text{ \#/hr}$
3. Environment Calibration, $\dot{W} = 0$, $T_{\text{IN}} = 0^{\circ}\text{F}$
4. Flow Stability Limit, $T_{\text{IN}} = 100^{\circ}\text{F}$, $\dot{W} = 176 \text{ \#/hr}$
5. Recovery From Flow Instability
6. Retraction, $T_{\text{IN}} = 100^{\circ}\text{F}$, $\dot{W} = 176 \text{ \#/hr}$
7. Half Deployment, $T_{\text{IN}} = 100^{\circ}\text{F}$, $\dot{W} = 88 \text{ \#/hr}$
8. Steady State Heat Rejection, Half Deployed, $T_{\text{IN}} = 100^{\circ}\text{F}$, $T_{\text{OUT}} = 40^{\circ}\text{F}$,
 $\dot{W} = 88 \text{ \#/hr}$
9. Flow Stability Limit, $T_{\text{IN}} = 100^{\circ}\text{F}$, Half Deployed
10. Recovery From Flow Instability, Half Deployed
11. Retraction, $T_{\text{IN}} = 100^{\circ}\text{F}$, $\dot{W} = 88 \text{ \#/hr}$
12. Steady State Heat Rejection, Retracted, $T_{\text{IN}} = 100^{\circ}\text{F}$, $T_{\text{OUT}} = 40^{\circ}\text{F}$,
 $\dot{W} = 10 \text{ \#/hr}$
13. Deployment, $T_{\text{IN}} = 200^{\circ}\text{F}$, $\dot{W} = 400 \text{ \#/hr}$
14. Steady State Heat Rejection, $T_{\text{IN}} = 200^{\circ}\text{F}$, $T_{\text{OUT}} = 40^{\circ}\text{F}$, $\dot{W} = 400 \text{ \#/hr}$
15. Flow Stability Limit, $T_{\text{IN}} = 200^{\circ}\text{F}$, $\dot{W} = 400 \text{ \#/hr}$
16. Recovery From Flow Instability
17. Half Retraction, $T_{\text{IN}} = 200^{\circ}\text{F}$, $\dot{W} = 400 \text{ \#/hr}$
18. Steady State Heat Rejection, Half Deployed, $T_{\text{IN}} = 200^{\circ}\text{F}$, $T_{\text{OUT}} = 40^{\circ}\text{F}$,
 $\dot{W} = 400 \text{ \#/hr}$
19. Flow Stability Limit, Half Deployed, $T_{\text{IN}} = 200^{\circ}\text{F}$
20. Recovery From Flow Instability
21. Retraction, $T_{\text{IN}} = 200^{\circ}\text{F}$, $\dot{W} = 200 \text{ \#/hr}$
22. Steady State Heat Rejection, Retracted, $T_{\text{IN}} = 200^{\circ}\text{F}$, $T_{\text{OUT}} = 40^{\circ}\text{F}$,
 $\dot{W} = 200 \text{ \#/hr}$
23. Deployment, $T_{\text{IN}} = 25^{\circ}\text{F}$, $\dot{W} = 176 \text{ \#/hr}$
24. Outlet Temperature Control, $\dot{W} = 176 \text{ \#/hr}$, $T_{\text{IN}} = 100^{\circ}\text{F}$
25. Outlet Temperature Control, $\dot{W} = 400 \text{ \#/hr}$, $T_{\text{IN}} = 200^{\circ}\text{F}$
26. Solar Exposure, $T_{\text{IN}} = 100^{\circ}\text{F}$, $\dot{W} = 176 \text{ \#/hr}$
27. Steady State Heat Rejection, $T_{\text{IN}} = 100^{\circ}\text{F}$, $T_{\text{OUT}} = 40^{\circ}\text{F}$, $\dot{W} = 176 \text{ \#/hr}$
28. Steady State Heat Rejection, $T_{\text{IN}} = 200^{\circ}\text{F}$, $T_{\text{OUT}} = 40^{\circ}\text{F}$, $\dot{W} = 400 \text{ \#/hr}$
29. Environment Calibration, $\dot{W} = 0$, $T_{\text{IN}} = 0^{\circ}\text{F}$
30. Measure α , ϵ

*Transient response data to be obtained during these test points.

22 Feb 1977

PRELIMINARY FLEXIBLE RADIATOR TEST
SEQUENCE-CONTINUED

B. COLD ENVIRONMENT , $T = -300^{\circ}\text{F}$

1. Deployment, $T_{\text{IN}} = 100^{\circ}\text{F}$, $\dot{W} = 450 \text{ \#/hr}$
2. Steady State Heat Rejection, $T_{\text{IN}} = 100^{\circ}\text{F}$, $T_{\text{OUT}} = 40^{\circ}\text{F}$, $\dot{W} = 450 \text{ \#/hr}$
3. Flow Stability Limit, $T_{\text{IN}} = 100^{\circ}\text{F}$, $\dot{W} = 450 \text{ \#/hr}$
4. Recovery From Flow Instability (IR Lamps)
5. Retraction, $T_{\text{IN}} = 100^{\circ}\text{F}$, $\dot{W} = 450 \text{ \#/hr}$
6. Half Deployment, $T_{\text{IN}} = 100^{\circ}\text{F}$, $\dot{W} = 225 \text{ \#/hr}$
7. Steady State Heat Rejection, Half Deployed, $T_{\text{IN}} = 100^{\circ}\text{F}$, $T_{\text{OUT}} = 40^{\circ}\text{F}$,
 $\dot{W} = 225 \text{ \#/hr}$
8. Flow Stability Limit, $T_{\text{IN}} = 100^{\circ}\text{F}$, $\dot{W} = 225 \text{ \#/hr}$, Half Deployed
9. Recovery From Flow Instability, Half Deployed (IR Lamps)
10. Retraction, $T_{\text{IN}} = 100^{\circ}\text{F}$, $\dot{W} = 225 \text{ \#/hr}$
11. Steady State Heat Rejection, Retracted, $T_{\text{IN}} = 100^{\circ}\text{F}$, $T_{\text{OUT}} = 40^{\circ}\text{F}$
12. Flow Stability Limit, $T_{\text{IN}} = 100^{\circ}\text{F}$, Fully Retracted, Recovery
13. Deployment, $T_{\text{IN}} = 200^{\circ}\text{F}$, $\dot{W} = 1000 \text{ lb/hr}$
14. Steady State Heat Rejection, $T_{\text{IN}} = 200^{\circ}\text{C}$, $T_{\text{OUT}} = 40^{\circ}\text{F}$, $\dot{W} = 1000 \text{ lb/hr}$
15. Flow Stability Limit, $T_{\text{IN}} = 200^{\circ}\text{F}$, $\dot{W} = 1000 \text{ lb/hr}$
16. Recovery From Flow Instability
17. Half Retraction, $T_{\text{IN}} = 200^{\circ}\text{F}$, $\dot{W} = 1000 \text{ lb/hr}$
18. Steady State Heat Rejection, $T_{\text{IN}} = 200^{\circ}\text{F}$, $T_{\text{OUT}} = 40^{\circ}\text{F}$, $\dot{W} = 500 \text{ \#/hr}$
19. Flow Stability Limit, Half Deployed, $T_{\text{IN}} = 200^{\circ}\text{F}$
20. Recovery From Flow Instability
21. Retraction, $T_{\text{IN}} = 200^{\circ}\text{F}$, $\dot{W} = 500 \text{ lb/hr}$
22. Steady State Heat Rejection, Retracted, $T_{\text{IN}} = 200^{\circ}\text{F}$, $T_{\text{OUT}} = 40^{\circ}\text{F}$
23. Flow Stability Limit, $T_{\text{IN}} = 200^{\circ}\text{F}$, Retracted
24. Recovery From Flow Instability
25. Deployment, $T_{\text{IN}} = 25^{\circ}\text{F}$, $\dot{W} = 450 \text{ \#/hr}$
26. Outlet Temperature Control*, $\dot{W} = 450 \text{ \#/hr}$, $T_{\text{IN}} = 50 - 100^{\circ}\text{F}$
27. Outlet Temperature Control*, $\dot{W} = 1000 \text{ \#/hr}$, $T_{\text{IN}} = 75 - 200^{\circ}\text{F}$
28. Steady State Heat Rejection, Deployed, $T_{\text{IN}} = 200^{\circ}\text{F}$, $T_{\text{OUT}} = 40^{\circ}\text{F}$

*Transient response data to be obtained during these test points.

DEVELOPMENT OF A PROTOTYPE FLEXIBLE RADIATOR SYSTEM

PROGRESS REPORT NO. 9

1 MARCH through 31 MARCH 1977

CONTRACT NO. NAS9-14776
DRL: T-1213, LINE ITEM 2
DRD: MA-182TD

Submitted to:

THE NATIONAL AERONAUTICS AND SPACE ADMINISTRATION
JOHNSON SPACE CENTER
HOUSTON, TEXAS

BY

VOUGHT CORPORATION
An LTV Company
Dallas, Texas 75222

PREPARED BY:


J. W. Leach

CHECKED BY:


J. A. Oren

APPROVED BY:


R. L. Cox

MONTHLY PROGRESS REPORT NO. 9
DEVELOPMENT OF A PROTOTYPE FLEXIBLE RADIATOR SYSTEM

1.0 OVERALL PROGRESS

Work during the ninth reporting period has been concentrated on the fabrication and test planning phases of the flexible radiator development program and addresses the following subjects.

1. Computer Math Models for Pre-Test Predictions
2. Preliminary Test Sequence and Requirements List

2.0 PROGRESS ON INDIVIDUAL MAJOR AREAS

2.1 Computer Math Model

Two SINDA thermal math models are being prepared to perform pre-test predictions for the flexible radiator thermal vacuum test. The first model is designed to expedite the development of a method for controlling the fluid outlet temperature by regulating the extent of deployment of the radiator panel. It models a typical flow path rather than a bank of parallel flow passages, accounts for fluid lag time in the manifolds and also models the thermal interactions between adjacent elements of the radiator panel as the radiator is rolled or unrolled from the deployment drum. This model will be employed to test candidate methods for controlling the system, and will not require excessive computation time. The second computer model being developed is much more complex, and simulates thermal interactions such as the heat transfer between adjacent tubes which are not accounted for in the first model. It will be employed to make the final pre-test predictions after a method of control has been established from the simpler model.

2.2 Preparation for Thermal Vacuum Testing

A preliminary list of instrumentation and NASA-SESSEL support equipment requirements was prepared and submitted to NASA-JSC. A detailed test schedule to be submitted to NASA-JSC is being prepared by M. L. Fleming.

3.0 PROGRESS MAJOR END ITEMS

Work is in progress in the fabrication and test planning phases.

4.0 WORK PLANNED DURING THE NEXT REPORTING PERIOD

Work will continue in the fabrication and test planning phases.

DEVELOPMENT OF A PROTOTYPE FLEXIBLE RADIATOR SYSTEM

PROGRESS REPORT NO. 10

1 APRIL THROUGH 30 APRIL 1977

26 MAY 1977

CONTRACT NO. NAS9-14776
DRL: T-1213, LINE ITEM 2
DRD: MA-182TD


Submitted to:

THE NATIONAL AERONAUTICS AND SPACE ADMINISTRATION
JOHNSON SPACE CENTER
HOUSTON, TEXAS

By:

VOUGHT CORPORATION
P. O. BOX 5907
DALLAS, TEXAS 75222

PREPARED BY:


J. W. Leach

CHECKED BY:


J. A. Oren

APPROVED BY:


R. L. Cox

MONTHLY PROGRESS REPORT NO. 10

1.0 OVERALL PROGRESS

Work during the tenth reporting period has been concentrated on the fabrication and test planning phases of the flexible radiator development program and addresses the following subjects:

1. Flexible radiator panel element fabrication
2. Flexible radiator panel element thermal-vacuum test
3. Solar absorptivity of the radiator fin material
4. Planning and Analysis of the prototype thermal-vacuum test at NASA-JSC.
5. Submittal of Technical Paper

2.0 PROGRESS ON INDIVIDUAL MAJOR AREAS

2.1 Element Fabrication

An element test panel was fabricated to check out materials and manufacturing techniques for the prototype radiator. No significant problems were encountered in fabricating the element, and no scale up problems are forecast for the prototype panel. The element was assembled using a grooved vacuum tooling plate described in earlier progress reports. Subsequently, the element panel was removed from the plate and heated in a vacuum bag to cure the adhesive used to bond the two halves of the fin material around the transport tubing. Thermocouples were installed between the two layers of fin materials.

Some small problems were noted which can be avoided when fabricating the prototype. When assembling the element, the half of radiator fin material which is placed on top of the transport tubing and the opposing half of the radiator held in place by the grooved plate was pre-formed to provide grooves for the transport tubing. However when the pre-formed half was placed in position it did not fit properly over the tubing at the outside edges of the tooling plate, and had to be reformed during assembly. This problem is believed to be caused by tolerance buildup in the depth of the grooves in the tooling plate. The grooves are slightly deeper than required so that more fin material is required for the bottom half of the radiator than for the top half. Further work with the element showed that it is not necessary to pre-form the entire top half of the radiator panel. If the center of the panel is pre-formed the top half can be aligned with the bottom half using the center tubes, and the outside edges of the panel can then be formed to fit as the system is assembled. This minimizes the wear of the fin material.

A-111

A second problem associated with wear during assembly occurs when the fin material is pressed too firmly against the sharp edges of the grooves of the cooling plate. If this is done the fin stock is severed where it connects to the transport tubing and the thermal contact between the transport fluid and radiator fin is lost. This occurred on one tube of the element over a distance of approximately 2 inches. This is less than 0.1% of the area of the element panel. A redesign of the rollers used to press the fin against the tubing is required. Additional elements should be made to check the new design before attempting to produce the prototype radiator.

Because the element panel was not constrained during the adhesive cure cycle the Teflon fin material shrank such that the area of the panel was reduced by approximately 10%. This will not occur in the prototype radiator because the panel will be secured to the aluminum tooling plate during the cure cycle. However, shrinkage of the Teflon is a potential problem for applications of the flexible radiator when the transport fluid temperature is maintained at a high level for long periods of time. Additional data are required to determine whether this problem will be significant for typical operating conditions.

The shrinkage of the Teflon did create a minor problem in the fabrication of the element because the spacing of the transport tubing changed during fabrication so that the tubing could not be easily attached to the rigid manifolds. It was necessary to loosen the glue line connection between the tubing and fin material for 0.75" sections at the ends of the element panel in order to attach the tubing to the manifolds. This destroyed the thermal connections between the tubing and the fin material at the ends of the panel (about 8.5% of the total panel area.)

The presence of the thermocouples between the layers of fin material does not appear to cause any detrimental effects. However, the appearance of the radiator is improved if the thermocouple wire is not permitted to cross the transport tubing.

There were no problems with leakage of transport fluid at the manifold connectors, and the flow distribution within the parallel tubing network was found to be uniform. The R.M.S deviation from the average flow for the individual tubes was found to be less than 5 %.

2.2 Element Test

Figure 1 shows the flexible radiator element as installed in the vacuum test chamber. The three tubes at the center of the panel are instrumented with thermocouples at the entrance, mid-plane, and exit sections as shown in Figure 2. Thermocouples were also installed at the fin mid points between the three center tubes to determine the thermal resistance between the fins and the tubes. The inlet and outlet temperatures are measured with immersion thermocouples, and the fluid temperature drop across the element is determined from delta connected immersion thermocouples. The cold walls of the vacuum chamber are instrumented at four locations above, below, and at the sides of the test article. The cold wall thermocouples are located at the mid points of the fins.

All test article and facility data were recorded by hand on data sheets. Readouts of the panel thermocouples were made on a digital temperature indicator capable of reading to 0.1°F. Readings from the delta connected thermocouples measuring inlet and outlet temperatures were displayed on a digital voltmeter capable of reading to 0.001 mv. The temperature of an ice bath was recorded with each data set to provide a real-time check of accuracy. A complete list of test equipment is given in Table I.

Prior to installing the element in the test chamber, the flow in individual tubes was measured by collecting water in open beakers. The flow distribution measured for the twenty five parallel tubes of the element is given in Figure 3.

Thermal-vacuum test data were recorded for inlet temperatures of 100°F and 200°F over a range of flow rates in the laminar flow regime. The vacuum chamber cold walls were maintained at approximately -300°F throughout the test.

Analysis of Environment

The chamber cold walls do not absorb all of the radiation emitted from the test article, but reflect part of it back on the panel. Part of the reflected radiation is absorbed by the element so that the net rate of heat rejection is reduced.

The radiosity from the element shown in Figure 4 is:

$$J_1 = \epsilon_1 E_1 + \rho_1 G_1 \quad (1)$$

when E_1 = blackbody emitted radiation ($\frac{\text{BTU}}{\text{hr-ft}^2}$)

G_1 = irradiation (BTU/hr-ft^2)

for the cold walls

$$J_2 = \epsilon_2 E_2 + \rho_2 G_2 \quad (2)$$

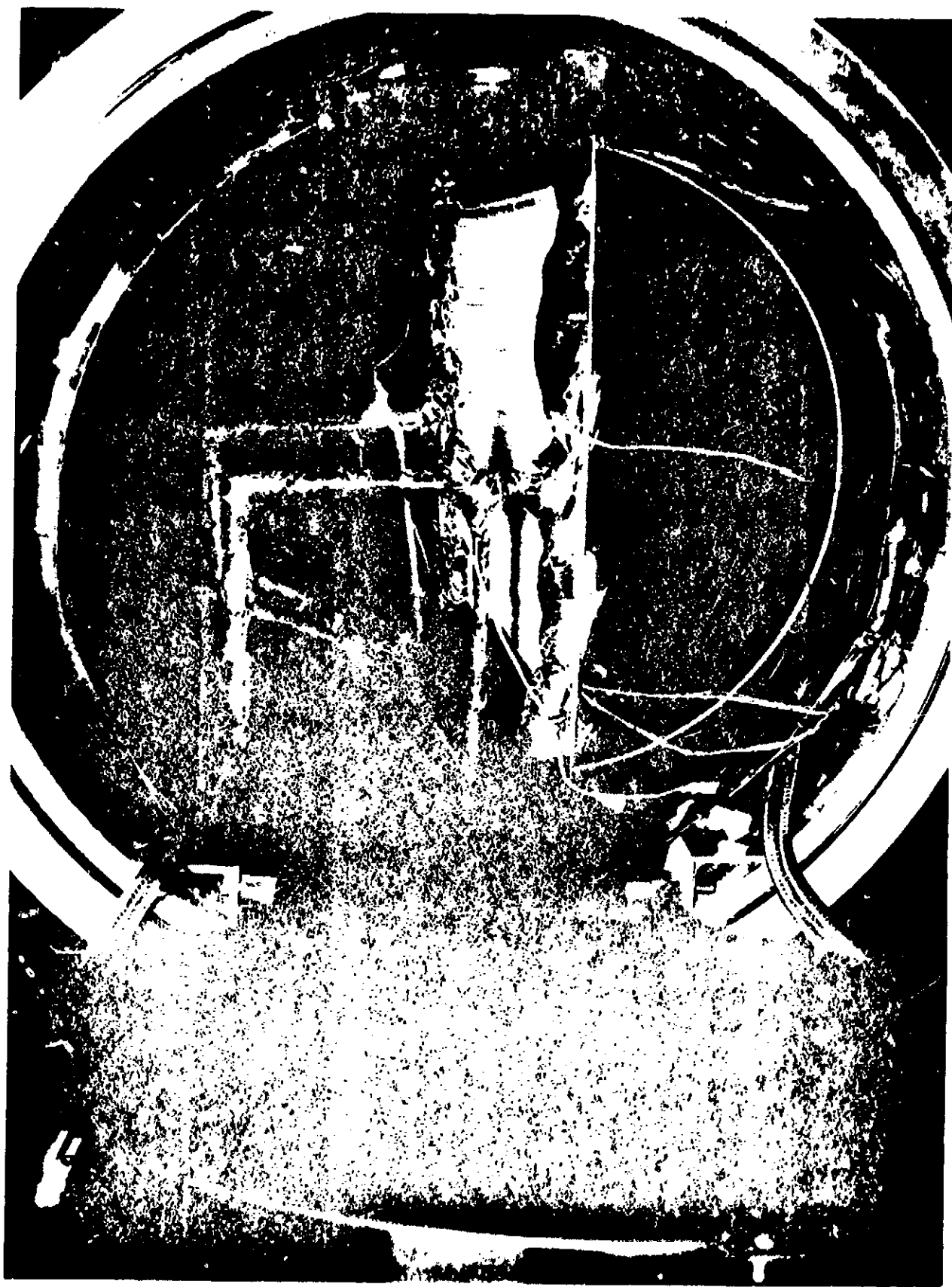
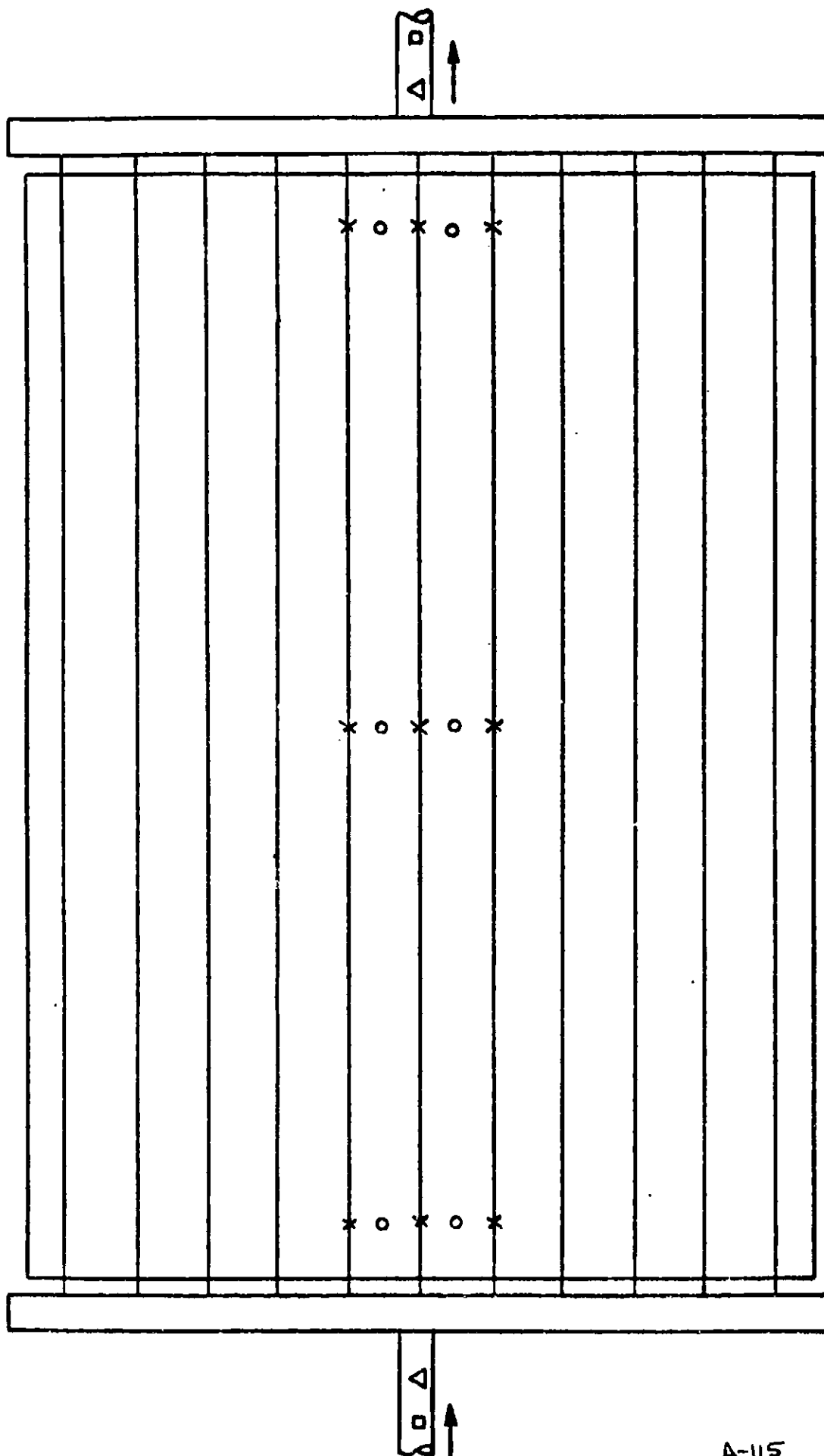


FIGURE 1 FLEXIBLE RADIATOR ELEMENT TEST ARTICLE



□ IMMERSION THERMOCOUPLE x TUBE WALL THERMOCOUPLE
 Δ DELTA CONNECTED IMMERSION TC o FIN MID-POINT THERMOCOUPLE
 FIGURE 2 TEST ARTICLE INSTRUMENTATION

A-115

TABLE I LIST OF EQUIPMENT FOR FLEXIBLE RADIATOR ELEMENT TEST

<u>INSTRUMENT</u>	<u>MANUFACTURER</u>	<u>MODEL NO.</u>	<u>RANGE</u>
DIGITAL THERMOCOUPLE INDICATOR	TRACOX WESTRONICS	7201-1750	-375°F to 750°F
DIGITAL MULTIMETER	SYSTRON DONNER	7205-158	1 V to 0.1V
THERMOCOUPLE SWITCH	THERMO ELECTRIC	3311353	
PRESSURE TRANSDUCER	BELL AND HOWELL	4-351-0050	+ 10 psi
THERMAC CONTROLLER	RI CONTROLS	TC 5122	
FLOWMETER	FLOW TECHNOLOGY	850913	0-133 #/HR
FLOWMETER	FLOW TECHNOLOGY	8501277	0-1130 #/HR
FLOWRATE MONITOR	FLOW TECHNOLOGY	PR-102A	0-100 %
RANGE EXTENDER	FLOW TECHNOLOGY	LPH-300	
PHASER POWER CONTROLLER	RI CONTROLS	PRW-460-175	175 AMP

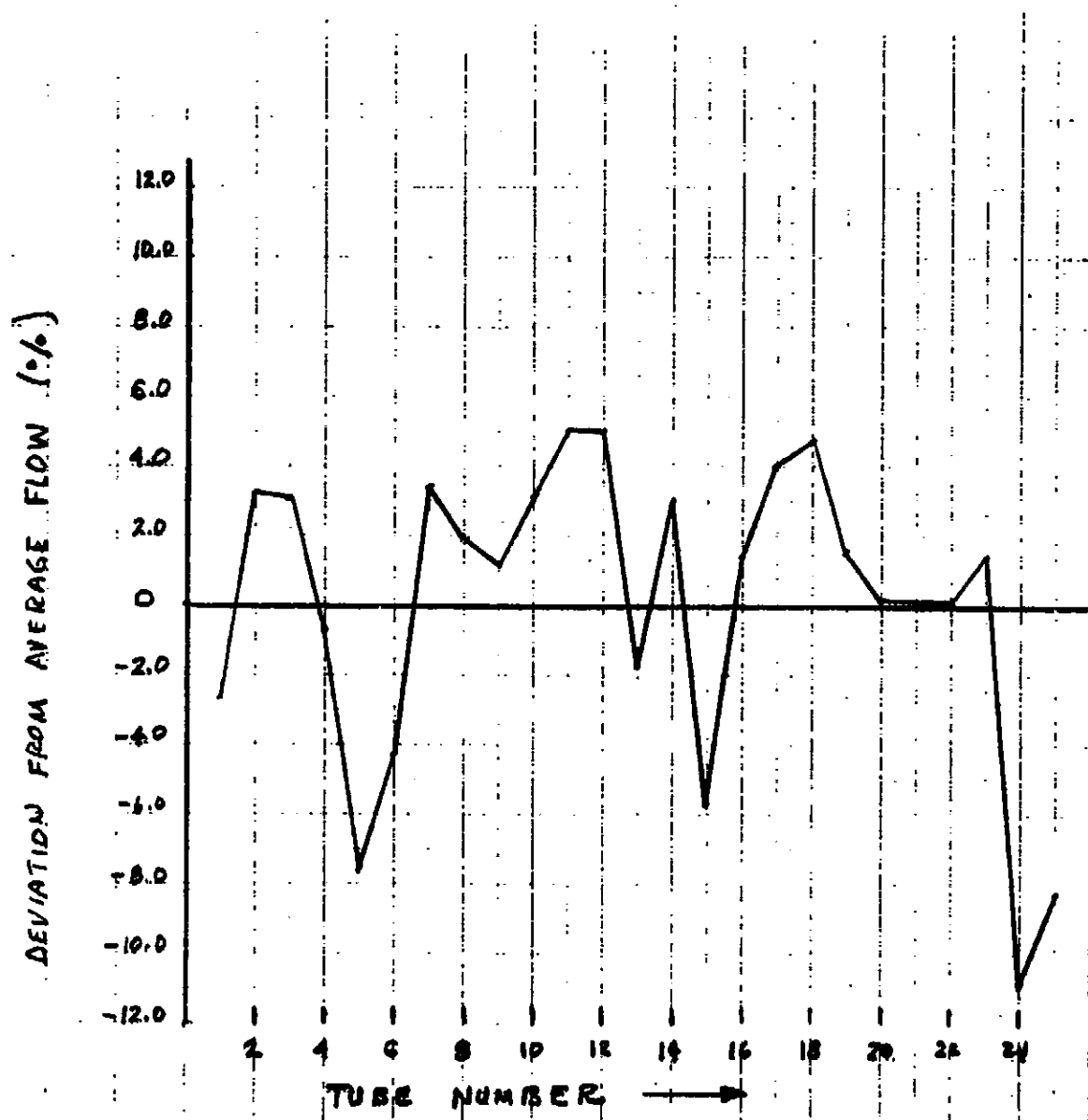


FIGURE 3 FLOW DISTRIBUTION IN TEST ARTICLE

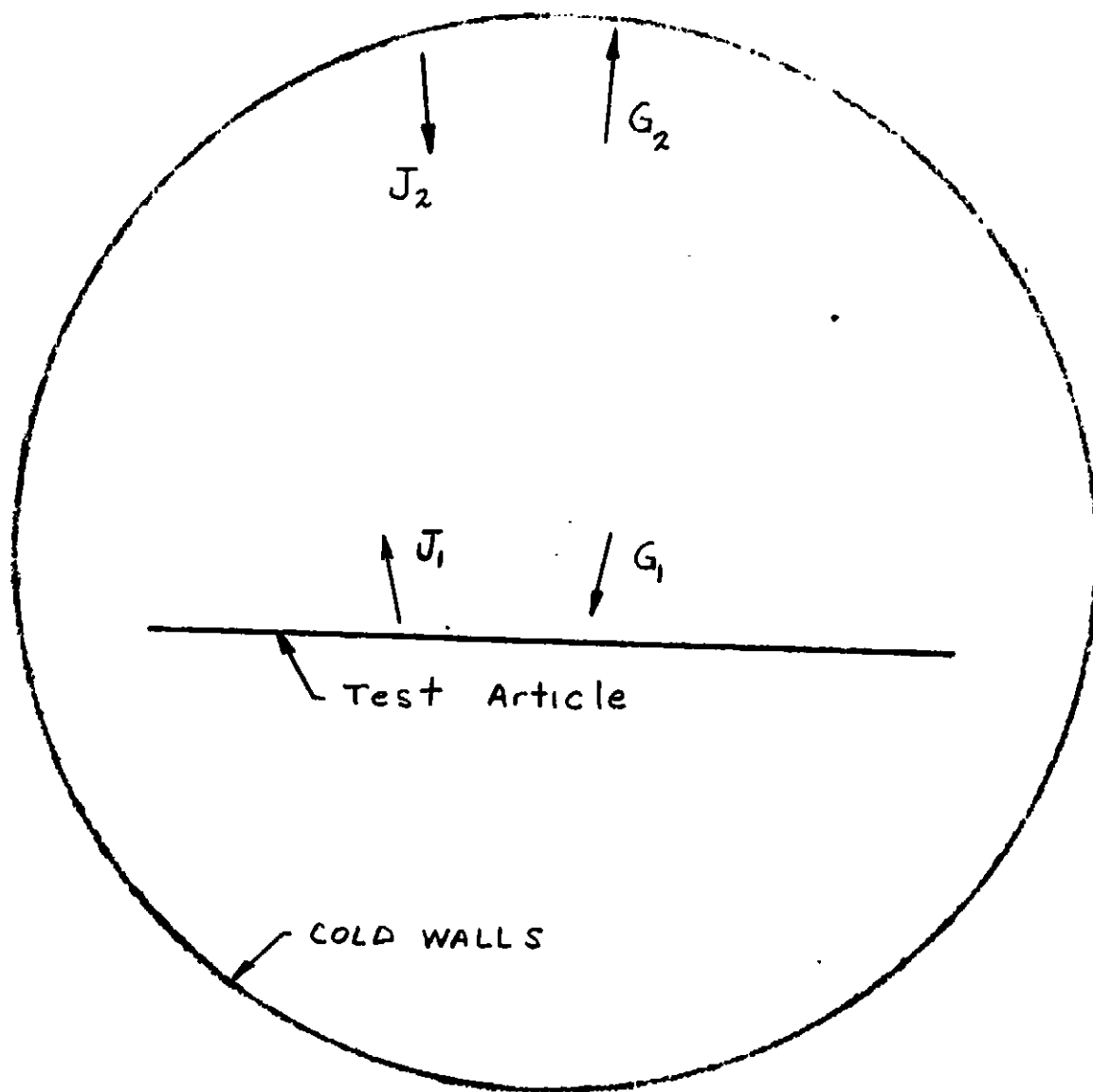


FIGURE 4 EFFECTIVE TEST ENVIRONMENT

The equations for irradiation are:

$$G_1 = F_{1-2} J_2 \quad (3)$$

$$G_2 = F_{2-1} J_1 + F_{2-2} J_2 \quad (4)$$

The net heat transfer from the element is:

$$(q/A)_1 = J_1 - G_1 \quad (5)$$

Solving (1) - (5) simultaneously gives:

$$(q/A)_1 = \frac{\epsilon_1 \epsilon_2 (E_1 - E_2)}{1 - \rho_2 F_{2-2} - \rho_1 \rho_2 F_{2-1}} \quad (6)$$

The approximate values for the view factors from the cold walls are:

$$F_{2-1} = .16$$

$$F_{2-2} = .84$$

Thus, for a cold wall emissivity of 0.9, Eq. (6) reduces to:

$$(q/A)_1 = 0.9875 E_1 (E_1 - E_2) \quad (7)$$

Eq. 7 shows that the heat rejection for the reflecting cold walls environment is approximately 1.25% lower than would occur in deep space.

Analysis of Data

The heat transfer from an element in the radiator panel is:

$$dq = \eta W \bar{\epsilon} \sigma (T_w^4 - T_\infty^4) dx \quad (8)$$

where:

η = radiator fin efficiency

W = width of radiator fin

T_w = tube wall temperature

T_∞ = ambient temperature

$\bar{\epsilon}$ = effective emissivity (for two sided radiators $\bar{\epsilon} = 2\epsilon$)

σ = Stefan Boltzmann Constant

The tube wall temperature may be expressed in terms of the fluid temperature through:

$$dq = \frac{1}{R} (T - T_w) dx \quad (9)$$

Where R is the thermal resistance between the fluid and the base of the radiator fin. Solving Eq. (9) for T_w^4

$$T_w^4 = (T - \frac{dqR}{dx})^4 \quad (10)$$

or

$$T_w^4 = T^4 [1 - \frac{4dqR}{T dx} + 6(\frac{dqR}{T dx})^2 + \dots] \quad (11)$$

From Eq. (9) the term $(\frac{dqR}{T dx})$ may be shown to be small

$$\frac{R dq}{T dx} = (\frac{T - T_w}{T}) \ll 1$$

Thus higher order terms may be neglected in Eq. (11)

$$T_w^4 = T^4 - \frac{4R dq T^3}{dx} \quad (12)$$

Eq. (8) becomes:

$$dq = \frac{\eta W \bar{\epsilon} \sigma (T^4 - T_\infty^4) dx}{1 + 4\eta R W \bar{\epsilon} \sigma T^3} \quad (13)$$

also, for conservation of energy:

$$dq = -\dot{W} C_p dT \quad (14)$$

Combining Eqs. (13) and (14),

$$-\frac{\eta W \bar{\epsilon} \sigma dx}{\dot{W} C_p} = \frac{(1 + 4R\eta W \bar{\epsilon} \sigma T^3) dT}{(T^4 - T_\infty^4)} \quad (15)$$

Integrating,

$$\begin{aligned} \frac{\eta A \bar{\epsilon} \sigma}{\dot{W} C_p} &= -\frac{1}{4T_\infty^3} \ln \left[\left(\frac{T_{in} + T_\infty}{T_{in} - T_\infty} \right) \left(\frac{T_{out} - T_\infty}{T_{out} + T_\infty} \right) \right] \\ &\quad - \frac{1}{2T_\infty^3} \left[\tan^{-1} \left(\frac{T_{in}}{T_\infty} \right) - \tan^{-1} \left(\frac{T_{out}}{T_\infty} \right) \right] \\ &\quad + \eta W \bar{\epsilon} \sigma R \ln \left(\frac{T_{in}^4 - T_\infty^4}{T_{out}^4 - T_\infty^4} \right) \end{aligned} \quad (16)$$

Equation (16) gives flow rate as a function of inlet and outlet temperature. Figures 5 and 6 compares the fluid temperature drop computed from Eq. 16 with measured value obtained in the thermal-vacuum test. The radiator parameters employed in Eq. (16) to predict the radiator performance are:

$$\begin{aligned} \eta &= 0.95 \\ A &= 2.47 \text{ Ft}^2 \\ \bar{\epsilon} &= (2)(0.71) = 1.42 \\ W &= 0.0583 \\ C_p &= 0.44 \text{ BTU/lb}_m \cdot ^\circ\text{F} \\ R &= 2.29 \text{ hr} \cdot ^\circ\text{F/BTU} \\ T_\infty &= -300^\circ\text{F} \end{aligned}$$

The measured temperature drop, and thus the heat rejection, is slightly lower than predicted for the ideal case analysis above. There are several small effects which collectively account for the discrepancy.

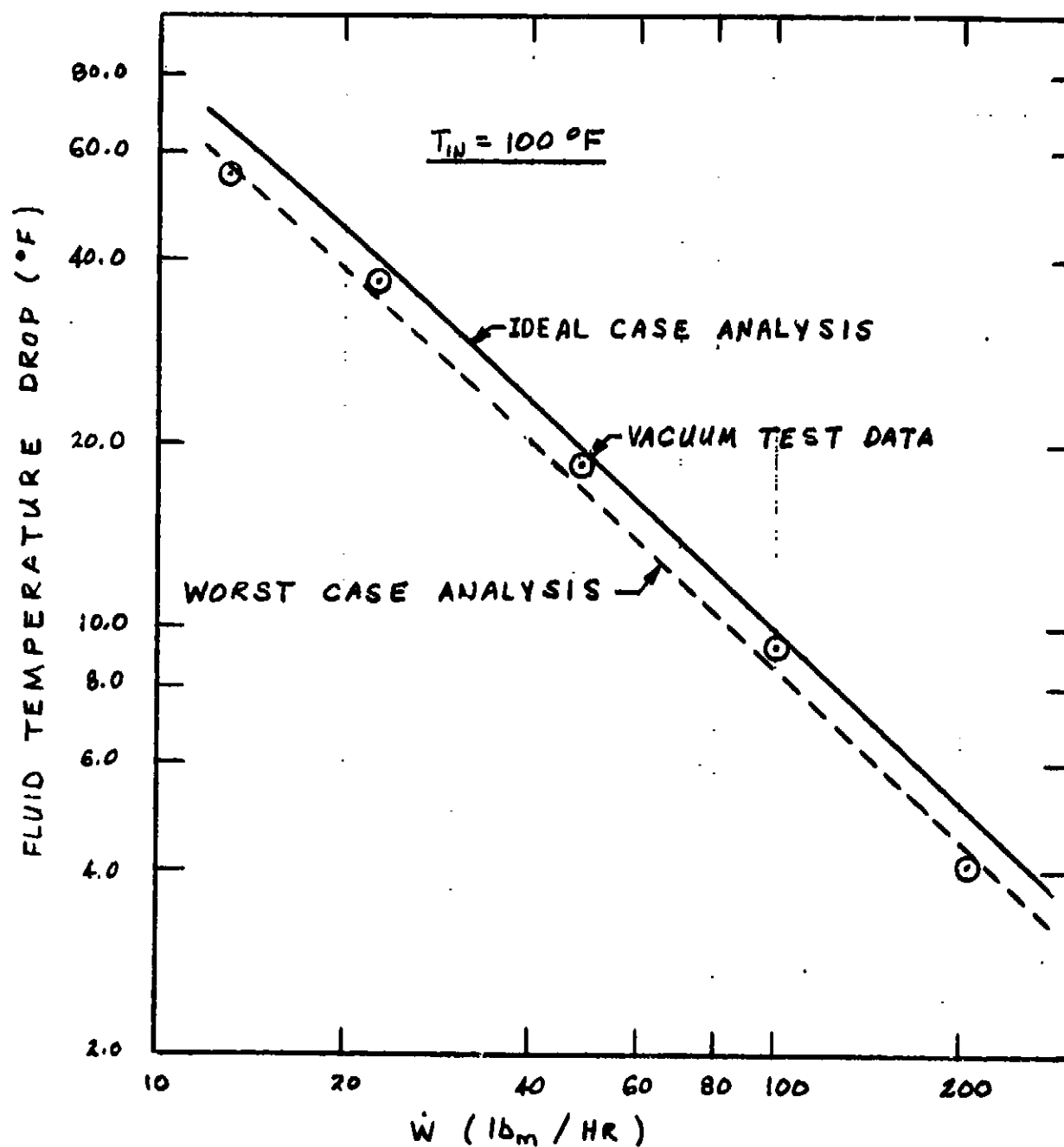


FIGURE 5 FLEXIBLE RADIATOR ELEMENT TEST DATA

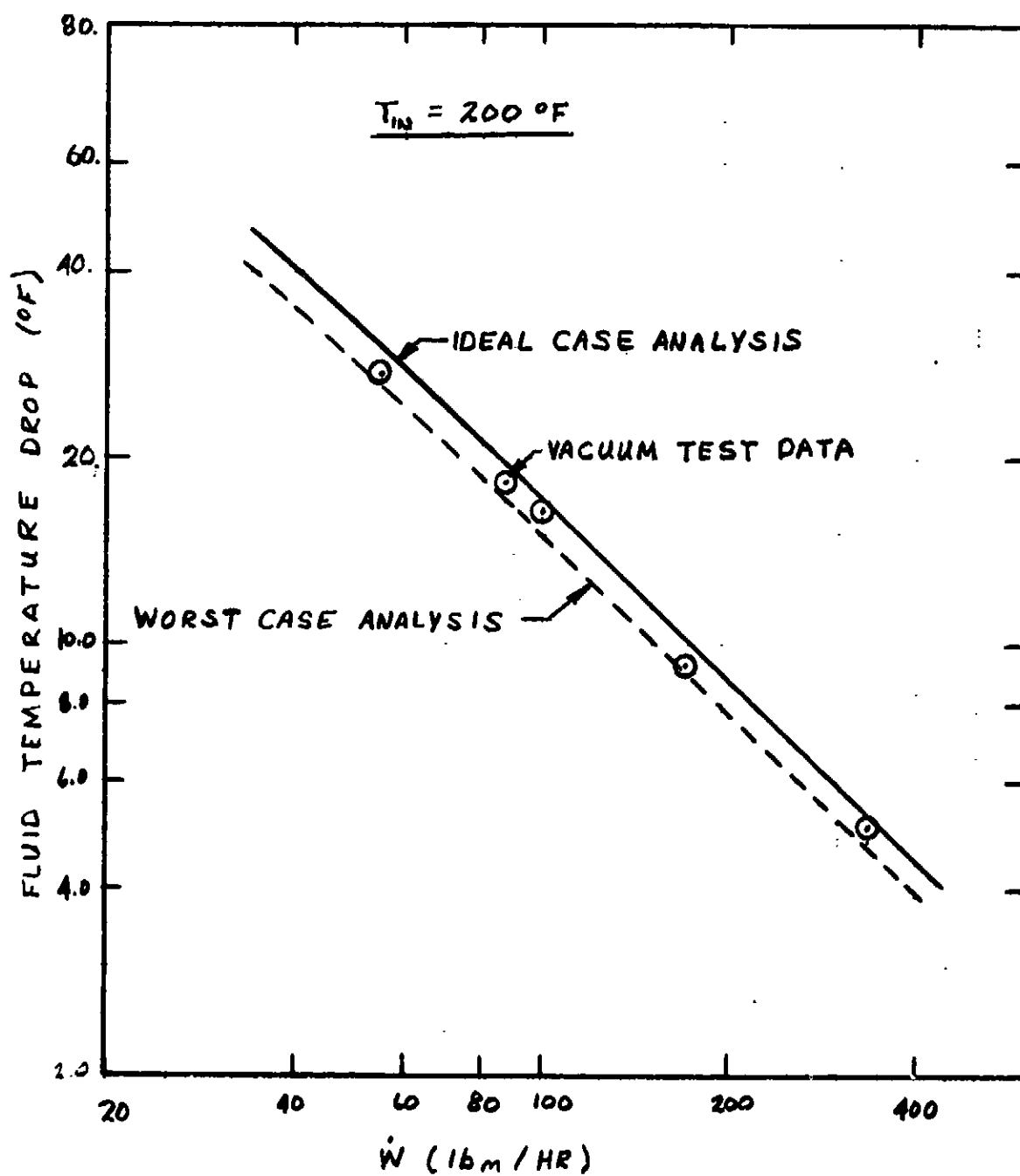


FIGURE 6 FLEXIBLE RADIATOR ELEMENT TEST DATA

The main cause is believed to be poor thermal connection between the transport tubing and the fin material at the ends of the radiator panel. The loose sections of fin material at the ends of the panel are significant because the radiating surface area of the element is relatively small. If it is assumed that there is no thermal connection at the ends of the radiator where the tubing was loosened to make connections with the manifolds, the heat rejection is reduced by approximately 8%. Variations in the silver wire mesh cross sectional area and spacing could lower the heat rejection by as much as 2%. The reflectivity of the vacuum chamber cold walls reduces the heat rejection by about 1%, and the cold wall temperatures averaged about 20°F higher than had been scheduled for the test. This would cause a 1% reduction in heat rejection.

The dashed lines in Figures 5 and 6 show the predicted fluid temperature drop when the worst case variations in panel construction and environment simulation are taken into account. The measured heat rejection falls between the ideal and worst case curves for all test points where the flow rate and fluid temperature drop can be accurately measured.

Figures 7-16 compare the measured and predicted panel temperatures for each test point. The agreement generally is within experimental error. The fin mid-point temperatures at the inlet and outlet planes are lower than expected because of the poor thermal connections between the fin and the tubing of these sections.

2.3 Solar Absorptivity of the Radiator Fin Material

The solar absorptivity of the silver backed Teflon (silver wire mesh laminate) was measured prior to fabricating the element test article. The measured values generally range from 0.17 to 0.25. This is considerably greater than the value of 0.12 obtained for small sections of fin material tested earlier. The silver/Inconel of the initial samples was applied in a bell jar whereas the large sheets of material were coated on a roll-to-roll basis in a larger vacuum chamber. The values of α measured for the large sheets will result in poor radiator performance, and will also impact the scheduled thermal-vacuum tests of the prototype panel. Additional studies will be made during the next reporting period to determine the cause of the problem and to evaluate its impact on the program.

$T_{in} (^{\circ}F)$

99.2

Δ



$T_{out} (^{\circ}F)$

95.9

Δ



PREDICTED EXP. PREDICTED EXP. PREDICTED EXP.

X	74.4	76.3	X	73.0	75.0	71.6	72.1	X
O	67.7	58.3	O	66.4	64.8	65.1	49.7	O
X	74.4	74.0	X	73.0	77.3	71.6	62.3	X
O	67.7	58.6	O	66.4	65.3	65.1	53.6	O
X	74.4	77.2	X	73.0	74.7	71.6	73.7	X

TEST POINT A-1

$\dot{W} = 2.15 \text{ lb}_m/\text{hr}$

$\Delta P = 1.7 \text{ PSI}$

DELTA T = $\frac{4.1}{^{\circ}F}$

Ice bath T = $\frac{32.5}{^{\circ}F}$

FIGURE 7 FLEXIBLE RADIATOR ELEMENT TEST DATA

$T_{12} (^\circ F)$
98.5
80 Δ
→

FIGURE 11 FLEXIBLE RADIATOR ELEMENT TEST DATA

TEST POINT B-4

FIGURE 15 FLEXIBLE RADIATOR ELEMENT TEST DATA

2.4 Planning and Analysis for Thermal Vacuum Tests

A meeting was held at NASA-JSC on 29 April 1977 to discuss the radiator test instrumentation, environment simulation, test time lines, and documentation for the thermal vacuum test in NASA Chamber B. A decision was made to simulate the space environment with solar and IR lamps. IR lamps were selected over fluid controlled IR panels because:

1. Reflected radiation from IR panels causes the environment to change with the radiator operating conditions, and causes the environment to be different for different locations on the radiator panel. Reflected radiation from the solar lamps when the radiator panel is partially retracted also complicates the environment simulation.
2. The ends of the radiator panel extend out of the region of the test chamber covered by solar lamps. Therefore, to provide a uniform environment for the radiator, the IR flux must be increased in the shaded areas. This is more conveniently done with IR lamps.
3. If IR lamps are used, the effective environment can be measured by stopping the flow of the transport fluid and measuring the equilibrium temperatures of the radiator panel.
4. Transient conditions can be simulated more easily with lamps than with panels.

NASA has previously had some difficulty measuring the flux from IR lamps. NASA/JSC will conduct a study to establish an accurate procedure for calibrating the lamps. He will also optimize the spacing and power setting of the lamps to insure that the emitted radiation has sufficient uniformity and correct wavelength.

Additional thermocouples will be installed on the radiator panel to measure the equilibrium temperatures at representative locations in conjunction with radiometers to calibrate the environment.

The test time line proposed in progress report No. 8 was reviewed and additional test points were discussed for 0°F equivalent sink temperatures with no solar flux. This was done to test the performance of the radiator with warm environments while avoiding the problems caused by non-uniformities of the solar absorptivity of the fin material. A revised test time line will be provided after the problem with the solar absorptivity of the fin material has been resolved.

Work in progress on test documents was also reviewed and assignments were made to individuals for writing sections of the test requirements document.

Ben McGhee of NASA-JSC requested that we consider rescheduling the test for July instead of September because of schedule problems of other programs requiring the NASA Space Environment Simulation Facility. After discussing the problems with the fin material and delivery requirements for the deployment/retraction system it was agreed that we probably could not test in July .

2.3 Submittal of Technical Paper

A technical paper entitled "Flexible Deployable - Retractable Space Radiators" was submitted to the American Institute of Aeronautics and Astronautics. The paper will be presented at the 12th Thermophysics Conference, Albuquerque, New Mexico, June 27-29, 1977. Review copies of the paper were also submitted to the NASA program monitor.

3.0 PROGRESS ON MAJOR END ITEM

Work is in progress in the fabrication and test planning phase. A problem has developed because of the high solar absorptivity of the fin material which impacts the testing phase of the program.

4.0 WORK SCHEDULED DURING THE NEXT REPORTING PERIOD

A study will be initiated to determine the cause of the solar absorptivity problem. Work will continue in the fabrication and test planning phase.

DEVELOPMENT OF A PROTOTYPE FLEXIBLE RADIATOR SYSTEM

PROGRESS REPORT NO. 11

1 May Through 31 May 1977

6 June 1977

CONTRACT NO. NAS9-14776
DRL: T-1213, LINE ITEM 2
DRD: MA-182TD

Submitted to:

THE NATIONAL AERONAUTICS AND SPACE ADMINISTRATION
JOHNSON SPACE CENTER
HOUSTON, TEXAS

BY

VOUGHT CORPORATION
An LTV Company
Dallas, Texas 75222

PREPARED BY:

J. W. Leach
J. W. Leach

CHECKED BY:

J. A. Oren
J. A. Oren

APPROVED BY:

R. L. Cox
R. L. Cox

MONTHLY PROGRESS REPORT NO. 11

Development of a Prototype Flexible Radiator System

1.0 Overall Progress

Work during the eleventh reporting period has been concentrated on the fabrication and test planning phases of the flexible radiator development program and addresses the following subjects:

1. Study of high solar absorptivity of radiator fin material.
2. Rescheduling of thermal vacuum test and re-allocation of budget to correct the solar absorptivity problem.
3. Substitution of Coolanol 20 for Coolanol 15 transport fluid.

2.0 Progress on Individual Major Areas

2.1 Solar Absorptivity of Radiator Fin Material

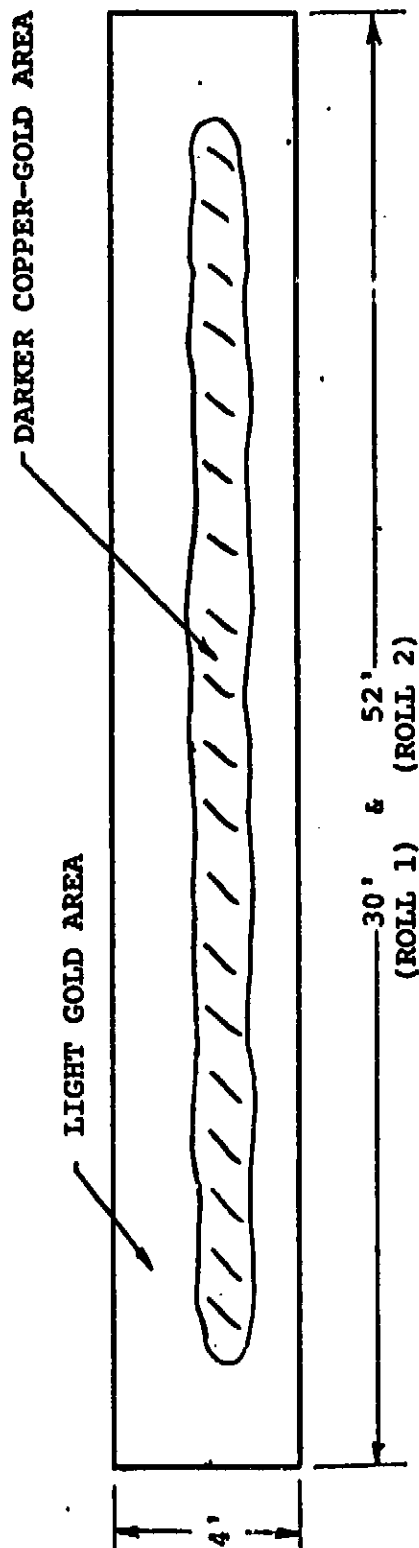
The radiator fin material fabricated by Sheldahl Advanced Products Division has higher solar absorptivity, α , than had been expected based on element test data. Two rolls of material were fabricated. The basic construction of the fin material is illustrated in Fig. 1. The measured values of α range from 0.18 in the light gold areas of Fig. 1 to 0.25 in the darker colored areas at the centers of the rolls. There is a small area on one roll where α is 0.45. This compares to values of approximately 0.12 obtained for elements initially fabricated to check out manufacturing processes.

A sequence of tests were conducted to isolate the cause of the problem. The tests indicate that the increased solar absorptivity is due to oxidation of the silver coating. To determine whether the transmittance of the Teflon film is contributing to the problem, the silver/Inconel coating was removed from a section of the fin material and the α of the remaining structured measured. The α measured for the stripped section is 0.03. This means that the silver/Inconel is the major absorbing element in the radiator fin.

The color of the silver coating suggested that the silver is oxidized. Thus tests were conducted to determine whether the oxidation process is still in progress, and whether the oxygen is reaching the silver through the Inconel layer shown in Fig. 1, or through the opposing Teflon/wire mesh side of the fin material. Sections of the fin material were heated to 350°F to accelerate any reaction which would change the solar absorptivity. The α of most of the heated sections increased by a factor of two or more, indicating that the reaction affecting the silver is still in progress. This data is supported by unquantitized observations that the color of the fin material had darkened after two months storage.

DESCRIPTION OF FLEXIBLE FIN MATERIAL

TWO ROLLS OF FIN MATERIAL:



2-MIL SILVER
WIRE SCREEN ROUGH SIDE OUT
FUSION BONDED 3-MIL FEP
TEFLON/SILVER WIRE
1000 Å Ag
150 Å INCONEL

OPTICAL PROPERTIES (TEFLON SIDE)	
	α
INITIAL (AT SHELDHAHL)	.18
AT VOUGHT (4-21-77)	75%
	23%
(ROLL 2 ONLY)	2%
	.45

FIGURE 1 FLEXIBLE RADIATOR FIN CONSTRUCTION

Additional tests were made to determine whether the agent reacting with the silver is internal to the fin material or is permeating through the protective layers of Teflon and Inconel. Sections of fin material heated in vacuum bags showed very little degradation. Also, when sections of Teflon were glued to the Inconel side of the radiator fin to prevent air from entering through the Inconel layer, the change in absorptivity occurring during heating was reduced markedly. This indicates that air permeating through the Inconel side of the fin material is oxidizing the silver layer. The Inconel side could not be completely isolated so that it is not possible to determine from this test data above whether all of the oxygen enters through the Inconel. However, other evidence indicates that this is the case. Dilute sulfuric acid applied to the Teflon side has no effect on the silver coating.* Also, the initial elements of fin material for which the silver/Inconel layers were applied in a bell jar did not degrade when exposed to the atmosphere.

Thus, the data indicates that the Inconel layer applied to the large sheets of fin material is inadequate. Since the Inconel applied to the small element sections does prevent oxidation, there apparently is some manufacturing scale-up problem which is responsible for the poor quality of the large sheets of material. It is not clear whether the problem is in the facilities or the methods employed to coat the material. The vacuum deposition facility was modified so that the radiator fin could be coated in continuous sections. Therefore, there is a possibility that the facility needs to be improved, or the process changed because of modifications to the facility. Scanning electron micrographs of the fin material given in Fig. 2 show that the surface is much rougher than that of silver backed Teflon for the Shuttle orbiter radiators. Because of the surface roughness, the thickness of the Inconel layer may have to be increased. Sheldahl Advanced Products Division is reviewing the problem and will make recommendations.

2.2 Program Re-direction

A meeting was held at NASA-JSC to discuss the problem of the high solar absorptivity of the fin material and to decide how the work schedule should be changed to minimize the impact of the problem on the flexible radiator development program. The meeting was attended by H. E. Battaglia, B. O. French, L. A. Trevino, W. E. Ellis, and W. W. Guy of NASA; M. L. Fleming, R. L. Cox, and J. W. Leach of Vought. After the data on the fin material had been reviewed, the following decisions were made:

- (a) Continue with the present high absorptivity fin material through fabrication of the full-scale test article and the conduct of ambient deployment tests. Do not fully instrument the panel for thermal vacuum tests, but only enough to resolve certain thermocouple installation questions.
- (b) Concurrent with the above effort, conduct tests and analyses necessary to rectify the high absorptivity problem. At the conclusion of ambient deployment testing refurbish the full scale article with the revised/new flexible fin material.
- (c) Slide the September 1977 thermal vacuum test to the next available test window at the NASA/JSC Space Environment Simulation Laboratory (May/June 1978).

*This same solution rapidly stripped the silver/Inconel when applied to the opposite side.

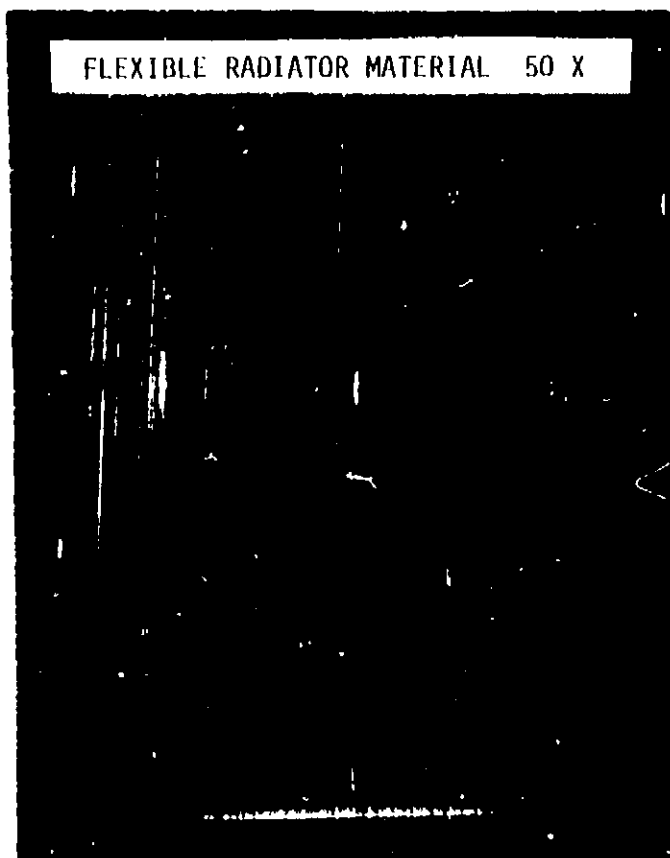


FIGURE 2 SCANNING ELECTRON MICROGRAPHS OF RADIATOR FIN MATERIAL

- (d) Re-allocate the approximately \$50K of FY'77 effort associated with the September 1977 thermal vacuum test to implementation of the Item (b) fin improvement and refurbishment.
- (e) Modify the contract to provide the above redirection and the additional funding necessary.
- (f) NASA agreed to make some additional solar absorptivity measurements on fin materials to be supplied by Vought. There is some question that this solar reflectometer used by Vought, a Gier Dunkle Instruments model MS-251, is adequate for measuring the absorptivity of the flexible fin material. NASA will try to locate an instrument more suitably designed for this application. There is no question that the Gier Dunkle reflectometer is adequate for determining that the fin material is severely degraded. However, more accurate measurements may be needed to determine the limiting values of the absorptivity for non-degraded materials and for diagnosis of potential problems with proposed new designs.

A revised schedule is given in Fig. 3.

2.3 Substitution of Coolanol 20 for Coolanol 15 Transport Fluid

Monsanto is discontinuing production of Coolanol 15, the transport fluid initially selected for use in flexible radiators. Therefore calculations were made to determine the required radiator size and operating limits for Coolanol 20, the fluid Monsanto recommends as an alternate. Coolanol 20 is slightly more viscous than Coolanol 15 so that the weight penalty for pumping power is increased by approximately 2 lb. per radiator panel. Also the low temperature stable operating limit is increased by 10°F - 30°F as shown in Fig. 4. The radiator design and operating characteristics for Coolanol 20 are similar to those for Oronite FC-100 as described in Progress Report No. 3. Materials compatibility tests are needed for each fluid before making a final selection.

3.0 Progress on Major End Items

Work is in progress in the fabrication phase of the program. The test phase has been rescheduled for May - June 1978.

4.0 Work Planned During the Next Reporting Period

A 6' radiator will be fabricated with radiator fin material for ambient deployment tests. Work will begin on the long life radiator study. Elements will be fabricated to demonstrate the feasibility of concepts and processes for correcting the high solar-absorptivity problem of the current design.

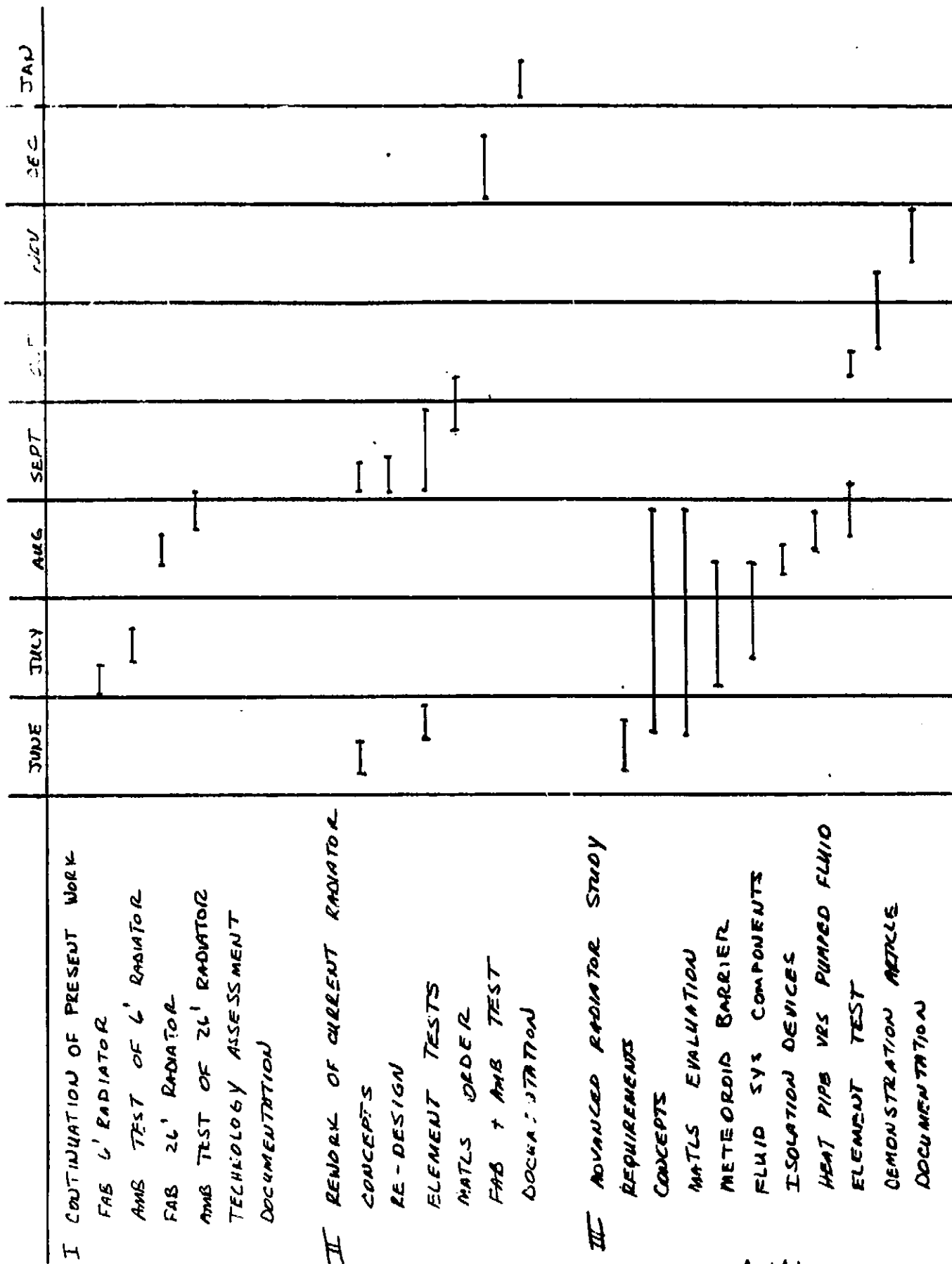


FIG. 3 REVISED PROGRAM SCHEDULE

DEVELOPMENT OF A PROTOTYPE FLEXIBLE RADIATOR SYSTEM

PROGRESS REPORT NO. 12
1 JUNE THROUGH 30 JUNE 1977

6 JULY 1977

CONTRACT NO. NAS9-14776
DRL: T-1213, LINE ITEM 2
ORD: MA-182TD

Submitted to:

THE NATIONAL AERONAUTICS AND SPACE ADMINISTRATION
JOHNSON SPACE CENTER
HOUSTON, TEXAS


BY

VOUGHT CORPORATION
An LTV Company
Dallas, Texas 75222


PREPARED BY:


J. W. Leach

CHECKED BY:


J. A. Oren

APPROVED BY:


R. L. Cox

MONTHLY PROGRESS REPORT NO. 12

Development of a Prototype Flexible Radiator System

1.0 Overall Progress

Work during the twelfth reporting period has been concentrated on the fabrication and long life study phases of the flexible radiator development program and addresses the following subjects:

- a. Fusion bonding of radiator fin/tubing assembly
- b. Aluminum foil/silver backed teflon design evaluation
- c. Testing of inflation tubing
- d. Presentation of technical paper at AIAA 12th Thermophysics Conference

2.0 Progress on Individual Major Areas

2.1 Fusion Bonding of Flexible Radiator

Small sections of flexible radiator fin material were fusion bonded to FEP Teflon tubing to determine whether the two halves of the radiator could be joined by this procedure without damaging the transport tubing. If this is possible, the radiator fin material with the degraded silver coating might be reclaimed for use in fabricating the prototype panel.

Two methods were investigated for maintaining pressure on the radiator panel assembly during the heat bonding process. One employs a heated platen press and matching grooved plates as shown in Fig. 1. The radiator components are held in position by the grooved plates while heat and pressure are applied through the press. Air is forced through the tubing so that the tube wall does not reach the melting point. Continuous sections of radiator are fabricated by incrementally bonding adjacent 6" sections of material. The grooves in one end of the plates are tapered so that the unbonded sections will slide into position without folding or tearing. The ends of the plates extend outside of the heated press so that the fin material at the edge of the plate is below the melting point. This prevents the material from being stressed while in the molten state, and provides a smooth transition between adjacent sections. The fin material is heated to $550 \pm 5^\circ\text{F}$ under a pressure of approximately 25 psi. The air flow is regulated so that the outlet temperature is approximately 300°F .

Sections of radiator approximately 6 inch wide by 18 inch in length were fabricated by this procedure without major problems. A few areas were observed in some of the samples where the silver wire mesh in the fin material was severed at the base of the tubes. This apparently occurred when the fin material was stretched and brought into contact with the sharp edges of the grooves in the aluminum plates. However, this problem was corrected by placing a buffer layer of Kapton between the aluminum plates and the radiator material.

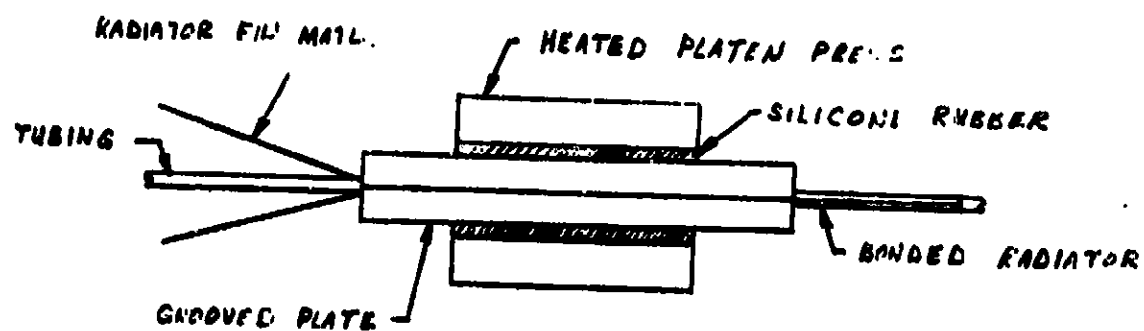


Fig. 1 Apparatus For Fusion Bending Flexible Radiators

Larger 4' x 6' grooved aluminum plates are being machined and will be employed to determine whether sections of sufficient size can be fusion bonded to make fabrication of a prototype flexible radiator practical. In this case, the prototype radiator could be produced from existing fin stock. The degraded silver/Inconel coating described in earlier progress reports was stripped from representative sections of the fin stock with dilute sulfuric acid, and fusion bonded so that the solar absorptivity could be determined. Measurements with a Gier Dunkle solar reflectometer ranged from 0.07 to 0.08. The coating can be removed without damaging the silver wire mesh, so that the stripped material would be entirely satisfactory for fabricating the prototype.

The second procedure investigated for fusion bonding the radiator employs an autoclave and vacuum bags in place of the platen press to provide pressure and heat. A description of the process developed and materials required is given in Appendix A. A potential problem with this method occurs because the tubing cannot be cooled during the bonding process. A tubing material must be selected which has a higher melting point than the FEP Teflon fin material. A small section was fabricated with PFA Teflon tubing. PFA Teflon is very similar to FEP except that its melting point is approximately 50°F higher. The small section was fabricated by heating the material to a temperature between the melting points of FEP and PFA. The bond formed between the tubing and fin material was found to be slightly stronger than is obtained by adhesive bonding, but not as strong as is possible with FEP tubing.

Samples of PFA tubing and cost quotes have been requested for additional testing. The autoclave process is attractive because it provides a means for bonding the entire radiator at one time. However, because of the materials delivery time required for PFA tubing and the potential of the platen press method, the fusion bonding work in the immediate future will employ the platen press.

2.2 Aluminum Foil Fin Material

An aluminum foil/silver backed Teflon radiator fin construction is being investigated as an alternative to fusion bonding for producing the prototype flexible radiator. This construction would have significant cost advantages over the present design, and would use conventional silver backed Teflon known to have stable optical properties. The aluminum foil provides thermal conductance necessary for a high radiator fin efficiency, and a smooth surface for attachment of the silver backed Teflon. This design has not been given detailed consideration in the past because it was believed that the aluminum foil would impact the deployment/retraction such that its size and weight would be increased to impractical limits. However, preliminary tests on small elements showed that the aluminum foil is stressed beyond the elastic limit the first time the radiator is stowed on the deployment drum. Then, when the radiator is straightened, small wrinkles develop which greatly increase the flexibility of the panel. The wrinkles are spaced approximately one eighth inch apart and do not appear to seriously weaken the connection between the tubing and fin material. Larger elements are being produced with 0.00035" and 0.001" aluminum foil. The stiffness of these elements will be measured and compared with that of the silver wire mesh design. If the results are favorable, an element should be fabricated and instrumented for thermal vacuum testing.

2.3 Test of Inflation Tubing

The 6' inflation tubes fabricated by Sheldahl Advanced Products Division were connected to the radiator mounting frame and deployment drum, and inflated to check their operation prior to attaching them to the radiator panel. Tests showed that the inflation tubes operated very smoothly and required less than 1 psi gas pressure for deployment. There was no observable imbalance in the system. The two tubes inflate and deflate at the same rate such that the stowage drum remains perpendicular to the inflation tubes during deployment and retraction. A section of radiator is being fabricated from excess fin material having poor optical properties to check the operation of the inflation tubing when attached to the radiator. If there are no problems with the 6' tubing, 30' tubes will be purchased for the prototype radiator.

2.4 Presentation of Technical Paper

A technical paper describing the development of the flexible deployable/retractable radiator system was presented at the AIAA 12th Thermophysics Conference, Albuquerque, N.M. June 28, 1977.

3.0 Work on Major End Items

Work is in progress in the fabrication phase of the program.

4.0 Work Planned During the Next Reporting Period

A 6' radiator will be fusion bonded to check out manufacturing processes for producing the prototype panel. Elements will also be produced by adhesively bonding aluminum foil and silver backed Teflon as an alternative to the fusion bonding process. Additional tests will be conducted with 6' inflation tubing prior to purchasing tubing for the prototype system. Work under the long life radiator study contract will be concentrated on heat pipes and future mission requirements.

DEVELOPMENT OF A PROTOTYPE FLEXIBLE RADIATOR SYSTEM

PROGRESS REPORT NO. 13

1 JULY THROUGH 31 JULY 1977

8 AUGUST 1977

CONTRACT NO. NAS9-14776
DRL: T-1213, LINE ITEM 2
DRD: MA-182TD

Submitted to:

THE NATIONAL AERONAUTICS AND SPACE ADMINISTRATION
JOHNSON SPACE CENTER
HOUSTON, TEXAS

BY

VOUGHT CORPORATION
An LTV Company
Dallas, Texas 75222

PREPARED BY:

CHECKED BY:

APPROVED BY:

J. W. Leach
J. W. Leach

J. A. Oren
J. A. Oren

R. L. Cox
R. L. Cox

MONTHLY PROGRESS REPORT NO. 13
DEVELOPMENT OF A PROTOTYPE FLEXIBLE RADIATOR SYSTEM

1.0 Overall Progress

Work during the thirteenth reporting period has been concentrated on the fabrication phase of the flexible radiator development program and addresses the following subjects:

- a) Fabrication and ambient deployment test of six foot length radiator
- b) Fabrication of aluminum foil/silver backed Teflon based elements

2.0 Progress on Individual Major Areas

2.1 Fabrication and Ambient Deployment Test of Six Foot Length Radiator

A 4' x 6' section of radiator was fabricated by adhesively bonding two layers of silver wire mesh/Teflon fin material around FEP Teflon tubing using a grooved vacuum tooling plate as shown in Fig. 1. The radiator panel was made to check out fabrication tooling and techniques, and was subsequently used in ambient deployment tests of 6' length inflation tubing.

The following procedure was followed in fabricating the panel.

- 1) The bottom half of radiator fin material is positioned on the grooved plate and pre-formed by pressing the material into the grooves of the tooling plate using Teflon tubing.
- 2) Vacuum is applied to hold the fin material in position.
- 3) General Electric SR-585 adhesive is applied to the two mating sections of fin material and tubing.
- 4) The tubing is placed in the grooves over the pre-formed half of fin material.
- 5) The top half of fin material is held by the edges and lowered over the bottom half until the mating surfaces touch along the radiator centerline.
- 6) The fin material is pressed together around the center tube using a roller.
- 7) The top half is gradually lowered until the fin material can be sequentially pressed together around the remaining tubes as shown in Fig. 1.



FIGURE 1 FABRICATION OF SILVER WIRE MESH DESIGN ELEMENT

The element produced following this procedure was generally satisfactory. The fin material tore where it connects to the tubing over about 1% of the radiator area. The bottom layer tore in several randomly located areas from wear against the sharp edges of the grooves in the tooling plate, and the top layer also tore occasionally next to the tubing as it was being pressed into position by the notched roller.

Excessive tearing of the bottom layer can be prevented by minimizing the motion of the material while it is in contact with the tooling plate. When fabricating the 6' length element, the vacuum pump was turned on and off several times. Each time new tears appeared. Thus, when the prototype radiator is produced, work will be planned so that the vacuum pump runs continuously. Also, a soft porous cloth will be placed between the vacuum plate and radiator panel to reduce the stress caused by the sharp edges of the grooves.

The top half apparently tears when the two sheets of fin material are permitted to stick together near the mid-point of adjacent tubes before the top layer has been pulled into position around the tubing by the roller. When this happens, there is insufficient material available to cover the distance around the tubes. This occurs very seldomly, but when it does, a tear several inches in length develops. The fin material has very little resistance to tearing so that whenever it begins to separate, the tear propagates readily. It is possible that the tears in the top half initiate at sites where small flaws exist in the fin material. A narrow roller was made which pulls the top half of fin material around the tubing without pressing it against the bottom half. After the narrow roller has been applied, the wider roller shown in Fig. 1 is used to press the fin material together between the tubing. When carefully done, this procedure gives satisfactory results.

Some wrinkles developed in the top half of fin material of the element which probably can be eliminated when producing the full sized radiator.

The wrinkles occurred when excess material accumulated in localized areas where the fin material had been stretched out of proportion, or was improperly supported. The fin material has localized areas such as may be seen near the technician's hand in Fig. 1 where it appears to have been stretched. Small wrinkles which may cover a length of 18" develop in these areas. The wrinkles sometimes begin and end without reaching the edge of the radiator panel. This problem can be minimized by carefully positioning the panel in the supporting frame and by applying force to the material in the lengthwise direction as it is being pressed against the bottom half.

The ambient deployment test of the 6' element panel was entirely satisfactory. The radiator deployed and retracted easily and had no tendency to malfunction. The radiator panel rolled up tightly and uniformly on the deployment drum during retraction, and could be deployed with a gas pressure less than 1 psig. The system of retraction springs and inflation tubing was sufficiently well balanced that the deployment drum remained perpendicular to the radiator panel throughout the deployment retraction cycle. Thus the radiator could be repeatedly deployed and retracted without becoming dis-oriented on the stowage drum.

Since the ambient deployment test of the six ft. radiator was successful, go-ahead was given to Sheldahl Advanced Products Division to fabricate the 30' tubing for the prototype radiator. Delivery is expected during August 1977.

2.2 Fabrication of Aluminum Foil/Silver Backed Teflon Elements

6" x 14" elements were constructed from aluminum foil and silver backed Teflon as shown in Fig. 2. The silver backed Teflon tape is manufactured in 4" wide strips. To increase the strength of the panel, the elements were constructed so that the opposing layers of tape overlap. The two halves of fin material were produced first by adhesively bonding the strips of silver backed Teflon to aluminum foil. The radiator panel elements were then assembled using the grooved vacuum plate as described previously. This procedure proved to be much better than that of applying silver backed Teflon tape to a radiator panel constructed of tubing and aluminum foil because the Teflon tape prevented the aluminum foil from tearing during handling.

The appearance of the aluminum foil based elements is much better than that of elements previously made with silver wire mesh fin material, but the aluminum foil elements are not as flexible.

Elements were constructed with .001" and .00035" thick aluminum foils. The thickness of the silver backed Teflon tape is 0.005". The 0.00035" thick foil has about half the thermal conductance of the silver wire mesh, and tears very easily. It is difficult to form this thickness of foil around the radiator tubing without tearing it. However, the radiator can be fabricated from the .001" thick foil without difficulty, and the thermal conductance of the fin material is about 50% greater than that of the silver wire mesh design. Therefore, it is recommended that the .001" thick foil be used in future work on this design.

Table I compares the measured and calculated stiffnesses of the aluminum foil and silver wire mesh radiator designs. The measured stiffness of the aluminum foil element is approximately twice that of the silver wire mesh element, and about one fourth of the calculated value. The large discrepancies between the measured and calculated values occur because the calculated values assume elastic deformation of the fin and tubing whereas the actual deformations are outside the elastic range.

The measured stiffness of the aluminum foil panel is low enough that it is practical to consider this design as a candidate for the prototype system. Since the existing deployment/retraction system for the prototype is based on the calculated stiffness of the wire mesh design, no rework of the deployment system would be required. An additional element is being constructed with .002" thick silver backed Teflon to determine how the thickness of the Teflon affects the stiffness.

It is recommended that a 2' x 2' element be constructed with the best thickness of silver backed Teflon and thermal vacuum tested before deciding on the final design of the prototype system. Also, additional tests and development work should be conducted on the fusion bonded wire mesh design described in Progress Report No. 12. Performance and cost data will be prepared for the two concepts for making a final decision.

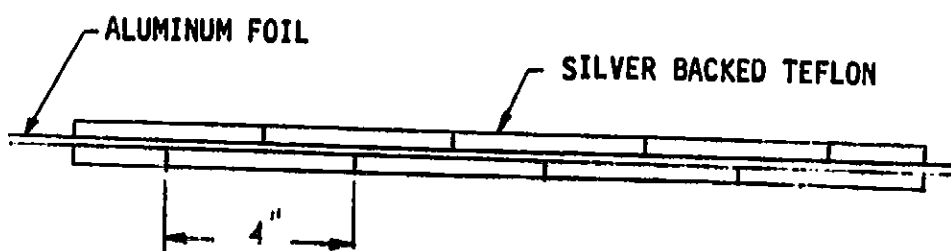


FIG. 2 ALUMINUM FOIL/SILVER BACKED TEFLON DESIGN

TABLE I STIFFNESS OF FLEXIBLE RADIATOR ELEMENTS

<u>Radiator Panel Construction</u>	<u>Bending Moment for 10" Drum (inch-lb/tube)</u>	
	<u>Calculated</u>	<u>Measured</u>
Fusion Bonded Silver Wire Mesh	0.235	0.16
.001" Al. Foil - .005" Teflon	1.042	0.28

3.0 . Work on Major End Items

Work is in progress in the fabrication phase of the program.

4.0 Work Planned During the Next Reporting Period

A 6' radiator will be fusion bonded to check out manufacturing processes for producing the prototype panel. Additional elements will also be produced with aluminum foil and silver backed Teflon. Concepts shall be evaluated in the long life study phase of the program.

DEVELOPMENT OF PROTOTYPE FLEXIBLE RADIATOR SYSTEM

PROGRESS REPORT NO. 14

1 AUGUST THROUGH 31 AUGUST 1977

20 SEPTEMBER 1977

CONTRACT NO. NAS9-14776
DRL: T-1213, LINE ITEM 2
DRD: MA-182TD

SUBMITTED TO:

THE NATIONAL AERONAUTICS AND SPACE ADMINISTRATION
JOHNSON SPACE CENTER
HOUSTON, TEXAS

BY

VOUGHT CORPORATION
An LTV COMPANY
DALLAS, TEXAS 75222

PREPARED BY:

J. W. Leach
J. W. Leach

CHECKED BY:

J. A. Oren
J. A. Oren

APPROVED BY:

R. L. Cox
R. L. Cox

MONTHLY PROGRESS REPORT NO. 14

1.0 OVERALL PROGRESS

Work during the fourteenth reporting period has been concentrated on the fabrication phase of the flexible radiator development program and addresses the following subjects:

- a) Fusion bonding of six foot length radiator with FEP Teflon tubing.
- b) Fusion bonding of two foot length radiator with PFA Teflon tubing.

2.0 PROGRESS ON INDIVIDUAL MAJOR AREAS

2.1 Fusion Bonding of 4' x 6' Panel With FEP Teflon Tubing

An unsuccessful attempt was made to fusion bond a 4' x 6' section of radiator panel. The 4' x 6' section was bonded in a heated platen press to determine the feasibility of producing the 4' x 25' prototype by this procedure. Earlier, 0.5' x 2' sections of radiator had been bonded successfully, as described in Progress Report No. 12, and tests were recommended with larger sections to determine whether problems would develop which could not be predicted from the small scale test results. The small sections were bonded by heating the radiator panel inside matching grooved tooling plates to 550°F while cooling the transport tubing with an internal flow of air.

For the larger sections, matching 4' x 6' grooved plates were machined to hold the radiator tubing in position while the fin material is heated to the melting point. Manifolds were attached to one end of the tubing so that air could be forced through the radiator to provide cooling for the transport tubing. It is necessary to keep the tubing below the melting point to prevent it from collapsing. Pressure and heat were applied

to the radiator assembly through a resistance heated platen press as shown in Fig. 1.

This attempt to fusion bond the radiator failed because the flow distribution of the cooling air in the parallel bank of radiator tubes was non-uniform. This created an uneven temperature field so that parts of the radiator became too hot while others did not reach the melting point.

Some non-uniformities in the air flow were anticipated, but not of the magnitude actually experienced. Manufacturing tolerances in the tubing diameter could cause some of the tubes to have greater flow resistance than others. Therefore, the diameters of individual tubes were measured prior to heating. There was no apparent correlation of the flow distribution with the tubing diameter. With pressure applied by the press, the flow in six of the tubes were noticeably low prior to heating. When the pressure was released, the flow was nearly uniform.

The restriction of the flow could have been caused by the tubing not being seated properly in the grooves of the tooling plate, or by tension in the fin material as it is pulled around the tubing by the tooling plate. Extreme care was taken when preparing the radiator assembly for bonding to prevent the press from interfering with the air flow. The ends of the tooling plates were secured with pins and clamps as shown in Fig. 2 to prevent the tubing from becoming dislodged from the grooves of the plate. A third removable clamp was placed across the center of the section to minimize the relative motion of the plates during handling. Also, to insure that the tubes were properly seated, the clamps were loosened slightly, and the tubes pulled at the ends to make sure that they would slide freely within the grooves of the plates. The radiator fin material was positioned around the tubing using rollers to insure that sufficient material was available to cover the entire surface of the tooling plates.

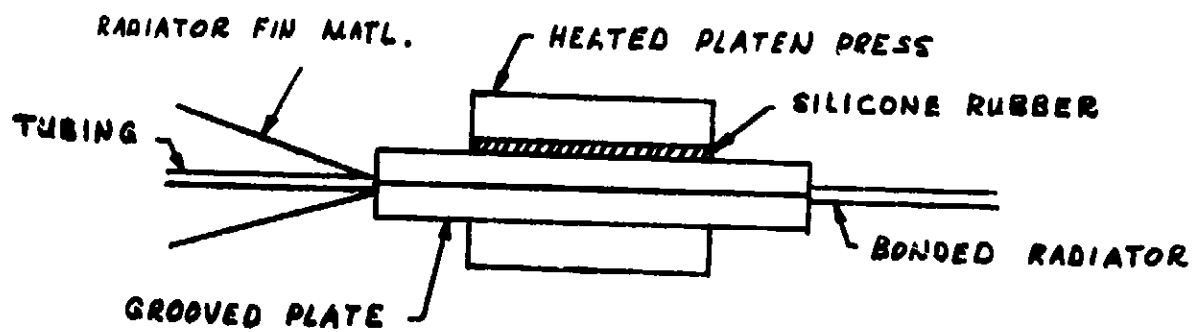


FIG 1 APPARATUS FOR FUSION BONDING FLEXIBLE RADIATORS

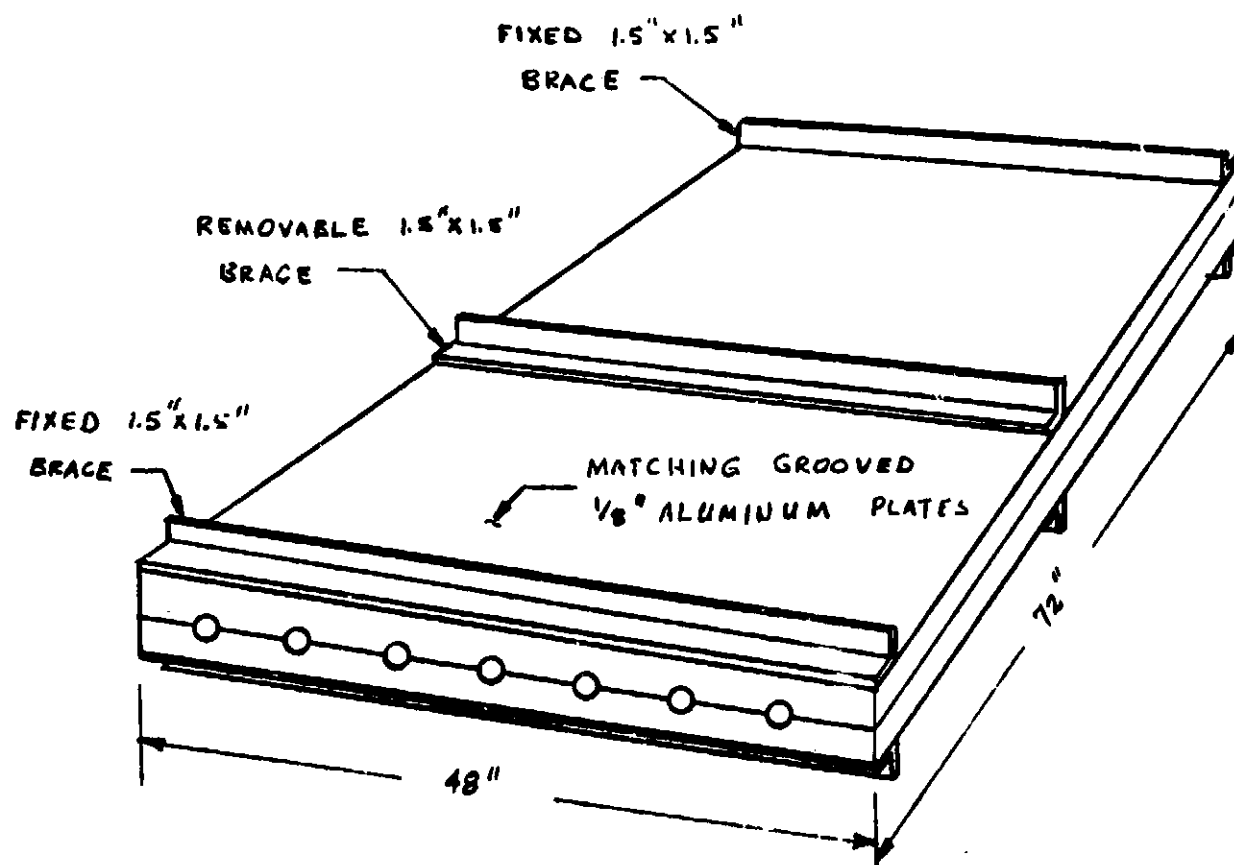


FIGURE 2 DETAILS OF GROOVED TOOLING PLATES

As the radiator was heated in the press, the flow in additional tubes began to diminish. At a temperature of about 350°F there was no measurable air flow in about 25% of the tubes. With continued heating, the temperature distribution within the press became increasingly uneven. The areas where the flow of air was greatest were about 150°F cooler than where the flow was stagnate. Five thermocouples were employed to measure the temperatures of the panel and of the cooling air. The measured panel temperatures ranged from 400°F to 550°F, while the exit temperature of the air reached 485°F. Before all of the panel could be heated to the temperature required for fusion bonding (540°F) a resistance heater burned out in the press causing a local power failure which lasted several hours. Thus the test was terminated at a point when part of the radiator had not reached the fusion point.

A post-test examination of the radiator panel showed that the tubing in the hot sections had completely collapsed while the underheated sections were unbonded.

There were several small areas where the radiator was stuck to a Kapton film which had been inserted between the radiator and tooling plates to prevent them from becoming bonded together. This indicates that these areas had become much hotter than the sections which were instrumented. It is possible that local hot spots on the heated press could have caused some of the problems discussed above. Therefore, if additional attempts are made with this approach, it is recommended that the system be heated very slowly to allow any transient temperature gradient to dissipate. Approximately 1.5 hours were required to heat the system from 100°F to 550°F in this test.

It is also recommended that the tooling plates be made shorter so that nonuniformities in the air flow can be tolerated.

1

Fanno flow calculations show that for shop air pressure, the mass flow rate of air is only marginally adequate for the heating length of this test. The shorter sections could also be prepared for bonding more easily than the larger ones, and flow restrictions would be less likely.

2.2 Fusion Bonding with PFA Teflon Tubing

A 6" x 20" section of radiator with PFA tubing was fusion bonded successfully. PFA Teflon has a melting point between 575°F and 590°F where the FEP fin material melts between 487°F and 540°F. Therefore the radiator assembly can be fusion bonded by heating it to a temperature intermediate to the melting point of the two materials without having to provide localized cooling as is required with FEP tubing. The bond formed between the PFA tubing and the fin material is not as strong as is obtained with FEP tubing, but is probably sufficient for the flexible radiator application. The strength of the bond increases as the bonding temperature approaches the fusion point of the PFA tubing, but the tubing deforms if the bonding temperature is too high. The most satisfactory results were obtained at bonding temperatures between 570°F and 575°F. No appreciable tubing deformation was noted at temperatures below 580°F.

Pressure was applied to the assembly by means of a vacuum bag, and the system was heated in an autoclave. The radiator tubing was held at the proper spacing as the panel was being assembled and transported to the autoclave by maintaining a partial vacuum in the vacuum bag.

A larger section of radiator will be fabricated as soon as additional PFA tubing can be purchased. If no problems develop, the prototype radiator will be fabricated by this method.

3.0 WORK ON MAJOR END ITEMS

Work is in progress in the fabrication phase of the program.

4.0 WORK PLANNED DURING THE NEXT REPORTING PERIOD

Elements will be produced with aluminum foil and silver backed Teflon for thermal vacuum testing. Materials will be purchased for fabricating large elements by fusion bonding PFA tubing to FEP fin materials. Ambient tests will be conducted with the 30' inflation tubes.

1

DEVELOPMENT OF A PROTOTYPE FLEXIBLE RADIATOR SYSTEM

PROGRESS REPORT NO. 15

1 SEPTEMBER THROUGH 30 NOVEMBER 1977

30 NOVEMBER 1977

CONTRACT NO. NAS9-14776
DRL: T-1213, LINE ITEM 2
DRD: MA-182TD

Submitted to:

THE NATIONAL AERONAUTICS AND SPACE ADMINISTRATION
JOHNSON SPACE CENTER
HOUSTON, TEXAS

BY

VOUGHT CORPORATION
AN LTV COMPANY
DALLAS, TEXAS 75222

PREPARED BY:

J. W. Leach
J. W. LEACH

CHECKED BY:

J. A. Oren
J. A. OREN

APPROVED BY:

R. L. Cox
R. L. COX

PROGRESS REPORT NO. 15

1.0 Overall Progress

Work during the fifteenth reporting period has been concentrated on the fabrication and advanced radiator study phases of the flexible radiator development program and addresses the following subjects:

- a) fabrication and testing of aluminum foil/silver Teflon based elements,
- b) fabrication and testing of a fusion bonded silver wire mesh based elements,
- c) advanced long life radiators study.

2.0 Progress on Individual Major Areas

2.1 Fabrication and Testing of Aluminum Foil/Silver Backed Teflon Elements

Two 17.5" x 18" elements were constructed from aluminum foil and silver backed Teflon, and tested in a vacuum environment for thermal performance and structural integrity. Table I summarizes the properties of the two test articles. The elements were fabricated by first bonding silver backed Teflon strips to sheets of aluminum foil to form a laminated radiator fin, and then bonding opposing sheets of this laminate around the transport tubing. The adhesive used to bond the radiator assembly is General Electric SR-585 adhesive thinned with toluene at a ratio of 1 part adhesive to 8 parts solvent. The element constructed from 2 mil Teflon proved to be difficult to fabricate because the laminated fin material tended to stretch and wrinkle, and was easily torn. No problems were experienced in fabricating the 5 mil test article.

Figures 1 - 4 compare the theoretical and measured thermal performances of the two elements. The measured temperature drop of the transport fluid, which is proportional to the heat transfer, indicates that both elements performed approximately as expected. The heat rejection of the 5 mil Teflon element is slightly higher than predicted. This probably indicates that the emissivity of the Teflon is slightly greater than the minimum value claimed by the manufacturers.

The test articles partially delaminated as a result of exposure to the vacuum environment. The delamination was not severe enough to degrade the thermal performance, but could be significant structurally if the panel were repeatedly deployed and retracted. It indicates outgassing of solvents used to thin the adhesive or to clean the surfaces of the aluminum foil and Teflon prior to applying the adhesive. The adhesive is the same as was used to fabricate earlier elements, and had been stored

TABLE I PROPERTIES OF ALUMINUM FOIL
BASED ELEMENTS

<u>DESIGN VARIABLES</u>	<u>ELEMENT #1</u>	<u>ELEMENT #2</u>
SILVER BACKED TEFLON THICKNESS (INCH)	.001	.005
ALUMINUM FOIL THICKNESS (INCH)	.001	.001
NO. LAYERS TEFLON	2	2
NO. LAYERS ALUMINUM FOIL	2	2
TUBE SPACING (INCH)	0.75	0.75
NO. OF TUBES	25	25
ADHESIVE	SR-585	SR-585

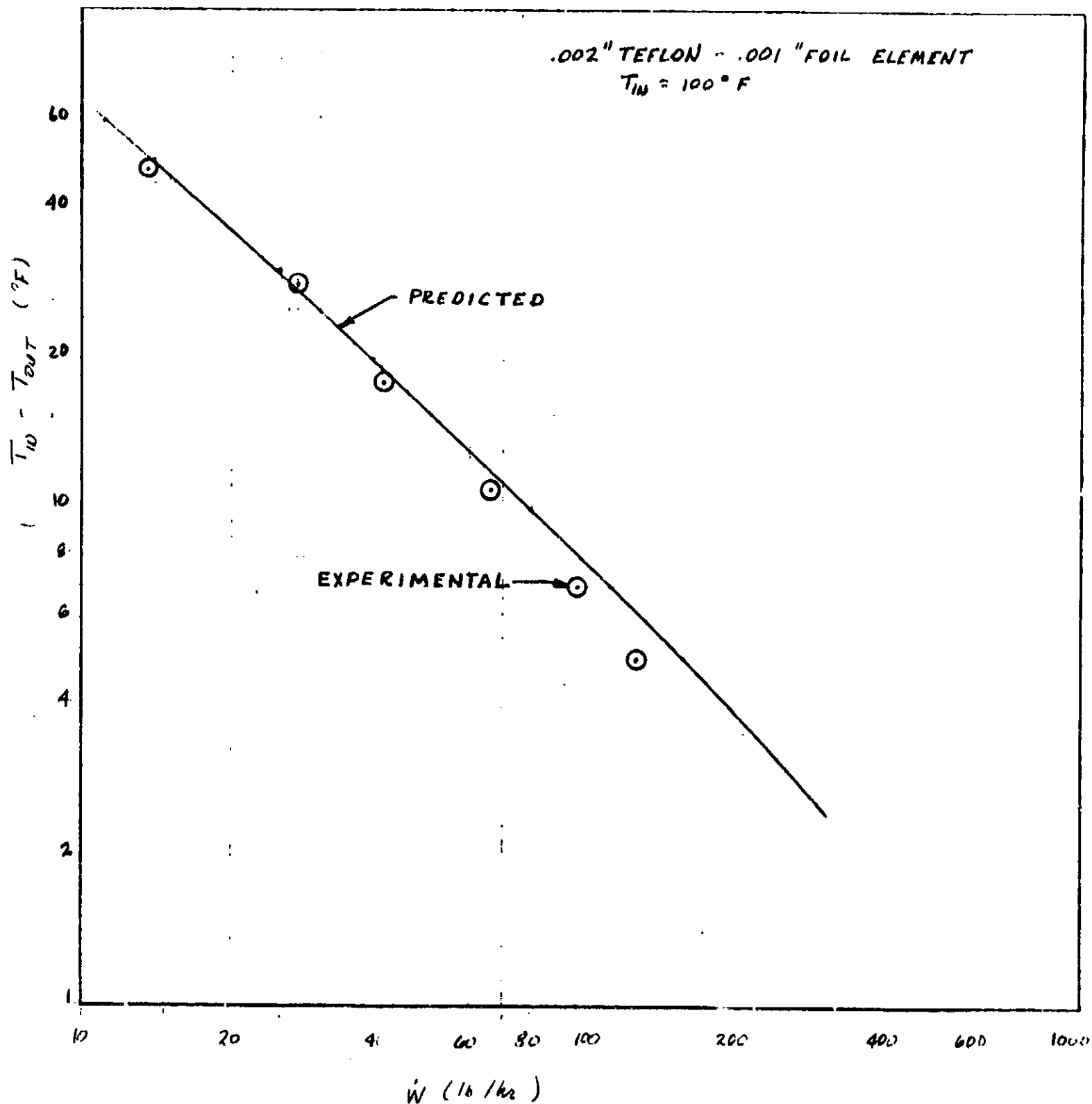


FIGURE 1 THERMAL PERFORMANCE OF ALUMINUM FOIL ELEMENT
A-165

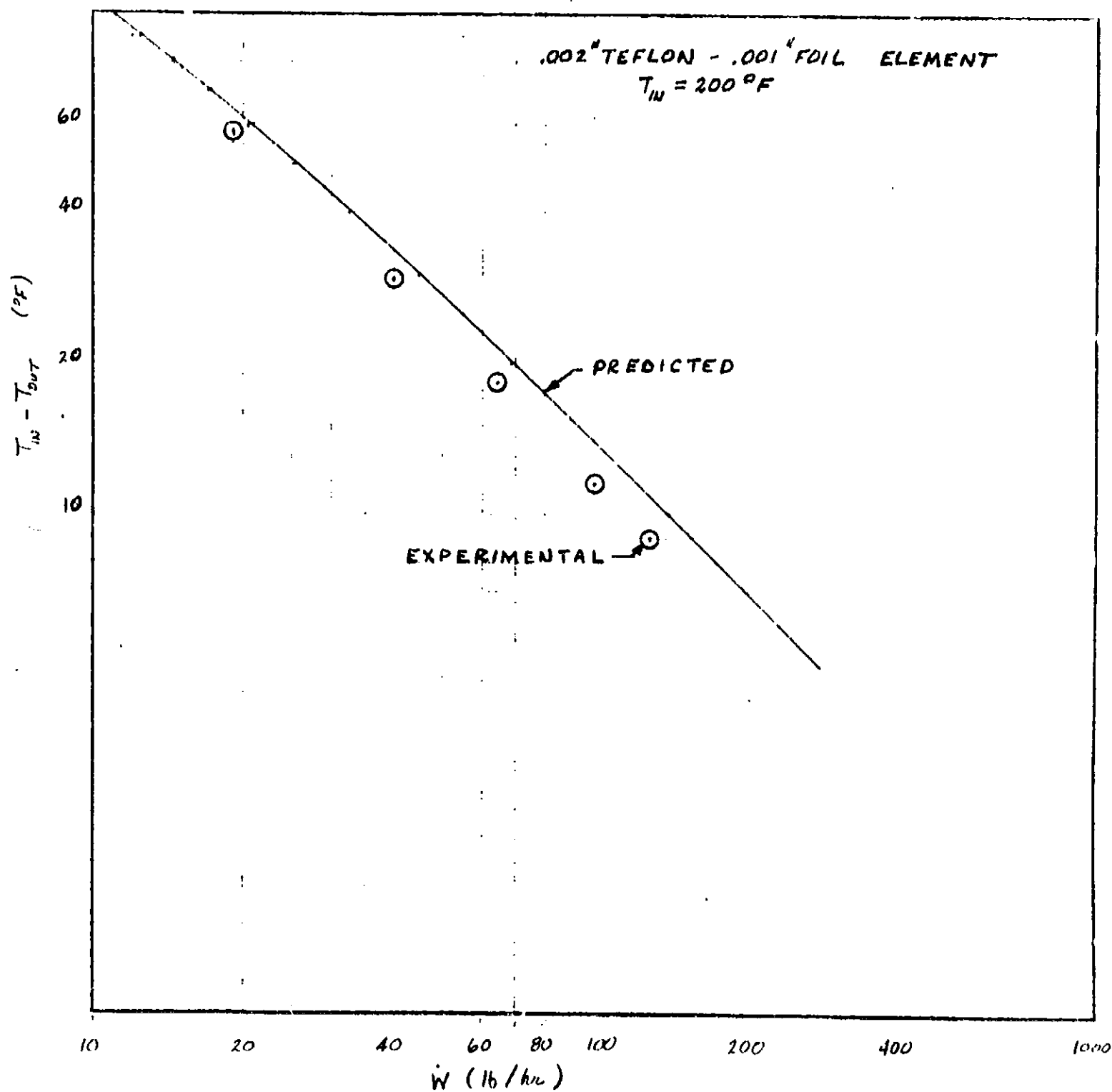


FIGURE 2 THERMAL PERFORMANCE OF ALUMINUM FOIL ELEMENT

A-166

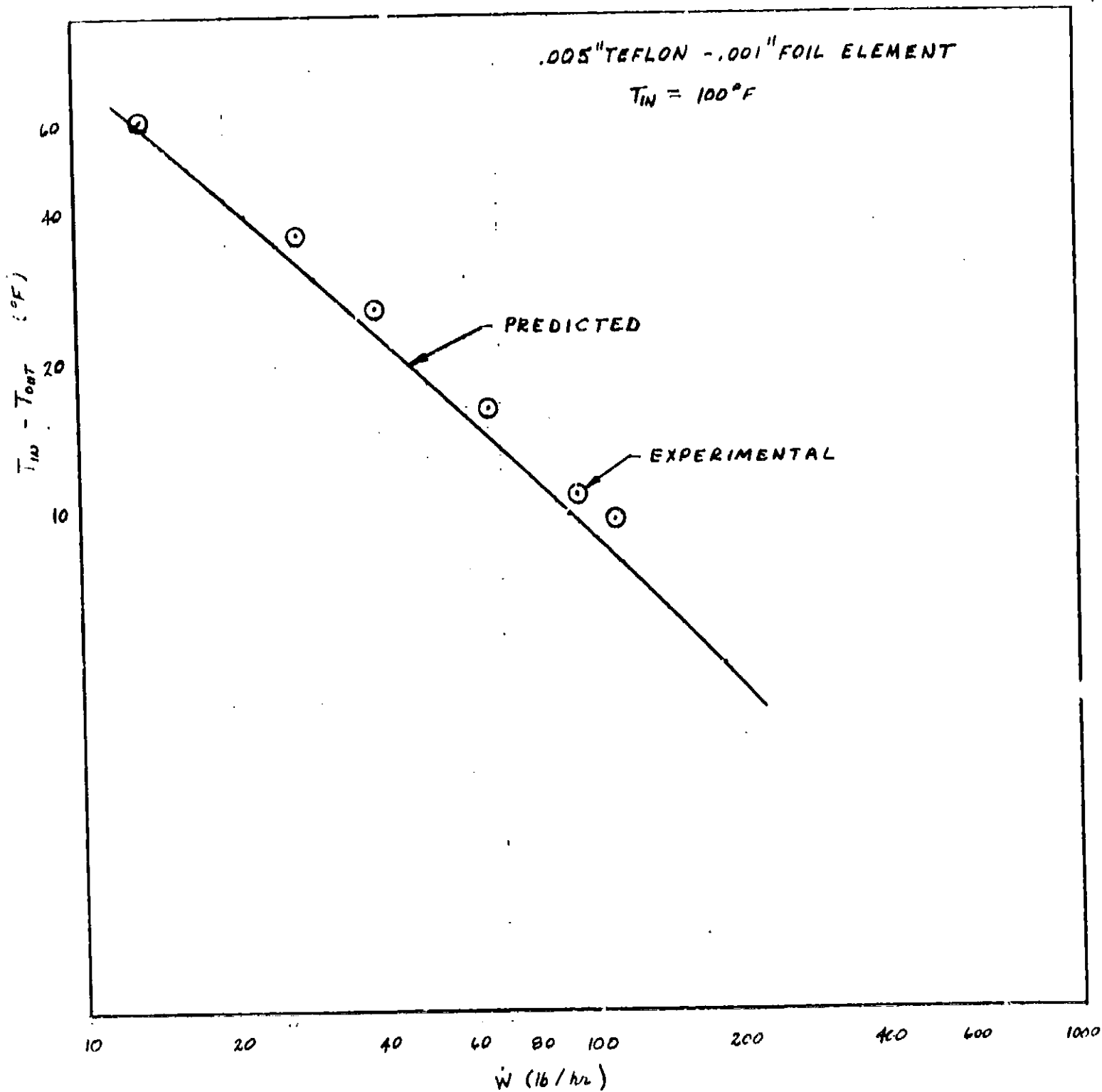


FIGURE 3 THERMAL PERFORMANCE OF ALUMINUM FOIL ELEMENT
 A-167

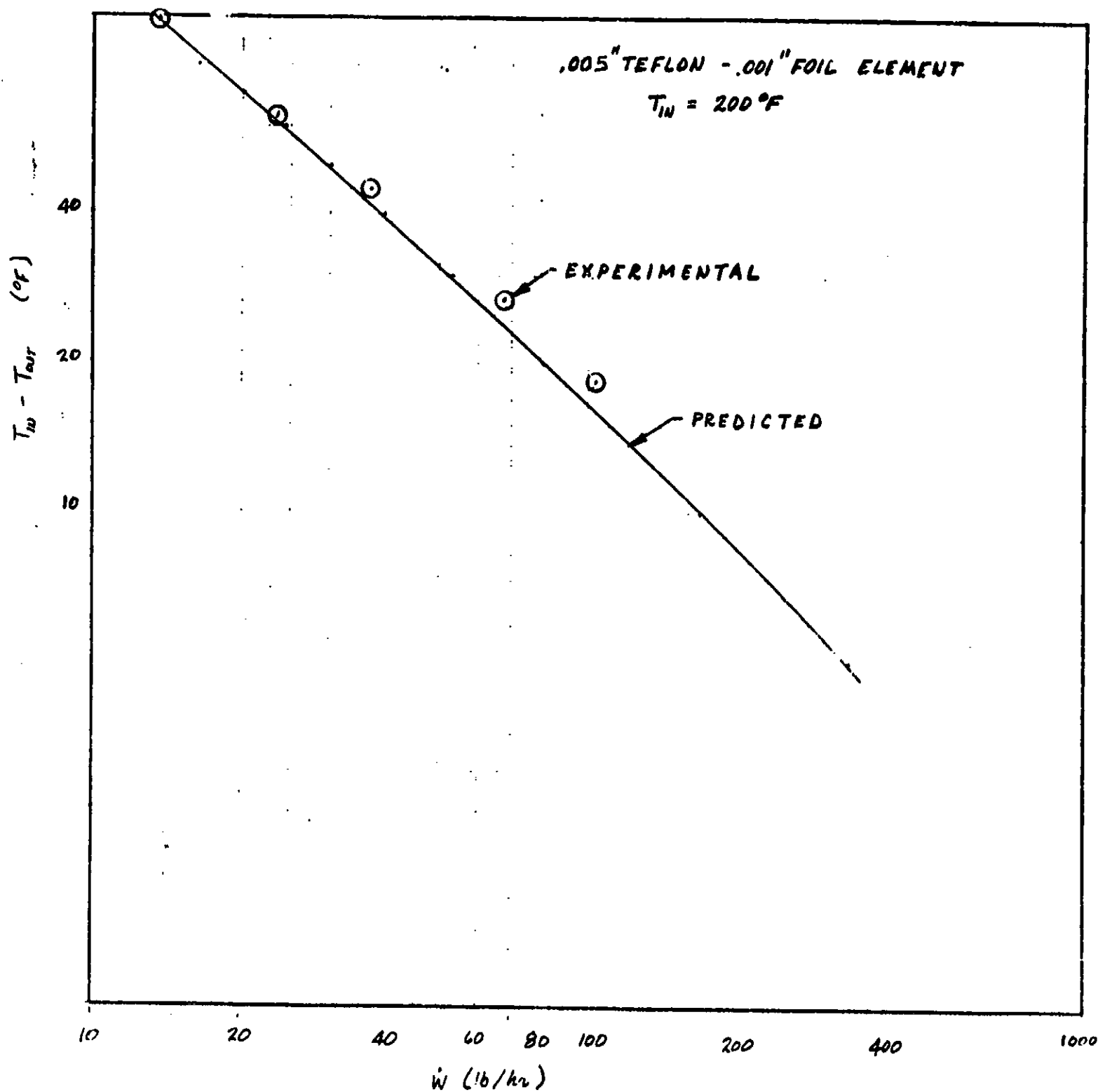


FIGURE 4 THERMAL PERFORMANCE OF ALUMINUM FOIL ELEMENT

in a sealed container for approximately 1 year. The coated surfaces were exposed to the atmosphere overnight before being pressed together to insure that the solvent would completely evaporate.

A separate four square inch element was made from a new supply of adhesive to determine whether aging of the adhesive had caused the delamination problem. Also, the new adhesive was thinned with one part toluene per one part adhesive to determine whether a thicker layer of adhesive would improve the strength of the bond. The adhesive was applied with cheese cloth. The element showed no tendency to delaminate when exposed to a vacuum, and a much stronger bond resulted. The measured thickness of the adhesive film is .001 inch. This compares to a thickness of .00025 inch obtained with the 8:1 solvent to adhesive mixture.

2.2 Fabrication and Test of Fusion Bonded Elements

A fusion bonded 18" x 18" element with PFA tubing and screen wire mesh fin material was fabricated and tested. The element was bonded together by heating it to 520°F so that the FEP Teflon in the fin material melted to form an adhesive. Pressure was applied to the assembly during the bonding process by means of a vacuum bag, and the system was heated in an autoclave. The radiator tubing was held at the proper spacing as the panel was being assembled and transported to the autoclave by maintaining a partial vacuum in the vacuum bag.

Thermal performance data for the fusion bonded element is presented in Figures 5 and 6. The thermal performance of the element is excellent, and the test article was not affected structurally by exposure to the vacuum environment.

2.3 Advanced Long Life Radiator Study

An advanced radiator concepts briefing was held at NASA-JSC on 10 November 1977. Ground rules and guidelines for conducting the study were agreed upon, and several long life radiator concepts were selected for additional study and analysis. A program plan and schedule was agreed upon.

3.0 Work on Major End Items

Work is in progress in the fabrication and advanced radiator study phases of the program.

4.0 Work Planned in the Next Reporting Period

The prototype flexible radiator panel will be fabricated by fusion bonding screen wire mesh fin material to PFA tubing. Work on the advanced radiator study will include continuation of concept generation and definition, concept screening, and trade studies.

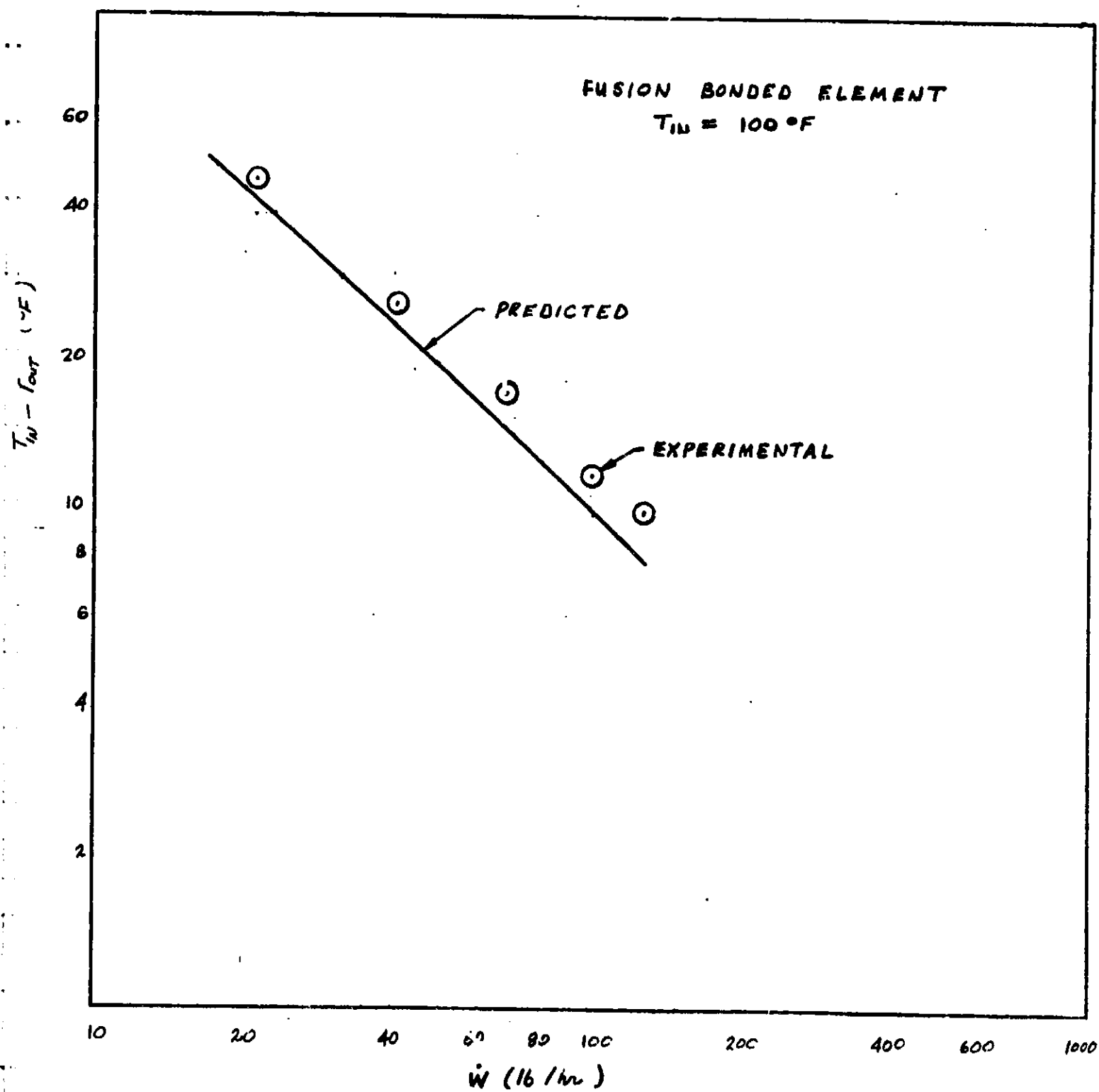


FIGURE 5 THERMAL PERFORMANCE OF FUSION BONDED ELEMENT
 A-76

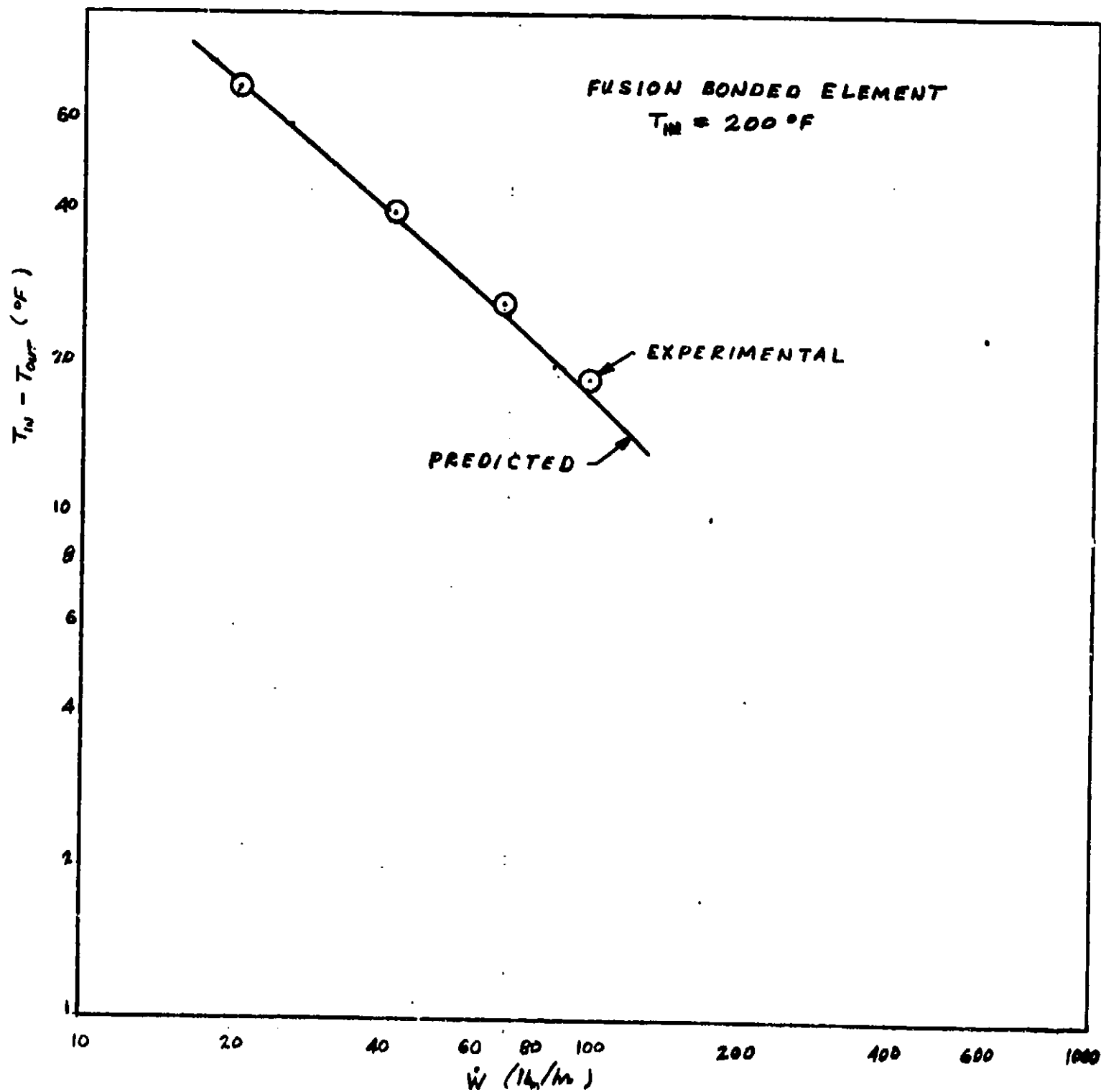


FIGURE 6 THERMAL PERFORMANCE OF FUSION BONDED ELEMENT

A-171

DEVELOPMENT OF A PROTOTYPE FLEXIBLE RADIATOR SYSTEM

PROGRESS REPORT NO. 16

1 DECEMBER 1977 THROUGH 28 FEBRUARY 1978

20 March 1978

CONTRACT NO. NAS9-14776
DRL: T-1213, LINE ITEM 2
DRD: MA-182TD

SUBMITTED TO:

THE NATIONAL AERONAUTICS AND SPACE ADMINISTRATION
JOHNSON SPACE CENTER
HOUSTON, TEXAS

BY

VOUGHT CORPORATION
DALLAS, TEXAS

PREPARED BY:

J. W. Leach
J. W. Leach

CHECKED BY:

J. A. Oren
J. A. Oren

APPROVED BY:

R. L. Cox
R. L. Cox

PROGRESS REPORT NO. 16

1.0 OVERALL PROGRESS

Work during the 16th reporting period has been concentrated on the fabrication and advanced radiator study phases of the flexible radiator development program and addresses the following subjects:

- a) fusion bonding of the prototype panel,
- b) flow distribution calibration of the prototype panel,
- c) ultrasonic welding of the radiator fin material,
- d) long life radiator study, and
- e) publication of technical paper.

2.0 PROGRESS ON INDIVIDUAL MAJOR AREAS

2.1 Fusion Bonding of The Prototype Panel

The prototype panel was fabricated successfully by pre-positioning the components as shown in Figure 1, and then heating the assembly until the FEP Teflon fin material melted. When the assembly was allowed to cool under a pressure of 1 atm., a strong bond formed between the two layers of fin material. A weaker bond is obtained between the fin material and the PFA transport tubing, with the strength of the bond depending on the maximum temperature experienced in the bonding process. The strongest bonds are obtained for processing temperatures in excess of 600°F. However, the PFA tubing has very little strength at such temperatures, and tends to collapse, apparently because of gravity or surface tension forces. Element tests showed that an adequate bond is obtained without deformation of the transport tubing if the processing temperature is maintained at $570 \pm 5^\circ\text{F}$.

When fabricating the prototype radiator, the seal of the vacuum bag was designed so that the ends of the transport tubes extended through the vacuum bag, and were open to the atmosphere. This equalizes the internal and external atmospheric pressure components, and prevents the vacuum bag from tending to flatten the transport tubing. The temperature variations across the panel were held within narrow limits by heating the oven slowly so that transient temperature gradients are minimized, and by covering the radiator panel with Beta cloth insulation to shield it from temperature variations in the heated atmosphere of the oven. The panel was heated on a large aluminum table which was insulated on the bottom side. The conductance of the table thus tended to reduce any remaining temperature gradients.

The temperature distribution across the radiator panel measured at the hottest point of the bonding cycle is shown in Figure 2. The temperatures were measured with Iron-constantan thermocouples placed inside the transport tubes. The transient temperature profile measured during the bonding process is shown in Figure 3. This profile was obtained by initially setting the thermostats of the oven heaters at 550°F, and observing the temperature distribution across the panel as it approached equilibrium. The thermostat settings of the individual oven heaters were then adjusted as required to achieve a uniform panel temperature of 570°F. The panel was bonded

in Vought's oven No. 12, building 22. This is a 5.5' x 5.5' x 33' oven with 6 individually controlled heated zones. The equilibrium temperatures of the individual zones are automatically controlled within $\pm 3^{\circ}\text{F}$. However, the transient responses of the individual heaters are significantly different so that it is necessary to manually adjust the control settings as described above.

The radiator panel fabricated by this procedure is entirely satisfactory for testing purposes. Very little shrinkage or distortion of the transport tubing occurred, and a strong bond was obtained. The transport tubes are straight and evenly spaced, and the appearance of the panel is satisfactory. A few isolated wrinkles developed when vacuum was applied prior to heating the panel. The wrinkles occurred where the Teflon film material had been locally stretched prior to assembly and could not be permanently removed by releasing the vacuum and straightening the material. The wrinkles recurred at approximately the same locations each time the vacuum was applied.

The stretching of the fin material probably occurred when the wire mesh was being embedded in the Teflon film. If additional panels are to be fabricated by this process, the screen mesh and Teflon film should be fusion bonded together at the same time that the fin material is bonded to the transport tubing. In this case the Teflon film will not have been deformed prior to assembly, and the cause of the wrinkles thus eliminated. Also, the screen mesh will serve as a bleeder cloth and assist in the removal of air pockets between the layers of fin material.

A second fabrication problem area which affects the appearance of the radiator concerns the separation of the fin material from the vacuum bag subsequent to heating the assembly to bonding temperatures. Kapton was selected as the material for the vacuum bag because it has adequate strength and does not tend to bond to FEP Teflon at the temperatures required for this application. Element tests on small radiator sections indicated that Kapton is an acceptable vacuum bag material. However, when the prototype panel was fabricated, the bond between the radiator and vacuum bag was much stronger than had occurred in the element tests. Apparently the additional time required to heat the large prototype panel contributed to the strength of the bond. When the Kapton vacuum bag was removed from the prototype radiator panel the surface of the Teflon radiator fin was found to have a diffuse appearance. Also, in a few small areas, the bond between the radiator fin and Kapton was so strong that the fin material would tear away from the transport tubing before it would separate from the Kapton. Liquid nitrogen was poured over small sections of the radiator in areas where the bond was exceptionally strong so that differences in the thermal expansion coefficients of Kapton and Teflon would cause the two layers to separate. In these sections the vacuum bag was easily removed from the radiator, and the panel surface was left with a glossy finish. This procedure was followed only when it was considered necessary to prevent the radiator fin from tearing because of concern over weakening the joint between the FEP Teflon radiator fin and the PFA Teflon transport tubing. However, subsequent visual inspections of the sections where LN_2 was applied revealed no areas where the tubing had separated from the fin material. The areas where the fin material had been torn were repaired by locally heating the material

past the melting point so that the torn surfaces fused together. This produced a relatively neat joint which blends in with the rest of the radiator panel and is un-noticeable when viewed from a short distance.

Additional studies and element tests should be conducted to prevent this problem from recurring in the future. It is probable that the Kapton film could be sprayed with a light silicone coating which would prevent the molten Teflon from adhering to the vacuum bag.

The solar absorptivity of the radiator panel was measured at several locations with a Gier Dunkle optical reflectometer. All of the measurements were made in areas where the Kapton vacuum bag had been peeled away from the radiator leaving a diffuse surface appearance. The measured values of α ranged from $\alpha = .055$ to $\alpha = .078$. Measurements could not be made at interior sections of the panel where the glossy surface areas were obtained by removing the vacuum bag with LN_2 . However, it is not expected that the α values would differ greatly from those of the diffuse areas.

2.2 Panel Flow Distribution Test

The flow distribution in the parallel tubes of the prototype panel was determined by measuring the flow in each individual tube. This was done by flowing water into the inboard manifolds at a constant pressure, and collecting the flow from individual tubes in glass beakers. The flowrates were determined by weighing the water collected during prescribed periods of time. Figure 4 gives the percentage deviations from the mean flow per tube for the 50 transport tubes. The results generally show a consistent and uniform flow distribution. Some of the scatter in the data is caused by water being lost from the open beakers by splashing or by spillage when the beakers were removed from the flow streams, and some to measurement error. Approximately 50 grams of water were collected for each tube, and the estimated measured error is ± 1 gram. Thus, measurement error would account for errors of the order of 2% whereas the RMS deviation measured for the 50 tubes is only 3.1%. Thus the measured flow deviations could be attributed to experimental error in most cases. It is significant that none of the tubes has a noticeably low flow. This indicates that the tubes were not damaged during the fusion bonding process.

The manifolds and fittings were checked for leakage with Freon leak detectors and found to be leak free. In addition, leakage rates were measured by pressurizing the panel with gaseous nitrogen and observing the decay of pressure with time. This procedure is not entirely satisfactory because the effects of the permeability of the transport tubing cannot be accurately accounted for, but indicates the presence or absence of gross leaks which might not have been discovered with the Freon leak detector. The pressure of the nitrogen gas entrapped in the manifolds and transport tubes dropped from 100 psi to 74 psi in a 24-hour period. The equation for pressure decay due to the transport tubing permeability is

$$\frac{P - P_{\infty}}{P} = \frac{P_0 - P_{\infty}}{P_0} e^{\frac{-\mu A P_{\infty} \tau}{Vt}} \quad (1)$$

where: P = pressure of entrapped gas at time τ
 P_{∞} = ambient pressure (1 atm)
 P_0 = initial pressure (100 psi)
 μ = permeability (380 cc/100 sq. inch/24 hr/atm/mil)
 A = surface area (3534 in²)
 t = tube wall thickness (32 mil)
 V = volume of entrapped gas (0.149 ft³)

Equation (1) predicts that the pressure of the entrapped nitrogen at the end of a 24 hour period should be 64.5 psi. This corresponds to a slightly larger leakage rate than was determined experimentally, and thus indicates that there are no sizeable leaks at the manifolds or fittings.

An accurate indication of the radiator panel leakage rate could be obtained by filling the radiator with the actual fluid to be employed in spaceflight applications, and observing the fall of the meniscus in a transparent small diameter fill tube over long periods of time. In this way the total fluid loss from tubing permeability and leakage at the manifolds and fittings could be readily determined. This measurement could probably be conveniently made just prior to thermal vacuum testing.

2.3 Ultrasonic Welding of Radiator Fin Material

Samples of flexible radiator fin material and transport tubing were supplied to Branson Sonic Power Company so that their applications lab could evaluate the feasibility of using ultrasonic welding in fabricating flexible radiators. The lab looked at several methods for tack welding the fin material together so that it would hold the transport tubing in position. The remainder of the radiator would then be fusion bonded by heating in an oven. Their report indicates that the radiator fin material cannot be ultrasonically welded at the present state of technology. A copy of the Branson lab report is enclosed.

This method was investigated as an alternative to the present procedure for fusion bonding the flexible radiator. It is not essential to the fabrication process. The Branson Company performed the study at their own expense.

2.4 Long Life Radiator Study

A computer routine is being developed for conducting trade studies and to optimize the designs of pumped fluid and heat pipe radiators for long duration missions. The literature is being surveyed, and researchers and

vendors are being contacted to obtain data on radiator system component life limits and design constraints. Materials were ordered for fabricating demonstration hardware and for testing conceptual designs with expanded metal fin materials, metal bellows materials, and stainless steel cross flow tubes. A flexible meteoroid bumper has been designed for the long life flexible radiator. Heat pipe radiator panels are being designed and tested under Vought internal research and development funding.

2.5 Publication of Technical Paper

The technical paper, "Flexible Deployable-Retractable Space Radiators" presented in June 1977 at the AIAA 12th Thermophysics Conference was revised and submitted for publication in the Heat Transfer Volume of the 1978 AIAA Progress in Astronautics and Aeronautics Series. The Volume will be published in May 1978.

3.0 WORK ON MAJOR END ITEMS

Work is in progress in the fabrication and advanced radiator study phases of the program.

4.0 WORK PLANNED IN THE NEXT REPORTING PERIOD

Inflation tubing will be attached to the prototype radiator, and ambient deployment tests performed provided retraction springs are delivered by the spring vendor. The delivery of the springs is expected within the next few days, but the exact date is uncertain. The spring vendor is awaiting materials which have been shipped from Ohio. Work will continue on the long life radiator study.

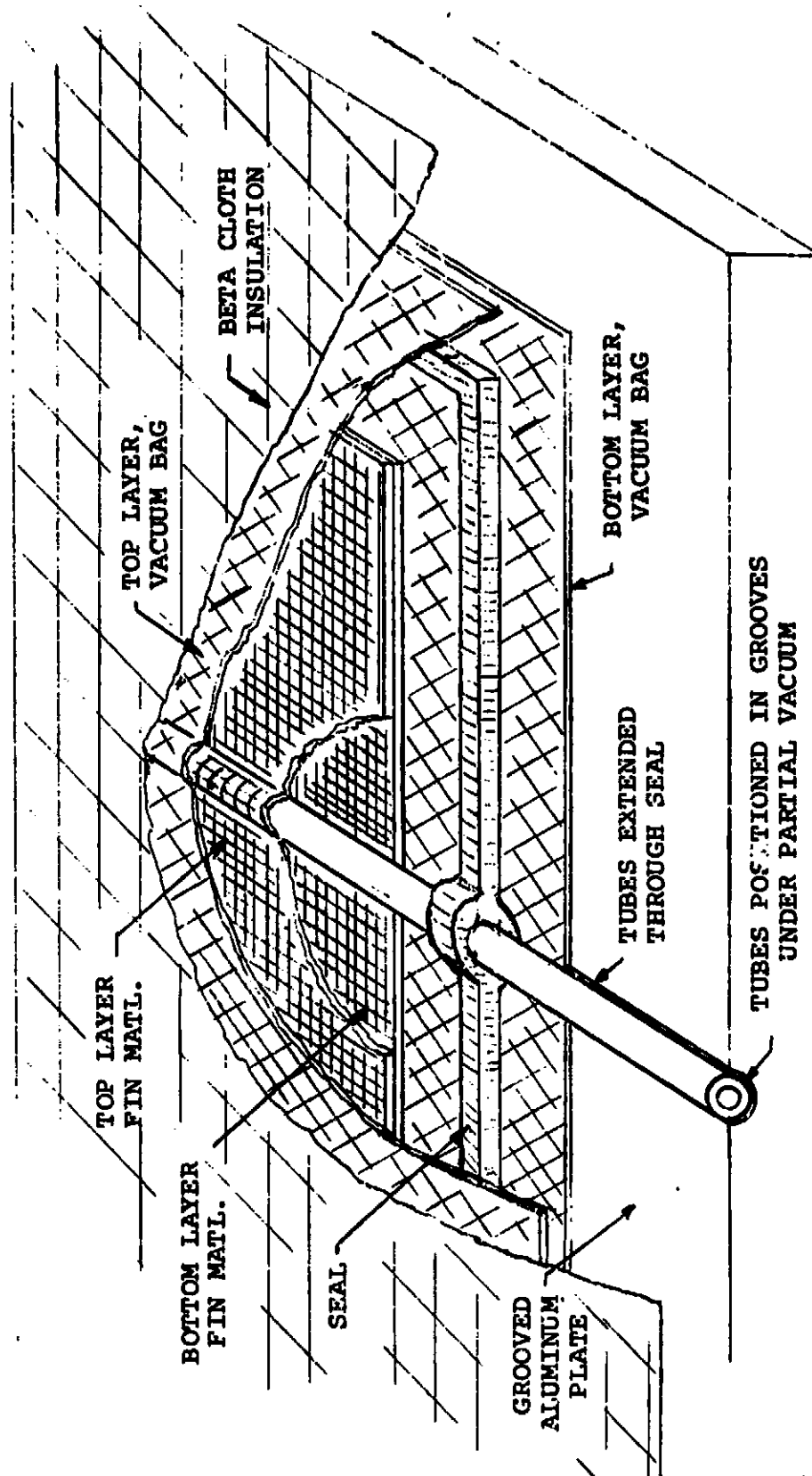


FIGURE 1 ASSEMBLY FOR FUSION BONDING RADIATOR

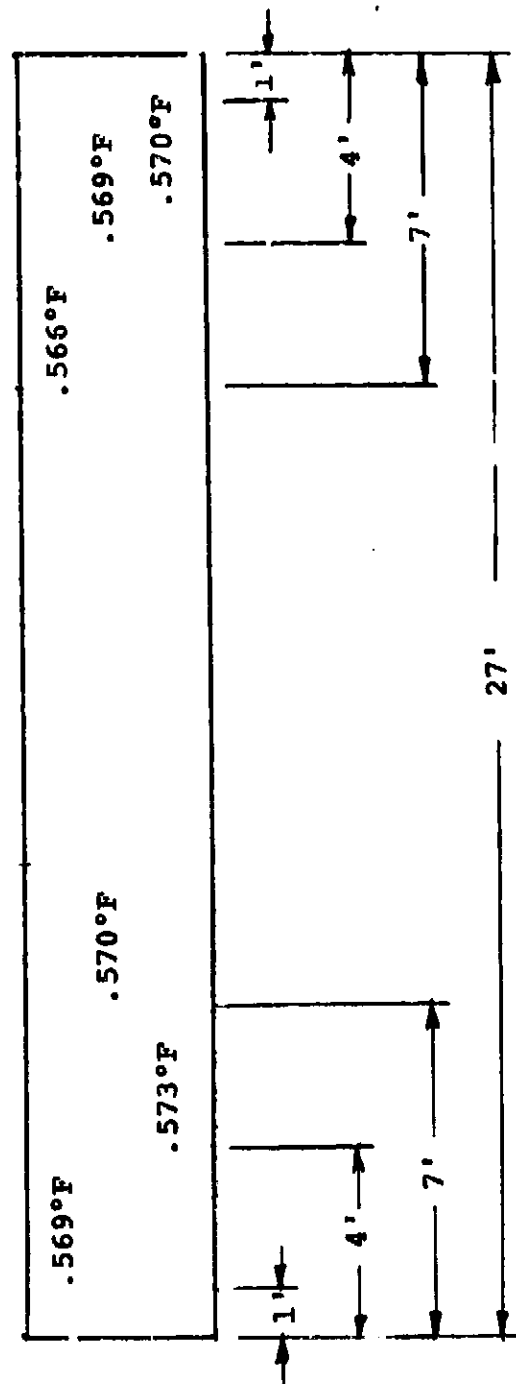


FIGURE 2 PEAK TEMPERATURE DISTRIBUTION IN FUSION BOND PROCESS

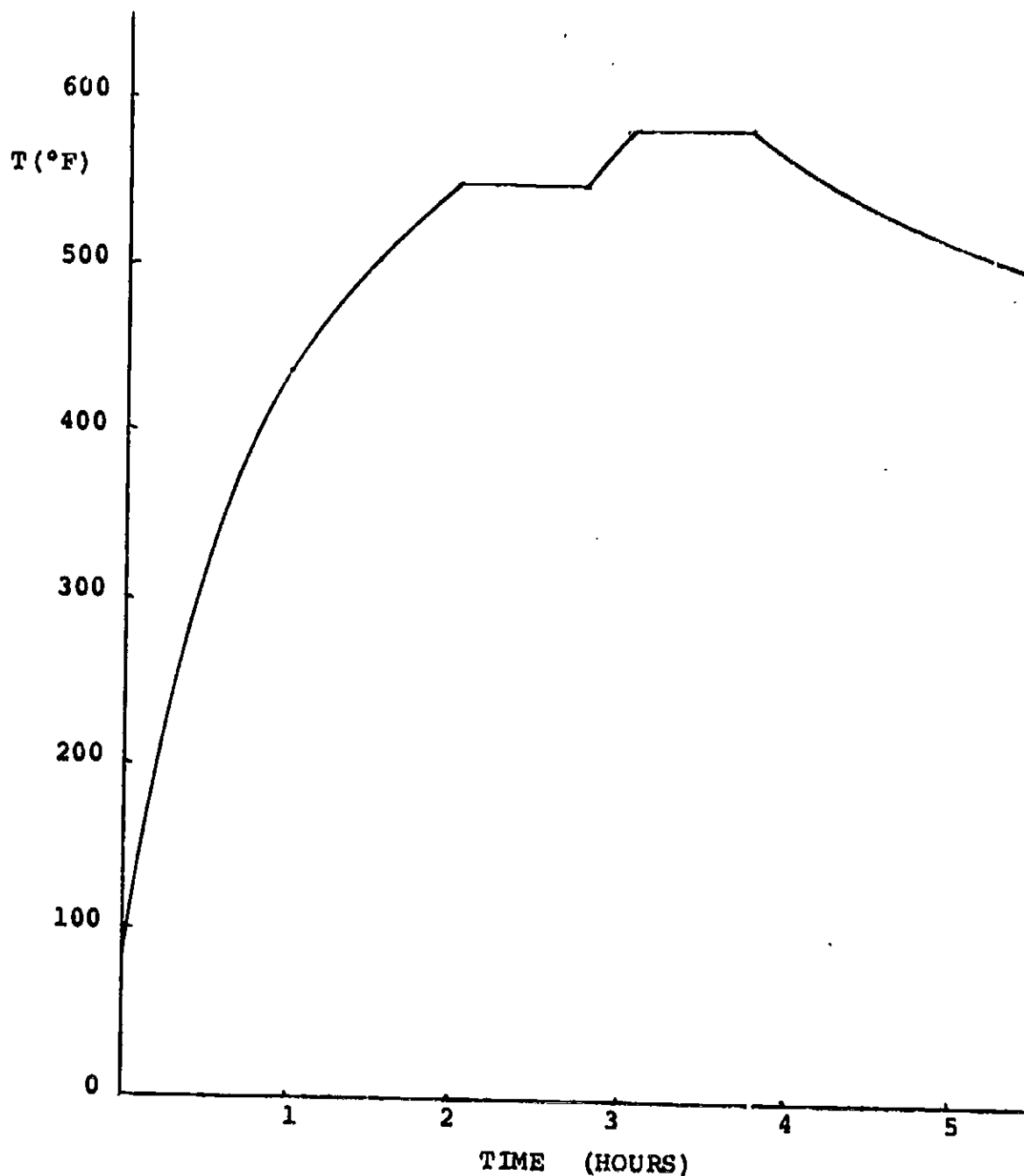


FIGURE 3
TRANSIENT TEMPERATURE OF OVEN ATMOSPHERE
DURING FUSION BONDING CYCLE

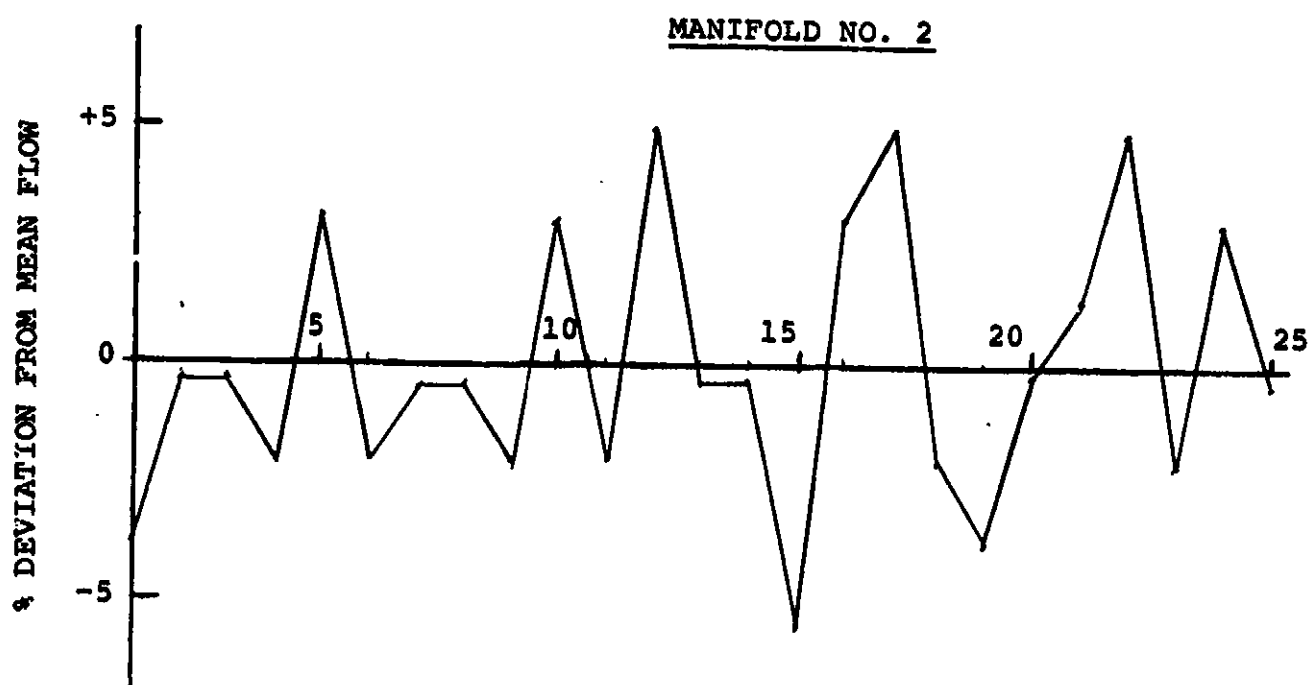
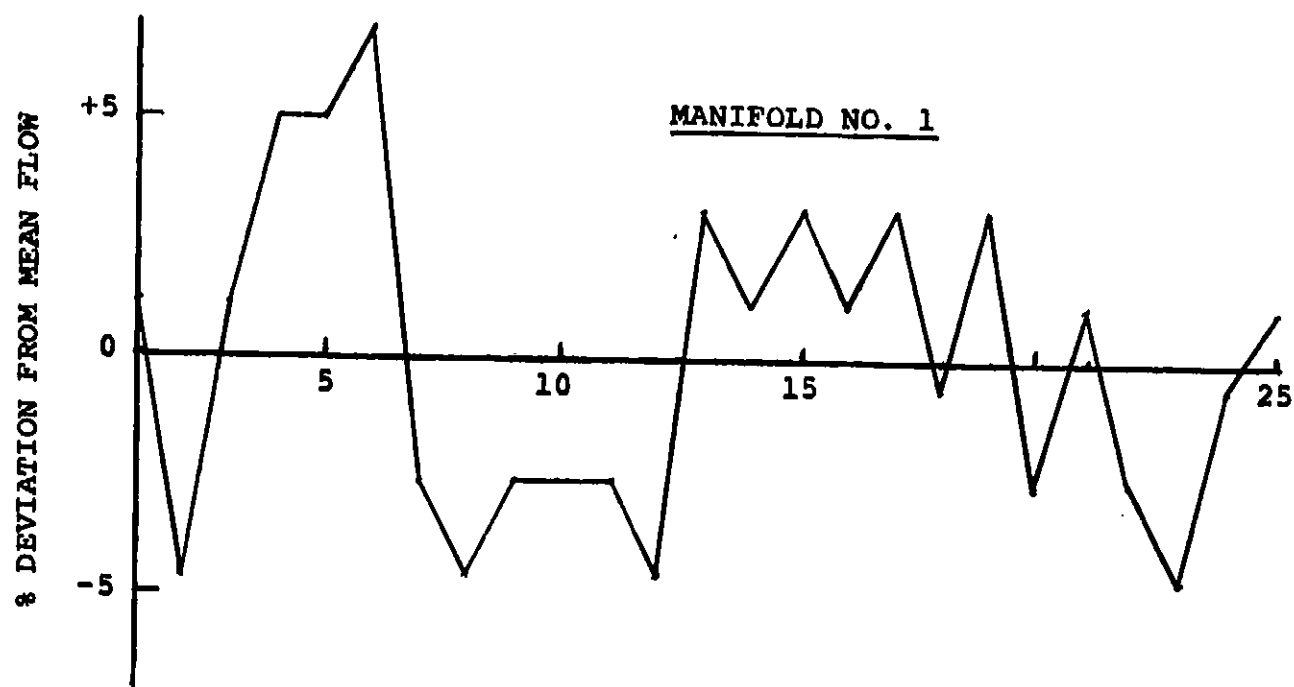


FIGURE 4 PROTOTYPE RADIATOR FLOW CALIBRATION RESULTS

BRANSON
SONIC POWER COMPANY

January 17, 1978

Mr. Jim Leach
VOUGHT
1701 W. Marshall
Grand Prairie, Texas 75050

Dear Mr. Vought:

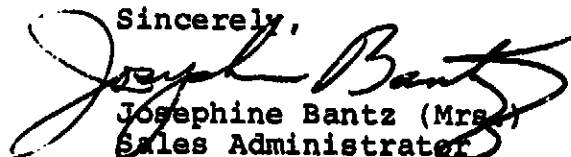
Enclosed is Application Laboratory Report #1177-1382 regarding the samples you provided.

Unfortunately, the report indicates that this particular application is not feasible for ultrasonics at the present state of our technology.

Our capabilities are continually expanding, however, and we may be able to satisfy such requirements in the future.

We regret that we are unable to help you on this occasion, but if you have other applications that you feel may lend themselves to ultrasonic assembly, please contact either our area Sales Engineer or Representative

Sincerely,


Josephine Bantz (Mrs.)
Sales Administrator

JB/yl

cc: Chuck Newby
I. P. Newby & Associates
6211 Denton Drive
Box 35846
Dallas, Texas 75235
(214) 357-8354

Bill Wilson

A-182

BRANSON SONIC POWER COMPANY

Eagle Road, Danbury, Connecticut - 06810 a subsidiary of Smith Kline & French Laboratories

Ph: (203) 744-0760
TWX 710-456-0452

APPLICATIONS LAB REPORT

CUSTOMER VISIT () APPLICATION INQUIRY (X)

COMPANY Vought

BSP# _____ LAB# 1177-1382

NAME Jim Leach REP. # _____

DATE IN 11/14/78 DATE OUT 1/11/79

ADDRESS 1701 W. Marshall

TYPE OF REPORT:

PRINT REVIEW ()

CITY & STATE Grand Prairie, Texas 75050

PART EVALUATION (X)

ITEMS tubing and film with wire screen

HORN TEST ()

attached

THIS APPLICATION APPEARS TO BE:

EXCELLENT () GOOD () FAIR ()

MATERIAL Teflon

POOR () NOT POSSIBLE AT THIS TIME (X)
BASED ON SAMPLES SUBMITTED.

TYPE OF APPLICATION: _____

WELDING (X)

ADHESIVE REACTIVATION ()

SCAN WELDING ()

INSERTION ()

SPOT WELDING ()

OTHER ()

SWAGING ()

SEWING (X)

SPECIFY:

STAKING ()

DEGATING ()

APPLICATION EVALUATION EQUIPMENT SET UP Various

STAND MODEL _____ POWER SUPPLY _____ ACCESSORY _____ BOOSTER _____

HORN _____

PRESSURE (PSIG) _____ FIXTURING _____

WELD TIME (SECONDS) _____ HOLD TIME (SECONDS) _____

PART WAS CONTACTED WITH HORN: TOP () BOTTOM () OTHER ()

EQUIPMENT RECOMMENDATIONS: None at this time.

STAND MODEL _____ POWER SUPPLY _____ ACCESSORIES _____ BOOSTER _____

HORN _____

FIXTURING _____

COMMENTS requirements: To seal a wire screen and film assembly around
several tube samples.

Various methods (plunge welding, continuous processing, hand held
welders) were tested for processing this material, but at this time
good welds could not be formed. Both the film and tubing degraded
before a weld could be formed.

I regret that we cannot recommend ultrasonic equipment for this
particular application. If there are other applications that we
may evaluate for you in the future, please contact us.

BY

John B. Roman

11 A-123 Applications Engineer

DEVELOPMENT OF A PROTOTYPE FLEXIBLE RADIATOR SYSTEM

PROGRESS REPORT NO. 17

1 MARCH 1978 THROUGH 23 APRIL 1978

25 April 1978

CONTRACT NO. NAS9-14776

DRL: T-1213, LINE ITEM 2

DRD: MA-182TD

SUBMITTED TO:

THE NATIONAL AERONAUTICS AND SPACE ADMINISTRATION
JOHNSON SPACE CENTER
HOUSTON, TEXAS

by

VOUGHT CORPORATION
DALLAS, TEXAS

PREPARED BY:

J. W. Leach
J. W. Leach

CHECKED BY:

J. A. Oren
J. A. Oren

APPROVED BY:

R. L. Cox
R. L. Cox

1.0 OVERALL PROGRESS

Work during the 17th reporting period has been concentrated on the Advanced Radiator Study Phase of the Flexible Radiator Development Program, and addresses the following subjects:

- a) Design of pumped fluid radiators for long duration missions
- b) Optimum subsystem module size for large radiator systems
- c) Manifold designs for heat pipe radiators
- d) Demonstration radiator elements constructed from expanded silver metal
- e) Design of meteoroid shield for the long life flexible radiator manifolds

2.0 PROGRESS ON INDIVIDUAL MAJOR AREAS

2.1 Design of Pumped Fluid Radiators for Long Duration Missions

A computer model was prepared for the generalized pumped fluid radiator system shown in Figure 1 to determine the values of radiator parameters such as tube diameter, tube spacing, transport fluid Reynolds number, and fin efficiency best suited for long life radiator systems. The program minimizes a function of the radiator weight and area to optimize radiator designs for various mission durations and subsystem survival probabilities. Documentation of the analysis shall be covered in an advanced radiator study report.

2.2 Subsystem Size Optimization

Statistical analyses are being performed to determine the best way to assemble large heat rejection systems from small subsystems. The analysis determines the most probable loss of radiating area as a function of module size and survivability, and compares the overall weight of systems having large numbers of modules to those having fewer numbers of more reliable subsystems.

2.3 Heat Pipe Radiator Manifold Designs

Several concepts for connecting heat pipe radiator panels to transport fluid manifolds are being analyzed for performance, weight, and manufacturability. Radiator optimization computations will be performed for the more promising manifold concepts to compare the weight and performance of heat pipe and pumped fluid radiators. The analyses shall seek to determine the mission applications for which each type of radiator system is best suited.

2.4 Expanded Metal Radiator Fin Elements

Small 4" x 4" sections of radiator fin were fabricated by fusion bonding expanded silver metal to FEP Teflon film. Elements were fabricated with two different expanded metal mesh dimensions. Table I gives data for the two elements. The element made with the 3AG5-6/0 expanded metal was constructed from a sample supplied by Exmet Corp. The sample was tarnished slightly when received, and was therefore subjected to a cleaning process prior to bonding. An attempt was made to remove the tarnish from the sample by immersing it in a 10% solution of sulfuric acid. This procedure had previously been employed to remove the silver coating from silver backed Teflon. However, in this case the acid did not clean the surface uniformly with exposure times for which the mesh would not be damaged. Several attempts were then made to degrease the metal by scrubbing it with MEK, Trichloroethylene, and a detergent/water mixture. However, the acid still would not completely remove the tarnish. A 20% solution of sulfuric acid also failed to clean the surface adequately.

The Vought materials section is studying this problem, and will recommend a procedure for cleaning silver screen and expanded metal.

The 5AG7-6/0 metal had a bright finish when received from Exmet Corp., but was also degreased and cleaned prior to bonding. The bonded element has a white shiny appearance whereas the element which could not be cleaned has a gold tint characteristic of oxidized silver. Both samples contained numerous small dark spots which resulted from contamination trapped within the assembly being charred during the bonding process. The particles are invisible prior to bonding, but are easily detected after being heated to 570°F. Some of the particles apparently are attracted to the Teflon film because of static charging whereas others are residual on the expanded metal following cleaning. After observing the particles on the first element, the laboratory technician was extremely careful when cleaning the Teflon and expanded metal before fusion bonding the second element. However, the dark spots still appeared on the bonded element. Small pieces of cotton from the cloth used to polish the surfaces are a surprisingly large source of contamination. Residual oil or grease left on the rough surface of the expanded metal because of improper cleaning also could be observed by close examination under a microscope. Additional work is needed to establish a cleaning procedure prior to fabricating the long life flexible radiator.

The measured solar absorptivity of the samples is larger than had been expected. The dark spots discussed above distract from the appearance of the surface but are far too sparse to have an appreciable effect on the solar absorptivity. The tarnished appearance of the first element probably accounts for its high absorptivity. The high absorptivity of the second sample could be caused by radiation entrapment in the cavities of the expanded metal. The ratio of the depth to diameter of the cavities is greater for this element than for the other fusion bonded surfaces tested in this work, and the transmissivity of the film is much lower. Calculations will be made to evaluate the entrapment effect, and additional elements having only one layer of expanded metal mesh shall be tested.

2.5 Meteoroid Shield for The Long Life Flexible Radiator Manifolds

The meteoroid shield shown in Figure 2 was designed for protecting the manifolds of the long life flexible radiator. The shield consists of Teflon sleeves and stainless steel spherical sockets. When the manifolds bend for stowage, the Teflon sleeves rotate without bending on the spherical sockets. The design of the socket insures that the liquid transport lines are shielded for all manifold orientations, and the diameter of the sleeves is adequate for unconstrained motion of the metal bellows.

3.0 WORK ON MAJOR END ITEMS

Work is in progress on the advanced radiator study phase of the program.

4.0 WORK PLANNED IN THE NEXT REPORTING PERIOD

Ambient deployment tests will be performed with the prototype flexible radiator. Work will continue on the long life radiator study.

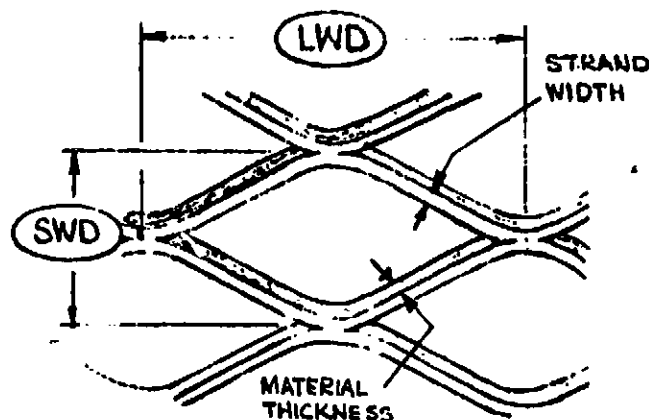
TABLE I
PROPERTIES OF EXPANDED METAL ELEMENTS

PROPERTY	MESH DESIGNATION	
	3 AG 5-6/0	5 AG 7-6/0
Mesh Thickness (inch)	.003	.005
Strand Width (inch)	.005	.007
Mesh Dimensions (inch)	.022 x .031	.022 x .031
Number Openings/inch ²	2600	2600
Fraction of Area Open	0.520	0.372
No. of Layers of Mesh	1	2
Calculated Transmissivity	0.520	0.138
Measured Transmissivity	0.522	0.065
Measured Reflectivity	0.361	0.748
Measured Solar Absorbtivity	0.117	0.187
Equivalent Thickness SWD ¹	.0026	0.0123
Equivalent Thickness LWD ²	.0052	0.0244

¹ Conductance across short dimension of diamond equal to that of aluminum fin of equivalent thickness.

² Conductance across long dimension of diamond equal to that of aluminum fin of equivalent thickness.

TABLE 1a



LWD

Long way of the diamond—measured from the center of one joint to the center of the next joint. This dimension is governed by the die used and never changes for that die. In fine expanded metal this is always parallel to the width of the coil.

SWD

Short way of the diamond—measured from the center of one joint to the center of the next joint. It will vary moderately with any given die as the strand width and degree of expansion are varied. The mesh count (openings per unit of length) decreases as expansion increases and conversely. Fine expanded metal is manufactured in coil form with this dimension running the length of the coil.

1. MESH DESIGNATION (Size)	1. MESH DIMENSIONS from center-to-center of joints LWD min. max.	Number openings per sq. in. approx.	2. THICKNESS OF ORIGINAL MATERIAL MIN. MAX.	3. STRAND WIDTH MIN. MAX.	4. MAX. SHEET WIDTH
1	.405" .20" .23"	25	.003" .025"	.007" .055"	18"
1/0	.280" .10" .125"	65	.003" .025"	.007" .055"	18"
2/0	.187" .077" .091"	120	.002" .020"	.007" .035"	18"
2/0E	.187" .048" .071"	170	.002" .015"	.007" .035"	12"
3/0	.125" .050" .065"	300	.002" .015"	.003" .020"	18"
FS	.100" .075" .085"	250	.005" .020"	.007" .025"	12"
4/0	.077" .038" .046"	625	.002" .012"	.003" .020"	12"
5/0	.050" .026" .030"	1400	.002" .010"	.002" .011"	10"
6/0	.031" .021" .024"	2600	.002" .007"	.002" .009"	6"

HOW TO ORDER

Exmet's customers have found the following method of specifying fine expanded metal useful and practical. Its use is recommended for positive identification of requirements.

For Example:

Sheet thickness (mils) 5
Metal (Chem. Symbol) NI
Strand width (mils) 7
Mesh designation 4/0

WRITTEN AS: 5 NI 7-4/0

This is a typical commercial specification.

When an application requires more specific details, they should be indicated, as for example:

- a) 250 grams (± 5%) per square inch (required weight)
- b) .010" overall thick (± .001") (required overall thickness)
- c) annealed (material to be soft)
- etc.

NOTE: Weight, overall thickness, strand width and original metal thickness must be compatible for mesh designation and total specification. See explanations above regarding chart.

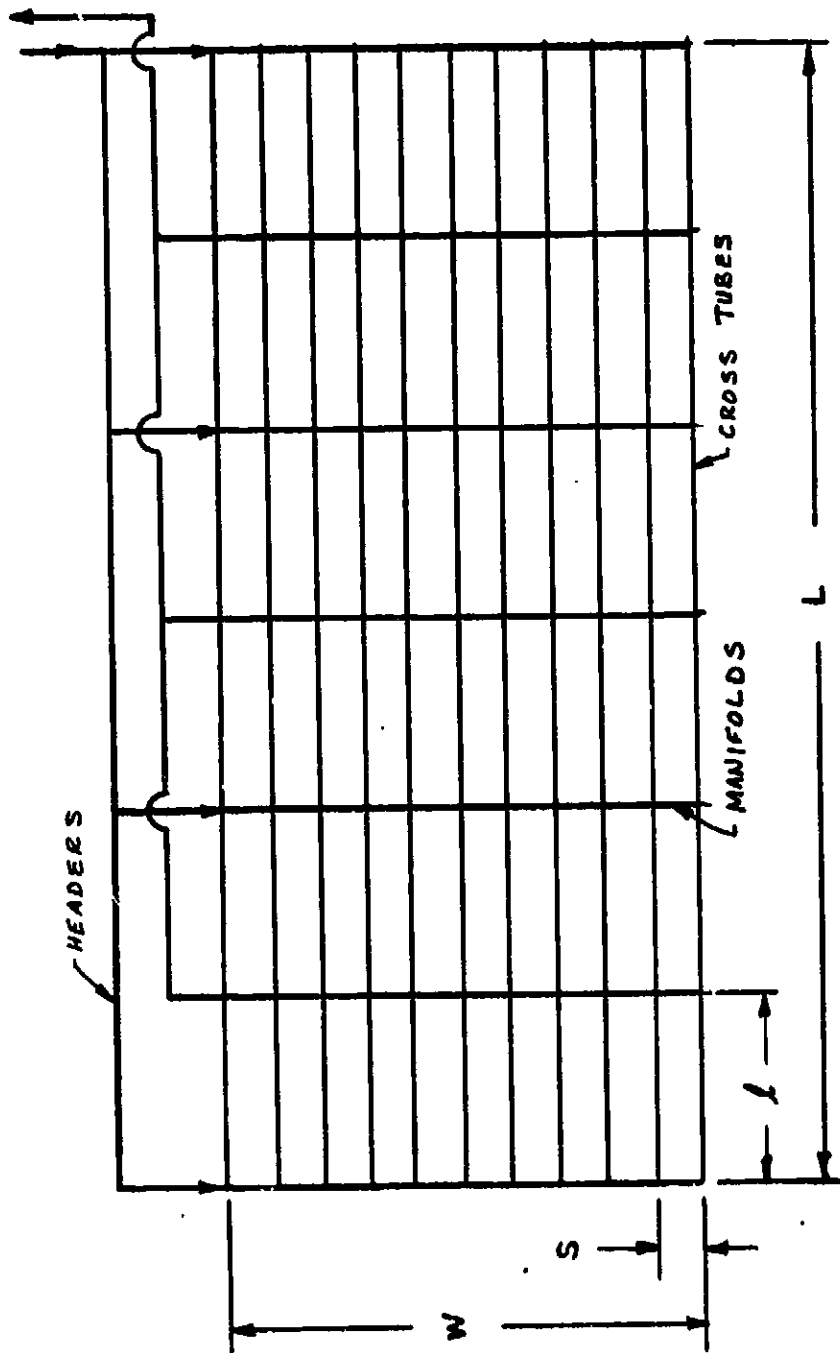


FIGURE 1 PUMPED FLUID RADIATOR SYSTEM

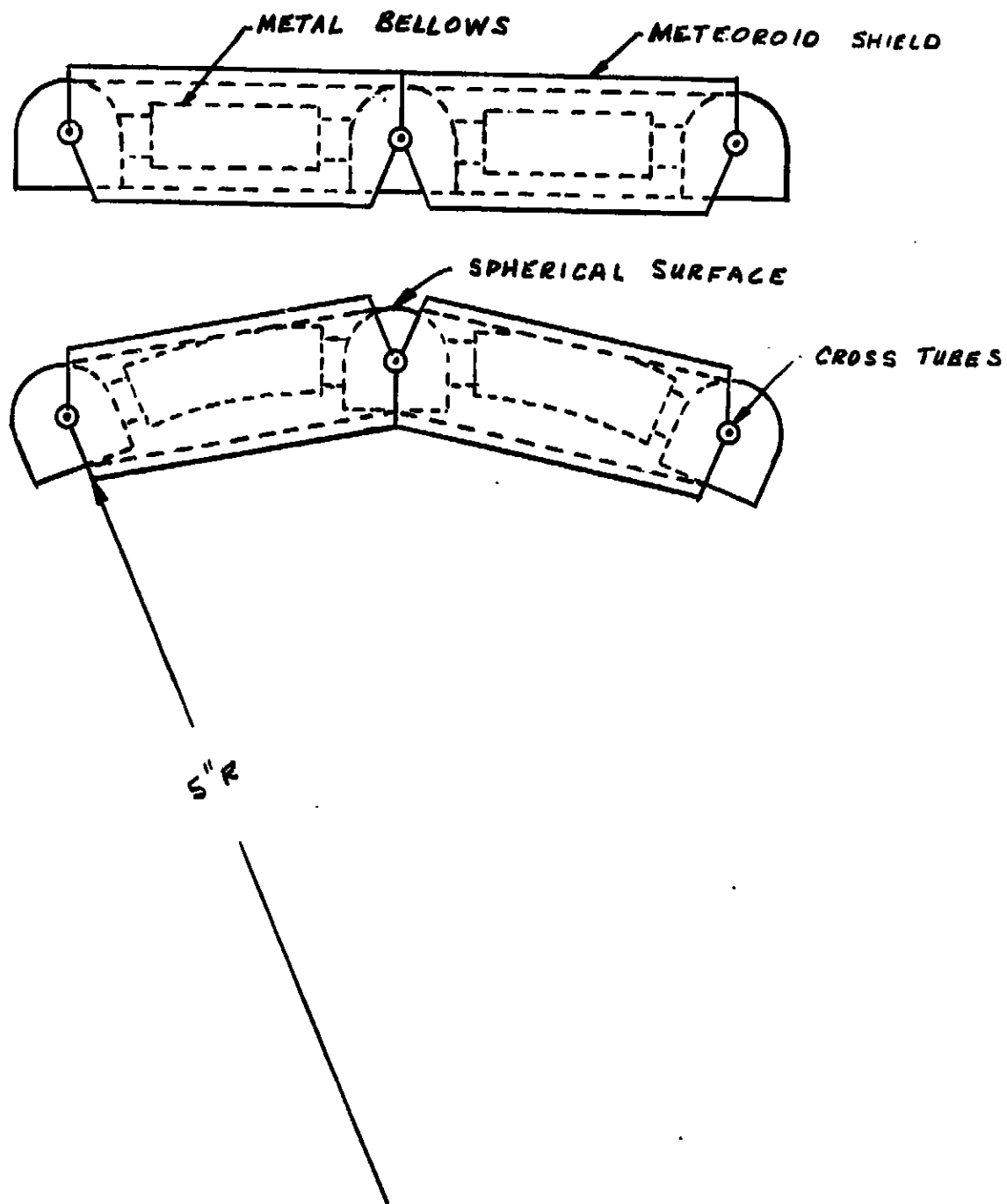


FIGURE 2 METEOROID SHIELD FOR LONG LIFE
FLEXIBLE RADIATOR MANIFOLDS

DEVELOPMENT OF A PROTOTYPE FLEXIBLE RADIATOR SYSTEM

PROGRESS REPORT NO. 18

24 APRIL 1978 THROUGH 31 MAY 1978

1 June 1978

CONTRACT NO. NAS9-14776

DRL: T-1213, LINE ITEM 2

DRD: MA-182TD

SUBMITTED TO:

THE NATIONAL AERONAUTICS AND SPACE ADMINISTRATION
JOHNSON SPACE CENTER
HOUSTON, TEXAS

by

VOUGHT CORPORATION
DALLAS, TEXAS

PREPARED BY:

J. W. Leach
J. W. Leach

CHECKED BY:

J. A. Oren
J. A. Oren

APPROVED BY:

R. L. Cox
R. L. Cox

1.0 OVERALL PROGRESS

Work during the 18th reporting period has been concentrated on the advanced radiator study phase of the Flexible Radiator Development Program, and address the following subjects:

- a) Optimization of heat pipe radiators,
- b) designs of radiators with meteoroid bumpers,
- c) contract review at NASA/JSC, and
- d) ambient deployment tests of the prototype radiator.

2.0 PROGRESS ON INDIVIDUAL MAJOR AREAS

2.1 Heat Pipe Radiator Optimization

Analyses are being performed to determine the values of heat pipe radiator design parameters that minimize weight and area. The analyses are concerned with the optimization of flow through heat exchanger core in the manifolds, the size and spacing of the heat pipes, the thickness of the radiating fin, and the geometric design of the radiator panel. Documentation of the analysis shall be covered in an advanced radiator study report.

2.2 Meteoroid Bumper Designs

A literature search was conducted to obtain equations for sizing meteoroid bumpers for radiator tubing. An equation was selected based on accuracy of prediction of depth of projectile penetration in laboratory tests. Computer models were prepared for heat pipe and pumped fluid radiators to determine the values of radiator parameters best suited for long duration missions. Radiator weight and area are compared with corresponding designs without meteoroid bumpers.

2.3 Contract Review at NASA-JSC

Preliminary results of the long life radiator study analyses were presented to NASA on 8 May 1978. NASA agreed with the study plan, and requested that Vought also look at large heat pipes in space radiators.

2.4 Ambient Deployment Tests of Prototype Radiator

Ambient deployment tests of the prototype radiator were successful. The new retraction springs supplied by Spring Engineers are not completely straight, but are much improved over the original springs which were rejected by Vought. The new springs have a slight curvature which causes the radiator to extend over the edge of the deployment drum during part of the deployment/retraction cycle. The lengths of the two springs can be adjusted so that the edges of the radiator coincide with the edges of the drum at the beginning

and end of the cycle. At the mid-point, the edge of the radiator overlaps one end of the drum by about two inches. This is not considered to be a serious problem, but would affect the stowage volume required for the retracted radiator. The pressure required to deploy the radiator is less than 2 psi.

3.0 WORK ON MAJOR END ITEMS

Work is in progress on the advanced radiator study phase of the program.

4.0 WORK PLANNED IN THE NEXT REPORTING PERIOD

Work will continue on the long life radiator study. A final report shall be submitted.

DEVELOPMENT OF A PROTOTYPE FLEXIBLE RADIATOR SYSTEM

PROGRESS REPORT NO. 19

1 JUNE 1978 THROUGH 30 JUNE 1978

21 July 1978

CONTRACT NO. NAS9-14776
DRL: T-1213, LINE ITEM 2
DRD: MA-182TD

SUBMITTED TO:

THE NATIONAL AERONAUTICS AND SPACE ADMINISTRATION
JOHNSON SPACE CENTER
HOUSTON, TEXAS

by

VOUGHT CORPORATION
DALLAS, TEXAS

PREPARED BY:

J. W. Leach
J. W. Leach

REVIEWED BY:

J. A. Oren
J. A. Oren

APPROVED BY:

J. A. Oren
for R. L. Cox

1.0 OVERALL PROGRESS

Work during the 19th reporting period has been concentrated on the advanced radiator study phase of the Flexible Radiator Development Program, and addresses the following subjects:

- a) Redundancy in Modular Build-up of Large Radiator Systems
- b) Quote for Development of Extended Life Flexible Radiator
- c) Contract Extension

2.0 PROGRESS ON INDIVIDUAL MAJOR AREAS

2.1 Redundancy Calculations

System designs with multiple independent subsystems were studied to determine how the total system weight and radiating area depends on the number and survivability of the subsystems. The studies show that significant weight reductions are possible in large systems if they are constructed from independent modules and are oversized such that the system maintains full capacity following the loss of one or more of the modules. High probabilities of mission success are possible.

2.2 Quote for Development of Extended Life Flexible Radiator

A cost quote was submitted to NASA for designing, fabricating and testing an extended life flexible radiator which would be applicable for mission durations of 5 years or more. The prototype flexible radiator and extended life flexible radiator will be tested simultaneously in 1979.

2.3 Flexible Radiator Contract Extension

A request for contract extension was submitted to NASA in order to maintain continuity between the current prototype development program and the forthcoming extended life radiator program which is expected to begin in September 1978.

3.0 WORK ON MAJOR END ITEMS

Work is in progress on the advanced radiator study phase of the program.

4.0 WORK PLANNED IN THE NEXT REPORTING PERIOD

Work will continue on the long life radiator study.

DEVELOPMENT OF A PROTOTYPE FLEXIBLE RADIATOR SYSTEM

PROGRESS REPORT NO. 20
1 JULY 1978 THROUGH 31 JULY 1978

18 August 1978

CONTRACT NO. NAS9-14776
DRL: T-1213, LINE ITEM 2
DRD: MA1&TD

SUBMITTED TO:

THE NATIONAL AERONAUTICS AND SPACE ADMINISTRATION
JOHNSON SPACE CENTER
HOUSTON, TEXAS

by

VOUGHT CORPORATION
DALLAS, TEXAS

PREPARED BY:

J. W. Leach
J. W. Leach

REVIEWED BY:

J. A. Oren
J. A. Oren

APPROVED BY:

R. L. Cox
R. L. Cox

1.0 OVERALL PROGRESS

Work during the 20th reporting period has been concentrated on the advanced radiator study phase of the Flexible Radiator Development Program and addresses the following subjects:

- a) Documentation of Advanced Radiator Study
- b) Fabrication of Extended Life Flexible Radiator Element

2.0 WORK ON INDIVIDUAL MAJOR AREAS

2.1 Advanced Study Documentation

Documentation of the Advanced Radiator Study which includes weight and radiating surface area trades of heat pipe and pumped fluid radiators, and redundancy/reliability considerations was initiated.

2.2 Extended Life Flexible Radiator Element

A 6" x 12" element with metal bellows manifolds is being fabricated to verify manufacturing techniques and to evaluate potential problem areas prior to initiating the design of the full scale radiator. No problems were experienced in fabricating the radiator panel. Meteoroid bumpers are being machined for the manifolds.

3.0 WORK ON MAJOR END ITEMS

Work is in progress on the advanced radiator study phase of the program.

4.0 WORK PLANNED IN THE NEXT REPORTING PERIOD

Work will continue on the long life radiator study.

DEVELOPMENT OF A PROTOTYPE FLEXIBLE RADIATOR SYSTEM

PROGRESS REPORT NO. 21
1 AUGUST 1978 THROUGH 31 AUGUST 1978

21 SEPTEMBER 1978

CONTRACT NO. NAS9-14776
DRL: T-1213, LINE ITEM 2
DRD: MA182 ID

SUBMITTED TO:

THE NATIONAL AERONAUTICS AND SPACE ADMINISTRATION
JOHNSON SPACE CENTER
HOUSTON, TEXAS

BY:

VOUGHT CORPORATION
DALLAS, TEXAS

PREPARED BY:

J. W. Leach
J. W. Leach

REVIEWED BY:

J. A. Oren
J. A. Oren

APPROVED BY:

R. L. Cox
R. L. Cox

1.0 OVERALL PROGRESS

Work during the 21st reporting period has been concentrated on fabrication and advanced radiator study phases of the Flexible Radiator Development Program, and addresses the following subjects:

- (a) final assembly of the prototype radiator
- (b) documentation of the advanced radiator study

2.0 WORK ON INDIVIDUAL MAJOR AREAS

2.1 Final Assembly of Prototype Radiator

Teflon clamps for attaching the radiator fin material to the inboard support frame and to the outboard deployment drum were machined in the Vought SES Lab. The aluminum frame and deployment drum were anodized, and the radiator components were then assembled for final inspection. The radiator will be placed in storage until it is shipped to NASA for testing.

2.2 Advanced Study Documentation

Documentation of the Advanced Radiator Study which includes weight and radiating surface area trades of heat pipe and pumped fluid radiators, and redundancy/reliability considerations was continued.

3.0 WORK ON MAJOR END ITEMS

Work is in progress on the advanced radiator study phase of the program.

4.0 WORK PLANNED IN THE NEXT REPORTING PERIOD

Work will continue on the long life radiator study.

DEVELOPMENT OF A PROTOTYPE FLEXIBLE RADIATOR SYSTEM

PROGRESS REPORT NO. 22
1 SEPT 1978 THROUGH 30 SEPT 1978

18 OCTOBER 1978

CONTRACT NO. NAS9-14776
DRL: T-1213, LINE ITEM 2
DRD: MA182TD

SUBMITTED TO:

THE NATIONAL AERONAUTICS AND SPACE ADMINISTRATION
JOHNSON SPACE CENTER
HOUSTON, TEXAS

by

VOUGHT CORPORATION
DALLAS, TEXAS

PREPARED BY:

J. W. Leach
J. W. Leach

REVIEWED BY:

J. A. Oren
J. A. Oren

APPROVED BY:

R. L. Cox
R. L. Cox

1.0 OVERALL PROGRESS

Work during the 22nd reporting period has been concentrated on the test planning and extended life radiator design phases of the Flexible Radiator Development Program and addresses the following subjects:

- a) solar degradation testing of the prototype radiator,
- b) thermal design of extended life flexible radiator, and
- c) documentation of advanced radiator study.

2.0 WORK ON INDIVIDUAL MAJOR AREAS

2.1 Solar Degradation Test of the Prototype Panel

A one-week solar degradation test of the prototype radiator panel in NASA Chamber B is being planned for the week beginning 12 November 1978. The panel has been instrumented with 24 thermocouples and shipped to NASA for testing. Plans for a test table and analysis of measurement error effects were also submitted to NASA.

2.2 Thermal Design of Extended Life Radiator

The manifolds of the extended life radiator are being designed for flow distribution, pressure retention, and flexibility. Analyses are also being performed to determine optimum tube diameters and spacing. Requests for quotes for materials are being prepared based on the results of the thermal analyses.

2.3 Advanced Radiator Study Documentation

Documentation of the Advanced Radiator Study which included weight and radiating surface trades of heat pipe and pumped fluid radiators, and redundancy/reliability considerations continues.

3.0 WORK ON MAJOR END ITEMS

Work is in progress on the advanced radiator study and extended life radiator development phases of the program.

4.0 WORK PLANNED IN THE NEXT REPORTING PERIOD

Work will continue on the advanced radiator study and extended life radiator development phases.

DEVELOPMENT OF A PROTOTYPE FLEXIBLE RADIATOR SYSTEM

PROGRESS REPORT NO. 23
1 OCT 1978 THROUGH 31 OCT 1978

10 NOVEMBER 1978

CONTRACT NO. NAS9-14776
DRL: T-1213, LINE ITEM 2
DRD: MA182TD

SUBMITTED TO:

THE NATIONAL AERONAUTICS AND SPACE ADMINISTRATION
JOHNSON SPACE CENTER
HOUSTON, TEXAS

BY:

VOUGHT CORPORATION
DALLAS, TEXAS

PREPARED BY:


J. W. Leach

REVIEWED BY:


J. A. Oren

APPROVED BY:


R. L. Cox

1.0 OVERALL PROGRESS

Work during the 23rd reporting period has been concentrated on the test planning and extended life radiator design phases of the Flexible Radiator Development Program and addresses the following subjects:

- a) solar degradation testing of the prototype radiator,
- b) thermal and mechanical design of extended life flexible radiator, and
- c) documentation of advanced radiator study.

2.0 WORK ON INDIVIDUAL MAJOR AREAS

2.1 Solar Degradation Test of the Prototype Panel

A one-week solar degradation test of the prototype radiator panel in NASA Chamber B is being planned for the week beginning 12 November 1978. The panel has been instrumented with 24 thermocouples and shipped to NASA for testing. Plans for a test table and analysis of measurement error effects were also submitted to NASA.

2.2 Thermal Design of Extended Life Radiator

The manifolds of the extended life radiator have been designed for flow distribution, pressure retention, and flexibility. Analyses were also performed to determine optimum tube diameters and spacing. Requests for quotes for materials are being prepared based on the results of the thermal analyses. Drawings are being prepared for fabricating the deployment/retraction mechanism.

2.3 Advanced Radiator Study Documentation

Documentation of the Advanced Radiator Study which included weight and radiating surface trades of heat pipe and pumped fluid radiators, and redundancy/reliability considerations continues.

3.0 WORK ON MAJOR END ITEMS

Work is in progress on the advanced radiator study and extended life radiator development phases of the program.

4.0 WORK PLANNED IN THE NEXT REPORTING PERIOD

Work will continue on the advanced radiator study and extended life radiator development phases.

DEVELOPMENT OF A PROTOTYPE FLEXIBLE RADIATOR SYSTEM

PROGRESS REPORT NO. 24
1 NOV 1978 THROUGH 30 NOV 1978

11 December 1978

CONTRACT NO. NAS9-14776
DRL: T-1213, LINE ITEM 2
DRD: MA182TD

SUBMITTED TO:

THE NATIONAL AERONAUTICS AND SPACE ADMINISTRATION
JOHNSON SPACE CENTER
HOUSTON, TEXAS

BY:

VOUGHT CORPORATION
DALLAS, TEXAS

PREPARED BY:

REVIEWED BY:

APPROVED BY:

J. W. Leach
J. W. Leach

J. A. Oren
J. A. Oren

R. L. Cox
R. L. Cox

1.0 OVERALL PROGRESS

Work during the 24th reporting period has been concentrated on the testing and extended life radiator design phases of the Flexible Radiator Development Program and addresses the following subjects:

- a) solar degradation testing of the prototype radiator,
- b) design of extended life flexible radiator, and
- c) documentation of advanced radiator study.

2.0 WORK ON INDIVIDUAL MAJOR AREAS

2.1 Solar Degradation Test of the Prototype Panel

A one-week solar degradation test of the prototype radiator panel was conducted in NASA Chamber B. Preliminary analyses of the data indicates the radiator performed as expected with no measurable degradation caused by solar exposure. Optical property measurements for sample radiator fin material exposed during the test also indicate no degradation occurred. Vought is preparing a quick look test report.

2.2 Design of Extended Life Radiator

Alternatives to the space deployable boom deployment/retraction system were studied. Boom suppliers were contacted to obtain cost and performance data. The cost of the booms could be substantial for flight hardware. Also, the boom design depends on flight loads, radiator dimensions, etc., that are mission dependent. Thus boom design changes could impact the cost and scheduling of future applications of the flexible radiator system. A strap drive system with self straightening manifold covers to provide structural support for the deployed radiator is being considered. Alternatives to the fluid swivels such as tubular springs, coiled flex hoses, and outboard drums are also being investigated. A design review is being planned with the NASA to discuss the results of the design studies.

2.3 Advanced Radiator Study Documentation

Documentation of the Advanced Radiator Study which includes weight and radiating surface trades of heat pipe and pumped fluid radiators, and redundancy/reliability considerations continues. A technical paper based on the study will be presented at the Ninth Intersociety Conference on Environmental Systems; 16-19 July 1979; San Francisco, California.

3.0 WORK ON MAJOR END ITEMS

Work is in progress on the advanced radiator study and extended life radiator development phases of the program.

4.0 WORK PLANNED IN THE NEXT REPORTING PERIOD

Work will continue on the advanced radiator study and extended life radiator development phases.

DEVELOPMENT OF A PROTOTYPE FLEXIBLE RADIATOR SYSTEM

PROGRESS REPORT NO. 25
1 DEC 1978 THROUGH 31 DEC 1978

19 January 1979

CONTRACT NO. NAS9-14776
DRL: T-1213, LINE ITEM 2
DRD: MA182TD

SUBMITTED TO:

THE NATIONAL AERONAUTICS AND SPACE ADMINISTRATION
JOHNSON SPACE CENTER
HOUSTON, TEXAS

BY:

VOUGHT CORPORATION
DALLAS, TEXAS

PREPARED BY:

C. W. Hixon
C. W. Hixon

REVIEWED BY:

J. A. Oren
J. A. Oren

APPROVED BY:

R. L. Cox
R. L. Cox

1.0 OVERALL PROGRESS

Work during the 25th reporting period has been concentrated on the test reporting and extended life radiator design phases of the Flexible Radiator Development Program and addresses the following subjects:

- a) solar degradation testing of the prototype radiator,
- b) design of extended life flexible radiator, and
- c) documentation of advanced radiator study.

2.0 WORK ON INDIVIDUAL MAJOR AREAS

2.1 Solar Degradation Test of the Prototype Panel

A one-week solar degradation test of the prototype radiator panel was conducted in NASA Chamber B. Preliminary analyses of the data indicates the radiator performed as expected with no measurable degradation caused by solar exposure. Optical property measurements for sample radiator fin material exposed during the test also indicate no degradation occurred. Vought has sent NASA a hand written final copy of the quick look test report. A typed, signed version will follow in January 1979.

2.2 Design of Extended Life Radiator

Alternatives to the space deployable boom deployment/retraction system were studied. Boom suppliers were contacted to obtain cost and performance data. The cost of the booms could be substantial for flight hardware. Also, the boom design depends on flight loads, radiator dimensions, etc., that are mission dependent. Thus boom design changes could impact the cost and scheduling of future applications of the flexible radiator system. A strap drive system with self-straightening manifold covers to provide structural support for the deployed radiator is being considered. Alternatives to the fluid swivels such as tubular springs, coiled flex hoses, and outboard drums are also being investigated. An informal design review was conducted 22 December 1978 with Gary Rankin, the NASA contract Technical Monitor, to discuss the results to date of the design studies. A design review at NASA-JSC is planned for January 1979.

2.3 Advanced Radiator Study Documentation

Documentation of the Advanced Radiator Study which includes weight and radiating surface trades of heat pipe and pumped fluid radiators, and redundancy/reliability considerations continues. A technical paper based on the study will be presented at the Ninth Intersociety Conference on Environmental Systems; 16-19 July 1979; San Francisco, California.

3.0 WORK ON MAJOR END ITEMS

Work is in progress on the advanced radiator study and extended life radiator development phases of the program.

4.0 WORK PLANNED IN THE NEXT REPORTING PERIOD

Work will continue on the advanced radiator study and extended life radiator development phases.

APPENDIX B

HYPERVELOCITY IMPACT EXPERIMENT TEST REPORT

TEXAS A&M UNIVERSITY

AEROSPACE ENGINEERING DEPARTMENT
COLLEGE STATION TEXAS 77843

January 17, 1977

Dr. James W. Leach
Unit 2-53002
Vought Corporation
Marshall Street Facility
Dallas TX 75222

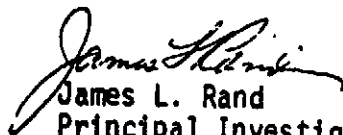
Dear Dr. Leach:

In accordance with the terms of your Purchase Order No. P-104433, I am forwarding to you all data and reports acquired during the contract period. I understand that your acceptance of this material will satisfy the contractual obligations of the Texas A&M Research Foundation.

As you will recall this program was a very low level, best effort, attempt to obtain meaningful penetration data on your materials. It is apparent that a more significant program could and should be attempted whereby low temperature effects could be investigated. I hope that in the future you will be able to provide a research assistantship at the master's level for at least a year to provide this needed information.

If you have any questions or if I can be of any further assistance to you, please do not hesitate to contact me.

Yours truly,


James L. Rand
Principal Investigator

Enclosure

cc: JoAnn Treat



B-2

**Hypervelocity Impact Experiments on
Materials for a Deployable Space Radiator**

by: Gary R. Henry

**Texas A&M University
December 1976**

ABSTRACT

Nylon and steel projectiles approximately .015g in weight were shot at Teflon sheets and polyurethane tubes. Velocities ranged from 1770 to 4480 M/sec. An attempt to ascertain penetration depths and compare it to an empirical equation already developed was made. Due to an insufficient number of data points, no strict conclusion could be drawn but initial indications show that for nylon velocity predictions may have been too high.

FOREWORD

This project was undertaken to provide hypervelocity impact data on materials for which no firm data was available. Many theories and equations exist, but their accuracy and applicability is questionable until the experimental stage is complete. This paper presents the results of some of those experiments.

At the same time, the author fulfilled the requirements for a senior level structures course in Aerospace Engineering at Texas A&M University.

ACKNOWLEDGEMENTS

The author wishes to thank Dr. James Rand of Texas A&M University for providing equipment, information, and advice to carry out this project.

Thanks are also in order to Dr. Jim Leach and the Vought Corporation for providing materials, information, and funding for this project.

TABLE OF CONTENTS

Abstract	11
Foreword	111
Acknowledgements	1v
List of Illustrations	vi
Nomenclature	vii
Introduction	1
Description of Experimental Apparatus	2
Test Procedure	5
Results	7
Recommendations for Further Testing	12
Conclusions	13
References	14
Appendix	15

LIST OF ILLUSTRATIONS

Figure

1	Gun System and Gun Instrumentation	3
2	Velocity Measuring System	4
3	Targets	6
4	Penetration Depth as a Function of Velocity - Steel and Nylon Projectiles	8
5	Water-filled Tube - Steel Ball Impact	11

NOMENCLATURE

- t = thickness penetrated (cm)
 ϵ_t = percentage elongation of target material
 ρ_t = mass density of sheet material (g/cm^3)
 ρ_m = mass density of meteoroid (g/cm^3)
 V_m = normal impact velocity (km/sec)
 d_m = meteoroid diameter (cm)

INTRODUCTION

Meteoroids encountered in space flight can cause considerable damage to space vehicles. The total meteoroid environment consists of a wide variety of masses at various velocities originating from comets and asteroids. As a result, damage to a structure may range from gradual deterioration over a period of time to catastrophic failure with one strike.

From a design standpoint, valuable information about hypervelocity impacts can be obtained using particle accelerators such as a light-gas gun. Much work has been done in this field and many empirical equations developed to relate penetration depths to target and projectile properties. Some of these equations are combined results of several experiments to attempt to develop a governing equation to the hypervelocity impact problem. For materials of specific interest, the best results came from actual tests on these materials.

The Vought Corporation of Dallas, Texas has a deployable space radiator constructed of plastic materials (Teflon* and polyurethane). It was desirable to obtain impact data for these materials to study meteoroid effects. The hypervelocity research facility at Texas A&M University was used to obtain this data. The data is compared to an empirical equation from another source. Teflon plates are the main focus of attention. Observational data on water-filled polyurethane tubes is also presented.

* Teflon in this case refers to Dupont FEP (fluorinated ethylene-propylene)

DESCRIPTION OF EXPERIMENTAL APPARATUS

The Light-Gas Gun

The light-gas gun is shown in figure 1. Burning gun powder is used to drive a piston down the pump tube. The piston compresses the hydrogen to high pressure. When the pressure is high enough, it bursts a diaphragm and drives a projectile down the launch tube, into the evacuated flight tube. The projectile impacts a target placed in the impact chamber which is also evacuated. Reference 1 gives a more complete description of this gun.

Velocity Measurement

Velocity was measured by shooting through two screens of ballistic paper. The screens were part of an electrical circuit shown in figure 2. Breaking the screens breaks the circuit and results in voltage changes. Each voltage change is input to a Hewlett-Packard timer. The projectile starts the timer when it breaks the first screen and stops it when it breaks the second. Therefore, the time to cross a known distance can be converted to velocity. The penetration of the ballistic papers has a negligible effect on its velocity for the masses used in this program.

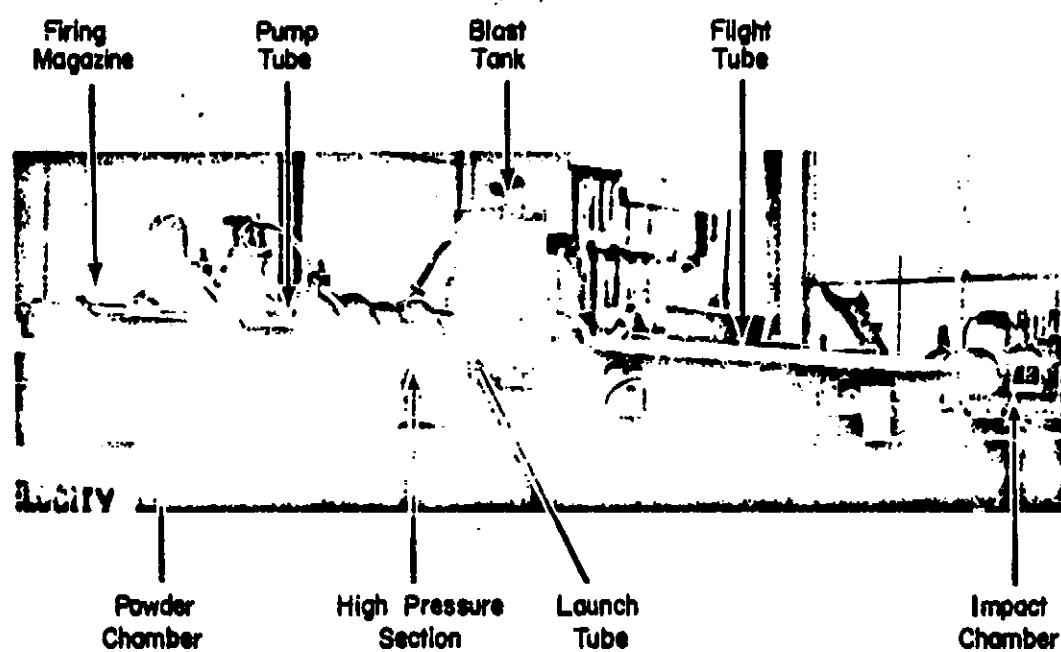


Figure A-1: The Gun System

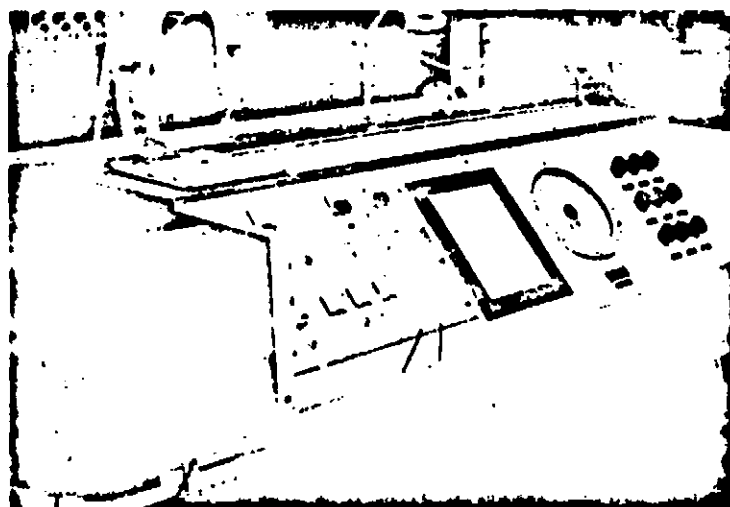
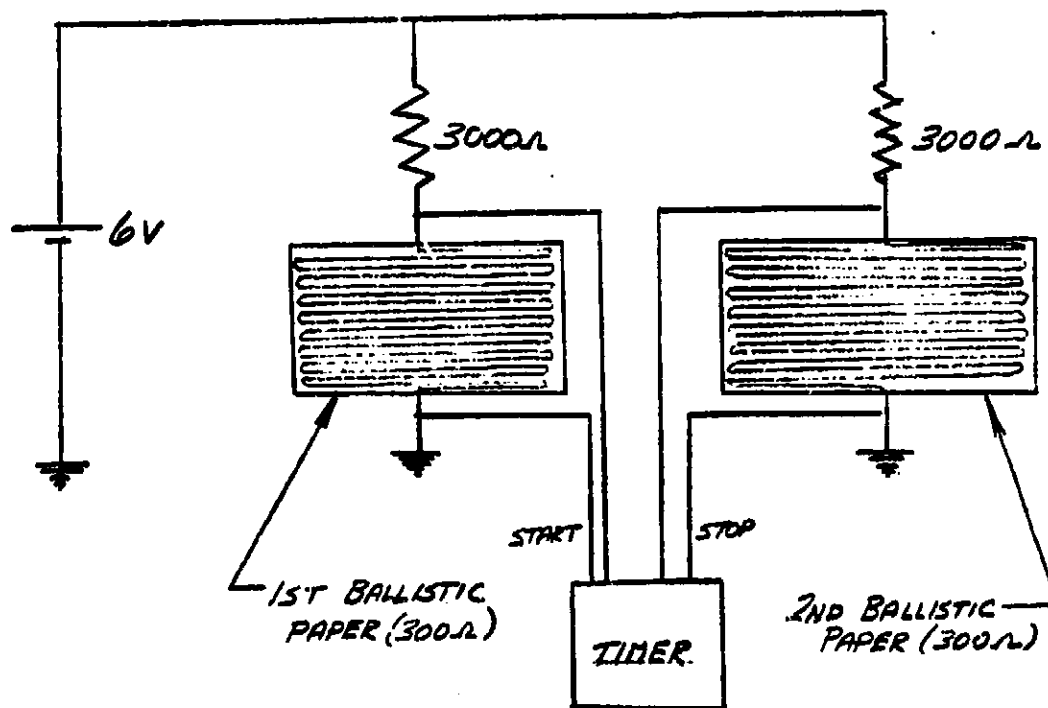


Figure A-2: Gun Instrumentation and the Control Console



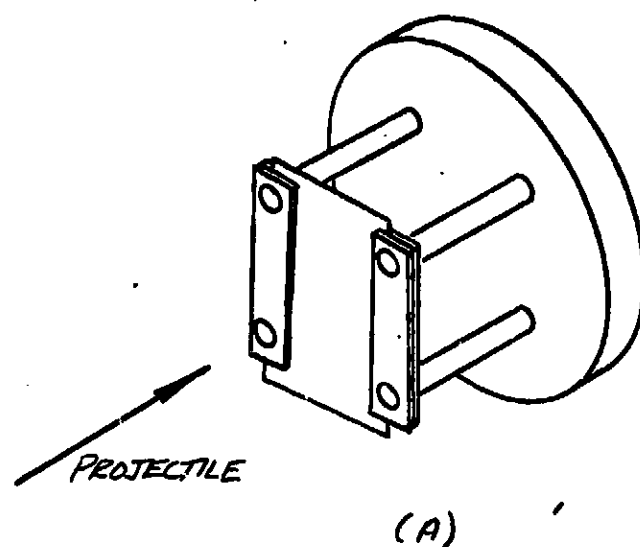
VELOCITY MEASURING SYSTEM
FIG. 2

TEST PROCEDURE

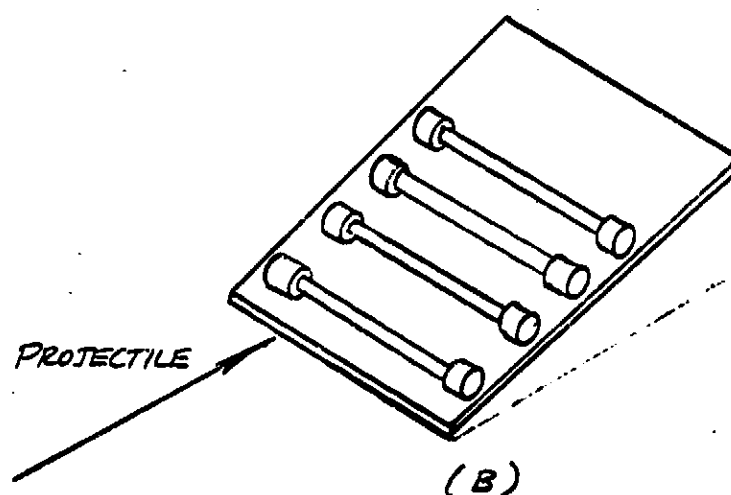
All testing was accomplished in the same manner except for using two different types of projectiles. Cylindrical shaped projectiles made of nylon were used for most shots because they were easily fitted in the base of the launch tube. These projectiles weighed approximately .014g, were .203cm in diameter and had a length to diameter ratio of 1. Steel spheres weighing .016g and .152cm in diameter were also used but had to be encased in a sabot to be fired.

The Teflon targets were 7.62cm x 7.62cm squares of various thicknesses (.1524cm and .203cm). The Teflon squares were made of .051cm layers. They were clamped on two sides and mounted in the impact chamber perpendicular to the projectile flight path as shown in figure 3A. The water-filled polyurethane tubes were sealed on the ends with swagelok fittings. Four of them were wired to a plate and mounted in the impact chamber at an angle so that the projectile would have a better chance of hitting them (figure 3B).

The impact chamber and flight tube were evacuated to less than 0.1 psia.



TEFLON TARGET



WATER FILLED TUBES

Figure 3

RESULTS

A survey of the literature revealed that there are many equations to predict penetration depth but there are certain limits to their usefulness. Much depends on the material properties of the target and the projectile.

Bjork (2) found that if the projectile and target were of the same material, cratering would be approximately hemispherical. Goodier (3) proposed different theories to predict penetration, depending on the behavior(deformation) of the projectile during impact.

Many theories have been tested using metal projectiles and targets. The data on testing of plastics is limited which is why this study was undertaken. Rittenhouse (4) presented an equation developed empirically to predict penetration in polyethylene. A form of the equation is given below.

$$\frac{t}{d_m} = .65 \left(\frac{1}{\epsilon_t}\right)^{1/8} \left(\frac{\rho_m}{\rho_t}\right)^{1/2} (v_m)^{7/8}$$

This equation will be used to compare with results of this program. Sample calculations are contained in the appendix.

Most of the shots were made using a cylindrical projectile of nylon. A total of fourteen shots were made at the Teflon specimens but due to timer malfunctions, not all shots produced useful data.

Shot number 4 (see appendix) was the first shot to provide information on the threshold of penetration for the Teflon sample. The target was .203cm thick and this was also the projectile diameter so that $(t/d_m) = 1$. The measured velocity was 4480 m/sec. According to equation 1 (plotted in figure 4), this is too slow for nylon to penetrate. However, it did penetrate all four layers.

46 1242

NOTE: 20 X 70 TO THE INCH 27 X 10 INCHES
NEUTRAL & LUBER CO. MADE IN U.S.A.

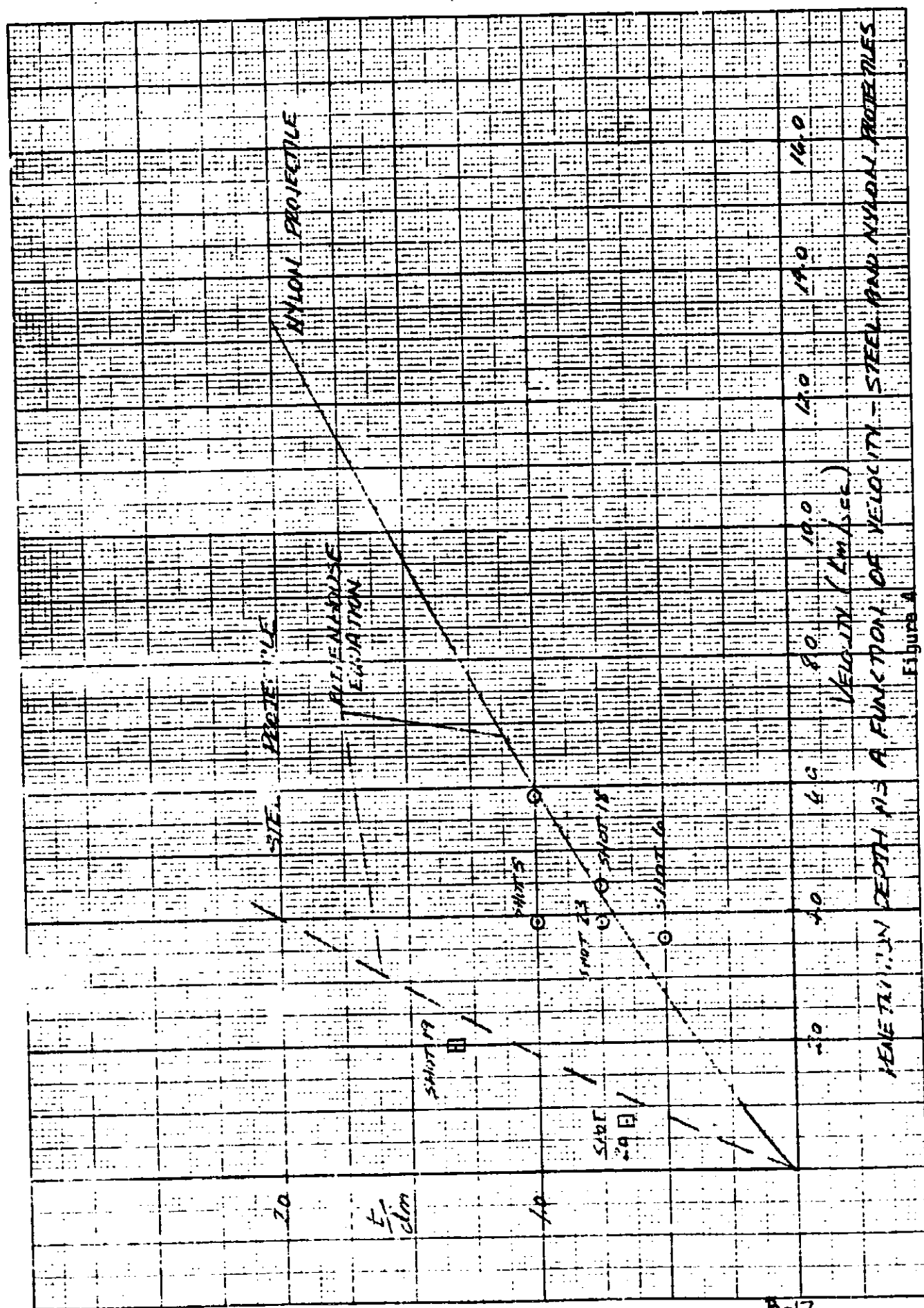


Figure 4

Shot number 5 provided the most valuable information during the program. The target was the same as above. The nylon projectile weighed .014g and had a velocity of 3900 m/sec. The Teflon was on the verge of penetration. The backside of the target specimen was drawn out from the impact but the material did not tear as in the previous shot. Depth of penetration would be impossible to determine due to the nature of the damage. The thin targets of relatively high elongation used here tend to extrude rather than crater. Therefore, penetration here means that a hole was formed through the thickness of the sample. Since penetration was incipient for this shot, the penetration depth was taken to be the thickness of the target. For this shot, (t/d_m) was equal to 1. This point is plotted in figure 4 at its measured velocity.

The projectile was slowed down for the sixth shot and it weighed .011g. The target was the same as before. At 3620 m/sec, the projectile penetrated the first two layers of the target to give a penetration depth of .102 cm (.04"). This makes the t/d_m ratio equal to .5. This shot is also compared to equation 1 in figure 4.

The next series of shots were at .1524cm thick Teflon samples. All resulted in penetration. The t/d_m ratio was .75 (shots 7 through 13). As predicted by equation 1, any projectile with a velocity less than 4300 m/sec should not have penetrated. But all were less and all did penetrate.

Shot number 14 illustrates the difference in projectile material. A .016g steel sphere, .1524cm (.06") in diameter was shot at 1770 m/sec at .203cm Teflon. This was the slowest shot but it did penetrate quite easily. Equation 1 for steel is also plotted in figure 4. For (t/d_m) of .75, penetration was predicted for this shot.

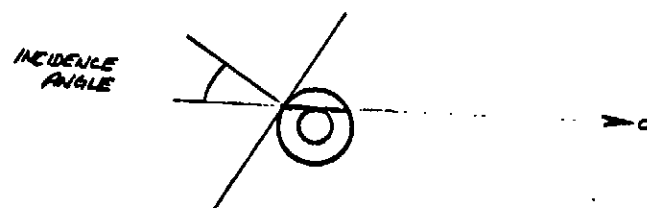
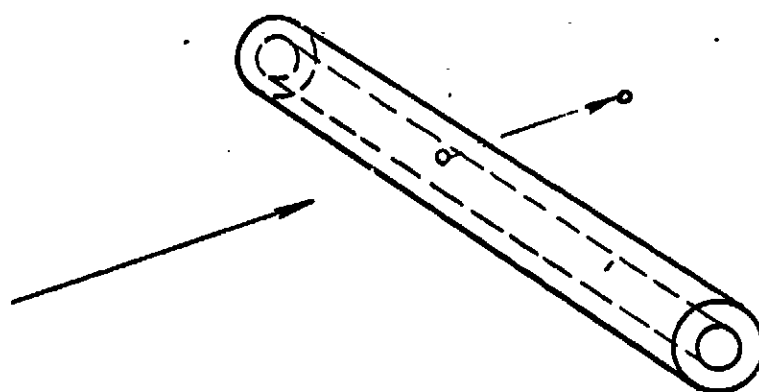
The difference in projectile material appears in the projectile/target density ratio in the Rittenhouse equations. Due to the differences in size

and strength of the steel sphere and nylon projectile a correlation in penetration is difficult to make. The mass of each was approximately the same. The diameter of the steel sphere was .051 cm (.02") less than the nylon. Also, the impact of the steel is approximately a point impact while the nylon is more of a blunt body. As a speculation, it may be that the steel sphere delivered less total momentum or energy to the target but more per unit impact area.

After obtaining thicker target samples of Teflon, a final series of shots were made (shots 18 through 24). The cases where the projectile penetrated all layers of the Teflon yielded no data. However, the cases of partial penetration produced useful results. Measuring penetration as stated before to find t , the penetration thickness/projectile diameter ratio is plotted as shown in figure 4. They show close agreement to the Rittenhouse equations.

A few shots were made using water filled polyurethane tubes. The tubes had an outside diameter of .635 centimeters and an inside diameter of .3175 centimeters. Swagelok fittings were used to seal the ends.

The timer malfunctioned on all three shots but all produced breaks in the tubes. The first two shots were with nylon projectiles, the third with a .016g steel sphere. The breaks were small, pinhole breaks and stopped by themselves. The water was not under pressure. The damage to the tubes consisted of a chip of polyurethane being knocked away while the projectile glanced off. The steel sphere went all of the way through a tube, penetrating both walls and causing it to leak. Again it left a small hole. It should be noted that the sphere impacted at an oblique angle (figure 5) and did not glance off.



WATER FILLED TUBE -
STEEL BALL IMPACT

FIG 5

RECOMMENDATIONS FOR FURTHER TESTING

From the differences in results of two different projectiles studied here, it is recommended that several masses, shapes, and densities be used for further study.

For the Vought radiator materials, thicker Teflon samples are needed to better study penetration depth. Vought also desires to cool down the tubes and Teflon to -60°F to study temperature effects similar to the space environment.

CONCLUSIONS

More data has to be obtained before a true comparison can be made with the Rittenhouse equation. Initially, it appears that this equation may predict too high a velocity for penetration. This illustrates the hazards of attempting to apply information from one test to another in which conditions have been altered somewhat. With more data, an equation applicable to Teflon can be developed.

REFERENCES

1. Ryneerson, R.J. and Rand, J.L., "Optimization of a Two Stage Light-Gas Gun", TEES 9075-CR-72-02, Aug. 1972, Texas Engineering Experiment Station, College Station, Texas.
2. Bjork, R.L., "Review of Physical Processes in Hypervelocity Impact and Penetration:", Proceedings of the Sixth Symposium on Hypervelocity Impact, Vol. II, Part I, Cleveland, Firestone Tire and Rubber Co., 1963.
3. Goodier, J.N., "On the Mechanics of Indentation and Cratering in Solid Targets of Strain Hardening Metal by Impact of Hard and Soft Spheres", Proceedings of the Seventh Hypervelocity Impact Symposium, Vol. III, Tampa, Florida, Martin Company, 1965.
4. Rittenhouse, J.B., "Meteroids", Space Materials Handbook, 3rd ed., Addison-Wesley, Reading, Mass., 1968.

Appendix

Table of Hypervelocity Tests

Sample Calculations

SUMMARY OF TESTS

SHOT	DATE	PROJECTILE	PROJECTILE WEIGHT (g)	TARGET	VELOCITY (M/SEC)	REMARKS
1	10-20-76	Nylon	.012	.08" Teflon	----	Penetrated 1st 3 layers Timer Malfunctioned
2	10-23-76	Nylon	.022	↓	----	Penetrated all layers Timer Malfunctioned
3	10-23-76	Nylon	.014		----	Penetrated all layers Timer Malfunctioned
4	10-24-76	Nylon	.014		4480	Punctured all layers
5	10-30-76	Nylon	.014		3900	Penetration threshold Good Data Point
6	10-30-76	Nylon	.011		3630	Penetrated 1st 2 Layers
7	10-30-76	Nylon	.011		4176	Penetrated all layers
8	10-31-76	Nylon	.008		----	Penetrated all layers Timer Malfunctioned
9	10-31-76	Nylon	.008		----	Penetrated all layers Timer Malfunctioned
10	10-31-76	Nylon	.010		3850	Penetrated all layers
11	11-3-76	Nylon	.010		2890	Penetrated all layers
12	11-31-76	Nylon	.005	↓	2410	Penetrated all layers
13	11-5-76	Nylon	.010		2270	Penetrated all layers
14	11-6-76	Steel Sphere	.016		1770	Penetrated all layers
15	11-20-76	Nylon	.014		----	Timer Malfunction Damaged tube, leaks
16	11-20-76	Nylon	.014	Tubing	----	Timer Malfunction Same Damage
17	11-20-76	Steel Sphere	.016	Tubing	----	Penetrated both walls
18	12-15-76	Nylon	.012	.10" Teflon	4460	Penetrated first 3 layers
19	12-15-76	Steel Sphere	.016	.18" Teflon	1984	Penetrated first 4 layers
20	12-16-76	Steel Sphere	.016	.12" Teflon	770	Penetrated first 2 layers
21	12-16-76	Steel Sphere	.016	.18" Teflon	3060	Penetrated all layers
22	12-16-76	Nylon	.011	.10" Teflon	3720	Penetrated all layers
23	12-16-76	Nylon	.010	.18" Teflon	3870	Penetrated 1st 3 layers
24	12-16-76	Nylon	.012	.14" Teflon	5862	Penetrated 1st 4 layers

Sample Calculations

Using the Rittenhouse Equation

$$t = .65 \left(\frac{1}{\epsilon_t} \right)^{1/8} \left(\frac{\rho_m}{\rho_t} \right)^{1/2} (v_m)^{7/8} (d_m)^{19/18}$$

ϵ_t is % elongation of Teflon (350)

ρ_t is the density of Teflon, 2.14 g/cm³

ρ_m is the projectile density, .94 g/cm³ for nylon and 7.83 gm/cm³ for steel.

$$(d_m)^{19/18} = (d_m)$$

The equation can be written as follows:

$$\frac{t}{d_m} = .65 \left(\frac{1}{\epsilon_t} \right)^{1/8} \left(\frac{\rho_m}{\rho_t} \right)^{1/2} (v_m)^{7/8}$$

The ratio of target thickness/meteoroid diameter can be plotted as a function of velocity.

If thickness penetrated is equal to the projectile diameter, we have for nylon:

$$1 = .65 \left(\frac{1}{350} \right)^{1/8} \left(\frac{.94}{2.14} \right)^{1/2} (v_m)^{7/8}$$

$$v_m = 6.04 \text{ km/sec}$$

APPENDIX C

HEAT BONDING PROCESS EVALUATION

PROTOTYPE FLEXIBLE RADIATOR

EVALUATIONS TO DETERMINE A PROCESS
FOR HEAT BONDING OF FLEXIBLE SPACE RADIATOR
PANELS BY AUTOCLAVE OR OVEN PROCESSING

In general, the heat bonding process to be used is an adaptation of the normal laminating procedures used for fabricating epoxy/fiberglass laminates for aerospace usage. The normal procedure consists of placing fiberglass cloth preimpregnated with a heat curing epoxy resin (prepreg) on a flat platen or contoured molding tool. The uncured prepreg layup is covered with a nonadhering porous fabric, one or more layers of a porous breather or bleeder material, such as fiberglass cloth, to allow entrained air or excess resin to be bled off during cure of the epoxy resin. This layup is covered by a non-porous plastic film (vacuum bag) such as high temperature resistant nylon or silicone film. The vacuum bag is sealed to the platen or molding tool with a pliable, adherent sealing compound. A special outlet connection is installed in the tool or the vacuum bag to allow a vacuum to be applied between the vacuum bag and the tool to apply a pressure on the enclosed layup. Vacuum pressure is applied to properly seat the prepreg layup on the tool and to hold it in position during handling from the layup area to the oven or autoclave for final curing.

Required adaptations to the normal laminating process include provision for bagging materials and sealing compounds suitable for temperatures as high as 550°F (288°C) which are required for heat bonding of FEP film materials.

A number of bagging and sealing materials have been evaluated by the Engineering Materials Laboratory for heat bonding of Space Shuttle flexible heat radiator panels. A brief summary and discussion of bagging and sealing materials and heat bonding procedures tried to this date is given below.

1. Bagging material - 2 mil thick Kapton polyimide film with 1/2 mil FEP Teflon coating on each side. (1 mil is 0.001")

Sealing compound - commercial sealing compound #5147 supplied by Schnee-Morehead Co. (a local producer of sealing compounds).

Result - The sealing compound lost adhesion at about 490°F and caused total loss of pressure on the test specimen. Test specimens did not heat seal because no bonding pressure was exerted at the FEP fusion temperature. The cause of the loss in sealing could not be determined since it could have been the loss of adhesion caused by sealant degradation or melting of the FEP coating on the Kapton film.

2. Bagging material - FEP coated Kapton film as described above.

Sealing compound - Dow Corning 30-121 one part silicone rubber (a silicone material which cures by moisture absorbed from ambient air).

Result - The sealing compound was found to cure too slow when covered by the bagging material. The test was discontinued when it was determined the sealing compound would not cure rapidly enough for practical use.

3. Bagging material - 1 1/2 mil thick Kapton film coated with FEP on one side only.

Sealing compound - Dow Corning 860 RTV two part silicone rubber.

Result - The viscosity of the sealing compound was too low to make an acceptable seal because of excessive flow and squeezeout when vacuum was applied to the layup. The test specimen did not have enough pressure at the FEP Teflon fusion temperature to heat bond properly.

4. Bagging material - FEP coated Kapton film as described for Trial 1.

Sealing compound - Adhesive backed Teflon pressure sensitive tape.

Result - Vacuum bag had acceptable seal at room temperature. However, seal was lost at approximately 450°F because the adhesive on the Teflon tape completely lost adhesion to the bag material. Test specimen did not heat bond because of loss of bonding pressure.

5. Bagging material - Heavy duty aluminum foil (1/2 mil thick).

Sealing compound - Dow Corning 93-044 two-part silicone sealer.

Result - Sealing compound set up too soon (approx. one hour) to make it acceptable for this application. Further work with this layup showed the aluminum foil developed pinholes when the vacuum was applied to the vacuum bag. No effort was made to complete the heat bonding cycle.

6. Bagging material - 2 mil thick aluminum foil

Sealing compound - Dow Corning 93-004 two-part silicone sealant (this sealant is used to seal the titanium fire wall bulkhead on the 747 airplane).

Result - The aluminum foil was found to tear badly when vacuum was applied to the layup which caused complete loss in sealing. Inspection of the sealing compound showed poor adhesion between the sealant and the aluminum foil bag which probably would have caused loss of sealing even if the foil had not torn.

7. Bagging material - 1 1/2 mil thick Kapton film coated with FEP on one side only.

Sealing compound - Dow Corning 93-046 two-part silicone adhesive/sealant.

Result - Some difficulty was encountered in mixing the extremely thick sealant, however, a satisfactory mix was obtained which could be extruded from a Semco sealant tube. The layup was completed with no difficulty and a good seal was maintained during the heat seal holding period of

520° to 540°F. A good test specimen was prepared with excellent heat sealing of the foil between the tubes. Inspection of the tubes in the test specimen showed considerable tube swelling and distortion which apparently cannot be avoided with FEP tubing.

Conclusions:

1. Kapton film with no FEP coating appears to be the most satisfactory bagging material.
2. Aluminum foil is unsuitable as a bagging material for the following reasons:
 - a. Cannot see through the vacuum bag to verify the FEP tubes are properly seated in the grooved mold.
 - b. Pinholes are easily formed under vacuum bag pressure when 1/2 mil thick foil is used.
 - c. The 2 mil thick foil tears too easily under vacuum bag pressure.
3. Dow Corning 93-046 two-part silicone adhesive/sealant is the best bag sealing compound tried to this time, even though there is considerable difficulty in mixing the extremely thick material.
4. The following sealing material candidates were found to be unacceptable as bag sealing materials for various reasons described earlier.
 - a. Dow Corning 30-121 one-part silicone adhesive
 - b. Dow Corning 860 two-part silicone rubber
 - c. Adhesive backed Teflon pressure sensitive tape
 - d. Dow Corning 93-044 two-part silicone sealant
 - e. Dow Corning 93-004 two-part silicone sealant

APPENDIX D

INSTRUMENTATION ERROR ANALYSIS
FLEXIBLE RADIATOR SOLAR DEGRADATION TEST

VOUGHT CORPORATION

SUBJECT: Instrumentation for Flexible Radiator
Solar Degradation Test at NASA-JSC

DATE: 9 October 1978

TO: J. G. Rankin

CC: R. L. Cox
R. J. French
J. A. Oren
J. C. Utterback

FROM: J. W. Leach

At NASA's request, instrumentation calibration tests and test sequences are outlined below for the forthcoming solar degradation test of the prototype flexible radiator in NASA Chamber B. The test will measure the change in the average value of solar absorptivity as a result of one week of vacuum/UV exposure. The extent of surface property degradation will be determined by measuring the surface temperatures and the heat rejected from the radiator at the beginning and end of the test. This is a difficult test because relatively large changes in solar absorptivity cause only small changes in the measured variables.

Vought will deliver the prototype flexible radiator to NASA instrumented with 36 gauge premium grade copper/constantan thermocouples. The signals from the thermocouples will be monitored on NASA supplied recorders. Flowrate measurements will be made with NASA supplied meters.

1. Sensitivity of Test Results to Measurement Errors

The heat rejected from the radiator surface is

$$q = \int [\epsilon \sigma (T^4 - T_A^4) - \alpha q_s] dA \quad (1)$$

where ϵ is the surface emissivity, α is the solar absorptivity, T is the tube wall temperature, T_A is the ambient temperature, and q_s is the incident solar irradiation. The absorbed solar and infrared terms may be combined to give an effective environment temperature

$$2\epsilon \sigma T_m^4 = 2\epsilon \sigma T_A^4 + \alpha q_s \quad (2)$$

Accounting for the difference between the fluid and tube wall temperatures by the resistance term $R = 1/\pi K_F N_u$, and integrating,

$$q = 2A\eta\epsilon\sigma(T_m - T_{WT})T_m^3 / \left[\frac{1}{4} \ln \left(\left(\frac{T_m - T_{\infty}}{T_m + T_{\infty}} \right) \left(\frac{T_{WT} + T_{\infty}}{T_{WT} - T_{\infty}} \right) \right) \right] \\ - \frac{1}{2} \left[\tan^{-1} \left(\frac{T_m}{T_{\infty}} \right) - \tan^{-1} \left(\frac{T_{WT}}{T_{\infty}} \right) \right] + 2\eta\epsilon\sigma R T_m^3 \ln \left(\frac{T_m^4 - T_{\infty}^4}{T_{WT}^4 - T_{\infty}^4} \right) \}$$

The fluid outlet temperature is given by

$$T_{out} = T_{in} - \frac{q}{\dot{m}C_p} \quad (4)$$

Equations (2), (3), and (4) may be solved to determine the sensitivity of the measured variables to changes in the radiator surface properties, and thus to evaluate the effect of measurement errors on the determination of surface property degradation. Table I compares values obtained from Equations (2) thru (4) for an initial value of $\alpha = 0.1$ and an example degraded value, $\alpha = 0.15$.

TABLE I EFFECT OF α DEGRADATION ON HEAT REJECTION

α	T_{∞} (°F)	\dot{m} (LB/HR)	T_{IN} (°F)	T_{OUT} (°F)	q (LB/HR)
0.1	387	285	90	50	11,413
0.15	421	285	90	53.4	10,420

The table shows that a 50% degradation in α changes the heat rejection by only 8.7%. Since the change in solar absorptivity is to be determined by measuring heat rejection, meaningful results can be obtained only if precise measurements are made. Differences between the inlet and outlet temperatures must be measured to within a few tenths of 1°F, and the flowrate to within 1%. Experience from previous thermal-vacuum radiator tests indicates that this order of accuracy can be obtained only with the highest quality instrumentation, and that instrument calibration tests prior to and following the thermal vacuum test are necessary.

2. Instrumentation Calibration Tests

The following calibration tests are recommended.

(a) Flowmeter Calibration Tests: Collect fluid flowing through the meter during a prescribed period of time in an open container. Determine the flowrate from the weight of the fluid taking account of the accuracy of the scales and the timing device. Perform the calibration tests prior to and following the vacuum tests.

(b) Thermocouple Calibration Tests: With the thermocouples connected to the recording device to be used in thermal vacuum testing, simultaneously record the signals from all immersion thermocouples in constant temperature baths covering the range of temperatures to be experienced in the thermal vacuum test. Calibrate the thermocouples against a secondary standard. To checkout thermocouples located on the radiator panel, cover the panel with an insulation blanket, and record simultaneously the signals from all thermocouples with no flow through the panel, and room ambient radiator environment conditions.

3. Test Sequence

With constant inlet temperature vary the flowrate to cover the maximum

possible range of outlet temperatures. This reduces the probability that instrumentation errors from a single source will obscure the test results. Thermocouple errors are most significant at high flowrates where the difference between the inlet and outlet temperatures are small. At low flowrates thermocouple errors are less significant, but flowmeters errors, which are proportional to the full scale reading, are most important. By examining discrepancies between predicted and measured performance over the range of test conditions, instrumentation effects can be separated from systematic type errors which are indicative of radiator performance degradation.

APPENDIX E
SOLAR DEGRADATION TEST QUICK LOOK REPORT

DESIGN INFORMATION ~~REQUEST~~ - RELEASE O-52042 R3

MODEL(S) AND EFF.

SOFT TUBE FLEXIBLE RADIATOR SOLAR EXPOSURE TEST, QUICK LOOK REPORT		DIR. NO. 2-30320/8DIR-62		REV.	
SYSTEM		REF. G.O. NUMBER 3519 CA 1160		DATE 1/9/79	
FILL IN BLOCK BELOW FOR INFORMATION REQUEST		FILL IN BLOCK BELOW FOR INFORMATION RELEASE			
TO	GROUP	IN REPLY TO DIR. NUMBER			
REQ. BY	GROUP	REL. TO R. L. Cox		GROUP 2-51400	
REASON:	PREPARED BY D.D. Stalmach		DATE 1/9/79	CHECKED BY J.W. Leach	DATE 1/10/79
<input type="checkbox"/> VSD ONLY <input type="checkbox"/> NASC <input type="checkbox"/> NPRO <input type="checkbox"/>	GROUP APP. J.A. Oren		DATE 1-12-79	PROJ OFFICE R.L. Cox	DATE 1/15/79

cc
R. J. French, M. Green, J. L. Williams, C. W. Hixon, J. L. Vann, J. C. Utterback

DESIGN INFORMATION:

INTRODUCTION

The "soft-tube" flexible/deployable radiator prototype was subjected to a solar exposure test from 13 November to 17 November 1978 in Chamber B at NASA-JSC. The purpose of this test was to evaluate possible degradation of the radiator optical properties or construction technique due to solar radiation by measuring:

- Thermal performance of the radiator when initially exposed to a deep space environment,
- Thermal performance when initially exposed to solar radiation,
- Thermal performance after exposure to solar radiation for ~ 100 hours, and
- Thermal performance when exposed to a deep space environment following solar exposure.

The radiator was instrumented with 20 thermocouples on the radiator surface and 8 thermocouples on the inlet and outlet fluid lines and manifolds. The locations of these thermocouples are illustrated in Figure 1. Two platinum resistance probes were used to measure the inlet and outlet fluid temperatures. In addition, a thermocouple was attached to the screen wire on which the radiator was lying and another was attached to the passive plate located in the center of the floor. The radiator fluid was water from the NASA potable hot

water supply. The inlet temperature of the water was approximately 113°F and the flowrate through the radiator was held at 160 lb/hr. The water flow schematic is illustrated in Figure 2.

The first deep space environment test point was reached at 1500 on 13 November. The solar flux was initiated at 1530 and the first steady state solar condition was reached at 2030 on 13 November. The solar flux was terminated at 1600 on 17 November and the second deep space environment test point was reached at 2100 on the same date.

DATA ANALYSIS

A FORTRAN computer program was written to process the measured temperatures and calculate the effective solar absorptance of the radiator at selected times. A listing of this program is included in Appendix A.

The average fin temperature of the radiator was calculated by averaging the measured temperatures on the radiator fin surface,

$$T_F = \left[\frac{\sum_{i=1}^{20} (T_i^4) - [T_5^4 + T_{15}^4 + T_{17}^4 + T_{18}^4]}{16} \right]^{.25} \quad (1)$$

where $T_1 \rightarrow T_{20}$ are the temperatures measured by the 20 radiator thermocouples. The values measured by thermocouples 15 and 17 were not included in the average because these thermocouples were located on tubes rather than the fin material. Also, the values measured by thermocouples 5 and 18 were not included because these thermocouples were giving erroneous (off-scale) readings. The equivalent structure temperature was calculated taking into account major sources of emitted and reflected IR. These sources included the solar module mirrors, the chamber floor, the chamber walls and ceiling, the passive circular floor plate, the wire table, the radiator inflation tubes, the radiator drum, and the rectangular floor plate located under the radiator. These sources have been numbered and are illustrated in Figure 3. The equivalent structure temperature was calculated with the following equation,

$$T_{ST} = \left[\sum_{i=1}^7 (\epsilon_i F_{R-i} T_i^4) + \epsilon_R T_R^4 \sum_{i=1}^7 F_{R-i} F_{i-R} \rho_i + \frac{\tau_R Q_S \rho_{8R}}{\sigma} \right]^{.25} \quad (2)$$

where the subscript R refers to the radiator. The equivalent sink temperature was calculated with the equation,

$$T_S = [T_{ST}^4 + K_1 \alpha Q_S]^{.25} \quad (3)$$

$$\text{where } K_1 = \frac{1 + (1 - \alpha_5)\tau_R}{2\epsilon_R\sigma}$$

The average tube temperature was then calculated with the equation,

$$T_T = \frac{1}{X} [T_F + (X - 1) T_S] \quad (4)$$

$$\text{where } X = \frac{T_{16} - T_S}{T_O - T_S} \quad \text{and } T_O = .5(T_{15} + T_{17})$$

The total radiated heat was calculated with the equation,

$$Q_{RAD} = K_2 \eta T_T^4 \quad (5)$$

$$\text{where } K_2 = 2 A_R \epsilon_R \sigma$$

The heat given up by the fluid loop was calculated as,

$$Q_{FLUID} = \dot{M}(\Delta T_{FLUID}) \quad (6)$$

The total absorbed heat was then calculated with the equation,

$$Q_{ABS} = Q_{RAD} - Q_{FLUID} \quad (7)$$

The effective solar absorptance was calculated by two different methods. Method A used the equation

$$\alpha = \frac{Q_{ABS} - K_3 T_{ST}^4}{K_4 Q_S} \quad (8)$$

$$\text{where } K_3 = 2A_R \epsilon_R \sigma \quad \text{and } K_4 = [1 + (1 - \alpha_5)\tau_R]A_R$$

Once α was calculated, this value was used to recalculate T_{ST} and T_S and a new value of α was then calculated. This procedure was performed three times, which was assumed to give sufficient convergence of α . Method B used the value

of α calculated by Method A and equation (3) to calculate T_S . The heat rejected by the radiator was then calculated with the equation,

$$Q = \frac{A}{B - C + D} \quad (9)$$

where,

$$A = 2 A_R \eta \epsilon_R \sigma (T_1 - T_O) T_S^3$$

$$B = 1/4 \ln \left[\left(\frac{T_1 - T_S}{T_1 + T_S} \right) \left(\frac{T_O + T_S}{T_O - T_S} \right) \right]$$

$$C = 1/2 \left[\tan^{-1} \left(\frac{T_1}{T_S} \right) - \tan^{-1} \left(\frac{T_O}{T_S} \right) \right]$$

$$D = 2 \eta \epsilon_R S R \sigma T_S^3 \ln \left(\frac{T_1^4 - T_S^4}{T_O^4 - T_S^4} \right)$$

$$T_1 = \text{inlet fluid temperature } (T_{31})$$

$$T_O = \text{outlet fluid temperature } (T_{32})$$

$$T_S = \text{environment sink temperature}$$

$$S = \text{radiator tube spacing}$$

$$R = \text{thermal resistance between the fluid and the radiator} = \frac{1}{\pi k_f Nu}$$

The effective solar absorptance is then the value of α (within some set limits) such that the function $F(\alpha) = |Q - Q_{\text{FLUID}}|$ is minimized. Note that in contrast to Method A which calculated the solar absorptance of the radiator based on the measured radiator fin temperatures, Method B calculated the absorptance based on the measured fluid inlet and outlet temperatures and the calculated thermal resistance between the transport fluid and the radiator surface.

RESULTS

The measured temperatures and calculated parameters at representative times during the solar exposure are presented in Table 1. The values of solar absorptance calculated by the two methods are in close agreement for the times presented and vary only slightly over the length of the solar exposure. The difference between the Method B values of α at the beginning and end of the solar exposure is less than 1%.

The measured temperatures for the two deep space environments are compared in Table 2. The temperatures at the two environments compare favorably and no difference in radiator performance is evident.

Visual inspection of the radiator indicated no optical or mechanical degradation due to the solar exposure.

CONCLUSIONS

Post test evaluation of the performance data indicate that no measurable degradation of the radiator occurred during the 96.5 hours of solar exposure. Visual inspection of the test article indicates no observable change in the physical appearance of the radiator.

TABLE 1 (a)

DATE=11/13/78

H=24 M=0 S=1

TC NO.	LOCATION	TEMP (F)
1	INLET FIN	83.1
2	OUTLET FIN	79.5
3	INLET FIN	87.0
4	OUTLET FIN	72.6
5	INLET FIN	*****
6	OUTLET FIN	76.7
7	INLET FIN	89.1
8	OUTLET FIN	76.3
9	INLET FIN	97.8
10	OUTLET FIN	77.0
11	INLET FIN	96.9
12	OUTLET FIN	75.9
13	INLET FIN	91.0
14	OUTLET FIN	73.3
15	INLET TUBE	102.9
16	INLET FIN	96.0
17	INLET TUBE	100.0
18	OUTLET FIN	*****
19	INLET FIN	98.3
20	OUTLET FIN	66.6
21	INLET FLUID (LEFT)	112.7
22	INLET FLUID (RIGHT)	112.7
23	OUTLET FLUID (LEFT)	76.5
24	OUTLET FLUID (RIGHT)	77.4
25	INLET MANIFOLD (LEFT)	109.9
26	OUTLET MANIFOLD (RIGHT)	77.6
27	OUTBOARD MANIFOLD (LEFT)	99.7
28	OUTBOARD MANIFOLD (RIGHT)	93.7
29	FLOOR PLATE	116.7
30	TABLE WIRE	78.1

PLATINUM PROBE INLET TEMP (F) =	113.4
PLATINUM PROBE OUTLET TEMP (F) =	77.2
PLATINUM PROBE DELTA TEMP (F) =	36.2
AVG FIN TEMP (F) =	83.8
WATER FLOW RATE (LB/HR) =	160.0
AVG STRUCTURE TEMP (F) =	-116.7
FLUID HEAT REJ (BTU/HR) =	5792.0
SOLAR FLUX (BTU/HR) =	468.5
AVG TUBE TEMP (F) =	85.2
TOTAL ABSORBED HEAT (BTU/HR) =	6489.0
FIN EFFECTIVENESS =	.960
TEMPERATURE RATIO =	.984
SINK TEMPERATURE (F) =	.1
TOTAL RADIATED HEAT (BTU/HR) =	12281.0
AVG SOLAR MOD MIRROR TEMP (F) =	87.1
AVG LUNAR PLANE TEMP (F) =	-290.2
AVG CHAMBER WALL AND CEILING TEMP (F) =	-296.9
EFFECTIVE SOLAR ABSORPTANCE (METHOD A) =	.153
EFFECTIVE SOLAR ABSORPTANCE (METHOD B) =	.159

TABLE 1 (b)

DATE=11/15/78

H= 3 M=70 S= 0

TC NO.	LOCATION	TEMP (F)
1	INLET FIN	83.1
2	OUTLET FIN	79.2
3	INLET FIN	88.3
4	OUTLET FIN	72.2
5	INLET FIN	*****
6	OUTLET FIN	77.0
7	INLET FIN	89.0
8	OUTLET FIN	76.2
9	INLET FIN	97.5
10	OUTLET FIN	76.5
11	INLET FIN	96.6
12	OUTLET FIN	76.5
13	INLET FIN	91.2
14	OUTLET FIN	73.7
15	INLET TUBE	102.9
16	INLET FIN	96.6
17	INLET TUBE	100.7
18	OUTLET FIN	*****
19	INLET FIN	98.2
20	OUTLET FIN	67.2
21	INLET FLUID (LEFT)	113.0
22	INLET FLUID (RIGHT)	112.3
23	OUTLET FLUID (LEFT)	77.1
24	OUTLET FLUID (RIGHT)	77.0
25	INLET MANIFOLD (LEFT)	110.6
26	OUTLET MANIFOLD (RIGHT)	78.6
27	OUTBOARD MANIFOLD (LEFT)	95.4
28	OUTBOARD MANIFOLD (RIGHT)	94.6
29	FLOOR PLATE	111.8
30	TABLE WIRE	80.2

PLATINUM PROBE INLET TEMP (F) = 113.4
 PLATINUM PROBE OUTLET TEMP (F) = 77.4
 PLATINUM PROBE DELTA TEMP (F) = 36.0
 AVG FIN TEMP (F) = 83.9
 WATER FLOW RATE (L3/HR) = 160.0
 AVG STRUCTURE TEMP (F) = -118.0
 FLUID HEAT REJ (BTU/HR) = 5760.0
 SOLAR FLUX (BTU/HR) = 468.5
 AVG TUBE TEMP (F) = 88.3
 TOTAL ABSORBED HEAT (BTU/HR) = 6610.1
 FIN EFFECTIVENESS = .945
 TEMPERATURE RATIO = .949
 SINK TEMPERATURE (F) = 2.2
 TOTAL RADIATED HEAT (BTU/HR) = 12370.1
 AVG SOLAR MOL MIRROR TEMP (F) = 86.5
 AVG LUNAR PLANE TEMP (F) = -294.3
 AVG CHAMBER WALL AND CEILING TEMP (F) = -296.9
 EFFECTIVE SOLAR ABSORPTANCE (METHOD A) = .158
 EFFECTIVE SOLAR ABSORPTANCE (METHOD B) = .159

TABLE 1 (c)

DATE=11/16/78

H= 3 M=30 S= 0

TC NO.	LOCATION	TEMP (F)
1	INLET FIN	92.8
2	OUTLET FIN	78.7
3	INLET FIN	86.7
4	OUTLET FIN	72.1
5	INLET FIN	****
6	OUTLET FIN	76.4
7	INLET FIN	91.1
8	OUTLET FIN	75.3
9	INLET FIN	97.0
10	OUTLET FIN	75.8
11	INLET FIN	96.5
12	OUTLET FIN	75.5
13	INLET FIN	91.7
14	OUTLET FIN	72.9
15	INLET TUBE	103.3
16	INLET FIN	97.3
17	INLET TUBE	100.5
18	OUTLET FIN	****
19	INLET FIN	99.0
20	OUTLET FIN	66.7
21	INLET FLUID (LEFT)	112.3
22	INLET FLUID (RIGHT)	112.3
23	OUTLET FLUID (LEFT)	76.6
24	OUTLET FLUID (RIGHT)	76.6
25	INLET MANIFOLD (LEFT)	109.8
26	OUTLET MANIFOLD (RIGHT)	77.4
27	OUTBOARD MANIFOLD (LEFT)	95.0
28	OUTBOARD MANIFOLD (RIGHT)	93.6
29	FLOOR PLATE	109.1
30	TABLE WIRE	78.3

PLATINUM PROBE INLET TEMP (F) =	113.7
PLATINUM PROBE OUTLET TEMP (F) =	77.2
PLATINUM PROBE DELTA TEMP (F) =	36.5
AVG FIN TEMP (F) =	83.7
WATER FLOW RATE (LB/HR) =	160.0
AVG STRUCTURE TEMP (F) =	-119.1
FLUID HEAT REJ (BTU/HR) =	5840.0
SOLAR FLUX (BTU/HR) =	468.5
AVG TUBE TEMP (F) =	87.8
TOTAL ABSORBED HEAT (BTU/HR) =	6673.5
FIN EFFECTIVENESS =	.960
TEMPERATURE RATIO =	.952
SINK TEMPERATURE (F) =	3.3
TOTAL RADIATED HEAT (BTU/HR) =	12513.5
AVG SOLAR MOD MIRROR TEMP (F) =	84.7
AVG LUNAR PLANE TEMP (F) =	-294.3
AVG CHAMBER WALL AND CEILING TEMP (F) =	-296.9
EFFECTIVE SOLAR ABSORPTANCE (METHOD A) =	.161
EFFECTIVE SOLAR ABSORPTANCE (METHOD B) =	.160

TABLE 1 (d)

DATE=11/17/78

H= 7 M=30 S= 0

TC NO.	LOCATION	TEMP (F)
1	INLET FIN	81.9
2	OUTLET FIN	78.2
3	INLET FIN	86.9
4	OUTLET FIN	72.1
5	INLET FIN	*****
6	OUTLET FIN	76.5
7	INLET FIN	89.7
8	OUTLET FIN	75.2
9	INLET FIN	95.4
10	OUTLET FIN	75.4
11	INLET FIN	95.7
12	OUTLET FIN	75.4
13	INLET FIN	90.8
14	OUTLET FIN	73.8
15	INLET TUBE	102.0
16	INLET FIN	96.7
17	INLET TUBE	100.4
18	OUTLET FIN	*****
19	INLET FIN	97.8
20	OUTLET FIN	67.5
21	INLET FLUID (LEFT)	112.3
22	INLET FLUID (RIGHT)	113.0
23	OUTLET FLUID (LEFT)	76.4
24	OUTLET FLUID (RIGHT)	76.6
25	INLET MANIFOLD (LEFT)	110.4
26	OUTLET MANIFOLD (RIGHT)	77.4
27	OUTBOARD MANIFOLD (LEFT)	95.1
28	OUTBOARD MANIFOLD (RIGHT)	93.7
29	FLOOR PLATE	107.5
30	TABLE WIRE	78.3

PLATINUM PROBE INLET TEMP (F) =	113.3
PLATINUM PROBE OUTLET TEMP (F) =	76.5
PLATINUM PROBE DELTA TEMP (F) =	36.8
AVG FIN TEMP (F) =	83.2
WATER FLOW RATE (LB/HR) =	160.0
AVG STRUCTURE TEMP (F) =	-119.9
FLUID HEAT REJ (BTU/HR) =	5888.0
SOLAR FLUX (BTU/HR) =	468.5
AVG TUBE TEMP (F) =	87.1
TOTAL ABSORBED HEAT (BTU/HR) =	6564.7
FIN EFFECTIVENESS =	.960
TEMPERATURE RATIO =	.955
SINK TEMPERATURE (F) =	1.5
TOTAL RADIATED HEAT (BTU/HR) =	12452.7
AVG SOLAR MOD MIRROR TEMP (F) =	74.8
AVG LUNAR PLANE TEMP (F) =	-294.5
AVG CHAMBER WALL AND CEILING TEMP (F) =	-236.9
EFFECTIVE SOLAR ABSORPTANCE (METHOD A) =	.158
EFFECTIVE SOLAR ABSORPTANCE (METHOD B) =	.157

TABLE 1 (c)

DATE=11/17/78

H=15 M= C S= 0

TC NO.	LOCATION	TEMP (F)
1	INLET FIN	82.3
2	OUTLET FIN	78.4
3	INLET FIN	86.7
4	OUTLET FIN	72.0
5	INLET FIN	****
6	OUTLET FIN	76.7
7	INLET FIN	89.5
8	OUTLET FIN	75.4
9	INLET FIN	97.0
10	OUTLET FIN	76.1
11	INLET FIN	96.8
12	OUTLET FIN	75.3
13	INLET FIN	91.3
14	OUTLET FIN	72.5
15	INLET TUBE	103.2
16	INLET FIN	97.4
17	INLET TUBE	100.7
18	OUTLET FIN	*****
19	INLET FIN	98.8
20	OUTLET FIN	67.3
21	INLET FLUID (LEFT)	112.2
22	INLET FLUID (RIGHT)	112.3
23	OUTLET FLUID (LEFT)	76.4
24	OUTLET FLUID (RIGHT)	76.5
25	INLET MANIFOLD (LEFT)	109.6
26	OUTLET MANIFOLD (RIGHT)	77.6
27	OUTBOARD MANIFOLD (LEFT)	94.9
28	OUTBOARD MANIFOLD (RIGHT)	93.4
29	FLOOR PLATE	110.3
30	TABLE WIRE	78.9

PLATINUM PROBE INLET TEMP (F) =	112.9
PLATINUM PROBE OUTLET TEMP (F) =	76.7
PLATINUM PROBE DELTA TEMP (F) =	36.1
AVG FIN TEMP (F) =	83.6
WATER FLOW RATE (LB/HR) =	160.0
AVG STRUCTURE TEMP (F) =	-118.9
FLUID HEAT REJ (BTU/HR) =	5776.0
SOLAR FLUX (BTU/HR) =	472.9
AVG TUBE TEMP (F) =	86.7
TOTAL ABSORBED HEAT (BTU/HR) =	6637.5
FIN EFFECTIVENESS =	.960
TEMPERATURE RATIO =	.964
SINK TEMPERATURE (F) =	2.7
TOTAL RADIATED HEAT (BTU/HR) =	12413.5
AVG SOLAR MCG MIRROR TEMP (F) =	76.6
AVG LUNAR PLANE TEMP (F) =	-294.7
AVG CHAMBER WALL AND CEILING TEMP (F) =	-296.4
EFFECTIVE SOLAR ABSORPTANCE (METHOD A) =	.158
EFFECTIVE SOLAR ABSORPTANCE (METHOD B) =	.158

TABLE 2
COMPARISON OF RADIATOR TEMPERATURES FOR
DEEP SPACE ENVIRONMENTS

T/C NO.	TEMPERATURE (°F)	
	11/13/78 1500	11/17/78 2100
1	50.5	51.2
2	45.4	45.2
3	49.2	49.3
4	39.2	39.2
5	-	-
6	39.2	39.1
7	61.4	62.1
8	40.0	40.6
9	61.9	62.0
10	34.0	33.0
11	66.8	66.4
12	31.4	32.2
13	69.8	69.7
14	26.9	24.6
15	81.4	81.1
16	71.7	72.1
17	83.7	83.5
18	-	-
19	76.1	75.9
20	28.3	30.1
31 (T_{in})	113.2	113.1
32 (T_{out})	50.0	49.8
ΔT_{FLUID}	63.2	63.3

FIGURE 1
FLEXIBLE RADIATOR THERMOCOUPLE LOCATIONS

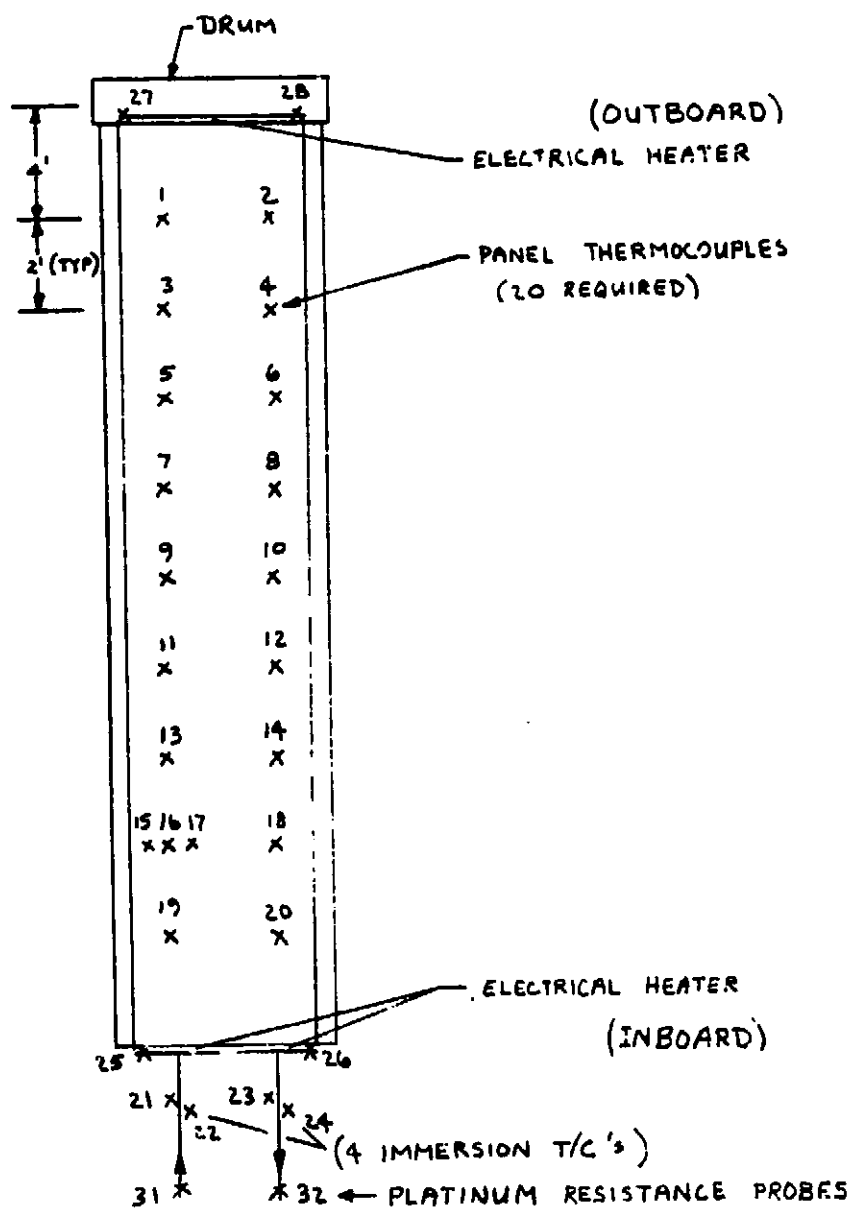
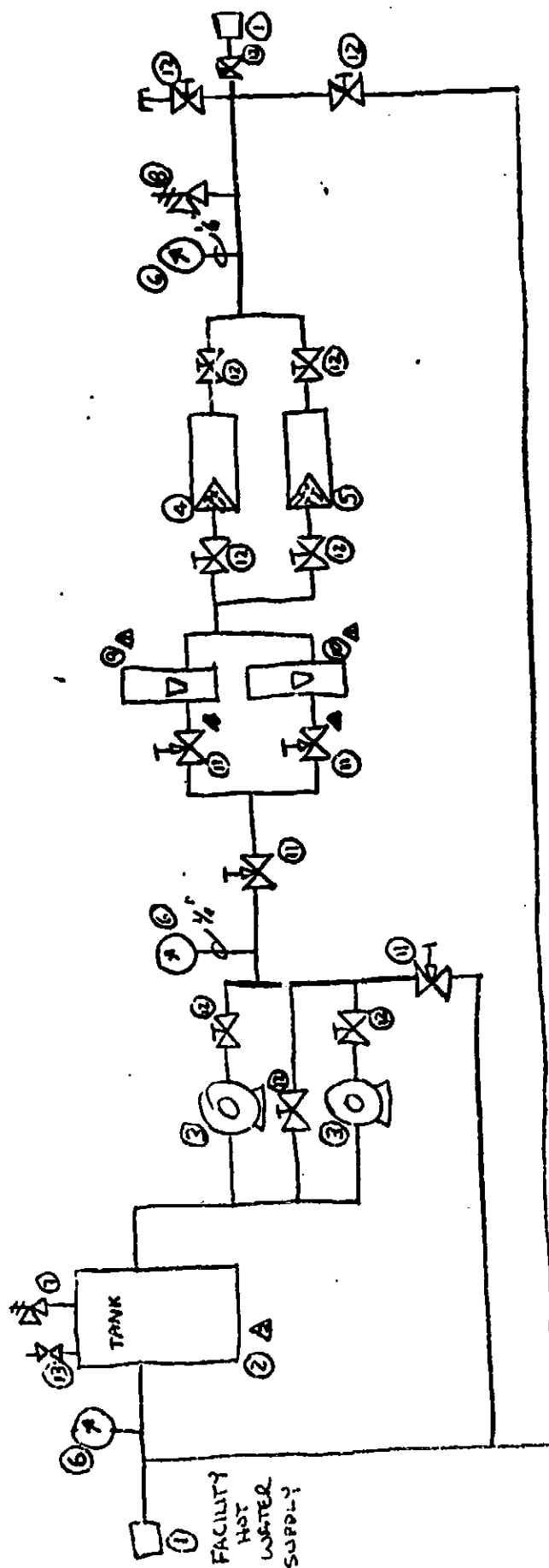


FIGURE 2
CSD FLOW BENCH SCHEMATIC



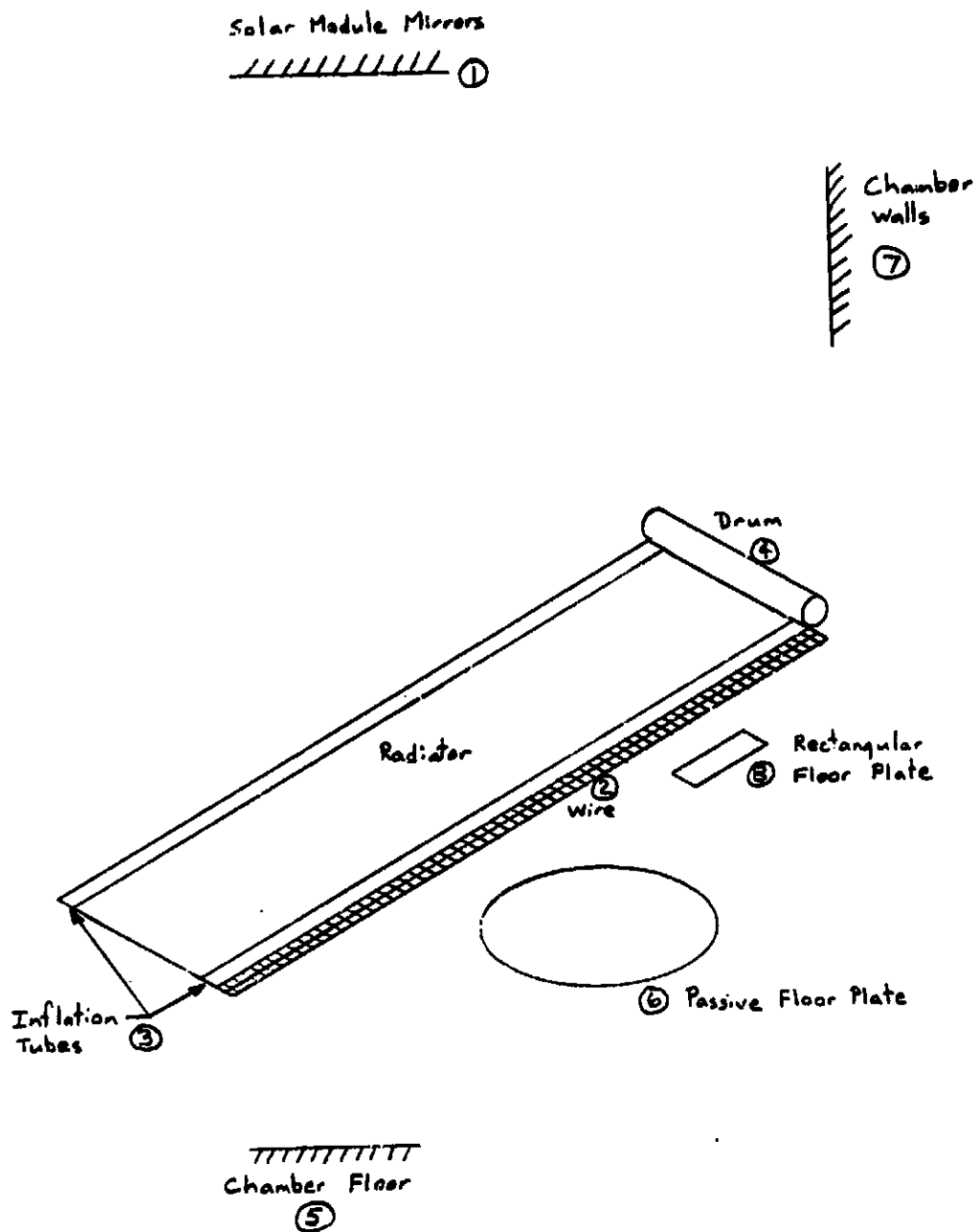
NOTES : ~~1. TANK IS TO BE LOCATED AT A HIGHER LEVEL THAN PUMP INLET~~

2. TANK IS TO BE LOCATED AT A HIGHER LEVEL THAN PUMP INLET
TUBING TO BE 1/2" STAINLESS STEEL
UNLESS OTHERWISE SPECIFIED

PARTS LIST

ITEM NO.	DESCRIPTION	MANUFACTURER	PART NUMBER	REMARKS
1	CONNECTION			1/2" Female NPT
2	WATER TANK	MILLIPORE	XYG700120	
3	PUMP	EASTERN NUPRO HARRIS	D-11	TEST 9000
4	INLINE FILTER	GELMAN		10A
5	FILTER	HEILIG		0-200 PSI 1/2"
6	PRESSURE GAGE	SAGE	231-88-BMC	0-200 PSI 1/2"
7	RELIEF VALVE	SAGE	231-88-BMC	0-200 PSI 1/2"
8	RELIEF VALVE	SAGE	231-88-BMC	0-200 PSI 1/2"
9	ROTAMETER	SHAPIRO SUPPLY CO.		150-200 PSI
10	ROTAMETER	SHAPIRO SUPPLY CO.		150-200 PSI
11	THROTTLE VALVES	WHITE	SS-ORANGE	1/2" SS
12	BALL VALVES	JAMESBURY	A232	1/2" SS
13	TOGGLE VALVE	HOKI	1151F25	1/2" SS

FIGURE 3 - IR SOURCES



APPENDIX - COMPUTER LISTING

```

PROGRAM FLEX(INPUT,OUTPUT)
COMMON/MAIN/TH,TFLR,T(32),TWALL,TF,DTF,QS,XK1,ETA,QFL
DIMENSION AL(3),Y(3)
TFUN(TI)=(TI+460.)**4
5  READ 100,RMJ,XK1,XK2,XK3,XK4
  IF(RMJ.LE.0.) GO TO 900
  READ 100,TH,TFLR,TWALL,DTF
  READ 100,QS,ALF,CHI,ETA
  READ 100,T
  READ 110,DATE,HR,M,S
  TF=J.
  DO 10 I=1,20
10  TF=TF+TFUN(T(I))
  TF=((TF-TFUN(T(5)))-TFUN(T(15))-TFUN(T(17))-TFUN(T(19)))/16.**.25
  1-460.
  DO 15 J=1,3
  TST=(.006*TFUN(TH)+.42*TFUN(TFLR)+.064*TFUN(T(29))+.035*TFUN(T(30))
  1)+.47*TFUN(TWALL)+.029*TFUN(TF)+1.79E6*ALF*QS)**.25-460.
  TS=(TFUN(TST)+XK1*ALF*QS)**.25-460.
  TT=(TF+460.+(CHI-1.)*(TS+460.))/CHI-460.
  QPAD=XK2*ETA*TFUN(TT)
  QFL=RMJ*DTF
  QABS=QPAD-QFL
15  ALF=(QABS-XK3*TFUN(TST))/(XK4*QS)
  AMAX=ALF+.02
  AMIN=ALF-.02
  DEL=(AMAX-AMIN)*.25
  DO 50 I=1,3
  AL(I)=AMIN+FLOAT(I)*DEL
  Y(I)=F(AL(I))
50  CONTINUE
51  ISUB=IS(Y)
  IF((2.*DEL).LE..001) GO TO 60
  DEL=DEL*.5
  AL(2)=AL(ISUB)
  Y(2)=Y(ISUB)
  AL(1)=AL(2)-DEL
  Y(1)=F(AL(1))
  AL(3)=AL(2)+DEL
  Y(3)=F(AL(3))
  GO TO 51
60  ALFB=AL(ISUB)
  PRINT 1,DATE,HR,M,S
  PRINT 200
  DO 20 K=1,13,2
  PRINT 201,K,T(K)
  KP1=K+1
  PRINT 202,KP1,T(KP1)
20  I=K
  I=I+2
  PRINT 203,I,T(I)
  I=I+1
  PRINT 201,I,T(I)
  I=I+1
  PRINT 203,I,T(I)
  I=I+1
  PRINT 202,I,T(I)

```

```

I=I+1
PRINT 201,I,T(I)
I=I+1
PRINT 202,I,T(I)
I=I+1
PRINT 203,I,T(I)
I=I+1
PRINT 204,I,T(I)
I=I+1
PRINT 205,I,T(I)
I=I+1
PRINT 206,I,T(I)
I=I+1
PRINT 207,I,T(I)
I=I+1
PRINT 208,I,T(I)
I=I+1
PRINT 209,I,T(I)
I=I+1
PRINT 210,I,T(I)
I=I+1
PRINT 211,I,T(I)
I=I+1
PRINT 212,I,T(I)
I=I+1
PRINT 213,I,T(I)
PRINT 214,T(31)
PRINT 215,T(32)
PRINT 216,QTF
PRINT 217,TF
PRINT 218,QMD
PRINT 219,TST
PRINT 220,QFL
PRINT 221,QS
PRINT 223,TT
PRINT 224,QABS
PRINT 225,ETA
PRINT 226,CHI
PRINT 227,TS
PRINT 228,QRAD
PRINT 229,TM
PRINT 230,TFLR
PRINT 231,TWALL
PRINT 232,ALF
PRINT 233,ALFB
GO TO 5
900 STOP
1 FORMAT(1H1,/,16X,*DATE=*,A8,5X,*H=*,A2,*M=*,A2,*S=*,A2)
100 FORMAT(8F10.0)
110 FORMAT(A8,A2,A2,A2)
200 FORMAT(///,14X,*TC NO. LOCATION*,19X,*TEMP (F)*,/)
201 FORMAT(15X,I2,5X,*INLET FIN*,20X,F5.1)
202 FORMAT(15X,I2,5X,*OUTLET FIN*,19X,F5.1)
203 FORMAT(15X,I2,5X,*INLET TUBE*,19X,F5.1)
204 FORMAT(15X,I2,5X,*INLET FLUID (LEFT)*,11X,F5.1)
205 FORMAT(15X,I2,5X,*INLET FLUID (RIGHT)*,10X,F5.1)
206 FORMAT(15X,I2,5X,*OUTLET FLUID (LEFT)*,10X,F5.1)
207 FORMAT(15X,I2,5X,*OUTLET FLUID (RIGHT)*,9X,F5.1)
208 FORMAT(15X,I2,5X,*INLET MANIFOLD (LEFT)*,8X,F5.1)

```

```

209 FORMAT(15X,I2,5X,*OUTLET MANIFOLD (RIGHT)*,6X,F5.1)
210 FORMAT(15X,I2,5X,*OUTBOARD MANIFOLD (LEFT)*,5X,F5.1)
211 FORMAT(15X,I2,5X,*OUTBOARD MANIFOLD (RIGHT)*,4X,F5.1)
212 FORMAT(15X,I2,5X,*FLOOR PLATE*,10X,F5.1)
213 FORMAT(15X,I2,5X,*TAGLE WIRE*,19X,F5.1,/)
214 FORMAT(15X,*PLATINUM PROBE INLET TEMP (F) =*,8X,F7.1)
215 FORMAT(15X,*PLATINUM PROBE OUTLET TEMP (F) =*,7X,F7.1)
216 FORMAT(15X,*PLATINUM PROBE DELTA TEMP (F) =*,8X,F7.1)
217 FORMAT(15X,*AVG FIN TEMP (F) =*,21X,F7.1)
218 FORMAT(15X,*WATER FLOW RATE (LB/HR) =*,14X,F7.1)
219 FORMAT(15X,*AVG STRUCTURE TEMP (F) =*,15X,F7.1)
220 FORMAT(15X,*FLUID HEAT REJ (BTU/HR) =*,14X,F7.1)
221 FORMAT(15X,*SOLAR FLUX (BTU/HR) =*,18X,F7.1)
223 FORMAT(15X,*AVG TUBE TEMP (F) =*,20X,F7.1)
224 FORMAT(15X,*TOTAL ABSORBED HEAT (BTU/HR) =*,9X,F7.1)
225 FORMAT(15X,*FIN EFFECTIVENESS =*,20X,F7.3)
226 FORMAT(15X,*TEMPERATURE RATIO =*,20X,F7.3)
227 FORMAT(15X,*SINK TEMPERATURE (F) =*,17X,F7.1)
228 FORMAT(15X,*TOTAL RADIATED HEAT (BTU/HR) =*,9X,F7.1)
229 FORMAT(15X,*AVG SOLAR MOD MIRROR TEMP (F) =*,8X,F7.1)
230 FORMAT(15X,*AVG LUNAR PLANE TEMP (F) =*,13X,F7.1)
231 FORMAT(15X,*AVG CHAMBER WALL AND CEILING TEMP (F) =*,F7.1)
232 FORMAT(15X,*EFFECTIVE SOLAR ABSORPTANCE (METHOD A) =*,F6.3)
233 FORMAT(15X,*EFFECTIVE SOLAR ABSORPTANCE (METHOD B) =*,F6.3)
END

```

SOLIS REFERENCE MAP (R=3)

IS DEF LINE REFERENCES

SN	TYPE	RELOCATION	REFS				
	REAL	ARRAY	42	DEFINED	30	35	37
	REAL		17		29	35	37
			8		19	25	26
	REAL		100	DEFINED	24		
	REAL		27	DEFINED	42		
	REAL		27		25		
	REAL		27		29	DEFINED	26
	REAL		2*20		93	DEFINED	8
	REAL		43	DEFINED	10		
	REAL		29		33	34	37
			27		34		
	REAL	MAIN	2		22	84	DEFINE
	REAL	MAIN	2		21	92	DEFINE
	REAL		43	DEFINED	10		
	INTEGER		13		2*29	2*30	51
			54	2*55	56	2*57	58
			62	2*63	64	2*65	66
			70	2*71	72	2*73	74
			78	2*79	80	2*81	DEFINE
			50	52	54	56	58
			66	68	70	72	74


```

FUNCTION F(ALF)
COMMON/MAIN/TM,TFLR,T(32),TWALL,TF,DTF,QS,XK1,ETA,QFL
TFUN(TI)=(TI+460.)**4
TST=(.016*TFUN(TM)+.42*TFUN(TFLR)+.064*TFUN(T(29))+.035*TFUN(T(30)
1)+.47*TFUN(TWALL)+.029*TFUN(TF)+1.79E6*ALF*QS)**.25-460.
T31=T(31)+460.
T32=T(32)+460.
TS=(TFUN(T31)+XK1*ALF*QS)**.25
A=1.4562E-7*ETA*DTF*TS**3
B=.25*ALOG((T31-TS)*(T32+T3)/(T31+TS)*(T32-TS)))
C=.5*(ATAN(T31/TS)-ATAN(T32/TS))
D=2.427E-10*E.A*TS**3*ALOG((T31**4-TS**4)/(T32**4-TS**4))
Q=A/(9-C+D)
F=ABS(Q-QFL)
RETURN
END
    
```

SOLID REFERENCE MAP (R=3)

DEF LINE REFERENCES
1 15

SN	TYPE	RELOCATION	REFS	13	DEFINED	9	
	REAL		REFS	13	DEFINED	9	
	REAL	F.P.	REFS	4	8	DEFINED	1
	REAL		REFS	13	DEFINED	10	
	REAL		REFS	13	DEFINED	11	
	REAL		REFS	13	DEFINED	12	
	REAL	MAIN	REFS	2	9		
	REAL	MAIN	REFS	2	9	12	
	REAL		DEFINED	14			
	REAL		REFS	14	DEFINED	13	
	REAL	MAIN	REFS	2	14		
	REAL	MAIN	REFS	2	4	9	
	REAL	ARRAY	REFS	2	2*4	6	7
	REAL	MAIN	REFS	2	4		
	REAL	MAIN	REFS	2	4		
	REAL	MAIN	REFS	2	4		
	REAL	MAIN	REFS	2	4		
	REAL		REFS	9	4*10	2*11	3*1
	REAL		REFS	8	DEFINED	4	
	REAL	MAIN	REFS	2	4		
	REAL		REFS	2*10	11	12	DEFINE
	REAL		REFS	2*10	11	12	DEFINE
	REAL	MAIN	REFS	2	8		

	TYPE	ARGS	REFERENCES
	REAL	1 LIBRARY	10 12
	REAL	1 LIBRARY	2*11
CTIONS	TYPE	ARGS	DEF LINE REFERENCES
	REAL	1 INTRIN	14
	REAL	1 SF	3 5*4 8

```

      FUNCTION IS(F)
      IS FINDS THE SUBSCRIPT OF THE MINIMUM VALUE OF THE ARRAY F
      DIMENSION F(3)
      FMIN=F(1)
      IF=1
      DO 10 I=2,3
      IF(F(I).GE.FMIN) GO TO 10
      FMIN=F(I)
      IS=I
10  CONTINUE
      RETURN
      END
  
```

ROLIC REFERENCE MAP (R=3)

TS	DEF LINE	REFERENCES
	1	12

SN	TYPE	RELOCATION	REFS	5	8	9	10	DEFINE
4	REAL	ARRAY	F.P.	4				
	REAL		REFS	8	DEFINED	5		
	INTEGER		REFS	8				
	INTEGER		DEFINED	6	10			DEFINE

LABELED	DEF LINE	REFERENCES
	11	7 8

EL	INDEX	FROM-TO	LENGTH	PROPERTIES
	I	7 11	48	INSTACK

LENGTH	268	22
--------	-----	----